XENOBIOTIC METABOLISM IN THE AUSTRALIAN MARSUPIAL KOALA (*PHASCOLARCTOS CINEREUS*)

A thesis submitted in fulfilment of the requirements for the degree of Doctor of Philosophy at the University of South Australia.

Suong Ngoc Thi Ngo (B. Pharm. (Hons))

School of Pharmaceutical Molecular and Biosciences
University of South Australia

March 2003

UNIVERSITY OF
SOUTH AUSTRALIA
12 MAR 2004
pmc LIBRARY

Contents

List of Figures vii
List of Tables xi
List of Appendices xiii
Abbreviations xiii
Single and Three Amino Acid Abbreviations xvi
Summary xvii
Declaration xx
Acknowledgements xxi
Publications in Support of Thesis xxiv

1 GENERAL INTRODUCTION **1**
1.1 XENOBIOTIC METABOLISM 4
1.2 CYTOCHROME P450 4
1.2.1 Historical aspects 5
1.2.2 Nomenclature of cytochrome P450 6
1.2.3 Catalytic cycle of cytochrome P450 enzymes 7
1.2.4 Key structural features of cytochrome P450 enzymes 7
1.2.5 Cytochrome P450 *CYP4A* family 10
1.2.6 CYP4A enzymes and their substrates 11
1.2.7 The roles of the CYP4A subfamily 11
1.2.8 Induction of CYP4A subfamily 13
1.3 PEROXISOMAL β-OXIDATION ENZYMES 15
1.3.1 Peroxisomes 15
1.3.2 Fatty acid metabolism 15
1.3.3 The peroxisomal β-oxidation pathway 16
1.3.4 The enzymes of the β-oxidation system 16
1.3.5 Acyl-CoA oxidases 18
1.3.6 Deficiencies of β-oxidation enzymes 20
1.4 PEROXISOME PROLIFERATORS AND PPAR-α 21
1.4.1 Historical aspects 21
1.4.2 Peroxisome proliferators 22
1.4.3 The overall effects induced by peroxisome proliferators 23
1.4.4 Peroxisome proliferator activated receptor-alpha: Molecular aspects 23

1.4.5 PPAR-α cofactors and the mechanism of action of peroxisome proliferators 29
1.4.6 Physiologic roles of PPAR-α 31
1.4.7 Species differences in response to peroxisome proliferators 31
1.5 XENOBIOTIC METABOLISM IN AUSTRALIAN MARSUPIALS 34
1.6 PROJECT AIMS 37

2 MATERIALS AND METHODS **38**
2.1 CHEMICALS AND KITS 38
2.2 EQUIPMENT 41
2.3 CONTROL AND TERPENE-TREATED POSSUM TISSUES 43
2.4 MARSUPIAL AND RAT TISSUES 43
2.5 HUMAN TISSUE AND SAMPLES 44
2.6 CENTRIFUGATION 44
2.7 BACTERIAL CELL CULTURE PREPARATION 45
2.8 ANTIBODIES 45
2.9 SUBCELLULAR HEPATIC FRACTION PREPARATION AND PROTEIN ASSAY 46
2.9.1 Microsomes and cytosol samples 46
2.9.2 Post-nuclear supernatants 46
2.9.3 Nuclear extracts 47
2.9.4 Determination of protein concentration 47
2.10 IMMUNOBLOT ANALYSIS 47
2.11 SPECTRAL DETERMINATION 48
2.11.1 Total cytochrome P450 content 48
2.11.2 Nicotinamide-adenine dinucleotide (NAD) and NADP (NAD phosphate) contents 48
2.12 ENZYME ACTIVITY ASSAYS 49
2.12.1 Lauric acid hydroxylation 49
2.12.2 Peroxisomal cyanide-insensitive fatty acid β-oxidation 49
2.12.3 Palmitoyl-CoA oxidase activity 49
2.13 GENERAL MOLECULAR CLONING METHOLOGY 49
2.13.1 Competent *E.coli* cell preparation 49
2.13.2 Ligation reactions 50
2.13.3 Transformation of DNA into competent cells 50
2.14 PLASMID DNA PREPARATION 51
2.14.1 Small scale purification of plasmid DNA 51
2.14.2 Large scale purification of plasmid DNA 52
2.14.3 Purification of plasmid DNA for transfection 52
2.15 DNA ANALYSIS 53

2.15.1 Restriction digest of DNA 53
2.15.2 Electrophoresis and visualisation of DNA 53
2.15.3 Extraction of DNA fragments from agarose gels 54
2.15.4 Quantification of DNA 54
2.16 DNA SEQUENCING 54
2.16.1 Sequencing primers 54
2.16.2 Sequencing reaction 55
2.16.3 DNA sequence analysis 55
2.17 cDNA PROBE PREPARATION AND LABELLING 56
2.18 SOUTHERN BLOT ANALYSIS OF GENOMIC DNA 56
2.18.1 Genomic DNA extraction 56
2.18.2 Electrophoresis of genomic DNA 57
2.18.3 Capillary transfer of genomic DNA to nylon membrane 57
2.18.4 Prehybridisation and hybridisation of membranes with α-^{32}P-labelled cDNA probe 58
2.19 RNA EXTRACTION AND PURIFICATION 58
2.19.1 Control of RNase activity 58
2.19.2 Total RNA extraction 59
2.19.3 Messenger RNA purification 59
2.19.4 Quantification of RNA and mRNA 60
2.20 NORTHERN BLOT ANALYSIS 60
2.20.1 Electrophoresis of RNA through denaturing formaldehyde agarose gels 60
2.20.2 Capillary transblotting 61
2.20.3 Prehybridisation and hybridisation of membranes with α-^{32}P-labelled cDNA probe 61
2.21 POLYMERASE CHAIN REACTION 61
2.21.1 First-strand cDNA synthesis 61
2.21.2 Reverse transcription-polymerase chain reaction (RT-PCR) 62
2.21.3 Rapid amplification of cDNA ends (RACE) 62
2.21.4 Expression of cloned cDNAs in Cos-7 cells 64

3 BRUSH TAIL POSSUM MODEL 65
3.1 INTRODUCTION 65
3.2 METHODS 68
3.2.1 Control and terpene-treated possum livers 68
3.2.2 Microsome, cytosol, post-nuclear supernatant, and nuclear extract preparations 68
3.2.3 Spectrophotometry measurement of hepatic nicotinamide co-factor contents 68
3.2.4 Lauric acid hydroxylase activity 70

3.2.5 Peroxisomal cyanide-insensitive fatty acid β-oxidation activity . . . 71
3.2.6 Statistical analysis . . . 72
3.2.7 Immunoblot analysis of CYP4A and PPAR-α in marsupial liver tissues . . . 72
3.2.8 Northern analysis . . . 73
3.3 RESULTS . . . 74
3.3.1 Lauric acid hydroxylase activity . . . 74
3.3.2 Peroxisomal cyanide-insensitive palmitoyl coenzyme A oxidation activity . . . 75
3.3.3 Pyridine nucleotide NAD, NADH, NADP and NADPH content measurement . . . 76
3.3.4 Immunoblot analysis . . . 77
3.3.5 Northern blot analysis . . . 79
3.4 DISCUSSION . . . 83

4 KOALA LIVER CYTOCHROME P450 4A15 (CYP4A15) 87
4.1 INTRODUCTION . . . 87
4.2 METHODS . . . 95
4.2.1 Cloning of koala liver *CYP4A15* cDNA . . . 95
4.2.2 Amplification of rat *CYP4A1* complete cDNA: . . . 99
4.2.3 Expression of koala liver CYP4A15 and rat CYP4A1 in Cos-7 cells . . . 99
4.2.4 Immunoblot analysis of cDNA-expressed koala and rat CYP4A enzymes and hepatic microsomes . . . 101
4.2.5 Determination of total P450 content from cDNA-expressed koala and rat CYP4A enzymes in Cos-7 cell lysates . . . 101
4.2.6 Lauric acid hydroxylase activity of cDNA-expressed koala and rat CYP4A proteins . . . 101
4.2.7 Microsomal preparations and protein assay . . . 101
4.2.8 Analysis of CYP4A mRNA by Northern blotting . . . 101
4.2.9 Analysis of the *CYP4A* gene by Southern blotting . . . 102
4.2.10 Comparative modelling and CYP4A15 3-D structure prediction 102
4.3 RESULTS . . . 104
4.3.1 Cloning and sequencing of koala hepatic *CYP4A15* cDNA . . 104
4.3.2 Expression of CYP4A protein in Cos-7 cells and immunoblot analysis of cDNA-expressed CYP4A proteins . . . 109
4.3.3 Determination of total CYP content from CYP4A protein expressed in Cos-7 cells . . . 110
4.3.4 Determination of lauric acid hydroxylase activity of cDNA-expressed koala CYP4A15 protein . . . 112
4.3.5 Northern blot analysis of CYP4A mRNA in koala liver and other hepatic tissues . . . 112
4.3.6 Southern blot analysis of *CYP4A* genes in koala liver and other hepatic tissues . . . 113

4.3.7 Comparative modelling of the koala CYP4A15 115
4.4 DISCUSSION 117

5 KOALA LIVER FATTY ACYL-COA OXIDASE 127
5.1 INTRODUCTION 127
5.2 METHODS 130
5.2.1 Isolation of koala liver fatty acyl CoA oxidase cDNAs by RT-PCR approaches 130
5.2.2 Isolation of rat full-length *AOX* cDNAs 133
5.2.3 Expression of koala and rat *AOX* cDNAs in Cos-7 cells 134
5.2.4 Preparation of liver homogenates 134
5.2.5 Determination of palmitoyl-CoA oxidase (AOX) activity 134
5.2.6 Northern analysis of hepatic acyl CoA oxidase mRNA 136
5.2.7 Southern analysis of hepatic genomic DNA 137
5.3 RESULTS 138
5.3.1 Cloning of koala liver acyl CoA oxidase cDNAs 138
5.3.2 Determination of palmitoyl-CoA oxidase (AOX) activity in koala liver homogenates 142
5.3.3 Expression of koala *AOXI* and *AOXII* in Cos-7 cells and determination of palmitoyl-CoA oxidase (AOX) activity 145
5.3.4 Northern analysis of acyl CoA oxidase mRNA 151
5.3.5 Southern analysis of the *AOX* gene 151
5.4 DISCUSSION 154

6 KOALA LIVER PPAR-α 157
6.1 INTRODUCTION 157
6.2 METHODS 160
6.2.1 Isolation of koala liver peroxisome proliferator activated receptor-alpha *PPAR-α* cDNA by RT-PCR approaches 160
6.2.2 Expression of koala liver *PPAR-α* cDNA in Cos-7 cells 163
6.2.3 Preparation of liver cytosol and nuclear extracts 163
6.2.4 Immunoblot analysis 163
6.2.5 Analysis of PPAR-α mRNA 163
6.2.6 Southern analysis of hepatic genomic DNA 164
6.3 RESULTS 165
6.3.1 Cloning of koala liver *PPAR-α* cDNA 165
6.3.2 Expression of koala and rat PPAR-α in Cos-7 cells and immunoblot analysis of cDNA-expressed PPAR-α 173
6.3.3 Immunoblot analysis of PPAR-α in cytosol and nuclear extracts 173
6.3.4 Northern analysis of PPAR-α mRNA 173
6.3.5 Southern analysis of the *PPAR-α* gene 175
6.4 DISCUSSION 178

7 VISUALISATION OF PEROXISOMES IN KOALA LIVER 182
7.1 INTRODUCTION 182
7.1.1 Historical background 182
7.1.2 Morphological characteristics 183
7.1.3 Biochemical characteristics 183
7.1.4 Function of peroxisomes 184
7.2 METHODOLOGY OUTLINE 185
7.2.1 Visualisation of peroxisomes by cytochemical localisation of catalase 185
7.2.2 Specimen preparation 185
7.2.3 Fixation and DAB staining 186
7.2.4 Dehydration 186
7.2.5 Infiltration and embedding 187
7.2.6 Sectioning 187
7.3 RESULTS 188
7.3.1 Visuálisation of peroxisomes in the koala livers 188
7.3.2 Quantification of peroxisomes 197
7.4 DISCUSSION 198

8 GENERAL DISCUSSION 200

A Restriction maps. 206
A.1 The restriction map of the koala *CYP4A15* 206
A.2 The restriction maps of the koala *AOX I* and *AOX II* 207
A.3 The restriction map of the koala *PPAR-α* 208

B Deduced amino acid sequence alignment. 209
B.1 Alignment of the deduced amino acid sequences of the koala CYP4A15 with other CYP4A proteins 209
B.2 Alignment of the deduced amino acid sequences of the koala AOX I and AOX II with other AOX proteins 209

C Transmission electron microscopy. 214

Bibliography 216

List of Figures

1.1 An overview of lipid metabolism depicting the functions of CYP4A and peroxisomal β-oxidation enzymes and the regulatory role of PPAR-α in controlling expression of these lipid-metabolising enzymes. 3

1.2 A schematic representation of the many roles of cytochrome P450 and the role of the CYP4A subfamily in fatty acid metabolism. 6

1.3 A schematic diagram of the catalytic cycle of the cytochrome P450 enzyme system. 9

1.4 The structural core of P450s. 10

1.5 A schematic representation of the role of CYP4A in lipid homeostasis. 13

1.6 A schematic representation of the formation of 20-HETE by CYP4A enzymes and the role of cytochrome P450 enzymes in the oxidative metabolism of arachidonic acid. 14

1.7 A schematic diagram depicting the peroxisomal β-oxidation system. . 17

1.8 Acyl CoA oxidases in rat and human livers and their substrate specificities. 20

1.9 Schematic representation of the structure of the fatty *acyl CoA oxidase* gene and the process of proteolytic cleavage of component A into components B and C. 22

1.10 Schematic representation of PPAR-α, coactivator complexes, and basal transcriptional element interaction, leading to increased transcription of target genes. 30

1.11 A schematic representation of the regulatory role of PPAR-α and cross-talk among peroxisomal, microsomal, and mitochondrial fatty acid oxidation systems. 32

3.1 The conversion of NAD and NADP into their reduced forms. 69

3.2 The chemical structure of lauric acid and positions of hydroxylation. . 71

3.3 Immunoblot analysis of CYP4A in microsomes from control and terpene-treated possum, rat, human and koala livers, using anti-rat CYP4A antibody. 77
3.4 Immunoblot analysis of PPRA-α in nuclear (A) and cytosolic (B) extracts from control and terpene-treated possum and rat livers, using anti-human PPRA-α polyclonal antibody. 78
3.5 Representative ethidium bromide stained gel of mRNA from control and terpene-treated possum, human, rat and koala livers. 79
3.6 Northern analysis of mRNA from control and terpene-treated possum, human, rat and koala livers, using a koala *CYP4A15* cDNA probe. . 80
3.7 Northern analysis of mRNA from control and terpene-treated possum, human, rat and koala livers, using a koala *AOX* cDNA probe. 81
3.8 Northern blot analysis of mRNA from control and terpene-treated possum, human, rat and koala livers, using a koala *PPAR-α* cDNA probe. 82

4.1 Homology model of CYP4A11. 90
4.2 Diagram of binding site of the heme to the CYP apoprotein and the mechanism for the formation of the ester bond between the heme and the protein 91
4.3 An overview of the process of comparative modelling of P450. 93
4.4 Circular map of pGEM-T vector and its multiple cloning sites. 97
4.5 Schematic diagram of the cloning strategy for koala *CYP4A15* cDNAs. 98
4.6 Circle map of pCMV-Script vector and its features. 100
4.7 Agarose gel analysis of PCR products generated from koala liver 5'RACE-ready cDNA using UPM and K4A5'r primers. 104
4.8 Agarose gel analysis of PCR products generated from koala first-strand cDNA 106
4.9 Agarose gel analysis of PCR products generated from koala first-strand cDNA (Large-scale PCR amplification). 106
4.10 cDNA and deduced amino acid sequence of CYP4A15 from koala liver. 107
4.11 Immunoblot analysis of cDNA-expressed koala and rat CYP4A. . . . 110
4.12 Immunoblot analysis of CYP4A proteins in koala liver microsomes as compared to human, rat, and wallaby. 111
4.13 Northern blot of hepatic CYP4A mRNA. 114
4.14 Southern blot analysis of the *CYP4A* gene. 116
4.15 A homology model of CYP4A15 and its substrate recognition regions. 119

4.16 A homology model of CYP4A15 showing the position of the two extra amino acid residues versus the substrate recognition site (SRS) regions. 120
4.17 The NH2-terminal amino acid sequence comparison between the koala CYP4A and CYP4A subfamilies from other species. 121

5.1 Schematic diagram of the cloning strategy for koala *AOX* cDNAs. . . 131
5.2 Circle map of pCI-neo vector and its features. 135
5.3 Agarose gel analysis of PCR product generated from koala liver cDNA using kAOXf2 and kAOXr2 primers. 139
5.4 Agarose gel analysis of PCR products generated from koala liver cDNA template using kAOX'3f and kAOX'3r primers at different annealing temperatures. 140
5.5 Agarose gel analysis of PCR products generated from koala liver 5' RACE-ready cDNA template using UPM and kAOX5'r primers. . . . 141
5.6 Agarose gel analysis of PCR products generated from koala 5'RACE-ready cDNA template using forward kAOXf and reverse kAOXr primers143
5.7 Agarose gel analysis of PCR products generated from koala liver cDNA template, using forward kAOXf and reverse kAOXr primers. 144
5.8 Nucleotide and deduced amino acid sequences of the fatty acyl-CoA oxidase (*AOX*) type I full-length cDNA isolated from koala liver. . . 147
5.9 Koala liver *AOX I* and *AOX II* cDNA and deduced amino acid sequences in the coding region located between nucleotides 269-429 (exon 3), where sequence differences were identified. 149
5.10 Northern blot analysis of hepatic AOX mRNA. 152
5.11 Southern blot analysis of the *AOX* gene. 153

6.1 A schematic diagram depicting the nuclear receptor PPAR-α structure. 158
6.2 Schematic diagram of the cloning strategy to obtain a full–length *PPAR-α* cDNA from koala liver. 161
6.3 Agarose gel analysis of PCR products amplified by KGPf and KGPr primers using koala liver cDNA template. 166
6.4 Agarose gel analysis of PCR products amplified by KGPf and KGPr primers from koala liver cDNA template with Q solution. 167
6.5 Agarose gel analysis of PCR products amplified from koala liver 5'RACE-ready cDNA using UPM and kPP5' primers. 169
6.6 Agarose gel analysis of PCR products amplified from koala liver cDNA using kPPfF and kPPfR primers. 170

6.7 Nucleotide and deduced amino acid sequences of the full-length koala *PPAR-α* cDNA isolated from liver. 171
6.8 Immunoblot analysis of cDNA-expressed koala and rat PPAR-α using sheep anti-human PPAR-α polyclonal antibody. 174
6.9 Immunoblot analysis of PPAR-α proteins in nuclear and cytosolic extracts utilising sheep anti-human PPAR-α polyclonal antibody. 175
6.10 Northern blot analysis of hepatic PPAR-α mRNAs. 176
6.11 Southern blot analysis of the PPAR-α gene. 177
6.12 Multiple sequence alignment of PPAR-α proteins from koala, human, rat and mouse. 181

7.1 The catalase reaction for visualisation of peroxisomes using DAB reagent. 185
7.2 DAB cytochemical visualisation of peroxisomes in koala liver by transmission electron microscopy. 190
7.3 DAB cytochemical visualisation of peroxisomes in koala liver by transmission electron microscopy showing a dark particle within the hepatocyte. 192
7.4 DAB cytochemical visualisation of peroxisomes in rat liver by transmission electron microscopy. 194
7.5 DAB cytochemical visualisation of peroxisomes in bandicoot liver by transmission electron microscopy. 196

A.1 The restriction map of the koala CYP4A15. 206
A.2 The restriction maps of the koala *AOX I* and *AOX* II. 207
A.3 The restriction map of the koala *PPAR-α*. 208

B.1 Alignment of the deduced amino acid sequence of the koala *CYPA415* clone with other CYP4A proteins. 210
B.2 Alignment of the deduced amino acid sequences of the koala *AOX I* and *AOX II* clones with other AOX proteins. 212

List of Tables

1.1 Substrates of peroxisomal β-oxidation. 18
1.2 Examples of natural and synthetic ligands of PPAR-α. 25
1.3 Overview of the main biological effects induced by peroxisome proliferators on peroxisomes, microsomes, mitochondria and other cellular components. 27

2.1 List of chemicals and kits required for experimental procedures. . . . 38
2.2 List of equipment used in experimental procedures. 41
2.3 Clinical data of human liver donors. 45
2.4 Routinely used antibiotics and their concentrations. 46
2.5 List of sequencing primers 55
2.6 Details of RACE Universal Primer Mix (UPM) 63

3.1 Lauric acid hydroxylase activities for control and terpene-treated possum, koala and rat livers. 74
3.2 Peroxisomal cyanide-insensitive palmitoyl coenzyme A oxidation activities for control and terpene-treated possum and rat livers. 75
3.3 Pyridine nucleotide concentrations for control and treated possum and rat liver homogenates. 76

4.1 List of CYP4A isoforms from nine different species and their tissue distribution. 88
4.2 Omega- and (omega-1)-hydroxylase activity of rat CYP4A1. 89
4.3 Details of oligonucleotide primers used for isolation of full-length koala and rat *CYP4A1* and *CYP4A15* cDNAs. 96
4.4 Total P450 content determined in Cos-7 cells transfected with koala and rat *CYP4A* cDNA and in koala and rat microsomes. 111
4.5 Lauric acid hydroxylase activity catalysed by cDNA-expressed koala and rat CYP4A proteins and in koala and rat microsomes. 113

4.6 Nucleotide and amino acid sequence identities between koala liver CYP4A15 and CYP4A subfamily members from other species. 122

5.1 Details of oligonucleotide primers used for isolation of full-length koala and rat *acyl CoA oxidase* cDNAs 132
5.2 Nucleotide and deduced amino acid sequence identities between the koala *AOX I* and *AOX II* cDNAs and *AOX* cDNAs from other species. 146
5.3 Total palmitoyl-CoA and acyl-CoA oxidase-dependent palmitoyl-CoA oxidase activities determined in koala and rat liver homogenates. . . . 150
5.4 Palmitoyl-CoA activity catalysed by cDNA-expressed koala and rat AOX enzymes. 150

6.1 Details of oligonucleotide primers for PCR amplification of koala *PPAR-α* cDNA. 162
6.2 Nucleotide and amino acid sequence identities between the koala liver kPPAR-α and PPAR-α from other species. 179

7.1 Quantification and measurement of peroxisomes in koala, rat and bandicoot livers. 197

List of Abbreviations

A	Adenine
aa	Amino acid
ACS	Aqueous Counting Scintillant
AOX	Acyl Coenzyme A oxidase
APS	Ammonium persulphate
β-NADP	β-Nicotinamide adenine dinucleotide phosphate
bp	Base pairs
BSA	Bovine serum albumin
C	Cytosine
cDNA	Complementary deoxyribonucleic acid
CoA	Coenzyme A
CYP450s	Cytochrome P450 enzymes
dATP	Deoxyadenosine triphosphate
Da	Dalton
D-BFE	D-bifunctional enzymes
DEPC	Diethyl pyrocarbonate
DMF	Dimethylformamide
DNA	Deoxyribonucleic acid
dNTP	Deoxyribonucleotide triphosphate
E.coli	*Escherichia coli*
EDTA	Ethylene diaminotetraacetate
EtBr	Ethidium Bromide
FMOs	Flavin-containing mono-oxygenases
G	Guanosine
g	gram
HRP	Horseradish peroxidase
HA	Homovanillic acid
IMVS	Institute of Medical and Veterinary Science
IPTG	Isopropyl-β-D-thiogalactopyranoside
kb	Kilobase pairs
kDa	Kilo Daltons
LA	Lauric acid
LB	Luria broth

L-BFE	L-bifunctional enzymes
min	Minutes
mRNA	Messenger ribonucleic acid
M	Molar
MCS	Multiple cloning sites
mg	Milligrams
ml	Millilitres
mM	Millimolar
μM	Micromolar
μl	Microlitre
μg	Microgram
MOPS	3-N-Morpholinopropane-sulphonic acid
NADPH	Nicotinamide adenine dinucleotide phosphate (reduced form)
NEM	N-Ethylmaleimide
ng	Nanograms
nm	Nanometres
PAGE	Polyacrylamide gel electrophoresis
PCR	Polymerase chain reaction
POD	Peroxidase
PP	Peroxisome proliferators
PPAR-α	Peroxisome proliferator activated receptor alpha
RNA	Ribonucleic acid
RNase	Ribonuclease
rpm	Revolutions per minute
RT-PCR	Reverse transcription-polymerase chain reaction
SDS	Sodium dodecyl sulphate
SSC (10X)	1.5M NaCl,150mM $Na_3C_6H_5O_7.2H_2O$
T	Thymidine
TAE	40mM Tris-acetate, 1mM EDTA (pH 8.0)
TBS	16mM Tris-acetate, 500mM sodium chloride
TLC	Thin layer chromatography
TTBS	0.05% v/v Tween-20 in TBS
U	Units of enzyme activity
UV	Ultraviolet
V	Volts

VLCFA	Very long chain fatty acid
v/v	Volume per volume
w/v	Weight per volume
X-gal	5-bromo-4-chloro-3-indole-β-D-galactoside
x g	Number of times unit gravitational force

Single and Three Amino Acid Abbreviations

Alanine	Ala	A
Arginine	Arg	R
Asparagine	Asn	N
Aspartic acid	Asp	D
Asparagine or Aspartic acid	Asx	B
Cysteine	Cys	C
Glutamic acid	Glu	E
Glutamine	Gln	Q
Glycine	Gly	G
Glutamine or Glutamic acid	Glx	Z
Histidine	His	H
Isoleucine	Ile	I
Leucine	Leu	L
Lysine	Lys	K
Methionine	Met	M
Phenylalanine	Phe	F
Proline	Pro	P
Serine	Ser	S
Threonine	Thr	T
Tryptophan	Trp	W
Tyrosine	Tyr	Y
Unassigned amino acid	X	X
Valine	Val	V

Summary

The Australian marsupial *Phascolarctos cinereus* has a unique diet, which consists exclusively of *Eucalyptus* leaves containing a high proportion of essential oils. In order to ingest and absorb such large quantities of monoterpenes, i.e. major constituents of essential oils, the koala must have developed highly specialised detoxification mechanisms involving a number of liver enzyme systems. Exposure to *Eucalyptus* terpenes has been reported to induce several rat cytochrome P450s and other xenobiotic metabolising enzymes including peroxisomal fatty acid β-oxidation enzymes. While higher CYP4A activity and cytochrome P450 content was observed in the koala liver than in rat or human livers, total peroxisomal β-oxidation activity was absent in the koala liver.

Peroxisomal fatty acid β-oxidation and microsomal ω-hydroxylation play an essential role in controlling lipid metabolism in the liver. Peroxisomal β-oxidation is responsible for chain shortening of fatty acids, while microsomal ω-hydroxylation, catalysed by CYP4A enzymes, represents a major pathway for the oxidative metabolism of branched-chain or substituted fatty acids. The peroxisome proliferator activated receptor-alpha (PPAR-α) has been shown to mediate the expression of CYP4A and peroxisomal fatty acid β-oxidation enzymes in most species studied. Many endogenous substrates and xenobiotics have been identified to be potent activators of PPAR-α, including peroxisome proliferators, fatty acids, and monoterpenes. Little data on CYP4A and peroxisomal β-oxidation enzymes has been obtained from the koala or any other marsupials, especially at the molecular level. To date, no biochemical or molecular studies have been conducted to examine PPAR-α in any marsupial species.

This project aimed to clone and complete the biochemical and molecular characterisation of CYP4A, the first and rate-limiting enzyme of the peroxisomal β-oxidation system, acyl CoA oxidase (AOX), and PPAR-α in the koala liver. The present project also examined the effects of *Eucalyptus* monoterpenes on the expression of these enzymes and the receptor PPAR-α.

The effects of *Eucalyptus* monoterpenes on the expression of liver CYP4A, acyl CoA oxidase, and the nuclear receptor PPAR-α were examined using a possum model. While the koala eats only *Eucalyptus* leaves, the brush tail possum is not an obligate eucalypt feeder. The control group (4 possums) was given an artificial diet of

fruit and cereal for ten days. The terpene-treated group (4 possums) was given the same artificial diet for the same number of days. In this diet, however, a mixture of monoterpenes including 1,8-cineole, α-pinene, *d*-limonene and *p*-cymene was added. In the livers of the terpene-treated group, peroxisomal cyanide-insensitive palmitoyl coenzyme A oxidative activity was significantly higher than is seen in the livers of the control group. No significant differences were observed for liver microsomal lauric acid hydroxylase activity between the control and the treated groups. Northern blot analysis, using the corresponding koala cDNA probes, revealed a higher acyl CoA oxidase (AOX) mRNA level in the livers of terpene-fed possums relative to that in livers of control possums. There was no detectable difference in CYP4A mRNA level in the livers between the two groups. The data demonstrated that *Eucalyptus* terpenes act as peroxisome proliferators to cause increased expression of liver AOX, without significant changes in expression of liver CYP4A and PPAR-α.

A 1544-bp koala liver *CYP4A* near full-length cDNA was isolated by reverse transcription - polymerase chain reaction (RT-PCR). The cDNA, designated *CYP4A15*, shares 69% nucleotide and 65% deduced amino acid sequence identity with human CYP4A11 and encodes a protein of 500 amino acids. Transfection of the koala *CYP4A15* cDNA into Cos-7 cells resulted in the expression of a protein that was recognised by a sheep anti-rat CYP4A polyclonal antibody. cDNA-expressed koala CYP4A15 exhibited lauric acid hydroxylase activity (nmole/mg protein/minute) comparable to that of cDNA-expressed rat CYP4A1. Higher levels of both liver CYP4A protein and mRNA were observed for the koala liver, as compared to those observed for non-*Eucalyptus* feeders such as humans, rat and other marsupials. Southern analysis of genomic DNA suggests the existence of a single *CYP4A* gene in all species studied. This study generated the first data confirming the presence of a functional *CYP4A15* gene in koala liver and suggests that higher lauric acid hydroxylation activity and CYP content in koala liver is due to increased expression of CYP4A.

Two 2039-bp koala liver *AOX* full-length cDNAs, designated *AOX I* and *AOX II*, were cloned by RT-PCR approaches and differed only in a small coding region of amino acid residues 89 to 130. The *AOX* cDNAs encoded proteins of 662 amino acids. Palmitoyl-CoA oxidase activity was detected for AOX I and AOX II cDNA-expressed enzymes with the apparent Km values of 28μM and 38μM, respectively. These values are within the order of magnitude reported for purified rat and human AOX enzymes. Northern analysis, utilising the koala *AOX I* cDNA as probe, de-

tected a more intense liver AOX mRNA band in the koala as compared to that in rat and humans. Southern blot analysis of genomic DNA samples suggests the existence of a single *AOX* gene in all species studied. This study generated the first molecular data confirming the presence of two functional AOX isoforms in the koala liver. The results also suggested that the absence of total liver peroxisomal β-oxidation activity in the koala is possibly due to deficiencies of one or more enzymes downstream of acyl-CoA oxidase and/or deficiencies of mitochondrial β-oxidation enzymes.

A koala liver *PPAR-*α full-length cDNA of size 1515-bp was cloned by RT-PCR and encodes a protein of 469 amino acids. cDNA-expressed koala *PPAR-*α was recognised by a rabbit anti-human PPAR-α polyclonal antibody. Immunoblot analysis revealed the expression of PPAR-α protein in both cytosolic and nuclear extracts of the koala liver. Northern analysis, utilising the koala *PPAR-*α cDNA as probe, detected a band corresponding to mRNA species of size approximately 7-kb in the koala liver. Southern blot analysis of genomic DNA suggests the existence of a single *PPAR-*α gene in all species studied. This study generated the first molecular data confirming that *PPAR-*α gene encodes the coding region of PPAR-α in koala liver.

Morphology examination of peroxisomes in the koala liver by light and electron microscopy indicated relatively more peroxisomes in koala liver than in non-*Eucalyptus* feeders such as bandicoot and rat.

Collectively, this project provided the primary molecular data confirming the presence of functional *CYP4A15*, *AOXI*, *AOXII*, and *PPAR-*α genes in koala liver. It appears that koala is a responsive species to peroxisome proliferators such as *Eucalyptus* monoterpenes.

Declaration

"I certify that this thesis contains no material that has been accepted for the award of any other degree or diploma in any other University; and to the best of my knowledge, this thesis contains no material that has been published or written by any other person, except where due reference is stated."

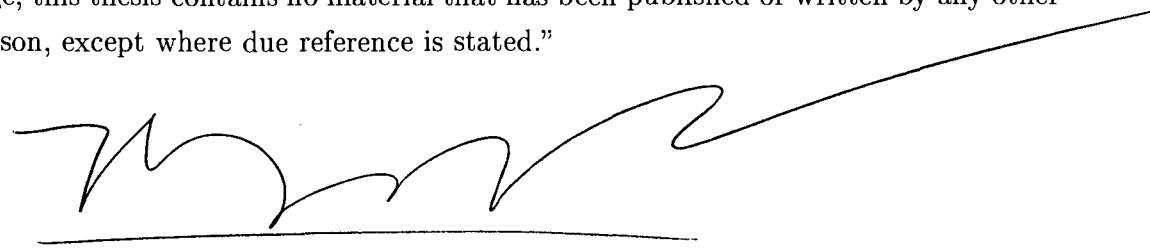

Suong Ngoc Thi Ngo

Acknowledgements

I wish to express my sincere gratitude to my principal supervisor Assoc. Prof. Ieva Stupans. Her guidance, encouragement and unlimited support throughout my candidature are very much appreciated.

Special thanks are due to my supervisor, Assoc. Prof. Ross Allan McKinnon, for his molecular biology expertise, great support and valued input into my research study, especially into the preparation of this thesis. His time and valued input into the preparation of the papers published in this project, his helpful guidance, inspiration and devoted supervisions are very much appreciated and will always be remembered.

I wish to thank Prof. Allan Evans for his expert advice on statistical data analysis. I would like to thank Mr. Andrew Beck for excellent technical assistance in electron microscopy, and to Assoc. Prof. Anthony Woods for his expert advice on this work.

I wish to thank all members of the School of Pharmaceutical, Molecular and Biomedical Sciences, University of South Australia, in particular Prof. Lloyd Sansom and Prof. Mary Barton, for creating a friendly and supportive environment for research, teaching, and social activities.

To my colleagues Brett Jones, John Skull, Mark Woolley, Sandra Kong, Tracy Delozier, Natalie Milic, Wei Ping and Shwu Fen Loh, their friendship, support and encouragement are very much appreciated.

I wish to thank Assoc. Prof. David Nelson, University of Tennessee (Memphis, TN, USA) for naming of the koala liver cytochrome P450 CYP4A15 cDNA, and to the GenBank submissions staff (Bethesda, Maryland, USA) for assigning the accession numbers for the isolated koala liver CYP4A15, AOXs and PPAR-α cDNAs.

I also wish to thank Assoc. Prof. Stuart McLean and Dr. Georgia Pass, University of Tasmania (Australia) for supplying the Terpene-treated and control possum liver tissues used in this project, and to Mr. Chris Leigh, Department of Anatomical Sciences, School of Medicine, Adelaide University, for his enormous effort in supplying the marsupial tissues.

Others to whom I am very grateful include Dr. Martin Lewis for his kind friendship and technical advice, Mr. Daniel Kissell for devoted and excellent computer assistance, Ms. Ceilidh Marchant, Ms. Amra Kirlich, Ms. Tamara Height, Mr. Richard Bennett, Ms. Karen O'Callaghan and Mr. Fred Stace for their technical, mechanical and ordering assistance.

I would like to thank the Australian Commonwealth for financial assistance in the form of an Australian Postgraduate Award.

Especially, my deepest gratitude to my husband Tan and my dearest daughter Amanda for their endless love, unlimited support, understanding, and encouragement throughout my study; finally, I owe my most heartfelt gratefulness to my family, especially my father and my mother, my sisters and brothers, for their long-distance caring and loving.

This thesis is dedicated to my husband & my daughter, Tan & Amanda; my father & my mother.

Publications in Support of Thesis

Publications in GenBank:

Ngo SNT, McKinnon RA, and Stupans I. (2001). Koala liver acyl-CoA oxidase type 1 (AOXI) full-length cDNA. GenBank, *ncbi.nlm.nih.gov*, Accession number AF463453.

Ngo SNT, McKinnon RA, and Stupans I. (2001). Koala liver acyl-CoA oxidase type 2 (AOXII) full-length cDNA. GenBank, *ncbi.nlm.nih.gov*, Accession number AF463454.

Ngo SNT, McKinnon RA, and Stupans I. (2001). Koala liver peroxisome proliferator activated receptor-alpha (PPAR-α) full-length cDNA. GenBank, *ncbi.nlm.nih.gov*, Accession number AF463455.

Ngo SNT, McKinnon RA, and Stupans I. (2001). Koala Liver cytochrome P450 CYP4A15 complete cDNA without the coding region for the last 10 amino acids before the stop codon. GenBank, *ncbi.nlm.nih.gov*, Accession number AF463456.

Published Manuscripts:

Ngo SNT, McKinnon RA, and Stupans I. (2003) The effects of *eucalyptus* terpenes on microsomal cytochrome P450 CYP4A, peroxisomal acyl CoA oxidase (AOX) and peroxisome proliferator activated receptor-alpha (PPAR-α) in the common brush tail possum liver, *Trichosurus vulpecula. Comparative Biochemistry and Physiology*, **136** (2C), 165-173.

Ngo SNT, McKinnon RA, and Stupans I. Cloning and expression of koala liver cytochrome P450 CYP4A15 (*Phascolarctos cinereus*) (Submitted to *Xenobiotica*).

Ngo SNT, McKinnon RA, and Stupans I. (2003) Identification and cloning of two forms of liver peroxisomal fatty acyl CoA oxidase from the koala (*Phascolarctos cinereus*). *Gene*, **309**, 91-99.

Ngo SNT, McKinnon RA, and Stupans I. Identification and cloning of koala liver peroxisome proliferator activated receptor-alpha (PPAR-α) (To be submitted to *Bio-*

chemical Pharmacology).

Ngo SNT, McKinnon RA, and Stupans I. Histological examination of peroxisomes in the koala liver by light and electron microscopy (In preparation).

Published Abstracts:

Ngo SNT, McKinnon RA, and Stupans I.(1999) Characterisation of CYP4A in the koala (*Phascolarctos cinereus*). *Proc. Aust. Soc. Clin. Exp. Pharmacol. Toxicol.* **6**:134.

Ngo SNT, McKinnon RA, Pass GJ and Stupans I. (2002) Induction of CYP4A, acyl CoA oxidase (AOX) and peroxisome proliferator activated receptor-alpha (PPAR-α) in brush tail possums (*Trichosurus vulpecula*) by *eucalyptus* terpenes. *IUPHAR XIVth World Congress of Pharmacology* **44**:176.

Ngo SNT, McKinnon RA, and Stupans I (2002) Cloning and expression of CYP4A15 in koala liver (*Phascolarctos cinereus*). *14th International Symposium on Microsomes and Drug Oxidations (MDO 2002)* **44** :157.

Ngo SNT, McKinnon RA, and Stupans I (2002) Identification and cloning of two forms of liver peroxisomal fatty acyl CoA oxidase from the koala (*Phascolarctos cinereus*) th *Australasian Pharmaceutical Society Association 2002 (APSA 2002)* Proceedings, 116.

Chapter 1

GENERAL INTRODUCTION

Like humans and other mammals, Australian marsupials are constantly exposed to a diverse array of exogenous compounds that are collectively termed xenobiotics. These xenobiotics come from a wide variety of sources including natural toxins in the diet, industrial and agricultural contaminants, and other environmental exposures. To facilitate the removal of xenobiotics from the body, highly complex detoxification mechanisms involving a number of enzyme systems have evolved. Such enzymatic mechanisms prevent xenobiotics from remaining in the body and exerting prolonged activity and toxicity. Knowledge of these enzymatic processes is vital in understanding the consequences of exposure to environmental chemicals.

Marsupials differ greatly from eutherian (placental) mammals in many aspects of their development and physical characteristics. These differences may alter their ability to tolerate environmental chemical exposure. Relative to eutherian animals, marsupials have a significantly shorter gestation period, often within a single oestrus cycle, resulting in limited intrauterine organogenesis. This leads to a very small, extremely undeveloped neonate in whom all the organs are defined but few are functional [1, 2]. With respect to most of their organs and systems, marsupial neonates appear not to reach the same stage of functional development as a neonatal eutherian until several months after birth. The majority of the marsupial neonatal growth phase happens in an air breathing environment. Marsupial neonates are therefore exposed to xenobiotics at a very early stage when they have few mature organs [1]. As a result, marsupial neonates are more vulnerable than neonatal eutherians to environmental chemical exposure. Since marsupial neonates are potentially exposed to environmental chemicals earlier in life and are lacking the maternal detoxification system, it is postulated that the detoxifying enzyme system of marsupials may have evolved differ-

ently from that of placental mammals. Little is known about the extent of chemical exposure encountered by Australian marsupials and their ability to metabolise and detoxicate these chemicals. Further research into xenobiotic metabolism of Australian marsupials is therefore prudent.

While most animals tend to select food low in potentially toxic chemicals, several marsupials rely on *Eucalyptus* leaves as a major or only food source (reviewed in [3]). These leaves contain a high proportion of toxic plant secondary metabolites, mostly phenolics and monoterpenes. *Eucalyptus* feeders include the koala (*Phascolarctos cinereus*), greater glider (*Petauroides volans*), ring tail possum (*Pseudocheirus peregrinus*) and brush tail possum (*Trichosurus vulpecula*). In order to ingest and absorb such large quantities of monoterpenes, specialist *Eucalyptus* feeders such as the koala must have evolved highly specialised detoxification mechanisms. These mechanisms presumably involve several liver enzyme systems including the cytochromes P450 [4]. Exposure to *Eucalyptus* monoterpenes has been reported to induce several rat liver cytochromes P450 and other metabolising enzymes including peroxisomal fatty acid β-oxidation enzymes [5, 6, 7] (reviewed in [3]). While higher CYP4A activity and cytochrome P450 content is observed in koala liver relative to rat or human livers, total peroxisomal fatty acid β-oxidation activity is absent in koala liver [8].

Peroxisomal fatty acid β-oxidation and microsomal ω-hydroxylation, catalysed by CYP4A enzymes, play an essential role in controlling lipid metabolism in the liver. Peroxisomal β-oxidation is responsible for chain shortening of fatty acids, while microsomal ω-hydroxylation represents a major pathway for the oxidative metabolism of branched-chain or substituted fatty acids. In humans, rat, and most species studied to date, the nuclear receptor, peroxisome proliferator activated receptor-alpha (PPAR-α), has been shown to control the expression of CYP4A and peroxisomal β-oxidation enzymes. Figure 1.1 shows an overview of the main enzyme systems responsible for oxidative metabolism of fatty acids and highlights the regulatory role of PPAR-α in controlling expression of these lipid-metabolising enzymes. Many endogenous substrates and xenobiotics have been identified as potent activators of PPAR-α, including peroxisome proliferators, fatty acids, and monoterpenes. In association with induction of CYP4A and peroxisomal β-oxidation enzymes, these structurally diverse compounds cause peroxisome proliferation.

To date, there is little data on CYP4A and peroxisomal β-oxidation enzymes of the

koala and other marsupials, especially at the molecular level. No biochemical or molecular studies examining PPAR-α have been carried out in the koala or any marsupials. The following sections provide a brief introduction to xenobiotic metabolism and focus on current reviews of cytochrome P450, fatty acid β-oxidation enzyme and PPAR-α. Current knowledge of xenobiotic metabolism in Australian marsupials is also discussed.

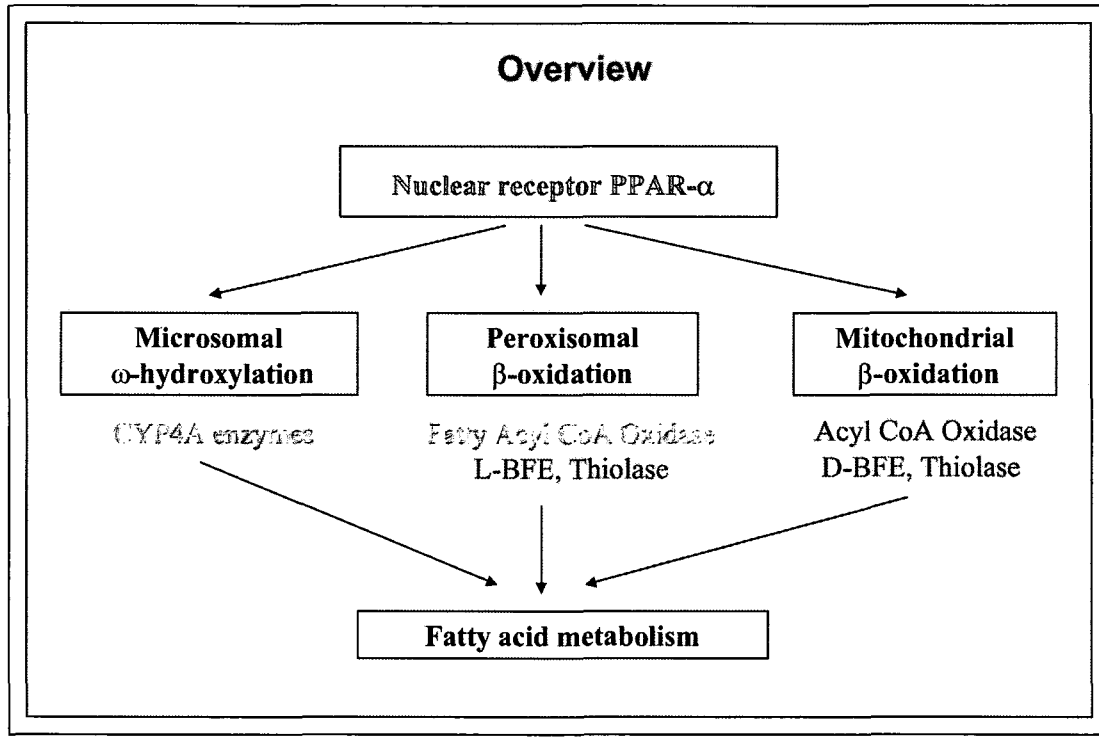

Figure 1.1: An overview of lipid metabolism depicting the functions of CYP4A and peroxisomal β-oxidation enzymes and the regulatory role of PPAR-α in controlling expression of these lipid-metabolising enzymes.
The three main lipid-metabolising enzyme systems include ω-hydroxylation, peroxisomal fatty acid β-oxidation and mitochondrial fatty acid β-oxidation. The enzymes highlighted in red are the marker enzymes of peroxisome proliferation as a result of exposure to PPAR-α activators. Fatty Acyl CoA Oxidase refers to the first and rate limiting enzyme Acyl CoA Oxidase of the L-hydroxy specific β-oxidation pathway (Section 1.3.5). D-BFE: D-bifunctional enzymes; L-BFE: L-bifunctional enzymes.

1.1 XENOBIOTIC METABOLISM

Xenobiotic metabolism refers to the biotransformation of chemicals which are foreign to the body. While the enzymes catalysing these processes are collectively termed xenobiotic-metabolising or drug-metabolising enzymes, many of these enzymes also participate in the metabolism of important endogenous compounds. The reactions involved in xenobiotic metabolism are generally classified into phase I (functionalisation) reactions and phase II (conjugative) reactions. While phase I reactions include oxidation, reduction, and hydrolysis, phase II reactions are mainly conjugation. Phase I metabolism introduces or unmasks a functional group in the parent compound to generate more polar metabolites. Phase I reactions are mainly catalysed by the cytochrome P450 system, although other enzymes including the flavin-containing mono-oxygenases (FMOs), aldehyde and alcohol dehydrogenases and xanthine oxidase are also involved. Phase I metabolism is also often a prerequisite for subsequent phase II metabolism. Phase II metabolism involves the coupling of a chemical (parent compound or metabolite) to a hydrophilic endogenous molecule to facilitate excretion. Phase II reactions are generally catalysed by several enzyme systems including the UDP-glucuronosyltransferases, sulphotransferases, N-acetyltransferases and glutathione transferases. While the major site of xenobiotic metabolism is the liver, xenobiotic-metabolising enzymes are also expressed in most other tissues.

1.2 CYTOCHROME P450

Cytochrome P450 is a generic term used to describe a family of hemoproteins which catalyse oxidative metabolism of a diverse range of endogenous substrates and xenobiotics [9]. Cytochrome P450 enzymes have been described in 136 prokaryote and eukaryote species, widely distributed in bacteria, fungi, plants and animals [10]. P450s generally fall into two major classes, depending on their location and the nature of the redox protein(s). Class I P450s, which are found on the eukaryotic mitochondrial membranes or in bacteria, are three-component systems made up of a flavin adenine dinucleotide (FAD)-containing reductase, an iron-sulfur protein (ferredoxin), and a P450. The bacterial P450cam from *Pseudomonas putida*, which was first characterised using x-ray crystallography, is an example of class I P450s [11]. Class II P450s, which are found in the endoplasmic reticulum of eukaryotes, are two-component systems comprising a diflavin reductase(FAD/flavin mononucleotide(FMN)-containing

NADPH-dependent cytochrome P450 reductase) and a P450 [12]. These are characterised by the liver microsomal P450s in mammalian cells. In addition to class I and class II, class III and class IV P450s have also been described. Class III P450s represent a fused system, made up of components of the eukaryotic class II enzyme in which the diflavin reductase is fused to the P450. An example of class III P450s is P450BM3, the bacterial soluble fatty acid ω-hydroxylase from *Bacillus megaterium* [13]. The bacterial P450RhF from *Rhodococcus sp.* represents class IV P450 comprising an FMN-containing reductase with a ferredoxin-like centre linked to a P450 in a single polypeptide [12].

The cytochromes P450 are encoded by a gene superfamily which currently comprises more than 2383 named P450 gene sequences [14]. The total number of different P450 families across species is 265 including 18 mammalian families and 43 mammalian subfamilies [15]. In any mammalian species, the estimated number of individual P450 genes is between 60 and 200 [16, 17]. The following sections focus on historical aspects of cytochrome P450 research and review current P450 understanding.

1.2.1 Historical aspects

Cytochrome P450 enzymes appear to be very ancient enzymes [18]. It is believed that about 400-500 million years ago, P450 enzymes evolved to enable animals to detoxify toxic chemicals [19]. Cytochrome P450 research holds a rich history based on the classic studies of the 1950s and 1960s. In 1951, the biochemical toxicology on the metabolism of a wide range of xenobiotics was established [20]. Studies of the pathways of cholesterol biotransformation to androgens, estrogens, mineralo- and gluco-corticoids were initiated in the same year [21]. The field of drug metabolism was initiated next [22], followed by the establishment of the principle of metabolic carcinogenesis, indicating the role of metabolic activation of procarcinogens [23]. Studies on the alternate pathways of lipid metabolism such as fatty acid ω-hydroxylation were then performed in 1964 [24]. Today, fatty acid ω-hydroxylation is known to be catalysed by the CYP4A subfamily (Section 1.2.6). A schematic representation of the many roles of cytochrome P450 is shown in Figure 1.2.

P450 enzymes were shown to catalyse the incorporation of molecular oxygen into organic molecules in 1955 [25, 26]. In 1958, a pigment exhibiting an unusual visi-

ble absorption at 450nm was observed in rat liver microsomes treated with sodium dithionite and carbon monoxide [27]. Subsequently, this pigment was identified as a hemoprotein and was termed cytochrome P450 [28, 29, 30]. The cytochrome P450 enzyme system was first identified as three components in 1968 [31]. These three components were then characterised as a hemoprotein (cytochrome P450), a flavoprotein termed NADPH-cytochrome P450 reductase, and a lipid termed phosphatidylcholine [32]. In mammals, while multiple cytochrome P450 enzymes have been isolated, only a single reductase has been described in mammalian P450s involved in xenobiotic metabolism. In plants and bacteria, multiple P450 reductases have been identified [33].

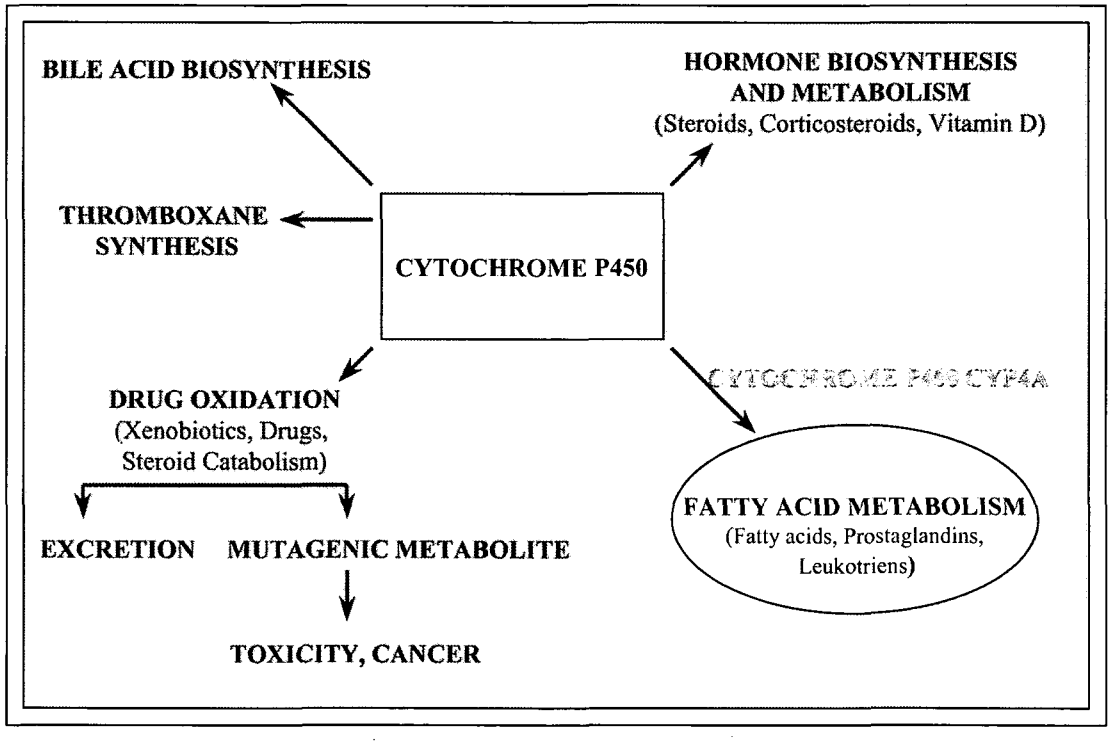

Figure 1.2: A schematic representation of the many roles of cytochrome P450 and the role of the CYP4A subfamily in fatty acid metabolism. (Reproduced from [34]).

1.2.2 Nomenclature of cytochrome P450

A uniform system of nomenclature for the cytochrome P450 gene superfamily is based on the extensive accumulation of protein sequence data derived from cDNA sequences.

In this system, the amino acid sequence identities and differences reflect evolutionary determinants of structure and function [35]. Recommendations for naming a P450 gene include the italicised root symbol *"CYP"* representing cytochrome P450 (capital letters are used for the mRNA, cDNA, and enzyme in most species, 'cyp' for mouse and Drosophila), an Arabic number designating the P450 family, a letter denoting the subfamily, and an Arabic number indicating the individual gene. The same numbers and non-italicised letters are used to designate the corresponding gene products. For example, the CYP4A15 enzyme is an individual member of the CYP4A subfamily that is in turn a member of CYP4 family. The gene responsible for the transcription of CYP4A15 mRNA that translates to the CYP4A15 protein is referred to as *CYP4A15*. While the protein sequences within a given CYP family have greater than 40% identity, mammalian sequences within the same subfamily always share greater than 55% identity [36]. The numbers of the individual genes are often assigned in the order in which the genes are identified (reviewed in [16]).

1.2.3 Catalytic cycle of cytochrome P450 enzymes

The cytochrome P450 enzyme system acts as an electron-transport group. In mammals, liver microsomal P450s are embedded tightly in the membranes of the endoplasmic reticulum. For these P450 enzymes, the membrane bound hemoprotein functions as the substrate and oxygen binding site, the NADPH-cytochrome P450 reductase is an electron carrier shuttling electrons one at a time from the reductase to the cytochrome P450. The phosphatidylcholine lipid facilitates the transfer of these electrons [37]. A schematic representation of the catalytic cycle of the cytochrome P450 enzyme system is shown in Figure 1.3. The insertion of cytochrome P450 enzymes into the membrane of the endoplasmic reticulum is highly specific. The heme containing portion of the enzyme is exposed to the cytosolic side of the membrane and orientated so that both lipophilic and hydrophilic substrates have access to the active site (reviewed in [18]).

1.2.4 Key structural features of cytochrome P450 enzymes

All cytochrome P450 enzymes appear to take on a similar structural fold within which a highly conserved structural core has been identified [38]. This was based on the comparison of the six crystallised bacterial P450s: $P450_{cam}$ (CYP101) [11], $P450_{BMP}$

(CYP102) [39], $P450_{terp}$ (CYP108) [40], $P450_{eryF}$ (CYP107A1) [41], $P450_{nor}$ (CYP55 A1) [42] and $P450_{sca}$ (CYP105A3) [43]. More recently, the crystallised structure of rabbit CYP2C5 has been resolved [44]. Cytochrome P450 enzymes are comprised of two main domains. One domain is predominantly α-helical, accounting for about 70% of the protein. The other is predominantly made up of β-sheets and accounts for approximately 22% of the protein [39, 40, 45, 46]. The heme and the oxygen binding sites of the cytochromes P450 are highly conserved. All cytochromes P450 possess similar requirements in performing their catalytic function [47]. The totally conserved cysteine residue functions as the fifth co-ordinating ligand bound to the heme prosthetic group. In mammalian P450s, this cysteine residue normally occurs around residues 450±15. Two other absolutely conserved residues are a glutamic acid and an arginine which are located in the K helix (described below) [39]. A highly conserved consensus F(G/S)XGX(R/H)XCXG sequence has been identified as a motif for identification of new cytochrome P450 enzymes [36, 47, 48].

The core structure of cytochrome P450 consists of the following highly conserved structural elements (Figure 1.4): a) a four α-helix bundle D, E, I, and L; b) helix J and K; c) sheets β1 and β2; d) the cysteinyl-containing heme binding loop; e) the coil termed the meander which is a 14 or 15 residue stretch carboxyl terminal immediately to the K helix. The highly conserved structural core of P450s is shown in Figure 1.4.

The four α-helix bundle is comprised of three parallel α-helices and one antiparallel α-helix. Helix I is long and largely hydrophobic at its amino-terminal end and forms one side of the heme pocket. Helix L forms a portion of the heme-binding region. Helix E is antiparallel. Beta-sheet 1 and 2 are simultaneously superimposable and are surrounded by the less-conserved helices, A, B, and K. The variable regions include the loop and other structures namely helices B′, F, G, H, β-sheets 3 and 4.

While the conserved structures are thought to be important in folding and heme binding, the regions of highest structural differences are involved in substrate recognition, substrate binding and binding to the redox partner (Figure 1.4) [38, 47].

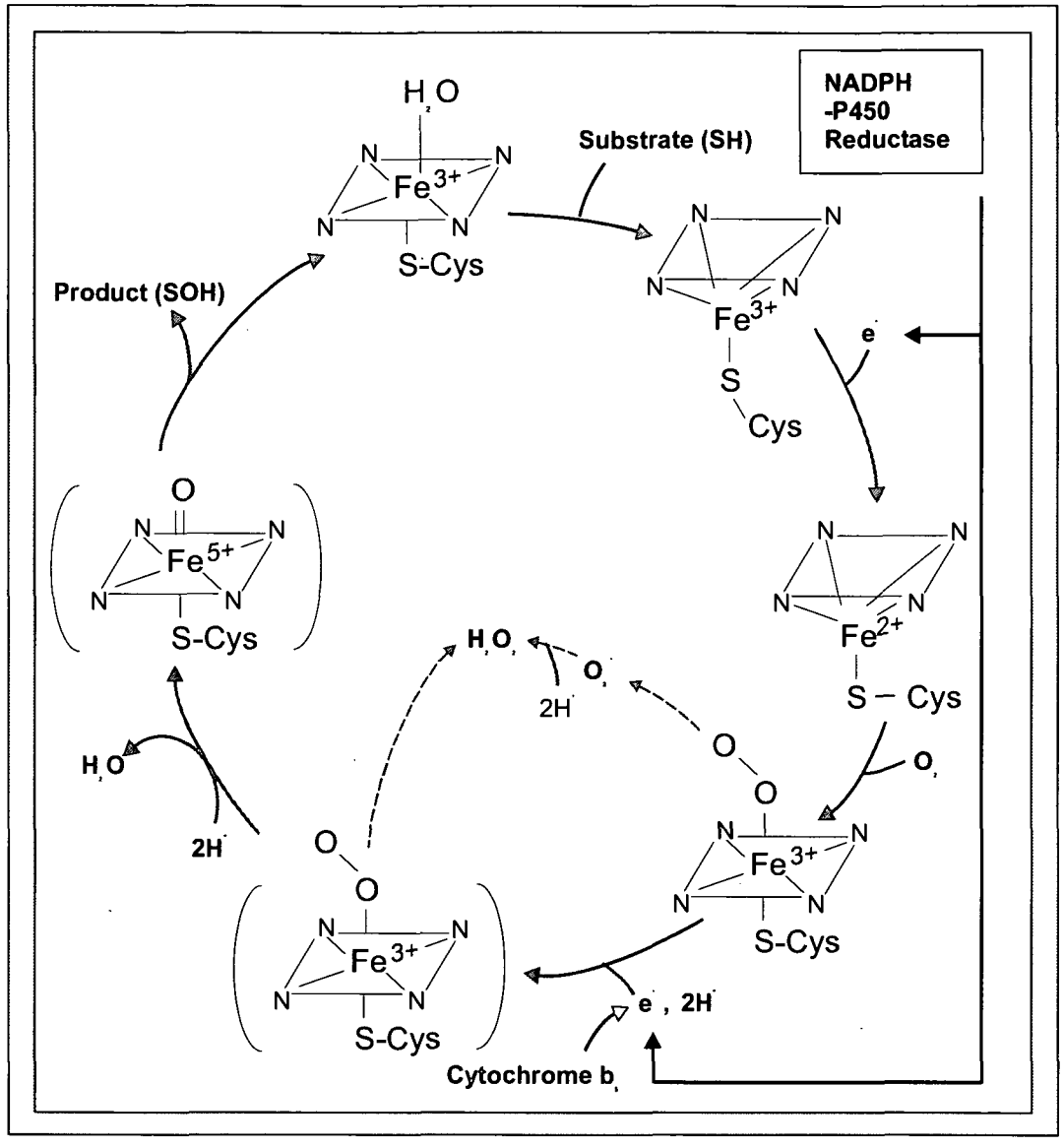

Figure 1.3: A schematic diagram of the catalytic cycle of the cytochrome P450 enzyme system.
(Redrawn from [9]). The hemoprotein functions as the substrate and oxygen binding site while NADPH-P450 reductase (or cytochrome b_5) acts as an electron carrier, shuttling electrons one at a time from the reductase (or cytochrome b_5) to the cytochrome P450.

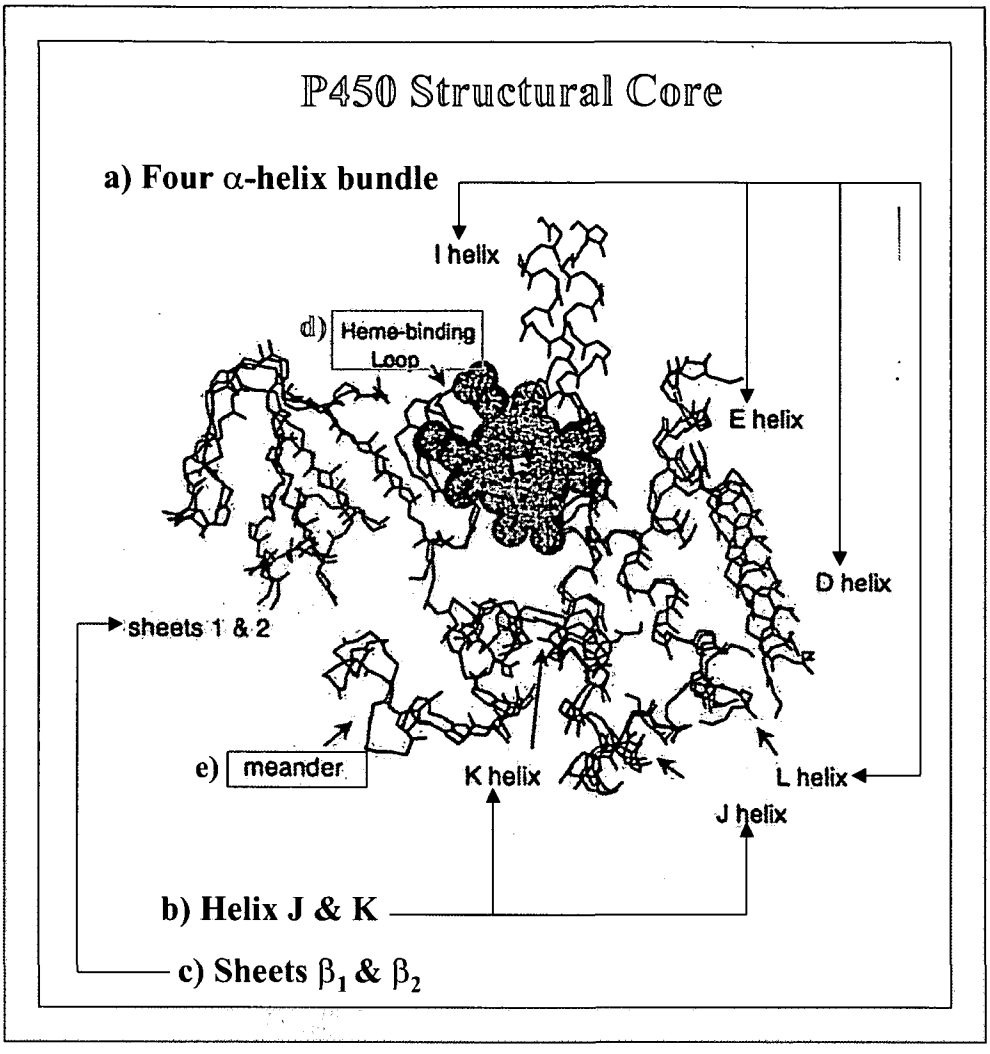

Figure 1.4: The structural core of P450s.
The core structure includes a) A four α-helix bundle D, E, I, and L; b) Helix J and K; c) Sheet $\beta 1$ and $\beta 2$; d) The cysteinyl-containing heme binding loop; e) and the coil termed the "meander", a 14 or 15 residue stretch carboxyl terminal immediately to the K helix. (Adapted from [47]).

1.2.5 Cytochrome P450 *CYP4A* family

The *CYP4* family appears to be one of the oldest eukaryotic cytochrome P450 gene families. The *CYP4* family is related to the enzyme family responsible for cholesterol metabolism and together they may have been involved in maintaining membrane integrity in early eukaryotes [49, 50]. The *CYP4* family was first recognised in 1987

when rat *CYP4A1* was designated the first member of the *CYP4* family [51] due to its protein sequence exhibiting less than 36% identity to other known P450s [35]. The *CYP4A* subfamily is one of eighteen subfamilies within the *CYP4* family and presently comprises twenty genes from nine different mammalian species. Multiple *CYP4A* genes have been identified in several species including rats [51, 52, 53, 54, 55, 56, 57], rabbits [58, 59, 60, 61], humans [62, 63], mouse [62, 64], hamsters, and pigs [65]. A single *CYP4A* gene has been described in guinea pigs [62] and cats (reviewed in [15]). CYP4A enzymes are predominantly expressed in liver, lung, and kidney and to a lesser extent in other tissues such as intestine, colon, heart, lung, and brain (reviewed in [66, 67]). Prior to these studies, CYP4A had not been studied in any marsupial species, except for the isolation of a partial *CYP4A15* cDNA from the koala liver [8].

1.2.6 CYP4A enzymes and their substrates

Fatty acids are the main substrates of CYP4A enzymes. Most CYP4A enzymes catalyse hydroxylation of fatty acids predominantly at their omega- (ω-) carbon. They also hydroxylate the ω-1 carbon to various degrees depending on the length of the fatty acid [34, 68, 69, 70, 71, 72, 73, 74] (reviewed in [34, 67]). Other CYP4A substrates include palmitate, arachidonate [68, 75], and to a lesser extent prostaglandins and leukotrienes [66]. Recently, other non-fatty acids have also been shown to be metabolised by CYP4A enzymes [67]. Pig liver CYP4A21 was found to catalyse the 6α-hydroxylation of chenodeoxycholic acid [65]. The capacity of CYP4A enzymes to metabolise fatty acids has focussed significant research due to the important role of ω-hydroxylated-fatty acids in physiological or pathophysiological processes (discussed in Section 4.1) [76, 77, 78]. Of relevance to this project is that in the koala liver, a higher lauric acid hydroxylation activity was found, as compared to human and rat livers [8].

1.2.7 The roles of the CYP4A subfamily

CYP4A roles in fatty acid metabolism: The oxidative metabolism of fatty acids occurs mainly in peroxisomes, microsomes and mitochondria. Microsomal omega-hydroxylation represents a major pathway for the oxidative metabolism of branched-chain or substituted fatty acids (Section 1.3.2). *In vivo*, this pathway also provides an essential alternate pathway for fatty acid metabolism where there is an increase in lipolysis and fatty acid transport to the liver [79, 80]. The increase in lipolysis and

fatty acid transport to liver cells may lead to fatty acid overload of the mitochondrial β-oxidation system. Examples of such conditions are ketotic states including diabetes and starvation, a high fat diet and administration of a hypolipidemic agent. The role of CYP4A in the oxidative metabolism of fatty acids during these states is depicted schematically in Figure 1.5.

Following ω-hydroxylation, the hydroxylated fatty acids are oxidised to dicarboxylic acids by alcohol and aldehyde dehydrogenase. These metabolites then undergo β-oxidation in peroxisomes to short chain dicarboxylic acids which are subsequently utilised in cellular reactions or secreted as C_6 or C_{10} metabolites. Together with the peroxisomal β-oxidation pathway (discussed in Section 1.3.3), fatty acid ω-hydroxylat-ion prevents mitochondrial dysfunction as a result of accumulation of fatty acids in liver cells [79, 80]. Elevated levels of monohydroxylated carboxylic and dicarboxylic fatty acids have been implicated in a number of serious lipid metabolising disorders such as Reye's syndrome, dicarboxylic aciduria, and sudden infant death syndrome. The role of CYP4A enzymes in the metabolism of arachidonic acid, which generates physiological factors involved in other critical processes, has been implicated in smoothly cooperative fatty acid metabolism in the liver (reviewed in [34]).

CYP4A roles in vascular homeostasis and other signalling pathways: As previously stated, the oxidative metabolism of arachidonic acid generates many important pharmacologically active metabolites involved in diverse biological processes including vascular homeostasis and signal transduction pathways. Within this complex oxidative process, cytochrome P450 enzymes play a major role. For example, CYP4A enzymes catalyse the ω-hydroxylation of arachidonic acid to 20-hydroxyeicosatetraenoic acid (20-HETE), an important component of signal transduction cascades activated by several hormonal systems. 20-HETE has been identified to be an activator of protein kinase C [81, 82] and mitogen activated protein kinase- mediated signalling pathways [83, 84], and also an activator of smooth muscle vaso-constrictor endothelin-1 and angiotensin II [85, 86, 87, 88, 89].

Several studies have reported a reduction in blood pressure as a result of inhibition of CYP4A expression or activity and an elevation in renal blood pressure associated with changes in renal CYP4A levels in male rats [90, 91]. Omega-hydroxylation is also an important step in the metabolism of 20-HETE and other pharmacologically active eicosanoids, prostaglandins (PG), and leukotrienes (LT) (reviewed in [66, 67]). A

schematic representation of the formation of 20-HETE by CYP4A enzymes is shown in Figure 1.6.

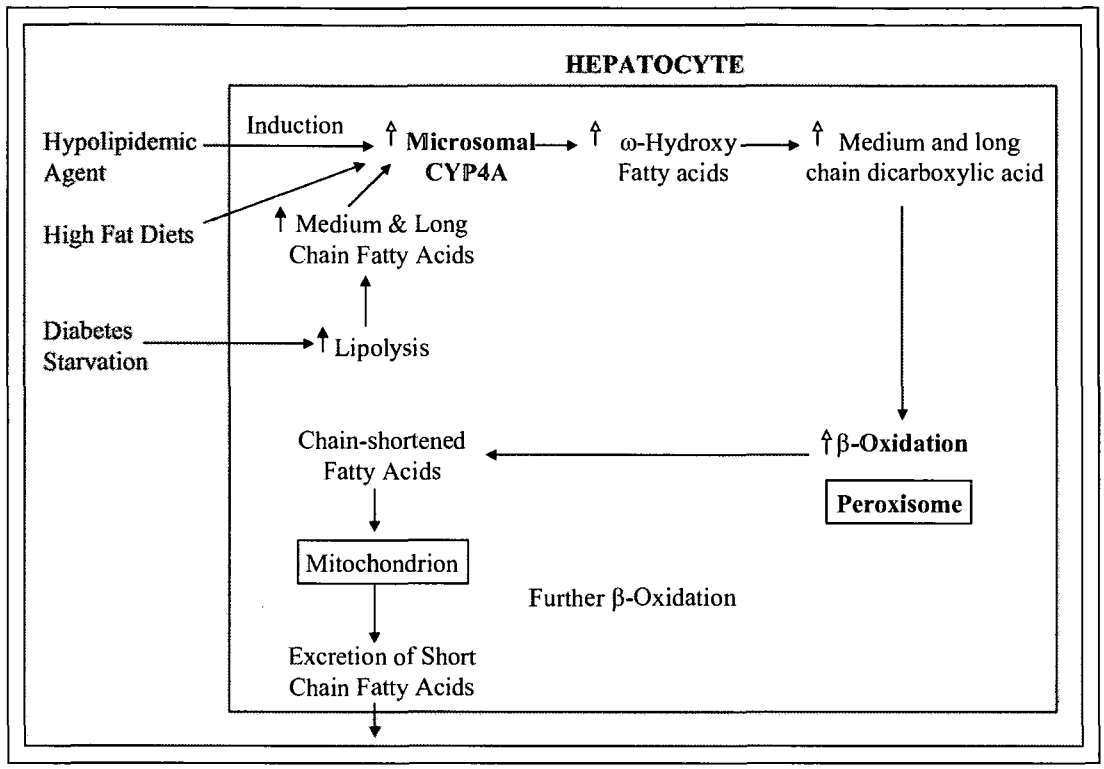

Figure 1.5: A schematic representation of the role of CYP4A in lipid homeostasis.
(Reproduced from [34]). During fatty acid overload, the induction of the microsomal fatty acid ω-hydroxylation and peroxisomal β-oxidation prevents the accumulation of fatty acids and their CoA derivatives in liver cells preventing mitochondrial dysfunction.

1.2.8 Induction of CYP4A subfamily

In susceptible rodents, CYP4A enzymes are inducible by several structurally diverse chemicals, collectively termed peroxisome proliferators (Section 1.4.2). In rat liver, CYP4A proteins represent about 1-4% of total P450 content, but are elevated up to 16-30% following administration of potent peroxisome proliferators [92, 93]. In the koala, an obligate Eucalypt feeder, total liver CYP content was found to be more than 3-fold higher than is seen in rat and humans [94]. The induction of CYP4A enzymes by acyclic monoterpenes found in *Eucalyptus* leaves such as citral has been reported

in rats[5]. The induction of CYP4A enzymes by xenobiotics appears to be associated with induction of peroxisomal β-oxidation enzymes [34, 67] (Section 1.4.3). While a higher hepatic CYP4A activity was found in the koala than in rat and humans, total liver peroxisomal β-oxidation activity was absent in the koala liver [8].

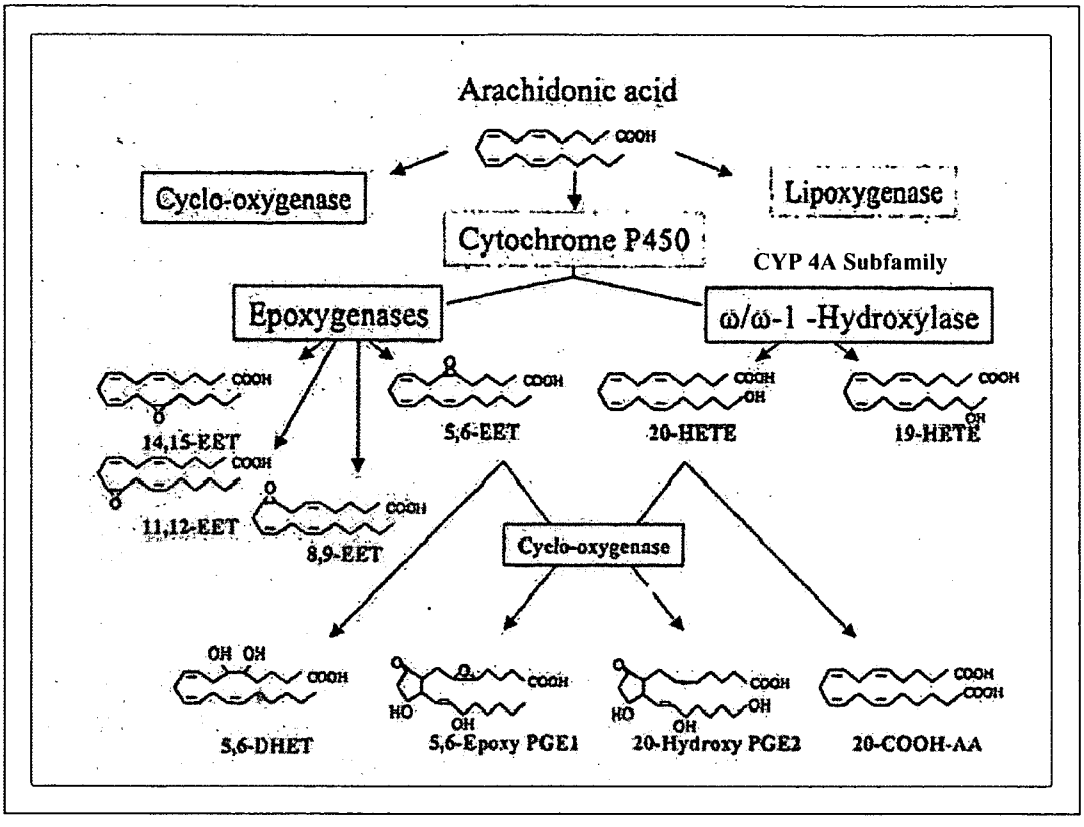

Figure 1.6: A schematic representation of the formation of 20-HETE by CYP4A enzymes and the role of cytochrome P450 enzymes in the oxidative metabolism of arachidonic acid.
(Adapted and modified from [9]).

CYP4A enzymes are also induced by endogenous compounds such as medium-chain triacylglycerols and progesterone and by pathophysiological states including pregnancy, streptozotocin-induced diabetes, [95], a high fat diet [96] and anti-inflammatory response [97] (reviewed in [98]). Other CYP4A inducers include fatty acids [99], retinoic acid [100], cisplatin [101], statin and nonsteroidal anti-inflammatory drugs [67, 102, 103, 104].

1.3 PEROXISOMAL β-OXIDATION ENZYMES

1.3.1 Peroxisomes

Peroxisomes are single membrane bound cytoplasmic organelles that participate in a variety of metabolic processes. In mammals, peroxisomes are most abundant in liver and kidney. The most well characterised process carried out by peroxisomes is fatty acid β-oxidation. Peroxisomes are capable of performing β-oxidative degradation of a vast array of substrates and each step of β-oxidation is catalysed by several enzymes with distinct substrate specificities. The most extensively studied β-oxidation enzyme is the first and rate limiting enzyme, fatty acyl CoA oxidase [105].

1.3.2 Fatty acid metabolism

As mentioned in Section 1.2.7, in mammalian liver, fatty acids are oxidised in three organelles namely microsomes, peroxisomes and mitochondria. While microsomes are responsible for fatty acid ω-hydroxylation, peroxisomes and mitochondria are responsible for β-oxidative chain shortening of acyl CoA fatty acids. Mitochondrial β-oxidation is mainly responsible for catabolism of short-, medium-, and long-chain fatty acids to provide energy to the cell whereas peroxisomal β-oxidation is more involved in the metabolism of less abundant and more toxic and biologically active substrates. These substrates include very long chain fatty acids containing more than 20 carbons, 2-methyl branched fatty acids, dicarboxylic acids, prostanoids and the C_{27} bile acid intermediates [106, 107]. Long chain and very long chain fatty acids also undergo ω-hydroxylation to form metabolites that serve as substrates for the peroxisomal β-oxidation system [51, 108].

Peroxisomal and mitochondrial β-oxidation processes co-exist in the same animal cell and the enzymes involved in the two systems are encoded by different genes. These two systems play functionally different but complementary roles [106, 107, 109, 110]. Very long chain fatty acids are almost exclusively processed in peroxisomes whereas long chain fatty acids up to 18 carbons are predominantly oxidised in mitochondria. This is because mitochondria are devoid of very long chain acyl CoA synthetase which is the enzyme responsible for adding CoA into fatty acids. The peroxisomal β-oxidation system is also involved in the oxidative metabolism of long chain fatty acids [107, 111, 112, 113] (reviewed in [114]). Fatty acyl CoAs generally undergo five

cycles of peroxisomal β-oxidation to remove ten carbon atoms and the resultant fatty acyl-CoAs enter mitochondrial β-oxidation for completion.

1.3.3 The peroxisomal β-oxidation pathway

The peroxisomal β-oxidation system is divided into two different but interconnected pathways based on the specificity of the substrates and the stereoselectivity of the enzymes involved [106, 115, 116]. While the L-hydroxy specific classical β-oxidation system acts on straight chain fatty acyl-CoAs, the D-hydroxy-specific β-oxidation system mainly oxidises branched chain acyl-CoAs [106, 116, 117, 118]. The same reactions occur in both the D- and the L-hydroxy specific pathways however the enzymes involved in each step are different. The enzymes of the L- peroxisomal β-oxidation system are markedly induced in the liver of rats and mice by peroxisome proliferators (Section 1.4) [118]. A schematic representation of the two pathways of peroxisomal β-oxidation is shown in Figure1.7.

Other important substrates of the peroxisomal β-oxidation system include eicosanoids such as prostaglandins, leukotrienes, thromboxane, long chain dicarboxylic fatty acids, pristanic acid, bile acid intermediates including di- and tri-hydroxycoprostanoic acids and xenobiotics. The main substrates of the peroxisomal β-oxidation system are listed in Table 1.1.

1.3.4 The enzymes of the β-oxidation system

The peroxisomal β-oxidation system consists of three distinct enzymes: acyl-CoA oxidase, L- or D-enoyl-CoA hydratase/3-hydoxyacyl-CoA dehydrogenase (multifunctional enzyme), and 3-keto-CoA thiolase or sterol carrier protein x. Peroxisomal β-oxidation is a four reaction cascade. In the first oxidation reaction, acyl CoA oxidase catalyses the conversion of acyl-CoA esters to their corresponding trans-2-enoyl-CoAs. The second step is a hydration reaction catalysed by enoyl-CoA hydratase to convert enoyl-CoA to 3-hydroxyacyl-CoA. The next reaction is the second oxidation reaction that oxidises the 3-hydroxyacyl-CoA to a 3-ketoacyl-CoA. The last step cleaves 3-ketoacyl-CoAs to acyl-CoA catalysed by 3-ketoacyl-CoA thiolase. This acyl-CoA is two carbons shorter than the original acyl-CoA molecule and can re-enter the β-oxidation system. [114, 118] (Figure 1.7).

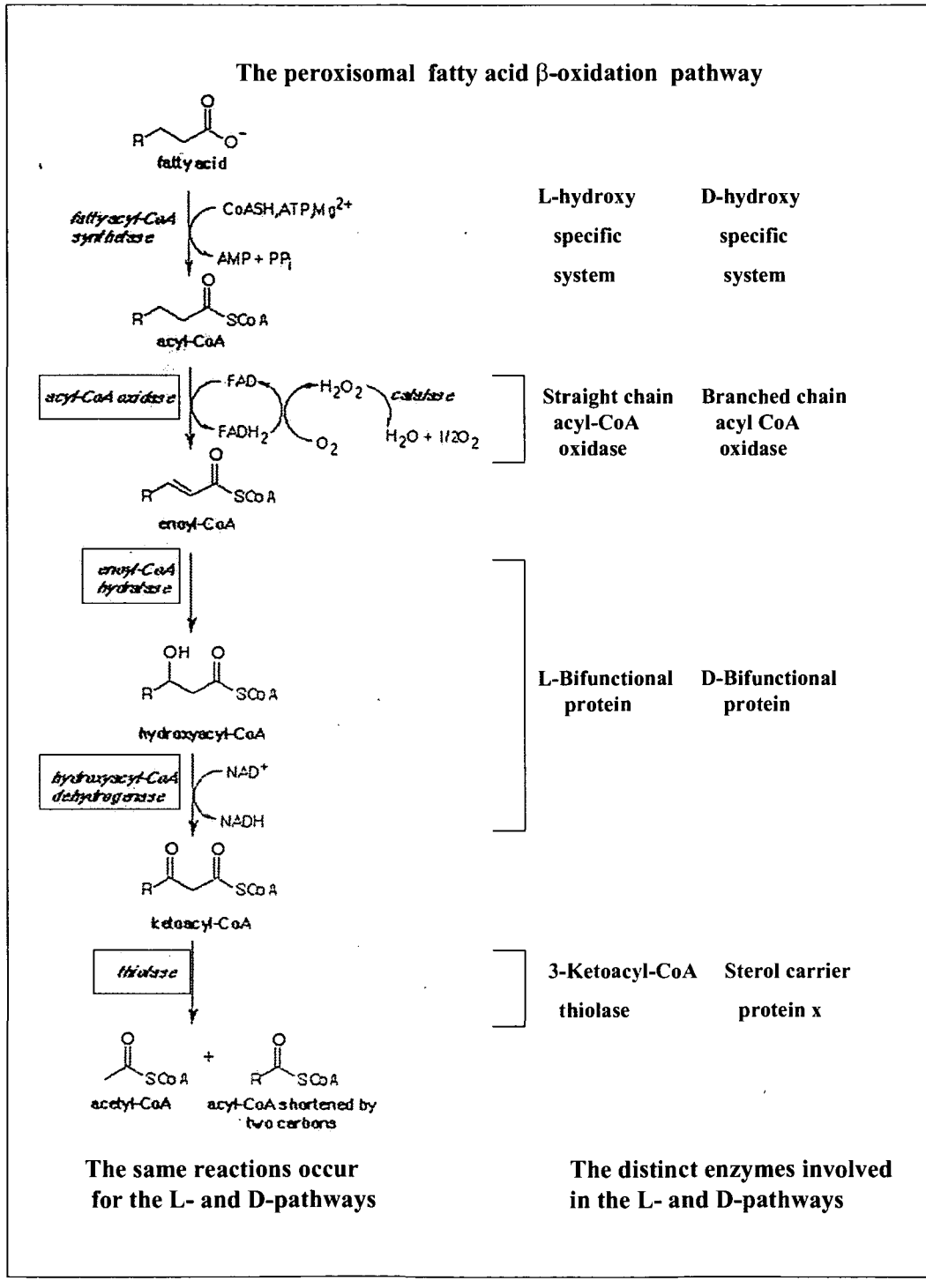

Figure 1.7: A schematic diagram depicting the peroxisomal β-oxidation system.
(Adapted and modified from [119]). The same reactions occur in both the D- and the L-hydroxy specific pathways, however, the enzymes involved in each step are different with very distinct substrate specificity.

Compound class	Substrates of peroxisomal β-oxidation
Fatty acids:	Very long chain fatty acids Long chain fatty acids 2-methyl-branched fatty acids
Fatty acid derivatives:	Eicosanoids: prostaglandins, leukotrienes thromboxane
Bile acid intermediates	Di- and tri- hydroxycoprostanoic acids
Others	Long chain dicarboxylic fatty acids Pristanic acid Other xenobiotics

Table 1.1: Substrates of peroxisomal β-oxidation.

1.3.5 Acyl-CoA oxidases

Historical aspects and biochemical properties: Acyl CoA oxidase (AOX) is a FAD-containing oxidase that transfers electrons directly to oxygen and generates hydrogen peroxide while converting acyl CoA ester to the 2-trans-enoyl-CoA ester. Acyl-CoA oxidase was first identified in peroxisomes from castor bean endosperm as part of the fatty acid oxidizing system [120]. Subsequently, it has been isolated from other sources including animal tissues [121, 122, 123], yeast [124, 125], several germinating fat seeds and other higher plant tissues [126, 127, 128]. Acyl CoA oxidase has been reported to be a unique marker enzyme of peroxisomal β-oxidation since it is present exclusively in peroxisomes and is not detected in mitochondria.

Species differences in the patterns of acyl CoA oxidases: Multiple acyl CoA oxidases have been identified in rat and humans and possess different substrate specificities. A schematic representation of acyl CoA oxidases and their substrates in livers of humans, rat and koala is shown in Figure 1.8. In rat liver, peroxisomes contain three acyl CoA oxidases. Palmitoyl CoA oxidase catalyses oxidation of the CoA esters of medium-, long-, and very long-chain fatty acids, medium- and long-chain di-

carboxylic acid, and prostaglandins. Pristanoyl CoA oxidase acts on the CoA esters of 2-methyl-branched fatty acids, straight chain fatty acids and dicarboxylic acids. Trihydroxycoprostanoyl CoA oxidase catalyses the oxidation of the CoA esters of bile acid intermediates [114, 129, 130, 131]. Human liver peroxisomes contain only two acyl CoA oxidases. Human palmitoyl CoA oxidase is similar to rat palmitoyl CoA oxidase and metabolises the same substrates. Branched chain acyl CoA oxidase possesses the catalytic actions of both rat pristanoyl CoA oxidase and trihydroxycoprostanoyl CoA oxidase [114]. Palmitoyl CoA oxidase is also known as fatty acyl CoA oxidase (AOX).

Fatty acyl CoA oxidase: Fatty acyl CoA oxidase (AOX) is the first and rate limiting enzyme that is critical for completion of peroxisomal straight chain fatty acid β-oxidation [118]. In most species studied, the *AOX* gene encodes two AOX proteins of approximately 660 amino acids which differ by the differential splicing of alternative exons 3 [114]. Before translocation to peroxisomes, AOX protein is a dimer composed of two identical subunits A. The polypeptide is cleaved proteolytically into component B and C when it is translocated into peroxisomes [132, 133, 134]. This cleavage process proposes that the full-length AOX polypeptide folds into two structural domains as shown in Figure 1.9. Within this 2 domain structure, the carboxyl terminus ends with a -Ser-Lys-Leu-COOH motif that forms a peroxisomal targeting signal [114, 134, 135].

In humans and rats, a single *AOX* gene exists that spans approximately 25-kb and comprises 14 exons and 13 introns. Component B derives from exons 1-9 and component C is derived from exons 10-14 [134]. The structure of the human fatty *acyl CoA oxidase* gene is depicted in Figure 1.9. Two different sequences were found for the third exon which is alternatively utilised in pre-mRNA splicing to yield two types of *AOX* mRNA. These two alternative third exons are probably generated by exon duplication and contain identical numbers of nucleotides with approximately 55% sequence identity. This region corresponds to the amino acid residues 90 to 144 with 50% protein sequence identity. This results in two types of AOX enzymes present in the peroxisomal matrix. This region has also been reported to be involved in substrate binding affinity. It appears that the two AOX enzymes have different selectivity against different chain lengths of fatty acyl CoA substrates [114, 134].

1.3.6 Deficiencies of β-oxidation enzymes

Deficiencies of peroxisomal β-oxidation enzymes have been reported to result in many critical fatty acid metabolising disorders [136]. In AOX knock-out mice, accumulation of unmetabolised acyl CoAs derived from very long chain fatty acids, dicarboxylic and other substrates of AOX were observed. This accumulation led to sustained elevation of CYP4A enzyme expression as a result of activation of PPAR-α (Section 1.3). In susceptible species, both AOX and CYP4A have been identified as the marker enzymes of peroxisome proliferation due to exposure to peroxisome proliferators. The following section focuses on the function of PPAR-α in controlling CYP4A and peroxisomal β-oxidation enzyme expression, and PPAR-α ligands.

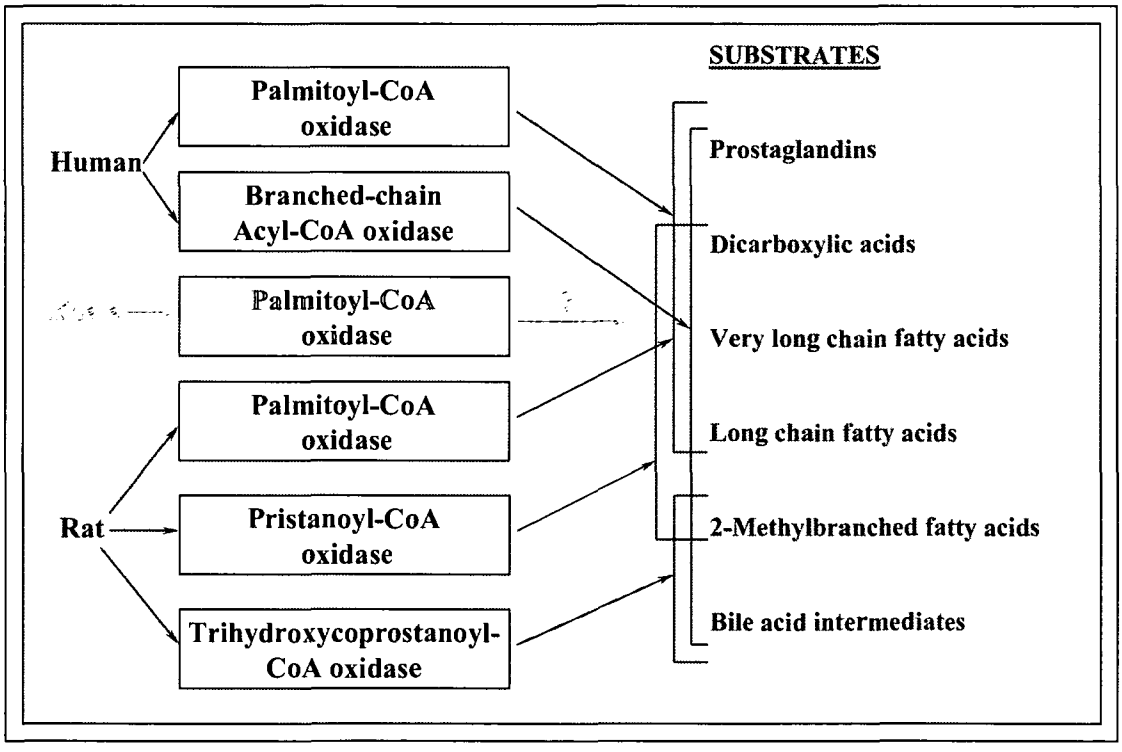

Figure 1.8: Acyl CoA oxidases in rat and human livers and their substrate specificities.
Total peroxisomal β-oxidation activity was found to be absent in the koala liver [8] and further study into peroxisomal β-oxidation enzymes has not been accomplished in the koala or any other marsupial species.

1.4 PEROXISOME PROLIFERATORS AND PPAR-α

Peroxisome proliferators (PPs) are a class of structurally diverse compounds of industrial, pharmaceutical, and agricultural importance. As the name implies, peroxisome proliferators cause a marked increase in the number and size of peroxisomes and an increase in liver weight in susceptible species such as the rat and mouse [114, 137, 138]. PPs also induce transcriptional activation of genes encoding the L-hydroxy specific β-oxidation and CYP4A enzymes [139, 140, 141]. Peroxisome proliferation has also been observed in rodents after treatment with a high fat diet, cold temperature, starvation and corticotrophin (ACTH) [142].

The peroxisome proliferator-activated receptor-alpha (PPAR-α) has been reported to mediate the biological and toxicological effects of peroxisome proliferators via transcriptional activation of target genes. PPAR-α is a member of the nuclear receptor superfamily and is able to be activated by several endogenous ligands. These ligands include leukotriene B_4 [143], 8S-hydroxyeicosatetraenoic acid [144], dietary unsaturated fatty acids and fatty acid metabolites [145, 146].

Evidence for the direct binding of PPs and endogenous ligands to PPAR-α has been reported [147, 148]. PPAR-α is most abundant in liver, kidney, heart, and muscle which are the main sites of peroxisome proliferation. PPAR-α proteins from different species have been reported to have similar function when studied *in vitro* [149]. PPAR-α plays an essential role in several physiological processes including inhibition of apoptosis, cell proliferation, mitogenesis and inflammatory responses [137, 138]. A brief history of peroxisome proliferation research and a current review of PPAR-α understanding follows.

1.4.1 Historical aspects

In the 1960s, several investigators documented the proliferation of hepatic microbodies after exposure to ethyl chlorophenoxy isobutyrate, a hypolipidemic agent. Peroxisomal β-oxidation of fatty acids was established in 1969 followed by the discovery of its inducibility by peroxisome proliferators in rat livers in 1976 [115, 150, 151]. At the end of 1980, the mechanism of action of peroxisome proliferators remained unclear

[138]. In 1990, cloning of the first PPAR-α from mouse provided a logical explanation of mechanisms by which peroxisome proliferation was triggered [152]. Since then, several studies have focussed on identification of PPAR-α from diverse species.

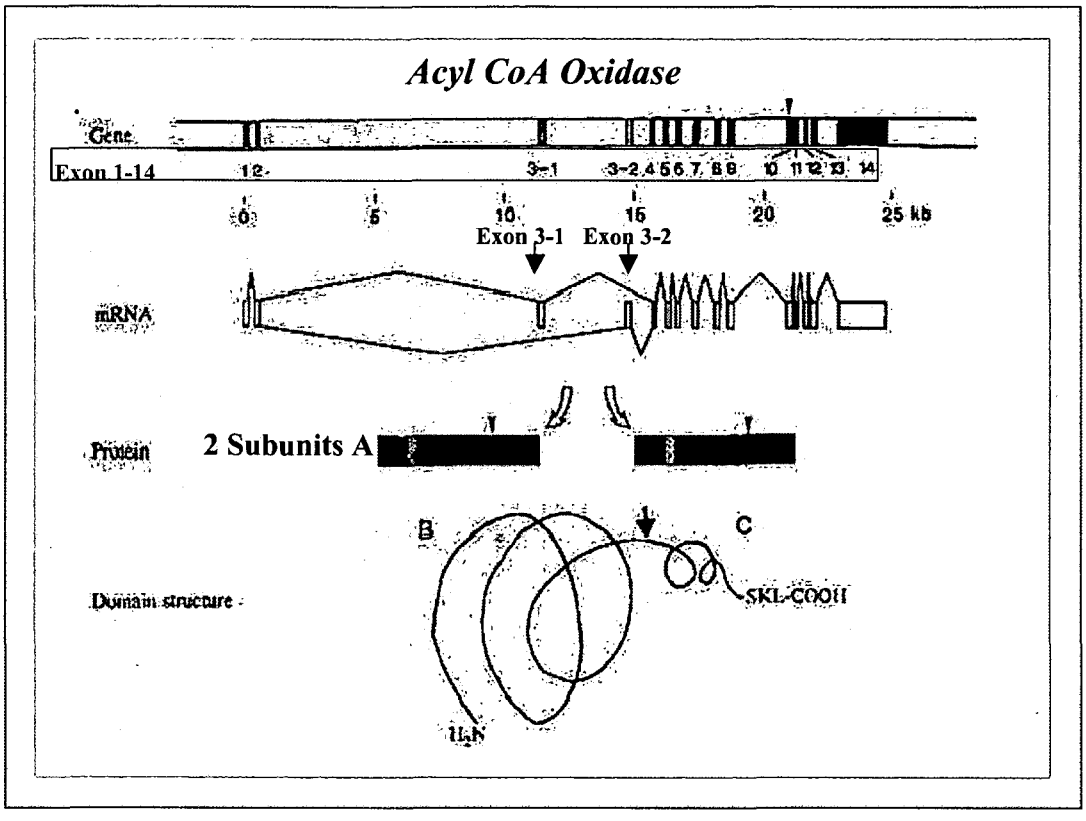

Figure 1.9: Schematic representation of the structure of the fatty *acyl CoA oxidase* gene and the process of proteolytic cleavage of component A into components B and C.
(Adapted and modified from [134]). The site of proteolytic cleavage of component A into components B and C is shown by a thick downward arrow on the domain structure and also indicated on the gene and protein sequence structures by arrowheads.

1.4.2 Peroxisome proliferators

Peroxisome proliferators form a class of structurally diverse compounds including several lipid and cholesterol lowering fibrate drugs, certain industrial phthalate plasticisers, herbicides, chlorinated hydrocarbons, perfluorinated fatty acids, prostaglandins, leukotriene D4 receptor antagonists and naturally occurring hormones. Certain fatty

acids and antifungal imidazole drugs have also been identified as peroxisome proliferators [145, 153]. Examples of each class of natural and synthetic ligands of PPAR-α are listed in Table 1.2. The ligands listed in the table are taken from various sources [137, 142, 152, 154, 155, 156, 157, 158] (reviewed in [139]). Evidence for direct interaction with PPAR-α is also shown. These compounds share very little obvious structural similarity except an aromatic ring, a aliphatic chain and a carboxylic acid group [159]. The carboxylic group may play an essential role in the binding and subsequent activation of PPAR-α [160].

1.4.3 The overall effects induced by peroxisome proliferators

In the liver, peroxisome proliferators exert their effects mainly on peroxisomes, microsomes and mitochondria. The inducible effects of PPs on these organelles and other components are listed in Table 1.3 (adapted and modified from [138]). Induction of hypolipidemia, increases in hepatocyte DNA synthesis and inhibition of apoptosis are also integral parts of the profound responses induced by PPs. Peroxisome proliferation due to exposure to PPs is tissue-specific and is most predominant in the liver [161].

1.4.4 Peroxisome proliferator activated receptor-alpha: Molecular aspects

During the last twenty years, much attention has focussed on the role of PPAR-α in the mechanism of action of peroxisome proliferators. PPAR-α was first postulated to mediate the action of PPs in 1983 based on the specificity of cellular and tissue responses and on the rapid transcriptional activation of fatty acid metabolising enzymes [142, 158]. This led to the isolation of mouse liver PPAR-α in 1990 [152] and the subsequent cloning of PPAR-α from Xenopus [162], rat [163], human [155], and guineapig [149].

PPAR isotypes and genomic organization: PPAR-α is most closely related to the thyroid hormone receptor and the retinoid receptor [139]. Two other related PPAR isotypes are PPAR-β and PPAR-γ, which share significant sequence identity with PPAR-α. Human and mouse PPARs comprise six coding exons [139, 152, 164]. One exon encodes the N-terminal domain and two exons encode the central part of

the receptor, a highly conserved DNA binding domain (DBD) that is responsible for sequence specific DNA recognition and dimerisation. The C-terminal is subdivided into D, E and F regions with one exon encoding each region. The E region (or E and F regions) function as the ligand-binding domain (LDB). The C-terminal F domain is essential for the interaction of the nuclear receptor with nuclear receptor coactivators and co-repressors [114, 139, 164].

PPAR-α response element and DNA binding properties: The DNA binding domain of PPAR-α consists of two finger like regions folded together to create a globular structure. This structure recognises a DNA target sequence comprised of 6 nucleotides. In the promoter region of PPAR-α target genes, two copies of such a core motif form a peroxisome proliferator response element (PPRE) to which a nuclear receptor binds as a dimer. The spacing of these two motifs and their relative orientation determines which receptors bind [165]. PPRE has been defined as an almost perfect direct repeat of two AGGTCA sequences (DR1 motif) spaced by one nucleotide. The first identified PPRE from the acyl CoA oxidase gene [162] and all subsequently found PPREs fulfil these DR1 criteria [139, 166, 167]. The DR1 rules allow PPREs to be discriminated from other direct repeat response elements of the thyroid or retinoic acid class receptors. The binding of PPAR-α to PPRE strictly depends on the presence of the nuclear 9-*cis* retinoic acid receptor (RXR) that functions as a DNA binding partner. Three additional discriminating parameters for PPAR and RXR binding selectivity include an extended 5'-half-site, an imperfect core DR1 and an adenine as the spacing nucleotide between the two DR1 motif [139].

The level of expression of PPAR-α within a cell is of great importance in the binding of PPAR-α to PPRE which is also recognised by other nuclear receptors. Single point mutations in the core DR1 motifs have been reported to differently affect the binding affinity of PPAR-α [139]. As a result, the presence of a DR1 motif that deviates from the consensus observed in many natural PPREs may increase preferential binding of PPAR-α [139].

Classification	PPAR-α ligands	Direct binding
Therapeutic agents	- Hypolipidemic drugs:	
	Clofibric acid	+
	Ciprofibric acid	+
	Pirinixic acid (WY-14643)	+
	Fibrate analog GW 2331, 2433	+
	Eicosatetraynoic acid (ETYA)	+
	Virtually all fibrates, tibrates	+
	- Non-steroidal anti-inflammatory drugs (indomethacin, ibuprofen, fenoprofen, flufenamic acid)	nd
	- Antifungal azole drugs (bifonazole, clotrimazole)	nd
Experimental and other synthetic ligands	- Herbicides: various chlorophenoxy-acetic acid derivatives	nd
	- Plasticisers: phthalate esters	nd
	- Prostaglandin 12 analogs: Iloprost, Carbaprostacylin (cPGI)	+
	- Leukotriene B_4 analogs: ZK 151657, ZK 158252, Trifluromethyl leukotriene B_4	+
	-Leukotriene D_4 antagonist Ly 171883	+
	-Fatty acyl CoA dehydrogenase inhibitors:	
	Ortylthiopropiocic acid (OTP)	+
	Nonylthioacetic acid (NTA)	+
	Tetradecylthioacetic acid (TTA)	+
	-Carnitine palmitoyl transferase I (CPT1) inhibitors: LY-171883	+
	2-Bromopalmitate (2Br-C16)	+
	Tetradecylglycidic acid (TDGA)	+

Table 1.2: Examples of natural and synthetic ligands of PPAR-α. Evidence for direct interaction with PPAR-α is indicated by +. nd: Compound has not been tested. (Taken from various sources [137, 142, 152, 154, 155, 156, 157, 158], (reviewed in [139])).

Classification	PPAR-α ligands	Direct binding
Natural ligands	- Leukotrienes	+
	- 8S-hydroxyeicosatetraenoic acid (HETE)	+
	- Phytanic acid	nd
	- Various unsaturated fatty acids:	
	α-Linolenic acid C18:3	+
	γ-Linolenic acid C18:3	+
	Eicosapentaenoic acid C20:5 (EPA)	
	Linolenic acid C18:2	
	Dihomo-γ-linolenic C20:3	+
	Arachidonic C20:4	+
	-Saturated fatty acids:	
	Lauric C12:0	nd
	Myristic C14:0	+
	Palmitic C16:0	+
	Stearic C18:0	+

Table 1.2 (continued): Examples of each class of natural and synthetic ligands of PPAR-α.

Evidence for direct interaction with PPAR-α is indicated by +. nd: Compound has not been tested. (Taken from various sources [137, 142, 152, 154, 155, 156, 157, 158], (reviewed in [139])).

Main effects of PPs* on peroxisomes	Degree of stimulation
Fractional volume of peroxisomes	Two to 10-fold increase
Peroxisomal β-oxidation of	
-monocarboxylyl-fatty acyl-CoA	More than 10-fold increase
-omega-hydroxymonocarboxylyl-CoA	More than 10-fold increase
- dicarboxylyl-CoA	More than 10-fold increase
- prostaglandyl-CoA	More than 10-fold increase
Carnitine acyltransferase (COT, CAT)	Less than 2-fold increase to 2- to 10-fold increase
Main effects of PPs* on microsomes	
Fractional volume of smooth endoplasmic reticulum	Less than two fold increase
Fractional volume of rough endoplasmic reticulum	Little or no change
Cytochromes P450 in general	Little or no change
CYP4A1(lauric acid hydroxylase)	Two to 10-fold increase to more than 10-fold increase

Table 1.3: Overview of the main biological effects induced by peroxisome proliferators on peroxisomes, microsomes, mitochondria and other cellular components.
This table mainly focuses on the metabolic alterations induced in susceptible rodent livers. PPs *: peroxisome proliferators. (Adapted and modified from [138]).

Main effects of PPs* on mitochondria	Degree of stimulation
Fractional volume of mitochondria	Little or no change to less than 2-fold increase
Mitochondrial β-oxidation of	
-monocarboxylic fatty acids	Less than 2-fold increase
-omega-hydroxymonocarboxylic acid	Less than 2-fold increase
- carnitine acyltransferase (CPT, CAT)	More than 10-fold increase
- prostaglandyl-CoA	More than 10-fold increase
Carnitine acyltransferase (COT, CAT)	Two to 10-fold increase to more than 10-fold increase
Enoyl-CoA reductase	Two to 10-fold increase
PP* effects on other components	
Fatty acid binding protein	Two to 10-fold increase
Acyl CoA hydrolase	Two to 10-fold increase
Total liver content of CoA	Less than 2-fold increase
Total liver content of carnitine	Less than 2-fold increase
Total liver content in polyamines	Less than 2-fold increase
17β-hydroxysteroid dehydrogenase type IV	Less than 2-fold increase

Table 1.3 (continued): Overview of the main biological effects induced by peroxisome proliferators on peroxisomes, microsomes, mitochondria and other cellular components.

This table mainly focuses on the metabolic alterations induced in susceptible rodent livers.* PPs: peroxisome proliferators.

PPAR tissue expression and regulation: PPAR-α is highly expressed in the liver and other tissues such as colon, kidney and cardiac muscle. The expression pattern of PPAR-α reflects the sensitivity of the tissues to the inducible effects of peroxisome proliferators. Expression of PPAR-α in rat liver is under positive and negative regulation by glucocorticoids and insulin respectively [168, 169]. The PPAR-α mRNA and protein levels cycle in parallel with the circadian level of circulating glucocorticoid. While synthesis of PPAR-α is increased in situations that elevate plasma glucocorticoid level such as stress and fasting, a marked decrease in PPAR-α level was observed in primary culture of rat hepatocytes exposed to glucocorticoid [170, 171]. PPAR-α is also up-regulated by its own ligands. Induction of PPAR-α expression level by fibrates, fatty acids and other PPAR-α ligands has been reported [118].

1.4.5 PPAR-α cofactors and the mechanism of action of peroxisome proliferators

PPAR-α mediates the action of peroxisome proliferators through transcriptional activation of target genes. PPAR-α forms a heterodimer with RXR and the PPAR-α:RXR complex binds to the PPRE located in the 5' upstream region of target genes [172]. The binding of PPAR-α to the PPRE has been well characterised [138, 162, 173]. PPREs have been identified in several PPAR-α target genes including rat and human acyl CoA oxidase, rabbit *CYP4A6*, rat *CYP4A1*, bifunctional enzymes and other peroxisome proliferator-inducible genes. It has been confirmed that PPAR-α can trans-activate PPRE in the presence of the RXR in human, guinea pig, rat and mouse [149, 155, 162, 173, 174]. A schematic representation of the interaction between PPAR-α, coactivator complexes and basal transcriptional element is shown in Figure 1.10.

Several protein components have been identified to be PPAR coactivators and to bind to the receptor in a ligand-dependent fashion [114, 175]. These cofactors include steroid receptor coactivator 1, PPAR binding protein, PPARγ coactivator 1, PPAR interaction protein and others [114, 164, 175, 176]. Not all of these cofactors are essential for the function of PPAR-α [114, 175].

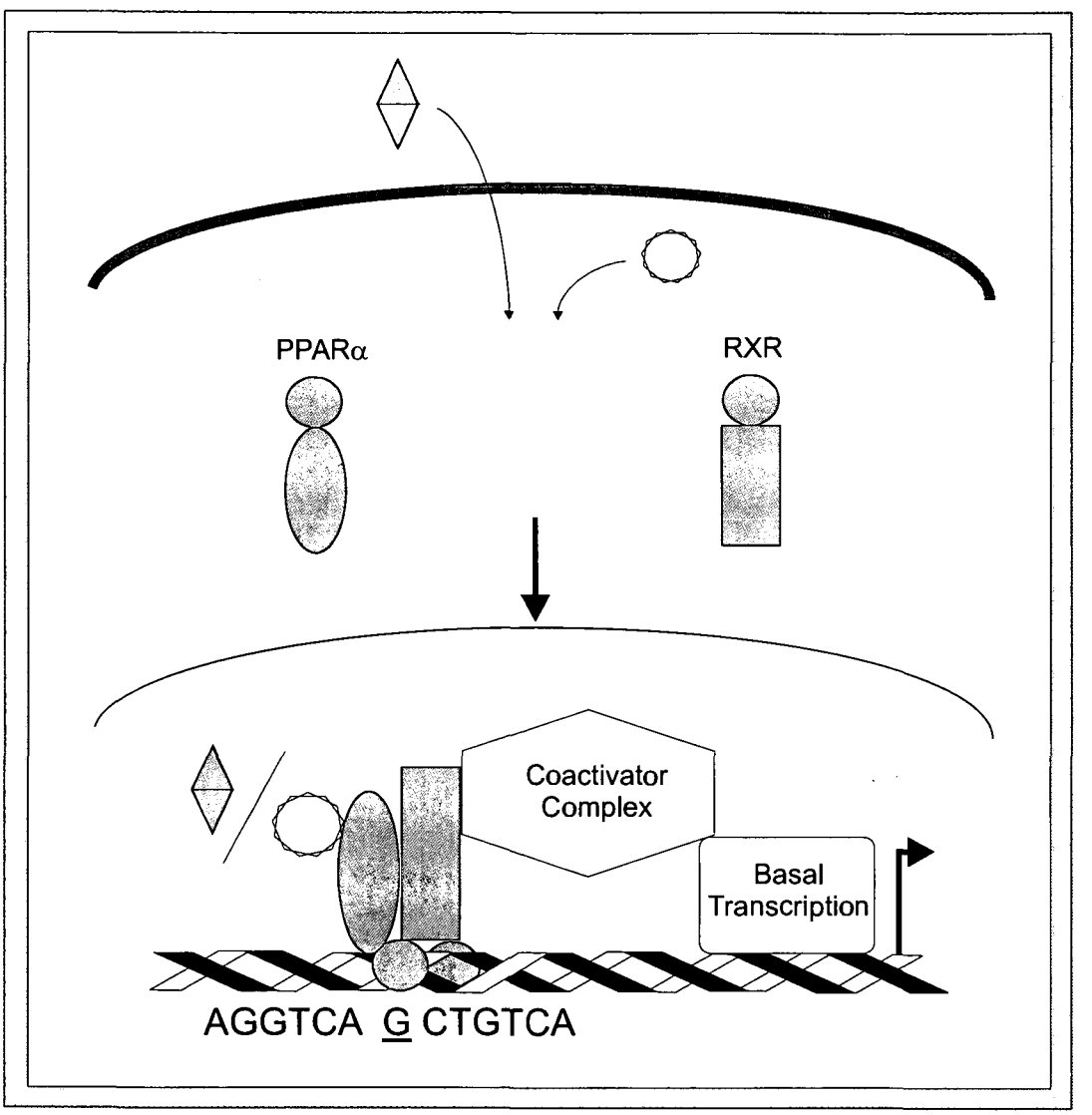

Figure 1.10: Schematic representation of PPAR-α, coactivator complexes, and basal transcriptional element interaction, leading to increased transcription of target genes.
Liganded PPAR-α interacts with 9-*cis*-retinoic acid receptor (RXR) to form PPAR-α/RXR heterodimer and recruit nuclear receptor coactivator complexes for linking with the basal transcriptional element. AGGTCA G CTGTCA sequence represents the PPRE of the human acyl CoA oxidase gene. The synthetic (diamond) and natural or biological ligands (asterisk) interact with PPAR-α. (Redrawn from [114]).

1.4.6 Physiologic roles of PPAR-α

PPAR-α exerts an important physiological role in the control of lipid homeostasis. At both constitutive and inducible levels, PPAR-α regulates both peroxisomal and mitochondrial β-oxidation enzyme expression as well as CYP4A expression [105]. As discussed in Sections 1.2.7 and 1.3.2, the oxidative metabolism of fatty acids is catalysed by the three main groups of enzymes including microsomal ω-hydroxylase, peroxisomal and mitochondrial β-oxidation enzymes. While these three enzyme systems play a functionally different but complementary roles in the maintenance of lipid homeostasis, PPAR-α is an essential receptor that controls the expression of these enzymes. The role of the receptor in lipid homeostasis is not only critical under normal conditions but is also essential in physiological conditions known to cause a imbalance between cellular lipid uptake and utilisation such as fasting, fatty acid dietary overload and diabetes [99, 177, 178, 179]. The cross-talk among peroxisomal, microsomal and mitochondrial fatty acid oxidation systems and the regulatory role of PPAR-α is summarised in Figure 1.11.

In addition, PPAR-α has been reported to mediate the inducible effects of peroxisome proliferators on the activation of fatty acid transport and binding proteins as well as on decreasing triglyceride level [180, 181, 182]. PPAR-α regulates blood cholesterol and triglyceride levels through the modulation of apolipoprotein A-I and A-II gene expression [183]. Gene expression in response to dietary polyunsaturated fatty acids and other genes not involved in lipid metabolism is also mediated by PPAR-α [184]. PPAR-α has also been reported to play a role in mitogenesis and cell cycle control [99, 177, 178, 179].

1.4.7 Species differences in response to peroxisome proliferators

Significant species differences in response to peroxisome proliferators have been reported [62, 185, 186, 187, 188]. While rodents such as rats and mice are highly responsive, humans and other species including rhesus monkeys, dogs, guinea pigs and marmosets appear to be weakly or nonresponsive [137, 187, 189, 190, 191, 192, 193, 194, 195, 196]. In rat, potent peroxisome proliferators such as ciprofibrate, benzafibrate, and LY 1711883 caused a dose-related 10-, 8- and 5-fold increase in liver β-oxidation enzymes respectively. In dog and monkey treated under the same conditions, the

increase in liver β-oxidation enzymes was less than 2-fold [137, 189, 197, 198].

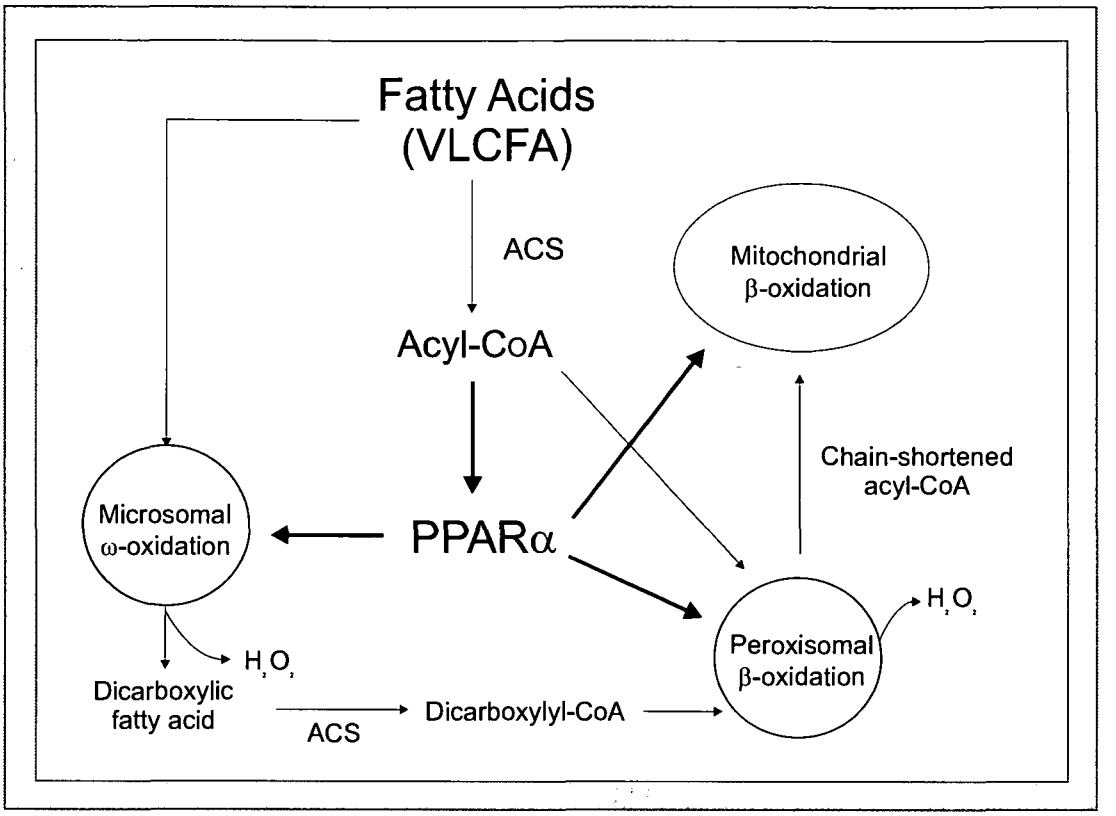

Figure 1.11: A schematic representation of the regulatory role of PPAR-α and cross-talk among peroxisomal, microsomal, and mitochondrial fatty acid oxidation systems.
Microsomal ω-oxidation catalysed by CYP4A generates dicarboxylic fatty acids which are further degraded by peroxisomal β-oxidation pathway. Fatty acyl-CoAs produced by peroxisomal β-oxidation are shunted to mitochondrial β-oxidation pathway for completion of oxidation. Acyl-CoA synthetase (ACS) converts fatty acid into acyl-CoA. VLCFA: very long chain fatty acid (Redrawn from [199]).

The molecular mechanism by which humans and nonhuman primates are either non-responsive or markedly less responsive is presently not fully understood. Species differences in response to peroxisome proliferators cannot be simply attributed to altered pharmacokinetics, disposition or metabolism of the peroxisome proliferators tested [194]. The nonresponsive nature of some species has been hypothesised to be due to fundamental deficiencies in PPAR-α [200]. For humans and guinea pigs, the lack of the receptor is not responsible for their refractory nature since both humans and guinea pigs possess a functional PPAR-α [149, 155, 185, 201, 202, 203]. While the gene specific binding sequence PPRE of the human acyl CoA oxidase gene has been reported as not being different from that of rodents [204] (reviewed in [137]), subsequent studies showed that this PPRE is inactive in most human individuals. This suggested a molecular basis for the nonresponsive nature of humans to peroxisome proliferators [205]. In addition, the transactivation response to peroxisome proliferators has been reported to differ. While the mouse and rat PPAR-α are more responsive to Wy-14,643 than the human receptor [201, 155], peroxisome proliferators induce the same potent lipid-lowering response in both human and rodents. This lipid-lowering response has been reported as being absolutely dependent on a functional PPAR-α [137, 183].

Species differences in response to peroxisome proliferators have important implications for the assessment of human safety and risk from peroxisome proliferators. In species that clearly exhibit peroxisome proliferation such as rodents, this profound response serves as an early indication of liver cellular carcinogenesis. In a species that is nonresponsive or weakly responsive to peroxisome proliferators, the response does not undergo the profound effect in its entirety [155, 206]. This explains the lack of increased cancer risk in humans following long-term therapeutic administration of the hypolipidemic drugs. In rat, acyclic monoterpenes found in *Eucalyptus* leaves such as citral have been reported to have the same effects of peroxisome proliferators in induction of CYP4A and peroxisomal β-oxidation enzymes. Since several marsupial species such as koalas digest a large amount of monoterpenes as their only food supply, it is essential to examine the effects of terpenes on the expression of these lipid metabolising enzymes in marsupial species.

1.5 XENOBIOTIC METABOLISM IN AUSTRALIAN MARSUPIALS

Detoxification and toxic effects of xenobiotics have been examined extensively in various mammalian species. Different sensitivity to the toxic effects of xenobiotics has been established to be attributed to the differences between species in xenobiotic-metabolising enzymes [37].

Unlike other mammals, several Australian marsupials such as the koala and the brush tail possum are capable of living wholly or partly on the leaves of certain *Eucalyptus* species, respectively (reviewed in [3]). *Eucalyptus* species are widely distributed throughout Australia and grow in a wide range of climatic environments [207]. *Eucalyptus* leaves contain high proportions of phenolics and essential oils, comprising up to 22% dry weight of leaf. *Eucalyptus* oil is a complex mixture of monoterpenes with its composition varying according to the *Eucalyptus* species, the age of the leaf, season and locality. For example, the oil from the *E. globulus* consists of 70% w/w cineol with large amounts of α-pinene, *d*-limonene and *p*-cymene [4]. Approximately 33-35% of the koala's digestible energy intake comes from the digestion of phenolics. Similarly, as much as 16% of the total digestible energy intake in the koala may be absorbed as essential oils [208]. While marsupial *Eucalyptus* feeders can consume as part of their diet several grams of *Eucalyptus* oil daily, a similar amount of *Eucalyptus* oil would be toxic to humans and other species [4, 209, 210, 211, 212] (reviewed in [3]). In order to tolerate such a high intake of *Eucalyptus* oil, it is hypothesised that *Eucalyptus* feeding marsupials have evolved efficient phase I and II enzyme systems to detoxify monoterpenes.

While much of the current information on xenobiotic metabolism in the literature derives from studies on rats, mice, rabbits and humans, a small number of studies examining xenobiotic metabolism in Australian marsupials have been published. These studies focussed mainly on cytochrome P450 (CYP) content and measurements of enzymatic activities with reference substrates (reviewed in [3]).

Early studies of xenobiotic metabolism in marsupials were carried out in the quokka (*Setonix brachyurus*) [213]. In this species, both the activities and the components of the P450 enzyme system, including P450, cytochrome b_5, and NADPH-cytochrome c reductase, were lower than in rat. Similarly, a lower hepatic metabolism rate was

found for other marsupial species examined relative to rat. These species include grey kangaroo (*Macropus fuliginosus*), bettong (*Bettongia penicillata*), short nose bandicoot (*Isoodon obesulus*) and brush tail possum (*Trichosurus vulpecula*). In addition, the development of the flavin-containing mono-oxygenase (FMO) system in the young of these marsupials was also slower than rat [214].

Higher hepatic CYP content and 7-ethoxyresorufin O-deethylase (EROD) activity was found in possums from a non-urban population as compared to those from urban population [215]. These differences were suggested to be due to potential *Eucalyptus* dietary effects. While in the non-urban possum population, *Eucalyptus* foliage would be the major food source, in urban areas, fruits, food scraps and other foliage are likely to constitute a major food source [215] (reviewed in [3]). Studies into the development of hepatic metabolising enzymes in the young of the possums indicated an increase in expression of the liver P450 enzyme system after weaning [216]. This suggested that exposure to chemicals from the diet may regulate the expression of these enzymes. In addition, higher CYPA4A activity and CYP content was found in the liver of the koala, an obligate *Eucalyptus* feeder, than is seen in livers of non-*Eucalyptus* feeders such as rat and humans [8].

The participation of P450 enzymes (phase I metabolising enzymes) in the metabolism of *Eucalyptus* terpenoids has been reported [217, 218, 219, 7]. Oxidative metabolism of dietary terpenes in the koala was first reported in 1975. In that study, novel monoterpenoid lactones were found to be excreted when the koala was fed on the leaf of *E. punctata*. These lactones originated from oxidative metabolism of α- and β-pinene to generate hydroxycarboxylic acids. These acids were then excreted unchanged or as labile glucuronides with subsequent cyclisation. Oxidative metabolism of 1,8-cineole was also observed in the brush tail possum with sex differences in the ratio of the enantiomers formed [4]. Both species- and sex-differences in phase I oxidative metabolism observed in marsupials suggest differences in the types and levels of metabolising enzymes [4, 213]. Species-specific patterns of urinary metabolite excretion were also found [220]. In general, marsupials relying solely on *Eucalyptus* leaves excreted extensively oxidised metabolites. Those relying partly on these leaves for their food excreted less oxidised metabolites which were also glucuronidated (review in [3]).

Phase II metabolism in marsupials has been examined using phenol as a model com-

pound. Marsupial species with various diets exhibited significant differences in phenol metabolism [221]. Folivorous marsupials such as koalas and brush tail possums showed a much lower (approximately 10-fold) capacity for sulfate conjugation of phenol than carnivorous marsupials such as the crested tailed marsupial rat or kowari (*Dasyroides byrei*). This may be due to limited protein and sulfate availability from the folivorous diet [221]. Phase II acetylation of sulphanilamide has been investigated in several marsupial species including the Tasmanian devil (*Sarcophilus harrisii*), brush tail possum, pademelon (*Thylogale billardierii*) and eastern-barred bandicoot (*Perameles gunnii*) [222].

While the induction of rat liver cytochrome P450s by *Eucalyptus* terpenes has been reported, few studies examined the adaptation of the marsupial folivores to their diet. In brush tail possums, the introduction of dietary terpenes into the diet has been found to increase the excretion of glucuronic acid in the urine. This was postulated to contribute to the increased phase II conjugation of the terpene metabolites. Liver microsomes from possums fed an artificial diet containing 1,8-cineole, α-pinene, p-cymene and limonene had a higher P450 content and also several other P450 activities than is seen in liver microsomes from control possums [6]. In rat, the induction of phase I metabolising enzymes, in particular CYP4A and the peroxisomal β-oxidation system, by *Eucalyptus* terpenes has also reported. In the koala, as mentioned previously, while higher liver CYP4A activity was observed, peroxisomal β-oxidation activity was found to be absent [8].

The hypothesis proposed by this project is that marsupials feeding on *eucalyptus* leaves, such as the koala, have evolved efficient phase I and phase II enzyme systems in order to detoxify dietary terpenes. From the preliminary findings in this laboratory (discussed in the project aims below), it is suggested that CYP4A enzymes and /or other parts of the peroxisomal metabolic system may be induced by dietary terpenes. This hypothesis was also based on the literature finding that terpenes were found to induce rat CYP4A [5]. Other CYP family such as CYP3A have been reported to be involved in the metabolism of terpenes [223]. This project will focus on CYP4A enzymes and the peroxisomal metabolic system.

1.6 PROJECT AIMS

Unlike other mammals, the koala has a unique restricted diet consisting exclusively of *Eucalyptus* leaves. Currently, knowledge of the metabolic capacity of koala and other Australian marsupials is limited, especially at the molecular level. Further research into the metabolic capacity of Australian marsupials is therefore clearly warranted.

Significant preliminary findings in this laboratory were a 3-fold higher mean cytochrome P450 content, a 3.5-fold higher microsomal CYP4A activity and an absence of liver total peroxisomal β-oxidation activity in koala livers, as compared to rat and other marsupials studied. Further studies of CYP4A, peroxisomal β-oxidation enzymes and PPAR-α has not been undertaken in the koala or any other marsupials. The present studies will contribute to our current understanding of the dependence of the koala on the highly specialised *Eucalyptus* terpene diet and provide primary molecular data on essential lipid-metabolising enzymes and PPAR-α.

The specific aims of these studies are:

1. To examine the effects of *Eucalyptus* monoterpenes on liver CYP4A, peroxisomal β-oxidation enzymes and PPAR-α expression in livers of possums given a mixture of monoterpenes for ten days.

2. To isolate a full-length koala liver *CYP4A15* cDNA and characterise the enzymatic properties of the cDNA-expressed CYP4A15 enzyme.

3. To isolate two putative types of koala liver acyl CoA oxidase (AOX) cDNA and establish the kinetic parameters of cDNA-expressed AOXI and AOXII.

4. To isolate and express a full-length koala liver PPAR-α cDNA.

5. To investigate expression of these lipid metabolising enzymes and PPAR-α at both protein and mRNA levels and examine their genomic DNA organisation across species.

6. To examine the morphology of peroxisomes in koala liver using tranmission electron microscopy (TEM).

Chapter 2

MATERIALS AND METHODS

2.1 CHEMICALS AND KITS

Reagents and kits required for analytical, enzyme assay and molecular procedures are listed in Tables 2.1.

Chemicals or kits	Supplier
Agar no. 3, tryptone, yeast extract	Oxoid Ltd. (Basingstoke Hampshire, UK)
Agfa G153A/B Developer, Agfa G153A/B Fixer	Agfa-Gevaert (Mortsel, Belgium)
Alcohol dehydrogenase, ampicillin bovine pancrease ribonuclease A, bovine serum albumin (BSA) Pentax fraction V, BSA (fatty acid free), bromophenol blue (sodium salt), Coenzyme A (CoA), deoxyribonuclease I (RNase free), diethyl pyrocarbonate (DEPC), ethylenediaminetetraacetic acid (EDTA), ethylmaleimide (NEM), flavin adenine	Sigma Chemical Co. (St. Louis, MO, USA)

Table 2.1: List of chemicals and kits required for experimental procedures.

Chemicals or kits (cont.)	Supplier (cont.)
Dinucleotide (FAD), durcupan ACM, formaldehyde, formamide, glucose-6-phosphate, glucose-6-phosphate dehydrogenase, herring sperm, DNA (free-acid), homovanilic acid, kanamycin A (monosulfate), 3-(N-Morpholino) propane-sulfonic acid (MOPS), NADPH, palmitoyl coenzyme A, peroxidase (POD), polyethylene glycol 8000, polyvinylpyrrolidone, proteinase K, unlabelled lauric acid, uric acid, uricase	Sigma Chemical Co (cont.) (St. Louis, MO, USA)
Aqueous counting scintillant (ACS), [1-14C]Lauric Acid, ultra-pure dNTP set (100mM), first-strand cDNA synthesis kit, mRNA purification kit	Amersham Pharmacia Biotech UK Ltd (Buckinghamshire, UK)
4-chloro-1-naphthol (4CN), 3,3' -diaminobenzidine (DAB), sodium dodecyl sulphate (SDS)	Bio-Rad Laboratories (Hercules, CA, USA)
DECA template^{TM} β-actin mouse probe	Ambion International (Austin, TX, USA)
DNA grade agarose, RNaseOUT ribonuclease inhibitor (recombinant) Dulbecco's Modified Eagle Medium (DMEM), restriction enzymes + 10X buffers, DNA marker, protein marker	Invitrogen (Mount Waverley, Vic, Australia)

Table 2.1 (continued): List of chemicals and kits required for experimental procedures.

Chemicals or kits (cont.)	Supplier (cont.)
Durcupan ACM mixtures 1 and 2	Fluka AG, Chemische Fabrik (Bucks, England)
Folin and Ciocalteu's reagent	Asia Pacific Specialty (APS) Chemicals Ltd (Seven Hills, NSW. Australia)
Guanidine HCl, isopropyl-β-D -thiogalactopyranoside (IPTG), low melt agarose, tetracycline HCl, 5-bromo-4-chloro-3-indolyl-β-galactoside (X-gal)	Progen Industries Ltd., (Darra Queensland, Australia)
Gigaprime DNA labelling kit	Geneworks (Thebarton, SA, Australia)
pCI-neo mammalian expression vector, restriction enzymes + 10X buffers, pGEM-T vector system	Promega Corporation (Madison, WI, USA)
QIAEX II gel extraction kit, QIAfilter midiprep spin kit, Qiagen plasmid maxi kit, Qiaprep spin miniprep kit, QIAquick nucleotide removal kit	Qiagen Pty. Ltd. (Victoria, Australia)
SMART RACE cDNA amplification Kit	Clontech Laboratories Inc. (Palo Alto, CA, USA)
XL1-blue *E.coli* strain cells, pCMV-Script pre-digested vector system	Stratagene (La Jolla, CA, USA)

Table 2.1 (continued): List of chemicals and kits required for experimental procedures.

Common laboratory solvents and other chemicals that are not listed were of at least analytical grade.

2.2 EQUIPMENT

Equipment used in experimental procedures is listed in Tables 2.2.

Equipment	Supplier
Agfa CP100 Automated Developer	Agfa-Gevaert N.V. (Mortsel, Belgium)
Air-cooled Thermal Cycler (PC-960)	Corbett Research (Australia)
Amersham Hypercassette with intensifying screen	Amersham Pharmacia Biotech UK Ltd (Buckinghamshire, England)
Beckman Optima XL-80 Ultracentrifuge	Beckman Instruments Inc. (Palo Alto, CA, USA)
DNA mini SubCell and SubCell Electrophoresis Systems	BioRad Laboratories (Hercules, CA, USA)
Eppendorf Centrifuge 5415C, Eppendorf Easypet 4420	Eppendorf- Netheler-Hinz GmbH (Hamburg, Germany)
Hoefer UVC 500 UV Crosslinker	Hoefer Scientific Instruments (San Francisco, CA, USA)
LKB 8800 ultratom III	LKB (Sweden)
Micromax OM2498 Minicentrifuge IEC	International Equipment

Table 2.2: List of equipment used in experimental procedures.

Equipment (cont.)	Supplier (cont.)
MP4R swinging bucket centrifuge	Company (IEC) (Needham Heights, MA, USA)
Philips EM 400	Philips (Holand)
Pipetman P20, P100, P200, P1000, P5000	Gilson (Villiers-le-Bel, France)
Ratek Orbital Mixer Incubator 0M10	Ratek Instruments Pty. Ltd. (Boronia, Victoria, Australia)
Micro Hybridisation Incubator 2000	Robbins Scientific Corporation (CA, USA)
Shimadzu UV-1601 UV-Visible Spectrophotometer	Shimadzu Corporation (Kyoto, Japan)
Sorvall Super speed Fixed-Angle RC5B Plus Centrifuge	DuPont Ltd. (Newtown, CT, USA)
Tri-Carb Liquid Scintillation Analyser	Canberra Packard Pty. Ltd. (Victoria, Australia)

Table 2.2 (continued): List of equipment used in experimental procedures.

2.3 CONTROL AND TERPENE-TREATED POSSUM TISSUES

Eight male common brush tail possum livers (4 treated and 4 control possums) were kindly donated by Dr Georgia Pass, University of Tasmania. These possum tissues have been used in other studies [6, 7, 224]. The possums were captured in wire cage traps in the urban area of Hobart (Tasmania), under National Parks and Wildlife Service's permission. The average weights of the possums were 4.19 ± 0.16 kg. The possums were initially kept in large holding enclosures ($6 \times 2 \times 2$m) in the Central Animal House (University of Tasmania). Four of the possums, randomly chosen for the terpene-treated group, were transferred to the Experimental Animal House (University of Tasmania) and housed in individual metabolism cages ($60 \times 45 \times 60$cm) under a 12:12 hour light:dark regime. The remaining four possums were allocated to the control group and housed in the Central animal house. Separate housing for the test and control groups was necessary due to the volatility of the tested terpenes [6, 7]. Briefly, control possums were fed an artificial diet containing apple, silverbeet, carrot, lucerne, brown sugar and water (39.6%, 26.6%, 8.2%, 4.5%, 3% and 14.9% wet matter, respectively) for 10 days prior to sacrifice. Treated possums were fed the same artificial diet into which 1,8-cineole, α-pinene, d-limonene and p-cymene were added. The amount of 1,8-cineole, α-pinene, d-limonene and p-cymene added into the wet mash were 566, 16, 69 and 214 mg/kg, respectively for the first 5 days, then 1212, 32, 138, and 428 mg/kg respectively, for the remaining 5 days. At the time of sacrifice, liver tissues from all animals were quickly removed, rapidly frozen in liquid nitrogen and stored at -80^{0}C until needed [7].

2.4 MARSUPIAL AND RAT TISSUES

Marsupial liver tissues were obtained from mature male koalas, wallabies, possums, and a single bandicoot, under the Adelaide Zoo and the Cleland Wildlife Park's permission (Adelaide, Australia). The animals, which were either road-injured or sustained injuries from domestic animal attacks or diseases, were ultimately euthanased using pentobarbital. Male Hooded Wistar rat liver tissues were obtained by scavenging the tissues from other projects. The animals were euthanased using pentobarbital. The use of these tissues was approved by the Ethics Committee of the Institute of Medical and Veterinary Science (IMVS).

Liver tissues: Liver tissues from all species were quickly removed at the time of death, rapidly frozen in liquid nitrogen and stored at -80^{0}C until required.

Morphological specimens: Liver sections for electron microscopy were immediately dissected within 5 minutes after sacrifice of the animals. The tissue sections were fixed in 2.5% (v/v) glutaraldehyde in 0.1 M sodium cacodylate buffer (pH 7.4) overnight, following routine procedures (Sections 7.3.2, 7.3.3 and 7.3.4) prior to processing into epoxide capsules for EM studies.

2.5 HUMAN TISSUE AND SAMPLES

The use of human liver tissue and samples in these studies had Flinders Medical Center Committee of Clinical Investigation approval and, where appropriate, the Coroner's permission.

Human liver tissues were obtained from four renal transplant donors from Flinders Medical Centre (Adelaide, Australia) who were maintained on life support systems until the kidneys could be removed. The liver sample was obtained within 30-60 minutes of removal of life support systems, quickly frozen in liquid nitrogen and stored at -80°C until needed. Human microsomes and cytosol samples were obtained under permit from the Department of Clinical Pharmacology, Flinders University of South Australia (SA, Australia). The human liver samples have previously been used in other studies [225, 226] and clinical details of the human livers have been published [227], as summarised in Table 2.3 (summarised from [227]).

2.6 CENTRIFUGATION

Small volume centrifugation was performed in eppendorf tubes using either an IEC Micromax^{TM} Minicentrifuge (model OM2498) at room temperature or in an Eppendorf Centrifuge 5415C at 4^{0}C. Larger volume centrifugations were accomplished in the Sorvall^{TM} Super speed Fixed-Angle RC5B Plus Centrifuge and the Beckman Optima XL-80 Ultracentrifuge for speeds up to and above 30,000 x g, respectively. Cells to be harvested from cell culture media were centrifuged in the swinging bucket IEC

Donor	Age	Sex	Smoking history	Alcohol	Drug treatment
H6	18	male	unknown	social	antibiotics (names not known)
H9	19	male	none	social	dopamine
H19	18	female	none	none	none
H21	52	male	unknown	unknown	unknown

Table 2.3: Clinical data of human liver donors.

Centra MP4R centrifuge.

2.7 BACTERIAL CELL CULTURE PREPARATION

Bacterial cells were grown in Luria Bertani (LB) broth (1% w/v tryptone, 0.5% w/v yeast extract and 1% w/v NaCl, pH 7) containing an appropriate antibiotic in an Orbital Mixer Incubator (Ratek Instruments) at 37^0C overnight with vigorous shaking. All media for bacterial culture were sterilised by autoclaving at 121^0C for 15 minutes. LB agar plates were prepared by adding 1% w/v of agar to the LB broth. After autoclaving and cooling to about 50^0C, appropriate antibiotics were added to the agar and poured into 90mm petri dishes. Routinely used antibiotics and their concentrations are summarised in Table 2.4. Antibiotics dissolved in water were sterilised by filtration through a 0.22 micron filter before use.

2.8 ANTIBODIES

Sheep anti-rat CYP4A polyclonal antibody was purchased from Chemicon International (UT, UK). Rabbit anti-human PPAR-α polyclonal antibody and mouse anti-rabbit secondary antibody, horseradish peroxidase (HRP) conjugated, were purchased from Santa Cruz (Germany). HRP-conjugated goat anti-sheep secondary antibody was obtained from Silenus Laboratories Pty. Ltd. (Boronia, Victoria, Australia).

Antibiotic	Stock concentration	Solvent	Working concentration
Ampicillin	50mg/ml	Water	100μg/ml
Kanamycin	10mg/ml	Water	50μg/ml
Tetracycline	12.5mg/ml	50% Ethanol	50μg/ml

Table 2.4: Routinely used antibiotics and their concentrations.

2.9 SUBCELLULAR HEPATIC FRACTION PREPARATION AND PROTEIN ASSAY

Preparation of hepatic microsomes, cytosol, post-nuclear supernatant and nuclear extracts were performed at 4^0C.

2.9.1 Microsomes and cytosol samples

Livers were homogenised in 0.1 M potassium phosphate buffer (pH 7.4) with 1.15% w/v KCl, using a Potter Elvehjem homogeniser. The homogenate was initially centrifuged at 9000 x g for 20 minutes, the supernatant collected and centrifuged at 108000 x g for 1 hour. The supernatant was reserved as cytosol and stored frozen at -80^0C until required. The microsomal pellet was resuspended in the above phosphate buffer and centrifuged at 108000 x g for 1 hour. The resultant microsomal pellet was resuspended in 0.1M phosphate buffer (pH 7.4) with 20% glycerol and kept at -80^0C prior to use.

2.9.2 Post-nuclear supernatants

For preparation of hepatic post-nuclear supernatant, liver was homogenised in cold 0.25M sucrose solution and the homogenate was centrifuged at 600 x g for 10 minutes. The resultant supernatant was used immediately for determination of peroxisomal

cyanide-intensive palmitoyl coenzyme A oxidation activity (Section 5.2.5).

2.9.3 Nuclear extracts

Nuclear extract was prepared using the method of Gebel *et al.*, [228]. Liver tissue was homogenised in three volumes of homogenisation buffer containing 20mM Tris-HCl (pH7.4), 1mM EDTA, 25mM KCl, 1mM PMFS (phenylmethanesulfonyl fluoride), 1mM DTT and 10% glycerol using 10 strokes of a drilling Teflon probe. The homogenate was centrifuged at 1000 x g for 5 minutes and the pellet obtained was resuspended in three volumes of the above homogenisation buffer. The resultant suspension was centrifuged at 1000 x g for 5 minutes to remove the remaining cytosol. After removal of the supernatant, the pellet was resuspended in two volumes of homogenisation buffer containing of 0.4M NaCl using a Potter Elvehjem homogeniser. The resultant suspension was stirred gently at 4^0C for 20 minutes with a magnetic stir bar and then centrifuged at 1000 x g for 1 hour. The collected supernatant representing the nuclear extract was stored at -80^0C until use.

2.9.4 Determination of protein concentration

Protein concentration was determined by a modification of the method of Lowry *et al.* [229]. Briefly, various hepatic fraction or cell lysate samples were diluted 1 in 20 in water to a final volume of 300μl. To the diluted samples were added 5ml of freshly prepared solution containing 0.28M Na_2CO_3, 0.1M NaOH, 1.4mM potassium sodium tartrate and 0.8mM $CuSO_4$, and the tube contents were incubated for 15 minutes at room temperature. To each sample was added 500μl Folin and Ciocalteus reagent (diluted 1:3 in water), mixed briefly and incubated for 15 minutes. The solution absorbances at 660nm were measured. The protein concentrations were calculated based on the standard absorbance curve, constructed by preparing a standard range of concentrations using BSA.

2.10 IMMUNOBLOT ANALYSIS

Fifty micrograms of microsomal, cytosolic or nuclear extract were separated by sodium dodecylsulfate-polyacrylamide gel electrophoresis (SDS-PAGE) on a 7.5% resolving

gel and 5% stacking gel, according to the procedure of Laemmli [230]. A prestained protein ladder (GibcoBRL, Rockville, MD, USA) was used as a reference. Prior to electrophoresis, all samples were heated to 100°C for 10 minutes. Following electrophoresis, proteins were transferred to nitrocellulose membrane (NitroBind, MIS, MA, USA) in 25mM Tris-HCl, 192mM glycine and 20% v/v methanol at 50V using a Hoefer (CA, USA) TE series transfer electrophoresis unit. The immunobloting procedure was accomplished essentially as described by Towbin and Gordon [231]. The filter was washed twice with Tween Tris buffered saline (TTBS containing 0.05% v/v Tween-20 in 16mM Tris-acetate and 500mM sodium chloride) and non-specific binding sites were blocked by incubating the filter in 5% w/v skim milk at 37°C for 1 hour. Immunoreactivity was detected by incubation with a corresponding primary antibody at 37°C overnight, followed by incubation with a corresponding horseradish peroxidase (HRP)-conjugated secondary antibody at 37°C for 1 hour. The reaction was detected by exposing the treated membrane to HRP colour development reagent [0.05% w/v 3,3'-diaminobenzidine (DAB) and 0.05% v/v hydrogen peroxide in 20mM imidazole buffer (pH 7.4)] to visualise the presence of immunoreactive proteins.

2.11 SPECTRAL DETERMINATION

2.11.1 Total cytochrome P450 content

Total cytochrome P450 content was determined by the method of Omura and Sato [29] using an absorption coefficient for the difference spectrum (450 to 490 nm) of 91 mM^{-1} cm^{-1}. Reduced-CO bound vs reduced difference spectra were determined after bubbling the sample cuvette with carbon monoxide.

2.11.2 Nicotinamide-adenine dinucleotide (NAD) and NADP (NAD phosphate) contents

Hepatic nicotinamide cofactor contents were measured at room temperature, essentially by the procedure of Klingenberg [232] as described in Section 3.2.3.

2.12 ENZYME ACTIVITY ASSAYS

2.12.1 Lauric acid hydroxylation

Lauric acid hydroxylase activity (a CYP4A activity marker) was determined using a modification of the method described by Parker and Orton [233] as described in Section 3.2.4.

2.12.2 Peroxisomal cyanide-insensitive fatty acid β-oxidation

Peroxisomal cyanide-insensitive fatty acid β-oxidation activity was determined essentially as described by Lazarow [234] as described in Section 3.2.5.

2.12.3 Palmitoyl-CoA oxidase activity

Palmitoyl-CoA oxidation, a measure of Acyl CoA oxidase (AOX) activity, was accomplished using a modification of the method described by Veldhoven using palmitoyl-CoA as the substrate as described in Section 5.2.5 [235].

2.13 GENERAL MOLECULAR CLONING METHOLOGY

2.13.1 Competent *E.coli* cell preparation

Preparations of competent cells, DH5α and XL1-blue *E.coli* strains, were performed using a calcium chloride method. Briefly, 30ml LB broth (containing tetracycline for XL1-blue and no antibiotic for DH5α) was inoculated with 0.5ml of an overnight culture and incubated at 37^0C until the OD of the culture at 600nm was between 0.3 and 0.4 (log phase). The cells were retrieved by centrifugation at 3000 x g for 15 minutes at 4^0C and resuspended in 15ml of cold 50mM $CaCl_2$. The cells were then recovered by further centrifugation, resuspended again in 3ml of cold $CaCl_2$ and placed on ice for 45 minutes. Sterile glycerol was added to a final concentration of 25% and cells were stored at -80^0C in small aliquots.

2.13.2 Ligation reactions

To check the efficiency of ligation into a vector, a series of control ligation reactions were set up: a ligation reaction with *Hind* III restricted lambda DNA to ensure that the ligase was active; a ligation reaction with control insert DNA (supplied) to check if the ligation was proceeding efficiently; a ligation reaction with cut plasmid to determine the number of background colonies; a ligation reaction with an uncut plasmid to check the transformation efficiency of the competent cells. Optimisation of insert vector molar ratios was performed using 1:3, 1:1, and 3:1 insert: vector molar ratio.

Ligation into pCMV-Script vector: Ligation reactions were set up using appropriate amounts of cDNA insert with 0.5μl T4 DNA ligase 10x buffer, 0.5μl rATP, 0.5μl DNA ligase (4 Weiss units/μl), 1μl pCMV-Script vector (10ng/μl) and sterile distilled water to a final volume of 5μl.

Ligation into pGEM-T or pCI-neo vectors: Ligation reactions were set up using appropriate amounts of cDNA insert with 1μl T4 DNA ligase 10x buffer or 5μl T4 DNA ligase 2x buffer, 1μl DNA ligase (3 Weiss units/μl), 1μl pGEM-T or pCI-neo vector (10ng/μl) and sterile distilled water to a final volume of 10μl.

The reaction mixtures were mixed gently by pipetting and then incubated at 4^0C overnight. One to 5μl of the ligation mixture was then used to transform 100μl of competent cells in subsequent transformation reactions.

2.13.3 Transformation of DNA into competent cells

Ligation reaction (2 to 5μl Section 1.13.2) was mixed gently with 100μl competent cells and placed on ice for 45 minutes. The cells were then heat shocked at 42^0C for 90 seconds and placed on ice for 2 minutes. The cells were allowed to recover in 1ml of LB broth at 37^0C for 90 minutes with gentle agitation. The cells were centrifuged briefly, resuspended in 100μl LB and then plated onto LB ampicillin (for transformation into pGEM-T or pCI-neo vectors) or kanamycin (for transformation into pCMV-Script vector) plates. The plates were incubated at 37^0C overnight. For colour selection of certain plasmids (pGEM-T or pCMV-Script vectors which contain the Lac-Z gene), IPTG (0.4M) and X-gal (50mg/ml) were added to the cell suspension at final concentrations of 0.067M and 0.83% (w/v), respectively, prior to plating.

Bacterial cells harbouring recombinant plasmid DNA appeared as white colonies.

2.14 PLASMID DNA PREPARATION

2.14.1 Small scale purification of plasmid DNA

Small scale plasmid DNA isolation for screening of recombinant cDNA clones was performed using a modification of the alkaline lysis method, which utilised the addition of a base to lyse the cells and phenol/chloroform extraction to purify the plasmid. Plasmid DNA for sequencing was isolated using the Qiaquick spin miniprep kit.

Alkaline lysis method: LB broth (5ml) containing appropriate antibiotic was inoculated with a single isolated bacterial colony (Section 2.7) and incubated at 37^0C overnight with shaking. Cells were harvested by centrifugation for 1 minute at 1000 x g, resuspended in 150μl of ice-cold resuspending buffer (50mM of glucose, 25mM Tris-HCl, pH 8.0, and 10mM EDTA) and placed on ice for 20 minutes. 300μl of cell lysis solution (2.0N NaOH and 1% w/v SDS) was added, mixed gently and placed on ice for 15 minutes. Ice-cold 3M potassium acetate, pH 4.8, (150μl) was added to neutralise the solution and to precipitate cell debris, and chromosomal DNA. The samples were placed on ice for 15 minutes and then centrifuged for 5 min. The supernatant was phenol (TE equilibrated, pH 8.0)/chloroform (1:1) extracted, chloroform extracted and then ethanol precipitated. The DNA pellet was washed with 70% ethanol, briefly dried, resuspended in appropriate volume of sterile water and stored at 4^0C until needed.

Qiaquick spin miniprep: Preparation of plasmid DNA by Qiaquick spin miniprep kit was performed at room temperature according to the manufacturer's protocol. Briefly, 3ml of the overnight culture was centrifuged for 30 seconds at 1000 x g and the pellet was resuspended in 250μl buffer P1. 250μl buffer P2 was added and the tube was inverted gently then left at room temperature for 5 minutes. To the lysed cell suspension was added 350μl buffer N3, mixed immediately and centrifuged for 10 minutes. The supernatant was applied to the Qiaprep spin column and the column was centrifuged for 1 minute. Buffer PE (750μl) was added and the column was centrifuged for 1 minute then centrifuged again for another minute to remove residual ethanol. Warm sterile water was added to the column and the column was

centrifuged for 1 minute to elute the plasmid DNA. P1, P2, N3 and PE buffers were supplied by the manufacturer.

2.14.2 Large scale purification of plasmid DNA

Large scale purification of plasmid DNA was performed using the Qiagen Maxi Plasmid Purification Kit as described in the manufacturer's protocol. Briefly, 100ml of LB containing an appropriate antibiotic was inoculated with 200μl overnight culture (Section 2.7) and incubated at 37^{0}C overnight with vigorous shaking. Cells were retrieved by centrifugation at 3000 x g for 10 minutes at 4^{0}C and resuspended in 10ml buffer P1. To the tube was added 10ml buffer P2 to lyse the cells, inverted a few times and left at room temperature for 5 minutes. Ice-cold buffer P3 (10ml) was added and the tube was mixed gently by inverting a few times then placed on ice for 20 minutes. The tube contents were centrifuged at 11,000 x g for 30 minutes at 4^{0}C to pellet cell debris. The supernatant was added to the Qiagen tip-500 column, which was equilibrated prior to centrifugation by applying 10ml of buffer QBT, and allowed to flow by gravity. The column was washed twice with 30ml QC buffer and plasmid DNA was eluted with 15ml QF buffer. To the eluate was added 10.5ml isopropanol and the tube contents mixed then centrifuged at 11,000 x g for 30 minutes at 4^{0}C. The DNA pellet was washed with ice-cold 70% ethanol, briefly dried, resuspended in appropriate volume of sterile water and stored at 4^{0}C until needed. P1, P2, P3, QBT, QC and QF buffers were supplied by the manufacturer.

2.14.3 Purification of plasmid DNA for transfection

For transfection into Cos-7 cells, high quality plasmid DNA was isolated using the QIAfilter Midiprep Spin Kit according to the manufacturer's instructions. Briefly, cells from a 25 ml bacterial cell culture containing recombinant cDNA clone in pCMV-Script XR or pCI-neo vector were retrieved by centrifugation at 3000 x g for 10 minutes at 4^{0}C and resuspended in 4ml buffer P1. To the tube was added 4ml buffer P2 to lyse the cells, mixed and placed at room temperature for 5 minutes. Ice-cold buffer P3 (4ml) was added, the tube contents were mixed gently and immediately poured into the QIAfilter cartridge then placed at room temperature for 10 minutes. The lysate was filtered gently into the Qiagen tip-100 column, which was equilibrated prior to centrifugation by applying 4ml of buffer QBT and allowed to flow by grav-

ity. The column was washed twice with 10ml QC buffer and plasmid DNA was eluted with 5ml QF buffer. To the eluate was added 3.5ml isopropanol and the tube contents were mixed then centrifuged at 11,000 x g for 30 minutes at 4^0C. The DNA pellet was washed with ice-cold 70% ethanol, briefly dried, resuspended in an appropriate volume of sterile water and stored at 4^0C until needed.

2.15 DNA ANALYSIS

2.15.1 Restriction digest of DNA

Following purification of plasmid DNA, a restriction digest was performed to screen DNA plasmid for the correct size inserts or to prepare cDNA probes for Northern and Southern blotting. Restriction digests were also performed to produce appropriate sticky ends of PCR amplified cDNA fragment prior to subcloning into pCMV-Script XR or pCI-neo mammalian expression vectors. Restriction digests were set up using 2 to 5U of each restriction enzyme, 0.4 to 1μg of DNA, in 1X buffer and sterile water to a final volume of 20μl. The restriction reactions were carried out at 37^0C for at least 2 hours or overnight.

2.15.2 Electrophoresis and visualisation of DNA

DNA fragments were separated by electrophoresis on agarose gels, which were prepared by melting an appropriate amount of agarose in 1 X TAE (1mM EDTA, pH 8.0 and 40mM Tris-acetate). For extraction of PCR amplified products, low-melt agarose gels from 0.7 to 1.% w/v were used, depending on the size of the DNAs. DNA fragments were visualised by adding ethidium bromide to the melted agarose to a final concentration of 0.5μg/ml and viewed under UV illumination. Gel electrophoresis was performed using the DNA SubCell Electrophoresis System at 10V/cm of the gel or at lower voltage when low-melt agarose was used to minimise the amount of heat generated in the tank. 100bp DNA ladder and λ DNA restricted with *Hind III* were used as DNA molecular weight makers.

2.15.3 Extraction of DNA fragments from agarose gels

Extraction of the DNA from the agarose gel was performed using the QIAEX II Gel Extraction Kit according to the manufacturer's protocol. Exposure to UV illumination was reduced to minimise damage to the DNA. Following electrophoresis, the portion of agarose gel containing the desired DNA fragment was excised, divided into 250mg portions, and placed into sterile eppendorf tubes. To the tubes were added 750μl QX1 buffer and 10μl of DNA QX2 resin suspension and mixed by vortexing. The tubes were then incubated at 55^{0}C for 10 minutes, centrifuged at 10,000 x g for 30 seconds and the resin pellet was washed with 500μl QX1 buffer to remove traces of agarose. After washing twice with 500μl buffer PE, the resin pellet was air dried for 5 to 10 minutes, resuspended in 20μl sterile water and incubated at 55^{0}C for 5 minutes to increase yield. The tubes were centrifuged at 10,000 x g for a minute and the DNA supernatant was collected and stored at 4^{0}C until required. QX1, QX2 and PE buffers were supplied by the manufacturer.

2.15.4 Quantification of DNA

Quantification of DNA was performed using the Shimadzu UV-1601 UV-Visible Spectrophotometer, by measuring the absorbance of the diluted DNA solution (1 in 1000 or 1 in 500 in sterile distilled water) at 260nm and 280nm. The purity of the DNA was determined by the ratio of the absorbance at 280nm to that at 260nm. The absorbance reading of 1 at 260nm corresponds to a DNA concentration of 50μg/ml of double stranded DNA.

2.16 DNA SEQUENCING

2.16.1 Sequencing primers

Sequencing of cDNA cloned in pGEM-T, pCMV-Script and pCI-neo vectors was accomplished using commercially available sequencing primers including M13 universal primer, M13 reverse primer, T3, T7 and $T7_{PCI}$, purchased desalted from Geneworks (Adelaide, Australia), and internal primers derived from known cDNA sequences. $T7_{PCI}$ primer sequence was modified from T7 primer in order to sequence cDNA clones inserted in the pCI-neo vector (Promega, Madison, WI, USA). Commonly

used commercial sequencing primers are listed in Table 2.5.

Sequencing primer	Nucleotide sequence (5'- 3')
M13 universal sequencing primer	GTA AAA CGA CGG CCA GT
M13 reverse sequencing primer	CAC ACA GGA AAC AGC TAT GAC CAT G
T3 primer	AAT TAA CCC TCA CTA AAG GG
T7 primer	GTA ATA CGA CTC ACT ATA GGG C
$T7_{PCI}$	TTA ATA CGA CTC ACT ATA GGC

Table 2.5: List of sequencing primers

2.16.2 Sequencing reaction

Each sequencing reaction was set up using 400ng of DNA, 8μl of the ABI Prism^{TM} Big-Dye reaction mix, 3.2pmole primer and sterile water in a final reaction volume of 20μl. The sequencing reaction was cycled for 25 cycles of 96^{0}C for 10 seconds, 50^{0}C for 5 seconds and 60^{0}C for 4 minutes. ABI Prism^{TM}Big-Dye reaction mix was purchased from Perkin Elmer through the IMVS, Adelaide and consists of A/C/G/T-dye terminates, Tris-HCl, $MgCl_2$, thermal stable pyrophosphatase and AmpliTaq DNA polymerase (FS).

Following cycling, the sequencing reaction was precipitated by adding 80μl 75% isopropanol, left at room temperature for 15 minutes, and then centrifuged at 10,000 x g for 25 minutes. The DNA pellets were washed with 200μl 75% isopropanol, dried and forwarded to the Molecular Pathology Sequencing Centre, IMVS, Adelaide, for analysis by electrophoresis in the Perkin Elmer ABI Prism 377 Sequencer.

2.16.3 DNA sequence analysis

Data obtained from the sequencing reactions were analysed using the MacVector^{TM} computer program (Version 6.5.3, Oxford Molecular Limited, 2000). ClustalW alignment of cDNA clone sequences was accomplished against sequences from other species

obtained from the GenBank database (http://ncbi.nlm.nih.gov/blast).

2.17 cDNA PROBE PREPARATION AND LABELLING

DECAtemplate^{TM} β-actin mouse cDNA probe (10ng/μl) was used as a loading control for Northern blot analysis. Koala CYP4A, AOX and PPAR-α cDNAs probes were prepared either by PCR amplification (Section 2.21.2) or restriction digest (Section 2.15.1) of plasmid DNA with the correct size insert. After the identity of the cDNA was confirmed by sequencing, the cDNA fragments were purified (Section 2.15.3 and 2.14.3) and labelled with α-^{32}P-dCTP using the Gigaprime cDNA Labelling Kit according to the manufacturer's protocol. Briefly, to denatured DNA (25ng in 7μl volume of distilled sterile water previously denatured at 95^{0}C for 10 minutes) was added 6μl decanucleotide solution, 6μl Buffer C, 5μl ^{32}P-dCTP (3000Ci/mM, 10mCi/ml) and 1μl Klenow enzyme (5I.U./ml). The tube was mixed by pipetting and incubated at 37^{0}C for 15 to 30 minutes. The reaction was terminated by the addition of 1μl 0.5M EDTA (pH 8.0) and non-incorporated nucleotides were removed from the labelled probe using the QIAquick Nucleotide Removing Kit as per the manufacturer's instructions. To the labelled probe was added 250μl Buffer PN and the tube contents were applied to the supplied column then centrifuged at 5000 x g for 30 seconds. The column was washed twice with 500μl of Buffer PE to remove traces of impurities by centrifuging at 5000 x g for 30 seconds. Sterile distilled water, 200μl was added and the column was centrifuged at 10,000 x g for 1 minute to elute the cDNA probe. The specific activity of the labelled probe was assessed by liquid scintillation counting with a count of 1.0 x 10^{8}cpm/μg of DNA considered acceptable.

2.18 SOUTHERN BLOT ANALYSIS OF GENOMIC DNA

2.18.1 Genomic DNA extraction

To approximately 0.1g of minced liver tissue was added 700μl of extraction buffer (50mM Tris, pH 8.0, 100mM EDTA, pH 8.0, 100mM NaCl and 1% w/v SDS) and

18μl of proteinase K (20μg/μl). The tube was incubated at 58^{0}C overnight and then centrifuged at 10,000 x g for 5 minutes at room temperature. To the collected supernatant was added 600μl of 100% isopropanol, the tube was inverted gently and the DNA pellet was lifted out with a sealed micropipette. The pellet was rinsed in 70% v/v ethanol and air-dried for 10 minutes. Genomic DNA pellet was dissolved in 300μl sterile water, phenol (TE-equilibrated)/chloroform (1:1) extracted, chloroform extracted, and precipitated with 0.1 volume of 3M sodium acetate, pH 5.2 and 2 volumes of ice-cold 100% ethanol at -20^{0}C for 2 hours. The DNA pellet was recovered by centrifugation at 10,000 x g for 20 minutes at 4^{0}C, washed in 70% ethanol, dried briefly, and resuspended in distilled sterile water.

2.18.2 Electrophoresis of genomic DNA

Genomic DNA samples (20 μg) were digested with *EcoR* 1 overnight at 37^{0}C. A second aliquot of *EcoR* 1 was added to the reaction mixture and the digestion was performed for another 6 hours at 37^{0}C to ensure complete digestion. DNA fragments were then separated by gel electrophoresis (Section 2.15.2) through a 0.7% w/v agarose gel at very low voltage (<1V/cm) overnight to ensure complete separation.

2.18.3 Capillary transfer of genomic DNA to nylon membrane

Following electrophoresis, the gel was visualised under UV illumination to confirm complete separation of DNA. Before transblotting, the gel was soaked in 1.5M NaCl and 0.5N NaOH for 45 minute and then in 1M Tris (pH 7.4) and 1.5M NaCl for 45 minutes. The treated gel was inverted and placed on the wick of the DNA apparatus with the bottom left hand corner being removed for orientation. The DNA apparatus was established by placing a piece of Whatman paper, previously soaked in transblotting buffer 10X SSC (1 X SSC: 0.15M NaCl, 15mM $Na_3C_6H_5O_7.2H_2O$, pH 7.0), on a glass plate support inside a large baking dish filled with the same blotting buffer. The gel was surrounded with plastic wrap to create a barrier to prevent liquid from flowing directly from the reservoir to the paper towels placed on top of the gel. A piece of nylon filter, previously soaked in 10 X SSC, was placed on top of the gel. The filter was overlayed with 2 sheets of pre-soaked Whatman paper, a 5-8cm high stack of absorbent paper was placed on top of the Whatman paper, and a 500g weight was placed over the paper to enhance capillary action. DNA transfer was allowed to

proceed overnight in 10 X SSC. After transfer, the gel was visualised with ethidium bromide under UV illumination to check the efficiency of the transfer. The DNA was fixed onto the nylon membrane by UV cross linking (120mJ/cm2).

2.18.4 Prehybridisation and hybridisation of membranes with α-^{32}P-labelled cDNA probe

Prehybridisation was accomplished at 42^{0}C for at least 2 hours in hybridisation solution containing 50% deionised formamide, 5 X Denhardt's solution, 6 X SSC, 0.5% w/v SDS, and 0.1mg/ml heat denatured sheared herring sperm DNA. The labelled probe (Section 2.17) was denatured by heating at 95^{0}C for 10 minutes, added to the prehybridised membrane (in fresh hybridisation solution) and allowed to bind at 42^{0}C overnight. Unbound probe was removed using a series of low to high stringency wash conditions as follows: twice in 6 X SSC and 0.5% w/v SDS at room temperature for 15 minutes, twice in 1 X SSC and 0.5-1% w/v SDS at 37^{0}C for 15 minutes, once in 0.1 X SSC and 1% w/v SDS at 37^{0}C for 15 minutes, then in the same solution at temperatures increased gradually to 65^{0}C. The degree of stringency in the washing condition was dependent on the specificity of the probe to the DNA on the nylon membrane and the procedure varied between experiments. After rinsing briefly in 4 X SSC to remove the SDS, the filter was placed in autoradiograph cassettes with intensifying screens and exposed to autoradiograph film at -80^{0}C for several days. Films were developed using the Agfa CP100 Automated Developer.

2.19 RNA EXTRACTION AND PURIFICATION

2.19.1 Control of RNase activity

To obtain high quality RNA preparations, it was important to minimise the activity of RNases liberated during cell lysis and to avoid the accidental introduction of trace amounts of RNases from other potential sources in the laboratory. General laboratory glassware was baked at 180^{0}C overnight prior to use. Plastic ware and other equipment were rinsed in diethyl pyrocarbonate (DEPC) treated water (0.1%) overnight and then autoclaved for 15 minutes at 121^{0}C to remove traces of DEPC that might modify purine residues in RNA by carboxymethylation. Milli-Q grade water and all solutions used in the preparation of RNA were also treated with 0.1%

DEPC overnight at room temperature and then autoclaved for 15 minutes. Other solutions were prepared using DEPC-treated water and molecular grade chemicals that were free of RNAase and DNAase, where possible.

2.19.2 Total RNA extraction

RNA extraction was performed using a modification of the method described by Chomczynski and Sacchi [236]. The phenol-chloroform extraction step of total RNA was repeated twice in order to obtain cleaner RNA. Approximately 1g of tissue was homogenised with 10ml freshly prepared denaturing solution (4M guanidium thiocyanate, 25mM sodium citrate, 0.5% N-laurylsarcosine, 0.1M 2-mercaptoethanol). To the homogenised tissues were added 1ml of 2M sodium acetate, pH 4.0, 10ml of phenol (DEPC-treated water saturated) and 2ml of chloroform:isoamyl alcohol (49:1) and mixed vigorously for 15 seconds. The tube contents were stored on ice for 15 minutes, then centrifuged at 11,000 x g at 4^0C for 20 minutes and the supernatant was collected. When needed, the solution was phenol, chloroform and isoamyl alcohol extracted again. An equal volume of isopropanol was added to the supernatant and stored at -20^0C for at least 1 hour to precipitate the RNA. After centrifugation at 11,000 x g for 20 minutes at 4^0C, the RNA pellet was dried briefly and resuspended in 300μl denaturing solution. To the resuspended RNA was added 300 μl isopropanol and the RNA was allowed to precipitate at -20^0C overnight. The solution was centrifuged at 4^0C for 15 minutes and the supernatant was discarded. The RNA pellet was rinsed in 70% ethanol, dried briefly and resuspended in 200μl DEPC-treated water. RNA was stored at -80^0C in small aliquots as ethanol precipitates or in DEPC-treated water with 0.2 I.U./l of RNaseOUT Ribonuclease inhibitor.

2.19.3 Messenger RNA purification

Purification of mRNA from total RNA samples was performed using the mRNA purification kit (Amersham Pharmacia, USA) as per the manufacturer's protocol. Spin columns were prepared by washing the oligo(dT)-cellulose twice with 1ml high salt buffer (10mM Tris-HCl, pH 7.4, 1mM EDTA and 0.5M NaCl). Approximately 1.25mg total RNA was dissolved in 1ml elution buffer (10mM Tris-HCl (pH 7.4) and 1mM EDTA) and the sample was heated at 65^0C for 5 minutes then placed on ice. To the tube was added 200μl sample buffer (10mM Tris-HCl (pH 7.4), 1mM EDTA and

3.0M NaCl) and the tube contents were poured into the prepared column then allowed to drain by gravity. The columns were centrifuged at 350 x g for 2 minutes at room temperature, washed twice with 250μl high salt buffer and three times with 250μl low salt buffer (10mM Tris-HCl (pH 7.4), 1mM EDTA and 0.1M NaCl). Between each wash, the columns were centrifuged at 350 x g for 2 minutes. The mRNA was eluted by applying 4 x 250μl elution buffer, preheated at 65^{0}C, to the column and centrifuging at 350 x g for 2 minutes. The eluted mRNA was precipitated with 100μl sample buffer, 10μl glycogen (10mg/ml) and 2ml of ethanol and stored at -20^{0}C overnight. mRNA pellet was recovered by centrifugation at 12,000 x g for 20 minutes at 4^{0}C, resuspended in DEPC treated water and stored at -80^{0}C in small aliquots as ethanol precipitates or with 0.2 I.U. / l of RNaseOUT Ribonuclease inhibitor.

2.19.4 Quantification of RNA and mRNA

Quantification of RNA and mRNA was performed as described for DNA (Section 2.15.4) except that absorbance reading of 1 at 260nm corresponds to a RNA concentration of 40μg/ml of single stranded RNA.

2.20 NORTHERN BLOT ANALYSIS

2.20.1 Electrophoresis of RNA through denaturing formaldehyde agarose gels

Formaldehyde gel electrophoresis of mRNA was accomplished according to the procedure adapted from those of Lehrach *et al.*, Goldberg, and Seed [237, 238, 239] (summarised in [240]). Briefly, denaturing formaldehyde gels were prepared by melting 1% agarose in DEPC-treated water and allowed to cool to about 50^{0}C before adding 1 X formaldehyde gel running buffer and formaldehyde to a final concentration 7.2% v/v. The molten gel was poured into the tray and allowed to set at room temperature for approximately 45 minutes. To 4 to 10μg mRNA was added 1 X formaldehyde gel running buffer (20mM MOPS, 8mM sodium acetate and 1mM EDTA pH 8.0), formaldehyde (7% w/v), deionised formamide (50% v/v) and DEPC-treated water to a final volume of 20μl. The tube contents were heated at 65^{0}C for 15 minutes and chilled quickly on ice. RNA loading dye (final concentration 4% glycerol, 0.8mM

EDTA, pH 8.0, and 0.3mM bromophenol blue) was then added to the RNA samples and mixed thoroughly. Prepared mRNA samples were loaded quickly, electrophoresed at 10V/cm of the gel for 10-15 minutes, and then electrophoresed at 5V/cm for at least 3 hours. The integrity of total and mRNA was assessed by UV illumination with ethidium bromide prior to RNA blotting.

2.20.2 Capillary transblotting

Before transblotting, the gel was treated in 0.05N NaOH and 0.15M NaCl for 30 minutes to denature the mRNA, rinsed briefly in DEPC-treated water and then soaked in 0.1M Tris (pH 7.5) and 0.15M NaCl for another 30 minutes to neutralise the mRNA. Messenger RNA was transferred onto a nylon membrane by capillary transfer as described for Southern blot in Section 2.18.3. After transblotting, the mRNA was fixed onto the nylon membrane by cross linking with UV light (120mJ/cm2) and stored at 4^0C until needed. The gel was then stained with ethidium bromide for 15 minutes and then visualised under UV illumination to check the efficiency of the transfer.

2.20.3 Prehybridisation and hybridisation of membranes with α-^{32}P-labelled cDNA probe

Prehybridisation and hybridisation with α-^{32}P-labelled cDNA probe were performed in 50% formamide at 42^0C as described for Sorthern blot analysis in section 2.18.4 except that 5 X SSC was used instead of 6 X SSC.

2.21 POLYMERASE CHAIN REACTION

2.21.1 First-strand cDNA synthesis

Synthesis of first-strand cDNA was performed using the First-Strand cDNA Synthesis Kit (Amersham Pharmacia, England, UK), essentially as described by the manufacturer's protocol. mRNA (10ng) in a volume of 8μl with RNase-free water was heated to 65^0C for 10 minutes and chilled on ice. To the tube was added 5μl of Bulk First-strand cDNA Reaction Mix (Cloned, FPLCpure Murine Reverse Transcriptase, RNA-guard (porcine), RNase/DNase-free BSA (0.24mg/ml), 135mM Tris (pH 8.3), 204mM

KCl, 27mM $MgCl_2$, 54mM of each dNTP), 1μl dithiothreitol (DTT) (200mM) and 1μl Not 1-d(T)18 bifunctional primer (0.2mg) (5'd[AAC TGG AAG AAT TCG CGG CCG CAG GAA T18]-3') and the tube contents were mixed and incubated at 37^{0}C for 1 hour, then stored at -20^{0}C until required.

2.21.2 Reverse transcription-polymerase chain reaction (RT-PCR)

Oligonucleotide primers: Oligonucleotide primers for PCR were custom-made by Sigma Genosys (Castle Hill, NSW, Australia). Primer design was based on conserved regions of aligned cDNA sequences of various species obtained from GenBank.

PCR reaction: PCR amplification was performed in an Air-cooled Thermal Cycler (PC-960) (Corbett Research, Australia). A standard 20μl PCR reaction was set up using 1μl first-strand cDNA template, 1 X PCR reaction buffer (20mM Tris pH 8.4, 50mM KCl), 250μM of each dNTP, 0.1μg of each forward and reverse primer, 1.5 I.U. Taq DNA polymerase (Qiagen) and varying concentrations of magnesium. DNA amplified by PCR was purified from low-melt agarose gel as described in Section 2.14.3

2.21.3 Rapid amplification of cDNA ends (RACE)

Rapid amplification of cDNA ends (RACE) was performed using the SMART RACE cDNA Amplification Kit (Clontech, Palo Alto, CA, USA) according to the manufacturer's instructions. RACE amplification was accomplished using Universal Primer Mix (UPM) and reverse gene specific primers, derived from known sequences (Sections 4.2.1, 5.2.1, 6.2.1), and 5' RACE ready cDNA as template. Details of the UPM (made up of two primers) are described in Table 2.6.

Synthesis of koala and control 5' RACE ready cDNAs: Synthesis of koala and control 5' RACE ready cDNAs was performed essentially as per manufacturer's protocol. Koala mRNA was extracted as per Section 2.19.3. SMART RACE first-strand cDNA synthesis reaction was set up in a final volume of 5μl containing 1μg koala mRNA (for koala 5' RACE ready cDNA synthesis) or human placenta total RNA (for control human placenta 5' RACE ready cDNA synthesis), 1μl 5' RACE cDNA synthesis primer (10μM, 5'-$(T)_{18}N_{-1}$N-3', where N=A, C, G, or T and N_{-1} = A, G or C), and

Universal Primer Mix primer sequence (5'- 3')	Concentration (mM)	Direction
1) CTAATACGACYCACTATAGGGCAAG CAGTGGTAACAACGCAGAGT	0.4	sense
2) CTAATACGACTCACTATAGGGC	2.0	sense

Table 2.6: Details of RACE Universal Primer Mix (UPM)

1 μl SMART II oligonucleotide (10μM, 5'-AAGCAGTGGTAACAACGCAGAGTACG CGGG-3'). The reaction mixtures were heated at 72^{0}C for 2 min and then chilled on ice for 2 min. To the reactions were added 2 μl first-strand buffer (250mM Tris-HCl (pH 8.3), 375mM KCl, 30mM $MgCl_2$), 1 μl DTT (20mM), 1μl dNTP Mix (10mM of each dATP, dCTP, dGTP, and dTTP), and 1 μl MMLV RT (Moloney Murine Leukaemia Virus-reverse transcriptase, 200IU/μl, PowerScript, Clontech) and the tube contents were incubated at 42^{0}C for 90 min. Finally, 250μl of Tricine-EDTA buffer [10mM Tricine-KOH (pH 8.5), 1mM EDTA] was added and the tubes were heated at 72^{0}C for 7 min, then stored at -20^{0}C until needed.

RACE amplification reaction: RACE amplification reaction was set up using 5 μl 10 X Advantage 2 PCR buffer, 1 μl dNTP mix (10 mM each), 1μl 50 X Advantage 2 Polymerase Mix, 5 μl 10 X Universal Primer Mix, 1 μl gene specific reverse primer (Sections 4.2.1, 5.2.1, 6.2.1), 2.5 μl koala 5' RACE ready cDNA and PCR-grade water to final volume of 50μl. Positive control PCR reactions were also performed using 2.5 μl control human placenta 5' RACE ready cDNA as the template and 1 μl of each 3' and 5'-RACE TFR primers (10μM). PCR reactions without the addition of DNA template were set up as negative controls. Touchdown cycling condition for positive control was as follows: 5 cycles of 94^{0}C for 30 sec and 72^{0}C for 3 min, 5 cycles of 94^{0}C for 30 sec, 68^{0}C for 30 sec and 72^{0}C for 3 min, and 27 cycles of 94^{0}C for 30 sec, 65^{0}C for 30 sec and 72^{0}C for 3 min. Touchdown cycling condition for amplification of koala cDNA clones varied according to a particular cloning strategy (Sections 4.2.1, 5.2.1, 6.2.1).

UNIVERSITY OF SOUTH AUSTRALIA
LIBRARY

2.21.4 Expression of cloned cDNAs in Cos-7 cells

Cos-7 cells (African green monkey kidney cells, *Ceropithecus aethiops*), which are able to amplify and over express the transfected cDNA under the control of the SV40 promoter (for example cDNA clone in pCMV-Script XR or pCI-Neo vector), were used for expression of koala and rat cloned cDNAs.

Cos-7 cells were grown in a monolayer in Dulbecco's Modified Eagle Medium (DMEM) supplemented with 10 % fetal bovine serum (FBS), 50 U/ml penicillin/streptomycin and 4 mM L-glutamine at 37^0C and 5 % CO_2. Cos-7 cells were seeded at 10^5 cells/well in a 6-well tissue culture plates (33mm) for small-scale transfection or at 6 x 10^5 cells/90 mm tissue culture plate for large-scale transfection. The cells were then allowed to grow in DMEM containing 10% FBS until 80-90 % confluent. Plasmid DNAs were isolated using the QIAfilter Midiprep Spin kit as described in Section 2.14.3. Just prior to transfection, the cells were washed gently with DMEM with no serum and the media removed. Koala and rat cDNAs cloned in pCMV-Script XR or pCI-Neo vector were transfected into Cos-7 cells using LipofectAMINE reagent. Two and 10 μl of LipofectAMINE were used for small-scale and large-scale transfections respectively, and the LipofectAMINE-DNA complexes were allowed to form for 30 minutes at room temperature before being overlaid on the cells. Media was replaced with fresh supplemented DMEM 16 hours post transfection and cells harvested three days following transfection. The cells were rinsed briefly in 0.1M phosphate buffer (pH 7.4), homogenised using a hand-held eppendorf homogeniser and used directly for protein assay, immunoblot analysis, CYP content measurement, and lauric acid hydroxylase activity assay.

Chapter 3

BRUSH TAIL POSSUM MODEL

3.1 INTRODUCTION

Eucalyptus species are native to Australia and have now been introduced worldwide into more than 90 other countries. *Eucalyptus* leaves contain low protein levels, high fibre levels and high concentrations of toxic secondary metabolites such as phenolics and essential oils [4, 241] (reviewed in [3]). Monoterpenes are major constituents of essential oils found in *Eucalyptus* leaves and include 1,8-cineole, α-pinene, β-pinene, d-limonene, *p*-cymene and menthol [242]. Several Australian folivorous marsupials are able to ingest and absorb large amounts of dietary terpenes that would be potentially toxic or fatal to other species [210, 211]. While the koala is capable of living wholly on *Eucalyptus* leaves, the brush tail possum, in residential conditions, consumes *Eucalyptus* leaves as part of its diet [3].

In an attempt to understand the interaction between Australian folivorous marsupials and their unique *Eucalyptus* diet, the oxidative metabolism of terpenes has been studied in these animals. *Eucalyptus* oil terpenes have been shown to be well absorbed and are almost completely absorbed prior to reaching the hindgut, the principal site of microbial activity (reviewed in [3]). *Eucalyptus* herbivores such as koalas and brush tail possums have been hypothesised to have evolved highly efficient enzyme systems in order to detoxify terpenes and phenolics to non-toxic substances. These metabolites can then be readily excreted in the urine [4, 243]. Enzymes involved in the biotransformation of *Eucalyptus* monoterpenes have been identified to be cytochromes P450 [7] (reviewed in [3]). A more detailed analysis of studies into the metabolism of terpenes in Australian marsupials is given in Section 1.5.

It has been suggested that many xenobiotics induce enzymes that are involved in their own metabolism [244]. The induction of xenobiotic-metabolising enzymes due to exposure to terpenoids and essential oils has been established [7, 244, 245, 246], in particular with rat liver P450s. For example, in rat liver, essential oils extracted from wood and leaves were found to elevate the levels and activities of some P450 enzymes [247]. In addition, oral administration of β-myrcene to rats was shown to induce several P450 enzymes [248]. 1,8-cineole and α-pinene have been shown to induce rat liver CYP2B1 [248]. Citral, a component of *Eucalyptus* leaves, has been reported to cause induction of peroxisomal β-oxidation activity and microsomal CYP4A activity in rat liver [5]. In brush tail possums given an artificial diet containing a mixture of monoterpenes such as 1,8-cineole, α-pinene, d-limonene and p-cymene, higher hepatic P450 content and elevations in several P450 activities were found relative to livers of control possums [6] (reviewed in [3]). In susceptible rodents, several structurally diverse chemicals, collectively termed peroxisome proliferators, have been reported to cause induction of peroxisomal β-oxidation enzymes and CYP4A (reviewed in [34]). Peroxisome proliferators have also been reported to significantly induce liver pyridine dinucleotides, in particular the highest abundance nicotinamide cofactors NAD and NADPH in rat liver [249, 250, 251].

In most species studied, induction of AOX and CYP4A expression by peroxisome proliferators has been shown to be mediated by PPAR-α. Induction of PPAR-α in rat liver after exposure to peroxisome proliferators has also been reported, which signifies one important measurement of the effects of peroxisome proliferators [228, 252]. The mechanism of induction of CYP4A and fatty acid β-oxidation enzymes by *Eucalyptus* terpenes such as citral could also be an adaptive response by liver cells to maintain cellular lipid homeostasis. For example, citral can be oxidised to a dicarboxylic acid that may then act to elevate peroxisomal β-oxidation enzymes. Alternatively, it is possible that citral may not be metabolised by CYP4A but induces CYP4A and peroxisomal β-oxidation by lipid overload effect. Citral inhibits mitochondrial β-oxidation enzymes such as carnitine-palmitoyl transferase to cause a lipid overload, resulting in induction of CYP4A and peroxisomal β-oxidation enzymes [5].

A reproducibly high CYP content and possible *Eucalyptus* induction of CYP4A enzymes and NAD cofactor content in livers of the koala has been reported [8, 94]. Prior to the commencement of this work, no studies had been performed to establish the effects of major *Eucalyptus* monoterpenes on the expression of lipid-metabolising

enzymes and PPAR-α. The present work aimed to investigate the enzymatic activities of CYP4A and peroxisomal β-oxidation enzymes in livers of possums given an artificial diet containing 1,8-cineole, *a*-pinene, *d*-limonene and *p*-cymene. The results were than compared with those obtained from livers of control possums. The expression of these enzymes and PPAR-α were investigated by Western and Northern blot analysis. Liver pyrimidine dinucleotide contents were also examined between the terpene-treated possums and the control possums.

3.2 METHODS

3.2.1 Control and terpene-treated possum livers

Frozen possum liver samples (four control and four terpene-treated possums) were kindly donated by Dr Georgia Pass, University of Tasmania. The possums were captured in wire cage traps in the urban area of Hobart (Tasmania), under National Parks and Wildlife Service's permission. Details of these tissues are given in Section 2.3.

3.2.2 Microsome, cytosol, post-nuclear supernatant, and nuclear extract preparations

Hepatic microsomes, cytosolic samples, post-nuclear supernatants, and nuclear extracts were prepared from livers of control and terpene treated possums, koalas, rat and humans as described in Sections 2.9.1, 2.9.2 and 2.9.3, respectively. The protein concentration of various subcellular fractions was determined by the method of Lowry *et al.* [229] as described in Section 2.9.4.

3.2.3 Spectrophotometry measurement of hepatic nicotinamide cofactor contents

Hepatic nicotinamide cofactors, NAD, NADH, NADP, and NADPH were measured from control and terpene-treated possum livers, according to the procedure of Klingenberg [232]. The method is based on the measurements of two produced extracts. The NAD and NADP contents were measured in the acid extract, while NADH and NADPH contents were measured in the alkaline extract.

In the acid extract, NADH and NADPH were unstable. The NAD content was measured by the appearance of NADH produced from the conversion of NAD to NADH, using ethanol and exogenously added alcohol dehydrogenase. Similarly, NADP content was measured by the appearance of NADPH, using glucose-6-phosphate and glucose-6-phosphate dehydrogenase to convert NADP to NADPH (Figure 3.1).

In the alkaline extract, NAD and NADP were unstable, NADH and NADPH were

converted into their oxidised forms, NAD and NADP. The level of generated NAD in the alkaline extract was measured by the appearance of NADH produced from the conversion of NAD to NADH, using ethanol and exogenously added alcohol dehydrogenase. The level of generated NADP in the alkaline extract was measured by the appearance of NADPH, using glucose-6-phosphate and glucose-6-phosphate dehydrogenase to convert NADP to NADPH as described above.

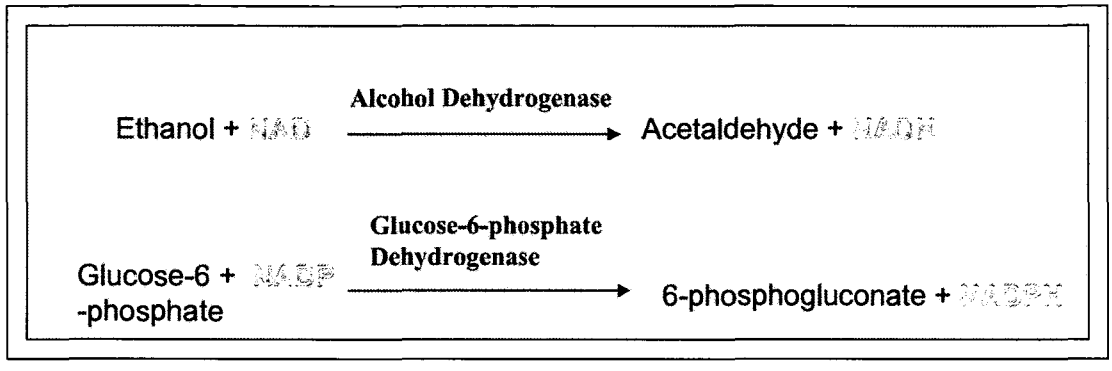

Figure 3.1: The conversion of NAD and NADP into their reduced forms.

Extraction of nicotinamide cofactors: For the acid extract, liver tissue (2g) was homogenised in 5 volumes of 0.6M $HClO_4$ and the homogenate was centrifuged for 5 minutes at 5000 xg. To the supernatant was added 200μl 1M K_2HPO_4 and the pH of the tube content was adjusted to 7.2 with 3M KOH. The sample was allowed to stand to sediment the $KClO_4$ and the resultant supernatant was used for determination of NAD and NADP contents.

For the alkaline extract, liver tissue (200mg) was homogenised in 2ml cold alcoholic potassium hydroxide solution (0.5M KOH in 50% v/v ethanol). The sample was allowed to stand in boiling water for 5 minutes and then incubated on ice. The tube content was adjusted to pH 7.8 with a buffer containing 5mM 2-oxoglutaric acid, 0.5M triethanolamine, and 30mM ammonium chloride in 0.5M potassium phosphate buffer. To the sample mixture was added glutamate dehydrogenase (2mg/ml) to final concentration of 0.001% w/v of the extract. After standing at room temperature for 15 minutes, 3M $HCL0_4$ was added to the tube to a final concentration 0.6M. The sample was centrifuged at 1000 xg for 5 minutes at 4^0C and the sample pH was adjusted to 7.2 with 1M KOH. The sample was allowed to stand to sediment the $KClO_4$ and the resultant supernatant was used for determination of NADH and NADPH contents.

Spectrophotometric measurement of nicotinamide cofactors: The content of NAD or NADH (in the acid extract or alkaline extract, respectively) was calculated using the extinction coefficient for NADH of $6.22\mu M^{-1}$ cm^{-1} at 340nm. Test samples were set up with 0.5ml extract, 0.5ml freshly prepared buffer (0.5% w/v semicarbazide hydrochloride in 0.1M sodium pyrophosphate buffer, pH 8.8) and $5\mu l$ ethanol. The reaction was initiated by adding $5\mu l$ (1IU) alcohol dehydrogenase. The absorbance changes against water were measured over 6 minutes at 340nm wavelength.

The content of NADP or NADPH (in the acid extract or alkaline extract, respectively) was calculated using the extinction coefficient for NADPH of $6.22\mu M^{-1}$ cm^{-1} at 340nm. Test samples were set up consisting of 1ml extract, $5\mu M$ $MgSO_4$ and $5\mu M$ glucose-6-phosphate. The reaction was initiated by adding 0.001% w/v glucose-6-phosphate dehydrogenase. The absorbance changes against water were measured at 340nm wavelength, over 25 minutes.

3.2.4 Lauric acid hydroxylase activity

Lauric acid hydroxylase activity was determined using a modification of the method described by Parker and Orton [233]. In humans, rat and other species, lauric acid hydroxylase has been widely used as a functional maker to identify the expression of CYP4A enzymes [8, 70, 71, 72, 73, 253, 254] (reviewed in [34, 67, 76]). Lauric acid is a 12 carbon fatty acid that is metabolised to form both (ω-1)- and ω-hydroxylated products. The hydroxylation of lauric acid at the ω-carbon is performed principally by CYP4A enzymes, which are the predominant lauric acid hydroxylase in the liver microsomes [51, 63, 67, 73]. The chemical structure of lauric acid and positions of hydroxylation are shown in Figure 3.2.

The assay method involved radiolabelled lauric acid and thin layer chromatographic (TLC) separation of (ω-1)- and ω-hydroxy lauric acid from the parent lauric acid. Lauric acid hydroxylase activity was expressed in terms of total (ω-1)- and ω-hydroxylated products. The incubation mixture contained [1-^{14}C]lauric acid (100nCi), lauric acid (0.1mM), liver microsomes (0.5mg/ml), NADP (1mM), $MgCl_2$ (8mM), isocitric acid (4mM), and isocitric dehydrogenase(1 I.U.) and sodium phosphate buffer (0.1M, pH 7.4) in a final volume of 2ml. Test and blank incubations were performed in triplicate

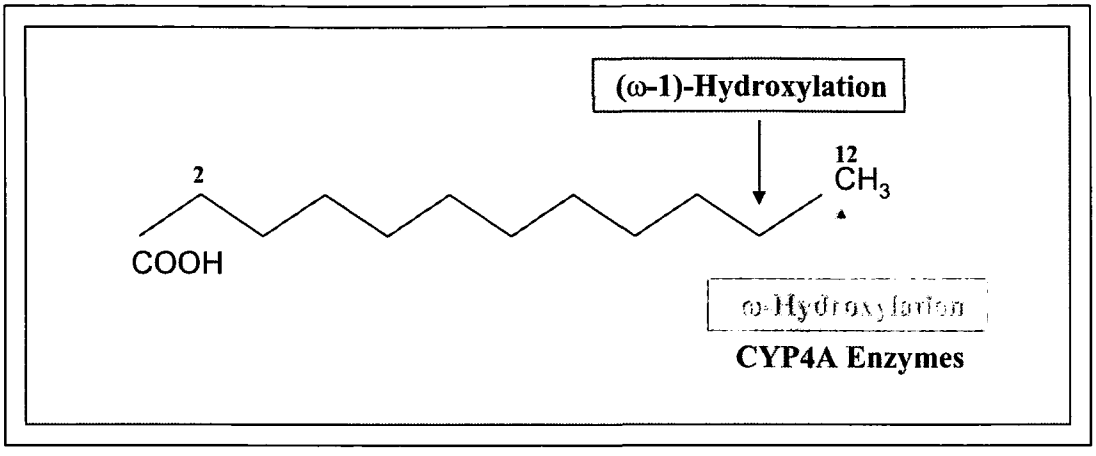

Figure 3.2: The chemical structure of lauric acid and positions of hydroxylation.
ω-hydroxylation of lauric acid is performed principally by CYP4A enzymes, which are the predominant lauric acid hydroxylase in the liver microsomes.

with no microsomes in the blank incubation. The mixture was pre-incubated for 5 minutes at 37^0C before adding the generating system, followed by a 5 minute incubation at 37^0C in a shaking water bath. After termination of the reaction, 5ml of diethyl ether was added, the tubes were vortexed for 30 seconds and centrifuged for 10 minutes. The organic phase was collected and the reaction mixture was re-extracted by adding another 5ml of diethyl ether. The pooled organic layer was evaporated under nitrogen (N_2) gas. The samples were reconstituted in 50μl diethyl ether and spotted on a silica gel TLC plate. The plate was developed in diethyl ether: light petroleum ether: formic acid, 70:30:1 [255]. Scraping and scintillation counting was performed to detect the parent lauric acid and its hydroxylated metabolites.

3.2.5 Peroxisomal cyanide-insensitive fatty acid β-oxidation activity

Peroxisomal cyanide-insensitive fatty acid β-oxidation activity was performed according to the method of Lazarow 1981 [234]. Peroxisomal β-oxidation of fatty acid occurs in a four reaction cascade, catalysed by four distinct groups of enzymes (Section 1.3.4, Fig 1.7). In this assay, measurement of the reduction of NAD to NADH will provide a measure of overall β-oxidation. The addition of potassium cyanide (KCN) prevents the reoxidation of the NADH by the endogenous enzymes. KCN does not inhibit

fatty acid β-oxidation in vitro.

The test and control reactions were set up with 0.2mM NAD, 1mM DTT, 0.0075% w/v BSA, 0.01% w/v Triton X-100, 0.1mM Coenzyme A (CoA), 0.01mM FAD (flavin adenine dinucleotide), 1mM KCN, 5μl of post nuclear supernatant (Section 2.9.2), and 50mM Tris-HCl buffer (pH 8.0) in a final volume of 1ml. The reaction was initiated by the addition of 2nM palmitoyl CoA to the test sample. The reaction was performed at 37^0C and the change in absorbance was recorded over 5 minutes. Peroxisomal cyanide-intensive fatty acid β-oxidation activity was calculated using the extinction coefficient for NADH of $6.22\mu M^{-1}cm^{-1}$ at 340nm.

3.2.6 Statistical analysis

Data were expressed as the mean of triplicate observations, except the quantification of nicotinamide content which was performed in duplicate. Population variability was indicated by a standard deviation (S.D). Statistical analysis was accomplished using a two-sample t-test for a 1-tail hypothesis.

3.2.7 Immunoblot analysis of CYP4A and PPAR-α in marsupial liver tissues

Immunodetection of CYP4A in liver microsomes from control and treated possums, koalas, rat and humans was performed using anti-rat polyclonal CYP4A primary antibody (1:200 dilution) raised in sheep as primary antibody and HRP-conjugated rabbit-anti-sheep IgG (1:2000 dilution) as secondary antibody. For immunodetection of PPARα in hepatic cytosolic and nuclear extracts, a polyclonal PPARα antibody (1:200) raised in rabbit and a HRP-conjugated mouse-anti-rabbit IgG (1:2000), were used as primary and secondary antibodies, respectively. Immunoblot analysis and the subsequent development of the nitrocellulose membrane using HRP colour development reagent was accomplished as described in Section 2.10.

3.2.8 Northern analysis

Total RNA was isolated from livers of control and terpene-treated possums, koala, rat and human as described in Section 2.19.2. Messenger RNA was then purified using the mRNA purification kit as per section 2.19.3. Messenger RNA was separated through denaturing formaldehyde agarose gel and transblotted onto nylon filter according to the methods described in section 2.20.1 and 2.20.2. The corresponding koala cDNA probe, *CYP4A* 417-bp or *AOX* 320-bp or *PPAR-α* 1.2-kb, was labelled with α-[^{32}P]-dCTP as described in section 2.17. Prehybridisation and hybridisation were accomplished at 42^{0}C in 50% formamide according to Section 2.20.3 and the filter was then exposed at 80^{0}C for several weeks in autoradiograph cassettes. After probing with the koala cDNA probe, the filter was stripped and reprobed with α-[^{32}P]-dCTP labelled β-actin cDNA probe for mRNA loading control. Spectrophotometric quantification of mRNA and ethidium bromide staining of the gel were performed as additional loading controls. For each blot, RNA was examined in one possum in each control and treated groups. The experiment was repeated in at least one more animal in each group.

3.3 RESULTS

3.3.1 Lauric acid hydroxylase activity

Lauric acid hydroxylase activity was determined in livers of control and terpene-treated possums, as a measure of CYP4A activity. Liver microsomes from rat and koala were included as positive controls. As shown in Table 3.1, lauric acid hydroxylase activity was 1.2-fold higher in livers of terpene-treated possums, as compared to that in livers of the control possums (4.40 ± 0.85 versus 3.60 ± 0.48 nmole/mg protein/minute). This difference did not reach statistical significance ($p<0.1$).

Samples	n	Lauric acid hydroxylase activities (nmole LA metabolite/mg protein/minute)
Rat	1	4.9 ± 1.6
Koala	1	9.4 ± 0.6
Control possums	4	3.6 ± 0.5
Treated possums	4	4.4 ± 0.9

Table 3.1: Lauric acid hydroxylase activities for control and terpene-treated possum, koala and rat livers.
Results for the possums are expressed as means ± S.D (n= 4 for each group). For each animal, the experiment was performed in triplicate. Results for koala and rat are expressed as means ± S.D of triplicate readings from one animal. The mean was different from that of control possums however this difference did not reach statistical significance ($p<0.1$, analysis of data was performed using a two-sample t-test for a 1-tail hypothesis).

3.3.2 Peroxisomal cyanide-insensitive palmitoyl coenzyme A oxidation activity

Peroxisomal cyanide-insensitive palmitoyl-CoA oxidation activity was determined as a measure of overall peroxisomal β-oxidation activity. A sample from rat liver was included as a positive control. Table 3.2 shows that a statistically significant 3-fold higher rate of peroxisomal cyanide-insensitive palmitoyl-CoA oxidation was observed in livers of terpene-treated possums, as compared to that in the control possums ($p<0.01$).

Samples	n	Peroxisomal cyanide-insensitive palmitoyl coenzyme A oxidation activities (nmole /mg protein/minute)
Rat	1	2.7
Control possums	4	1.0 ± 0.9
Treated possums	4	3.1 ± 1.0*

Table 3.2: Peroxisomal cyanide-insensitive palmitoyl coenzyme A oxidation activities for control and terpene-treated possum and rat livers. Results for the possums are expressed as means $\pm$ S.D (n= 4 for each group). For each animal, the experiment was performed in duplicate. Result for rat is expressed as an average of two readings from one animal. *Significantly different from the control group at $P< 0.01$. Analysis of data was performed using a two-sample t-test for a 1-tail hypothesis.

3.3.3 Pyridine nucleotide NAD, NADH, NADP and NADPH content measurement

Pyridine NAD, NADP, NADH and NADPH concentrations for control and terpene-treated possum and rat livers are summarised in Table 3.3. A higher NAD/ NADP ratio was observed in livers of terpene-treated possums, as compared to control possums (4.7 ± 0.6 versus 3.5 ± 0.6 nmole/mg protein per min, $p<0.05$). No other statistically significant differences in pyridine nucleotide contents were observed in livers between the two groups.

Samples	n	NAD	NADH	NADP	NADPH
Rat	1	265.0 ± 61.1	59.0 ± 31.2	212.0 ± 33.0	84.0 ± 43.2
Control	4	487.5 ± 147.8	136.3 ± 59.3	139.0 ± 37.6	146.3 ± 77.0
Terpene	4	435.0 ± 87.5	152.0 ± 22.7	92.5 ± 17.1	299.0 ± 171.0
Samples	n	NAD/ NADP	NAD/ NADH	NADP/ NADPH	
Rat	1	1.3	4.5	2.5	
Control	4	3.5 ± 0.6	4.0 ± 1.4	1.4 ± 1.2	
Terpene	4	4.7 ± 0.6*	3.0 ± 1.0	0.35 ± 0.1	

Table 3.3: Pyridine nucleotide concentrations for control and treated possum and rat liver homogenates.
Values are expressed as nmole/g tissue. Results for the possums are expressed as means ± S.D (n= 4 for each group). Result for rat is expressed as mean of two separate determinations. For each individual animal, each nicotinamide ratio was calculated. Each ratio shown is the mean of ratios from four animals ± S.D. *Significantly different from control group at $P< 0.05$.

3.3.4 Immunoblot analysis

Detection of CYP4A immunoreactive proteins: Microsomal fractions from control and terpene-treated possum livers were examined by immunoblotting, using a sheep anti-rat CYP4A polyclonal antibody. The antibody was reported to recognise rat CYP4A1, CYP4A2 and CYP4A3 proteins (Chemicon International, UT, UK). Microsomal samples from human, rat and koala livers were included for comparison. Immunoblot analysis of CYP4A in microsomes from terpene-treated and control possum, rat, human, and koala livers is shown in Figure 3.3.

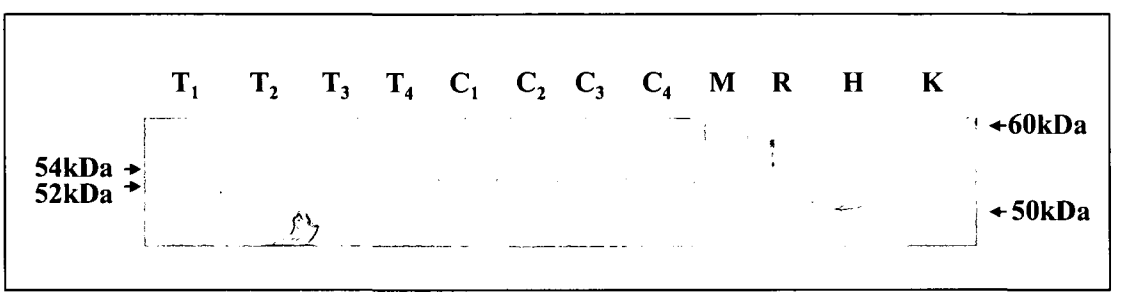

Figure 3.3: Immunoblot analysis of CYP4A in microsomes from control and terpene-treated possum, rat, human and koala livers, using anti-rat CYP4A antibody.
Liver microsomal proteins (50 μg/lane) from: C1-C4, possums given a control diet of fruits and vegetables only; T1-T4, possums given mixture of 4 terpenes in the control diet over 10 days; M, pre-stained protein ladder; R, rat; H, human; K, koala.

CYP4A immunoreactive proteins of mass approximately 52-kDa and 54-kDa were detected in livers of both control and treated possums, with the intensity of the 54-kDa band appears to be fainter and more variable in treated samples than control samples. Another band of mass less than 50-kDa was also seen for both the control and treated groups. Immunoreactive protein of mass approximately 52-kDa was detected in the rat, two immunoreactive proteins of mass 52-kDa and 50-kDa were detected in the human and the koala immunoreactive proteins were of mass approximately 54-kDa and 50-kDa.

Detection of PPAR-α immunoreactive proteins: A rabbit anti-human PPAR-α polyclonal antibody was used to detect PPAR-α protein in cytosolic and nuclear extracts from control and terpene-treated possum livers. The anti-human PPAR-α polyclonal antibody was reported to recognise human and rat PPAR-α proteins (Santa Cruz, Germany). Cytosolic and nuclear extracts from rat liver were included as positive controls. A representative immunoblot analysis of PPAR-α in cytosolic and nuclear extracts from control and terpene-treated possum and rat livers is shown in Figure 3.4. The anti-human PPAR-α polyclonal antibody detected more intense bands of mass approximately 52-kDa and 54-kDa, in both cytosolic and nuclear extracts of the terpene-treated possum livers as compared to those of the control possum livers. An immunoreactive protein of mass 54-kDa was observed for rat cytosolic and nuclear extracts.

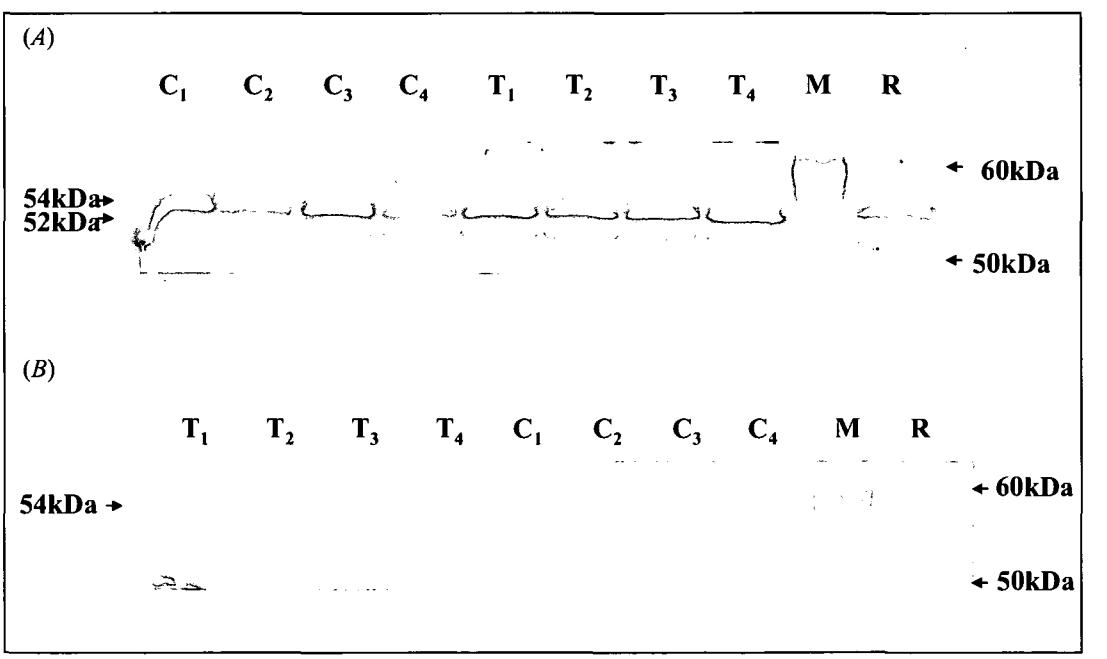

Figure 3.4: Immunoblot analysis of PPRA-α in nuclear (A) and cytosolic (B) extracts from control and terpene-treated possum and rat livers, using anti-human PPRA-α polyclonal antibody.
Samples (50 μg cytosolic or nuclear extract protein/lane) from: C1-C4, possums given a control diet of fruits and vegetables only; T1-T4, possums given mixture of 4 terpenes in the control diet over 10 days; M, pre-stained protein ladder; R, rat hepatic nuclear (A) and cytosolic (B) extracts.

3.3.5 Northern blot analysis

Messenger RNA from the livers of terpene-treated and control possums was analysed by Northern blot hybridisation to detect the mRNA level of CYP4A, peroxisomal acyl-CoA oxidase and PPAR-α. Messenger RNA from koala, rat and human livers was examined for comparison. Figure 3.5 shows an ethidium bromide stained gel of mRNA from control and terpene-treated possum, human, rat and koala livers.

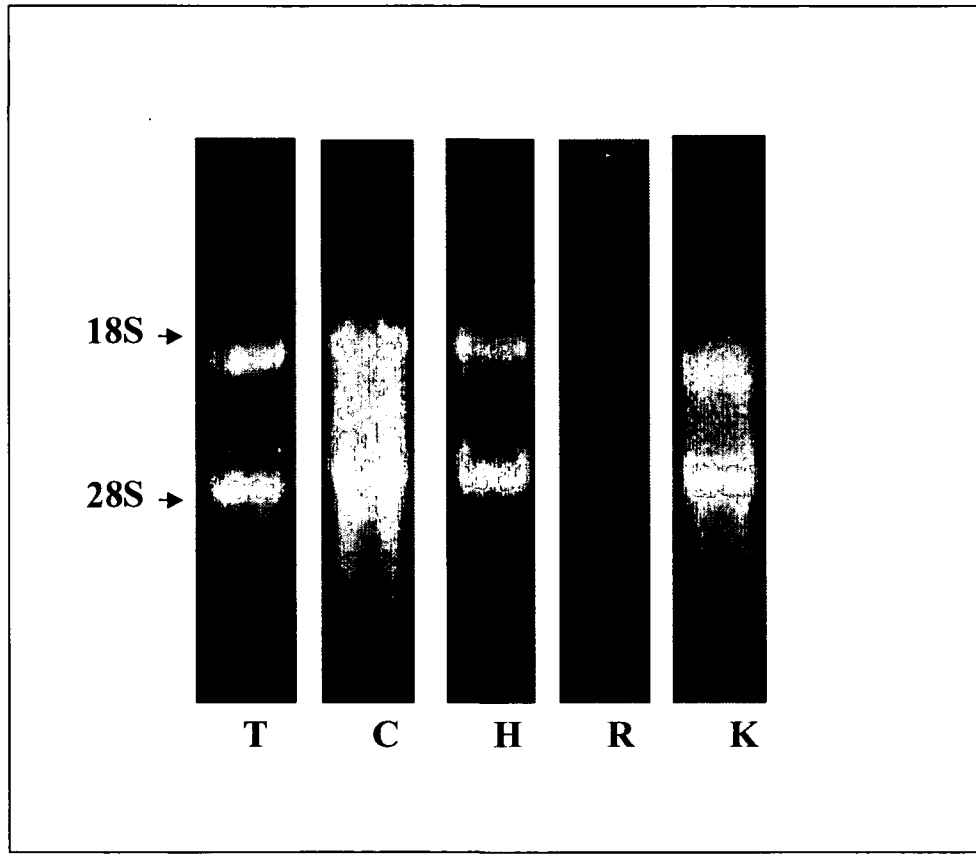

Figure 3.5: Representative ethidium bromide stained gel of mRNA from control and terpene-treated possum, human, rat and koala livers.
Liver mRNA (10μg) from terpene-treated possum (T), control possum (C), human (H), rat (R) and koala (K). Sections are from the same gel. The figure indicates that approximately equal amount of mRNA from control and terpene-treated possum, human and koala livers were loaded into each lane of the gel. The amount of mRNA from rat liver appears to be lower than that from other species.

Detection of CYP4A mRNA in control and terpene-treated possum livers: Northern analysis of control and terpene-treated possum, human, rat and koala livers, using a koala *CYP4A15* 417-bp cDNA probe, is shown in Figure 3.6. The blot shows a more intense mRNA band of approximately 2.6-kb in the liver of terpene-treated possum as compared to that of control possum. It is worth to note that the β-actin signal for the terpene-treated possum is also stronger, suggesting that this stronger signal was due to the presence of more mRNA in the treated sample. A messenger RNA species of the same size was detected in koala. Human and rat CYP4A mRNAs were of approximately 2.5-kb. In human liver, a mRNA species of 2-kb was also observed.

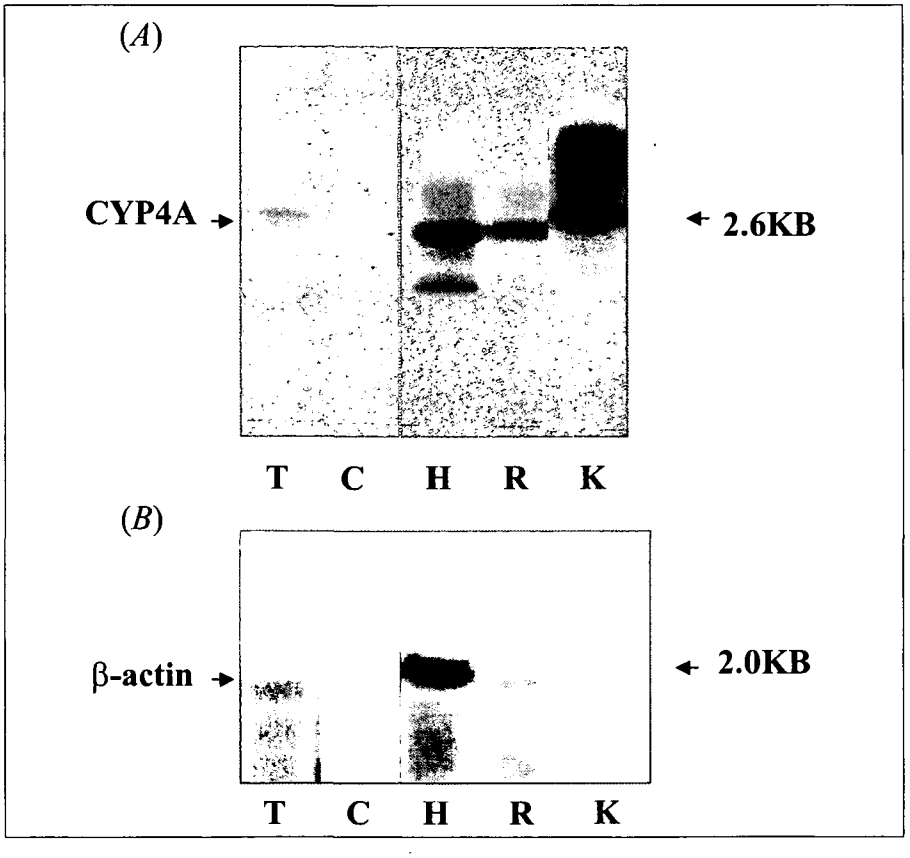

Figure 3.6: Northern analysis of mRNA from control and terpene-treated possum, human, rat and koala livers, using a koala *CYP4A15* cDNA probe. Liver mRNA (10μg) from terpene-treated possum (T), control possum (C), human (H), rat (R) and koala (K). (A) Hybridisation with koala *CYP4A15* 417-bp cDNA probe; (B) Hybridisation with mouse β-actin. Sections are from the same blot.

Detection of AOX mRNA in control and terpene-treated possum livers: Northern analysis of control and terpene-treated possum, human, rat and koala livers, using a koala *AOX* 320-bp cDNA probe is shown in Figure 3.7. A more intense band corresponding to a mRNA species of approximately 4.5-kb was observed in liver of terpene-treated possum as compared to that from control possum. Messenger RNA species of the same size was detected for rat liver while those for human and koala livers were of approximately 3-kb and 5-kb, respectively. Other bands of smaller size were also observed in koala, rat and treated possum livers.

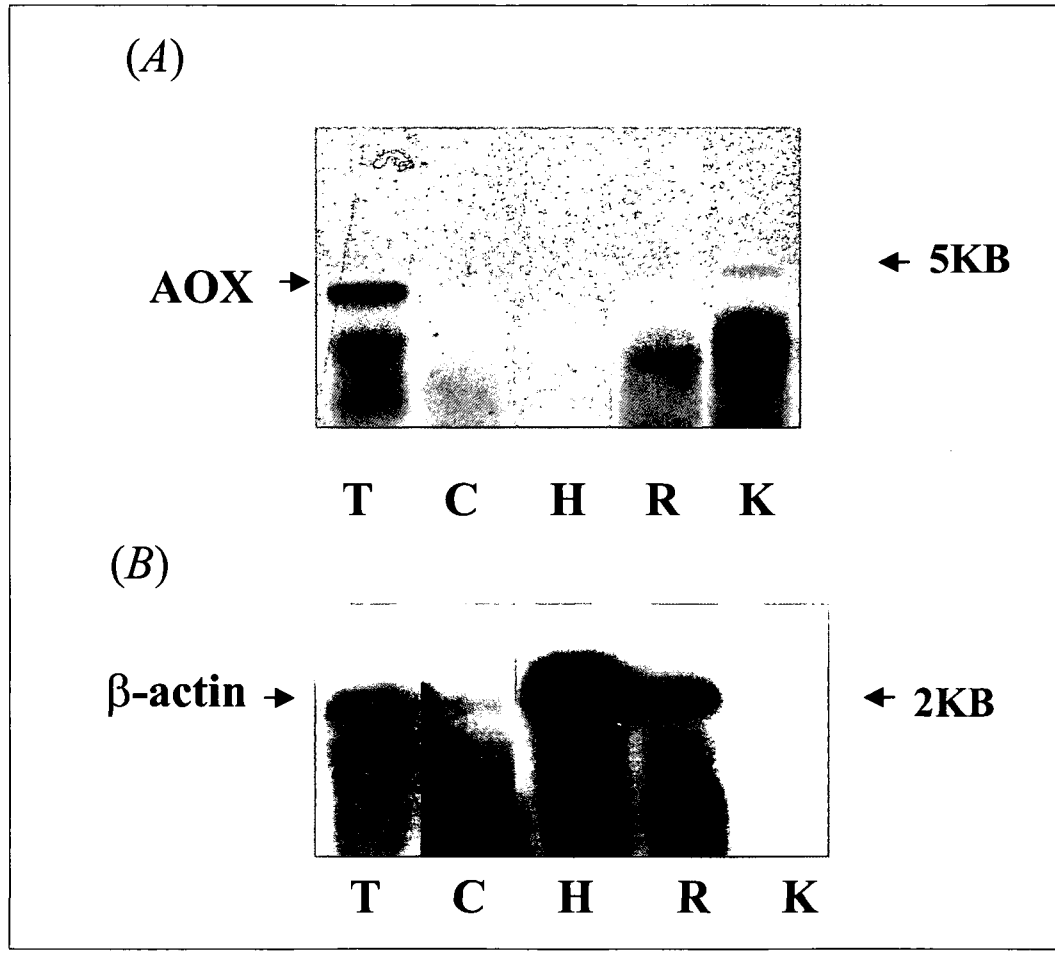

Figure 3.7: Northern analysis of mRNA from control and terpene-treated possum, human, rat and koala livers, using a koala *AOX* cDNA probe. Liver mRNA (10μg) from terpene-treated possum (T), control possum (C), human (H), rat (R) and koala (K). (A) Hybridisation with koala *AOX* 320-bp cDNA probe; (B) Hybridisation with mouse β-actin. Sections are from the same blot.

Detection of PPAR-α mRNA in control and terpene-treated possum livers: Northern analysis of control and terpene-treated possum, human, rat and koala livers, using a koala *PPAR-α* 1.2-kb cDNA probe, is shown in Figure 3.8. The blot detected mRNA species of approximately 2-kb and 4.5-kb in liver from terpene-treated possum. A mRNA species of approximately 8-kb was detected for koala liver and no signal was observed for control possum, rat and human livers.

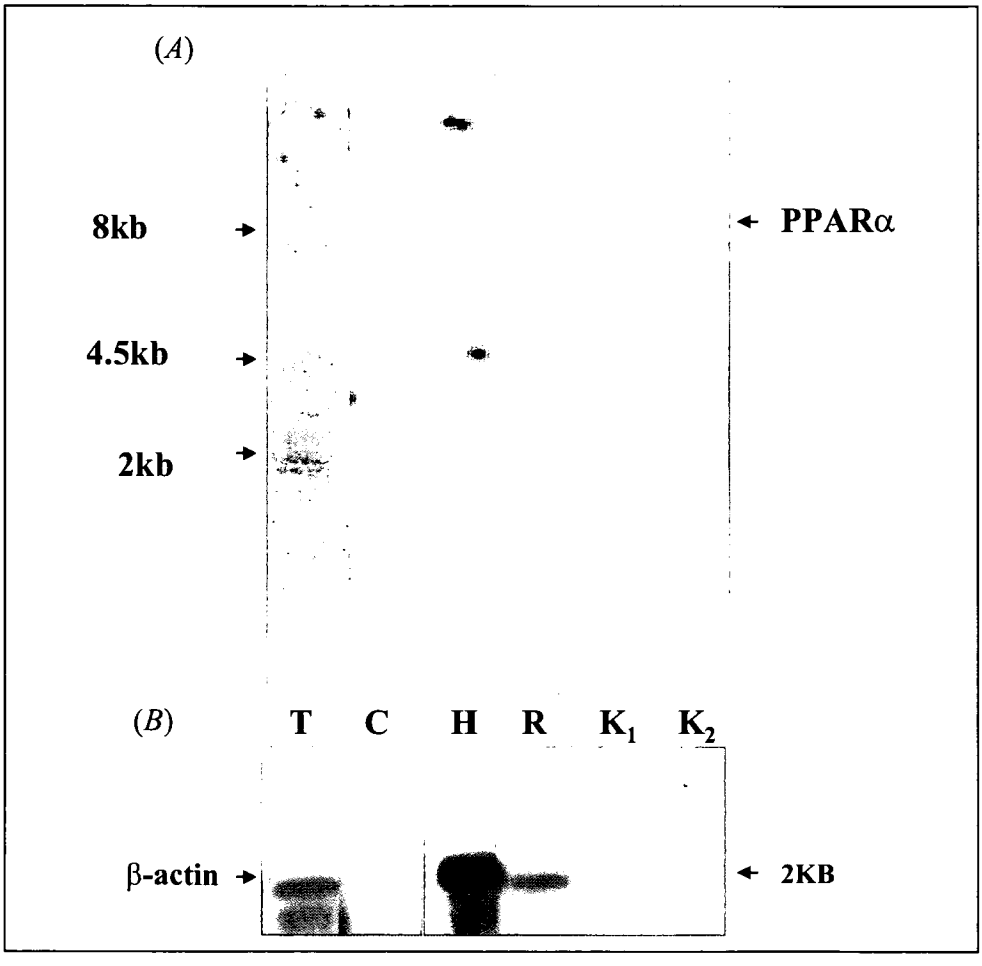

Figure 3.8: Northern blot analysis of mRNA from control and terpene-treated possum, human, rat and koala livers, using a koala *PPAR-α* cDNA probe.
Liver mRNA (10μg except K_2 (4μg) from terpene-treated possum (T), control possum (C), human (H), rat (R) and koalas (K). (A) Hybridisation with koala *PPAR-α* 1.2-kb cDNA probe; (B) Hybridisation with mouse β-actin. Sections are from the same blot.

3.4 DISCUSSION

Eucalyptus leaves contain a high proportion of essential oils which are comprised of a complex mixture of monoterpenes such as 1,8-cineole, α-pinene, β-pinene, *d*-limonene, *p*-cymene, and menthol. Using a possum model, the present studies examined the effects of *Eucalyptus* monoterpenes on the expression of CYP4A, acyl CoA oxidase, and PPAR-α. While the koala is an obligate *Eucalypt* feeder, the brush tail possum, in residential conditions, replies on *Eucalyptus* leaves only as part of their diet. They also eat vegetables, fruits and cereals. The control group (4 possums) was given an artificial diet of fruit and cereal for 10 days. The terpene-treated group (4 possums) was given the same artificial diet supplemented with a mixture of monoterpenes including 1,8-cineole, α-pinene, d-limonene and p-cymene for the same number of days. The induction protocol had previously been shown to result in a significant increase in CYP2C and CYP2E [6].

In the present studies, a significant 3-fold higher peroxisomal cyanide-insensitive palmitoyl coenzyme A oxidation activity was observed in livers of terpene-treated possums than in livers of control possums. This higher activity was not associated with significant changes in CYP4A activity. In comparison to the maximal induction of up to 15-fold reported for rats exposed to peroxisome proliferators, the fold induction of palmitoyl coenzyme A oxidation activity by *Eucalyptus* terpenes in this study is much smaller [256, 257, 258]. Peroxisomal cyanide-insensitive palmitoyl coenzyme oxidation and lauric acid hydroxylation activities detected in the rat were similar to the activities reported by others [5] and consistent with those reported previously [8].

In rat, induction of CYP4A by peroxisome proliferators is often associated with induction of peroxisomal β-oxidation enzymes, in particular acyl CoA oxidase [92, 93, 256, 257, 258] (reviewed in [34]). This was not the case with exposure to *Eucalyptus* terpenes. The results reported in this chapter are similar to the results of Roffey and co-workers who found that oral administration of linalool, a monoterpene, caused a 2-fold induction of palmitoyl coenzyme A oxidation activity but not of CYP4A activity [5]. The present work clearly demonstrated that Eucalyptus terpenes cause increased peroxisomal cyanide-intensive palmitoyl coenzyme A oxidation activity in livers of terpene-treated possums.

Peroxisome proliferators have been previously reported to cause significant induction

of hepatic pyridine nucleotides NAD, NADP and NADPH, with a significant decrease in the NAD/NADH ratio, reflecting stimulation of fatty acid oxidation in peroxisomes [249]. In the present studies, a significantly higher ratio of NAD/NADP was obtained for treated possums as compared to control possums ($p<0.05$) (Table 3.3). Although mean NADPH content observed in terpene-treated possums was higher as compared to the control group, data analysis showed that this difference was not statistically significant ($p<0.1$) (Table 3.3). Similarly, the lower mean NAD/NADH and NADP/NADPH ratios observed in treated possums relative to control possums were found not to be statistically significant ($p<0.1$). Hepatic nicotinamide cofactor contents and ratios for rat were consistent with those reported in other studies [232, 250, 259, 260] and similar to the results obtained previously in this laboratory [8]. Our results suggest that *Eucalyptus* terpenes elevate hepatic NAD/NADP ratio with no significant changes in other pyridine nucleotide parameters.

Western blot analysis using anti-rat CYP4A polyclonal antibody indicated no significant differences in the intensity of the CYP4A immunoreactive bands detected in the livers between the two groups (Figure 3.3). This result was consistent with the results obtained for the activity study with no significant differences in CYP4A activity detected between the two groups.

PPAR-α has been reported to mediate induction of genes encoding peroxisomal AOX and CYP4A by peroxisome proliferators in liver of mouse and human. This induction is mediated via transcriptional activation of target genes [261]. Disruption of the *PPAR-α* gene has been reported to result in abolition of the profound effects of peroxisome proliferators [159]. Induction of PPAR-α protein after exposure to peroxisome proliferators has been observed in rat liver [228, 252] which was thought to represent one important measurement of the effects of peroxisome proliferators. From the immunoblot analysis of hepatic cytosol and nuclear extracts (Figure 3.4), two of the nuclear extracts of control possums show the same intensity as those of treated samples while the other two were markedly fainter. Overall, more intense signals for PPAR-α immunoreactive proteins detected in both cytosol and nuclear extracts of treated possums suggested higher expression of PPAR-α protein in the treated-possums as compared to two control possums.

The level of hepatic CYP4A, AOX and PPAR-α mRNA was examined by Northern analysis, using corresponding koala cDNA probes. Although ethidium bromide

stained gel of mRNA samples shows some degree of degradation of mRNA samples, particularly for the rat, it is apparent that mRNA samples for other species were intact and that approximately equal amount of mRNA from control and terpene-treated possum, human and koala livers were loaded into each lane of the gel. The amount of mRNA from rat liver appears to be lower than that from other species and this may be due to sample degradation. Although the signal intensity of CYP4A mRNA species in the terpene-treated group is more intense than in the control group, it is difficult to draw conclusions since from the β-actin blot, the amount of mRNA from the control possum liver appears to be lower than that from the treated possum. The β-actin blot also shows different band intensity in various species, suggesting differences in the abundance of CYP4A RNAs across species. Similarly, from the β-actin blot for the AOX mRNA blot, the amount of mRNA from the control possum liver appears to be lower than that from the treated possum. However, the signal intensity of AOX mRNA species in the terpene-treated group is much more intense than in the control group. The blot actually shows that no band observed for the control group. This suggested that AOX mRNA level in the terpene-treated possums is higher than in the control possums . This finding was consistent with the results of the activity study. While hepatic peroxisomal cyanide-intensive palmitoyl coenzyme A oxidation activity was 3-fold greater ($P<0.01$), no significant differences in hepatic lauric acid hydroxylase activity were observed between the two groups. PPAR-α mRNA reactive species was detected in treated possum only (Figure 3.8), indicating higher hepatic PPAR-α mRNA level in treated possum. This result may also be due to the presence of less mRNA from control possum (Figure 3.8, Panel B). Although the bands observed in terpene-treated possum (2-kb, 4.5-kb) and koala (8-kb) (Figure 3.8) were clearly visible on the autoradiography film, some resolution has been lost due to photographic reproduction and imaging.

Variation in the sizes of PPAR-α mRNA has been previously reported. While Issemann and Green reported two major mRNA species, of approximately 1.8- and 2-kb, in mouse liver mRNA samples [152], others have reported mouse PPAR-α mRNA species of approximately 8.5- to 9.5-kb [149, 159]. Rat PPAR-α mRNA detected by Gebel and colleagues (1992) was approximately 6-kb whereas that reported by others was approximately 9.5-kb [149]. The size of human PPAR-α mRNA has been reported to be approximately 9.5-kb [149]. In the present studies, no bands of either 6-kb or 9.5-kb were observed in either human or rat liver. The absence of PPAR-α mRNA in rat tissue observed in the present studies is consistent with the results of

Sterchele and colleagues who found low expression of PPAR-α mRNA in untreated rat liver [252]. Gebel *et al.,* (1992) also reported no hybridisation signal when probing untreated rat RNA with a *PPAR-α* cDNA probe [228].

Species differences in the response to peroxisome proliferators have been reported. While humans, non human primates, dog and guinea pigs are either nonresponsive or weakly responsive, rodent species including mice and rats are very responsive species[62, 185, 187]. Based on the results of the present studies, marsupial possums appeared to be a moderately responsive species to terpene peroxisome proliferators.

Collectively, the present work shows that in terpene-treated possums, significantly higher hepatic AOX expression is evident at both protein and mRNA levels, as compared to control possums. In contrast, no significant changes in CYP4A expression was observed. The present work also suggests that dietary *Eucalyptus* terpenes possibly increase PPAR-α. From the overall results of this chapter, considerable inter-individual variability between animals in both the control and treated groups was observed. This was evident from the high SD values seen in the palmitoyl coenzyme A oxidation assay as well as in the measurement of pyridine nucleotide content and from the results of the two western blot analyses. Although the limitations of the data obtained in this chapter made it difficult to draw more rigorous conclusions on the overall effects of dietary *Eucalyptus* terpenes on CYP4A, peroxisomal acyl CoA oxidase (AOX) and peroxisome proliferator activated receptor-alpha (PPAR-α), it is apparent that dietary terpenes act like peroxisome proliferators to increase peroxisomal β-oxidation enzyme AOX activity and mRNA. It is also apparent that higher expression of peroxisomal β-oxidation enzyme AOX is not always associated with higher expression of CYP4A.

Chapter 4

KOALA LIVER CYTOCHROME P450 4A15 (CYP4A15)

4.1 INTRODUCTION

The cytochrome P450 *CYP4* family appears to be one of the oldest eukaryotic cytochrome P450 gene families and is closely related to the enzyme family responsible for cholesterol metabolism [49]. The *CYP4A* subfamily is one of eighteen subfamilies within the *CYP4* family and presently comprises twenty three genes [10]. All presently known CYP4A enzymes, their tissue distribution and the species from which they have been identified is shown in Table 4.1. CYP4A enzymes hydroxylate fatty acids predominantly at their omega (ω) carbon atom. CYP4A enzymes also hydroxylate fatty acids at the omega-1 (ω-1) carbon to varying degrees depending on the length of the fatty acid [67, 70, 71, 72, 73]. The capacity of CYP4A enzymes to metabolise fatty acids has focussed significant research because of the important role of ω-hydroxylated-fatty acids in physiological or pathophysiological processes [76, 77, 78]. The most extensively studied member of the CYP4A subfamily is rat CYP4A1. Examples of substrates and catalytic activities of rat CYP4A1 are shown in Table 4.2 (adapted from [66]).

The majority of CYP4A enzymes are inducible by several structurally diverse xenobiotics collectively termed peroxisome proliferators. Under normal conditions, CYP4A proteins represent about 1-4% of total P450 content in rat liver. Following exposure to potent peroxisome proliferators such as clofibrate, CYP4A enzymes are induced up to 16-30% of the total P450 enzyme content [92, 93]. For example, in susceptible rodent

Species	CYP4A Forms	Tissue
Rat	4A1	Liver, kidney
	4A2	Liver, kidney
	4A3	Liver, kidney
	4A8	Prostate, kidney, retina
Rabbit	4A4	Lung, kidney, liver, uterus, placenta
	4A5	Kidney, liver, small intestine
	4A6	Kidney, liver
	4A7	Kidney, liver, small intestine
Human	4A11	Kidney, liver
	4A22	Liver
Mouse	4A10	Kidney, liver
	4A12	Liver, kidney
	4A14	
Hamster	4A17	
	4A18	
	4A19	
Guinea Pig	4A13	Liver
Koala	4A15	Liver
Cat	4A16	
Pig	4A21	Liver
	4A23	
	4A24	
	4A25	

Table 4.1: List of CYP4A isoforms from nine different species and their tissue distribution.
(Data were obtained from [10])

species such as rats, constitutive levels of P4504A1 are increased approximately 5- to 15-fold on treatment with peroxisome proliferators [98]. The link between peroxisome proliferator induced expression of CYP4A and peroxisomal β-oxidation enzymes, in conjunction with peroxisome proliferation, is well characterised [34, 67]. These inducible effects of peroxisome proliferators have been reported to be mediated by the nuclear receptor PPAR-α. CYP4A expression is also increased by endogenous compounds and other pathophysiological states including pregnancy [98], streptozotocin induced diabetes [95], a high fat diet [96] and the anti-inflammatory response [97, 102, 103, 104]. Acyclic monoterpenoids, such as citral and linalool, have been reported to cause peroxisome proliferation and induction of CYP4A1 and peroxisomal β-oxidation enzymes [5]. These monoterpenoids are used widely as food and cosmetic additives.

Substrate	ω-hydroxylase	(ω-1)-hydroxylase
Stearic acid (C18)	3.50	2.00
Palmitic acid (C16)	7.50	6.73
Lauric acid (C12)	13.50	1.20
Myristic acid (C10)	16.80	3.42
Vitamin D3	0.15	0.00
Cholesterol	0.13	0.00
Prostaglandin E1	0.60	0.02
Prostaglandin A1	2.50	0.05
Prostaglandin B4	0.87	0.00

Table 4.2: Omega- and (omega-1)-hydroxylase activity of rat CYP4A1. Activities are expressed as (nmol/min/nmol P450) (Data were obtained from [66]).

Over recent years, a number of high resolution three-dimensional (3-D) structures of P450s have been generated by X-ray crystallography. These studies have given valuable insights into the relationship between P450 structure and catalytic function. The work by Ortiz de Montellano and colleagues has generated substantial insight into the four active site amino acid residues that determine the regiospecificity of the CYP4A subfamily [70, 71, 262]. These studies have mainly focussed on rat CYP4A1, 4A2, 4A3, and human CYP4A11. On the human CYP4A11 model, these key residues are Tyr-120, Leu-132, Thr-325, and Val-386 [262]. For rat CYP4A3, mutations in ac-

tive site residues Tyr(117) and Leu (129) are found to alter the heme binding and catalytic properties of the enzyme [70, 71]. CYP4 proteins possess a highly conserved amino acid residue that plays an essential role in heme binding. This residue is glutamic acid 320 (CYP4A1), 315 (CYP4A2), 318 (CYP4A3), 319 (CYP4A8) and 321 (CYP4A11). This absolutely conserved glutamic acid residue is part of the highly conserved I-helix that forms the substrate recognition site in CYP4A enzymes (Section 1.1.4). The position of the glutamic acid residue with respect to the I-helix and the active site residues is shown in Figure 4.1.

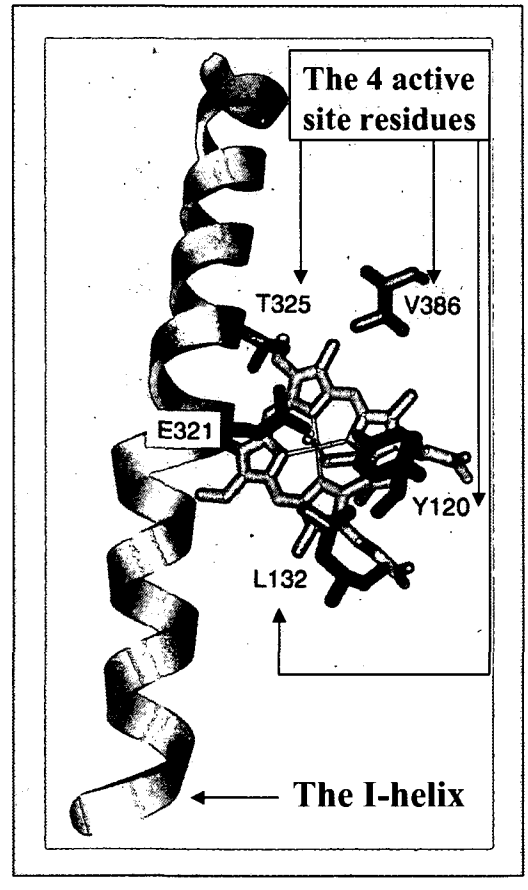

Figure 4.1: Homology model of CYP4A11.
A critical region of the CYP4A11 protein structure (the I-helix, the heme and the four active site residues) that form the substrate recognition site are shown. The figure indicates the position of Glu-321 (E-321) on the I-helix with respect to the active site residues Tyr-120, Leu-132, Thr-325, and Val-386. (Adapted and modified from [262]).

The heme in CYP4A enzymes has been found to be attached to the protein via an ester link to the glutamic acid residue [262]. Figure 4.2 shows a schematic diagram of the binding of the heme to the protein and the mechanism for the formation of the ester bone between the heme and the protein. Recently, the glutamic residue has been identified to be covalently linked to a hydroxyl group on the heme 5-methyl group. Fatty acid oxidation is sensitive to the presence or absence of the heme covalent link [49].

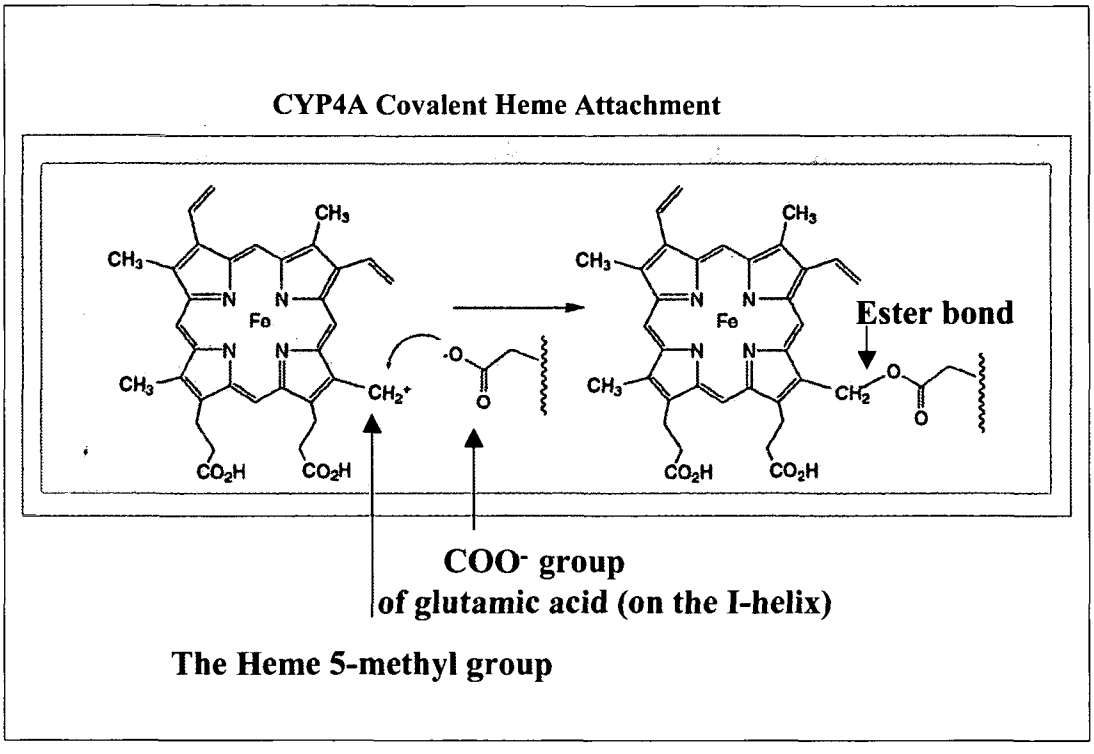

Figure 4.2: Diagram of binding site of the heme to the CYP apoprotein and the mechanism for the formation of the ester bond between the heme and the protein
(Adapted and modified from [49]).

As noted in Chapter 3, unlike other mammals, the obligate eucalypt feeder koala has a unique restricted diet, consisting exclusively of *Eucalyptus* leaves. These leaves contain a high quantity of monoterpenes that are major constituents of essential oils [4]. The induction of xenobiotic-metabolising enzymes, including CYP4A and β-oxidation enzymes, due to exposure to terpenoids and essential oils is well established [5, 6, 7, 217, 218, 219, 244, 245, 246]. Hepatic cytochromes P450 have been reported to participate in the metabolism of some terpenoids in eutherian species [5, 6, 7].

A reproducibly higher CYP4A activity and CYP content is observed in the koala relative to human, rat and wallaby [8, 94]. Isolation of the koala *CYP4A15* cDNA followed by activity studies using cDNA-expressed CYP4A15 will provide valuable insights into the significance of high CYP content and CYP4A activity in the koala liver. Prior to the commencement of these studies, no CYP4A partial or full-length cDNAs had been isolated from any marsupial species, except for the isolation of a partial koala liver *CYP4A15* 1188-bp cDNA in this laboratory [8]. This partial clone exhibits approximately 65% nucleotide and amino acid sequence identities to other CYP 4A enzymes and was named CYP4A15 [8]. The present work aimed to clone the full-length koala liver *CYP4A15* cDNA using PCR approaches and to investigate the lauric acid hydroxylase capacity of cDNA-expressed CYP4A15, using a Cos-7 cell expression system. CYP4A protein and mRNA expression and genomic DNA organisation across species were also examined by immunoblot, Northern and Southern blot analyses respectively.

To gain insight into the structure and function of the koala CYP4A15 enzyme, comparative modelling was used to generate a 3-D model of the koala CYP4A15 enzyme, based on the knowledge of the CYP4A15 amino acid sequence and the empirically determined 3-D structure of CYP2C5 [44]. Comparative modelling is a predictive tool, involving the generation of the 3-D structure of a protein for which the amino acid sequence, but not the 3-D structure, is known. The comparative modelling procedure employs three item inputs.

1. The sequence of the protein with unknown 3-D structure, referred to as target protein (CYP4A15).

2. A known 3-D structure template(s) chosen by virtue of having the highest sequence identity with the target protein. In this study, the 3-D structure of CYP2C5 was used as the template for modelling the 3-D structure of CYP4A15 since it is the only mammalian P450 3-D structure available.

3. An alignment between the target sequence (ie. CYP4A15) and the template sequence (ie. CYP2C5).

An overview of the process of comparative modelling of P450s is depicted in Figure 4.3.

The procedure of comparative modelling of P450s involves the following steps:

(a) Submission of a P450 amino acid sequence into the Protein Data Bank (PDB)

(b) Identification of 3-D structural templates

(c) 3-D structural alignment of templates

(d) Alignment of query amino acid sequence to template profile

(e) Model building: comparative modelling

(f) Model validation and analysis

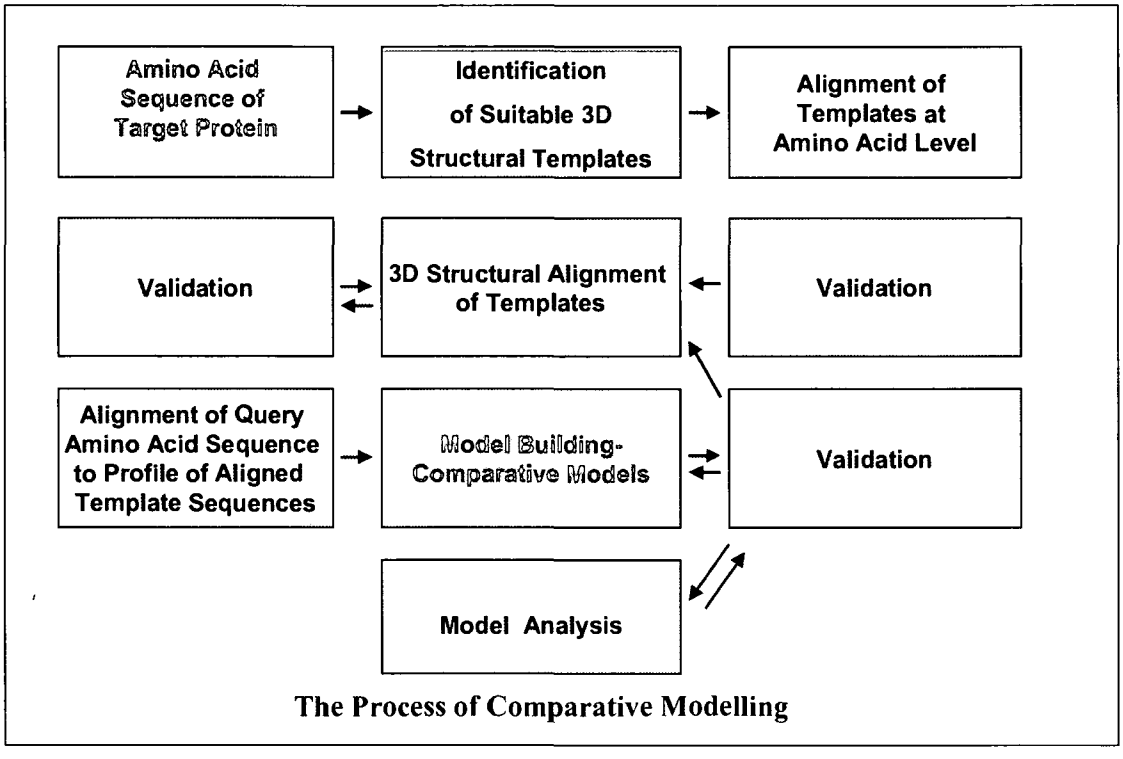

Figure 4.3: An overview of the process of comparative modelling of P450. (Reproduced from [44]).

Structural templates that have highest sequence homology with the target P450 are used for comparative modelling since proteins with similar amino acid sequences tend to adopt similar 3-D structures [263]. Homologous proteins could be selected by scanning the target P450 sequence against the sequences of published 3-D structures in the Protein Data Bank(PDB) [264, 265]. Currently, the rabbit CYP2C5 crystal structure is the only mammalian P450 crystal structure available and is most homologous structure for modelling mammalian P450s [44]. 3-D structural alignment of templates enables the identification of the active site of an unknown P450. Once the sequence alignment is created, a 3-D model is derived. The results are critically dependent on the choice of structural templates and the sequence alignment utilised. While the most popular modelling method has been to base the model on a single

3-D structure that is the most homologous one, multiple template approaches are also used widely for generating 3-D structure of target proteins. This chapter utilised a single template approach to model the CYP4A15 3-D structure using the rabbit CYP2C5 crystal structure.

4.2 METHODS

4.2.1 Cloning of koala liver *CYP4A15* cDNA

A near full-length koala liver *CYP4A15* cDNA, including the start codon ATG, was isolated using rapid amplification of cDNA ends (RACE) and conventional RT-PCR. Total RNA was isolated from koala liver using a modification of the method of Chomczynski and Sacchi [236] as described in section in Section 2.19.2. Purification of mRNA from total RNA samples was performed using the mRNA purification kit as per section 2.19.3. Koala first-strand cDNA was synthesised using the First-strand cDNA kit as described in Section 2.21.1.

Amplification of CYP4A15 5'end cDNA by RACE: The 5'end of koala liver *CYP4A15* cDNA was isolated using the SMART RACE cDNA Amplification kit as described in Section 2.21.3. The SMART technique utilises a Moloney Murine Leukaemia Virus-Reverse Transferase (MMLV-RT) that adds 3 to 5 dC nucleotides to the 3' end of the first-strand cDNA and uses the SMART II oligonucleotide primer, containing a stretch of dGs to bind to the resultant dC-rich cDNA tails. This generates a complete cDNA copy of the mRNA by reverse transcription with the additional SMART II primer at the end and ensures the production of clones containing complete coding regions. This is because the MMLV-RT adds the dC oligo most efficiently at the end of mRNA template.

To amplify *CYP4A15* 5' cDNA, RACE reactions were set up as described in section 2.21.3 using Universal Primer Mix (UPM) (Table 2.6) and a specific anti-sense primer, designated K4A5'r (Table 4.3), derived from the koala partial *CYP4A15* sequence [8]. Synthesis of koala and control 5' RACE ready cDNAs was performed as described in Section 2.21.3 and stored at -20^{0}C until needed. An *EcoR* 1 restriction site was added to the 5' end of the anti-sense primer to facilitate screening by restriction digest analysis. Touchdown PCR conditions for RACE reactions were as follows: 5 cycles of 94^{0}C for 5 seconds and 72^{0}C for 2 minutes; 5 cycles of 94^{0}C for 5 seconds, 70^{0}C for 10 seconds and 72^{0}C for 2 minutes, and 32 cycles of 94^{0}C for 5 seconds, 68^{0}C for 10 seconds and 72^{0}C for 2 minutes.

Amplified RACE fragments were analysed by gel electrophoresis as described in Section 2.15.2. For subsequent cloning into pGEM-T vector, polymerase was removed from the RACE reactions by adding 110 μl TE buffer (pH 8.0) and 1 μl of 2% w/v SDS

Name	Sequences (5'-3')	Origin	A*
K4A5'r	**GAATTC**ACCCATTAAGGACCAGCAGC	(+)73 - (+)92	a
K4Af1	**CCGGAATTC**ATTGGGGTAGTGGCATC **ATG**AAT	(-)17 - (+)6	b
K4Af2	**CCGGAATTC**AGTGGCATC**ATG**AATTC TCCGCT	(-)9 - (+)14	b
K4Ar	**CCGCTCGAG**TTTTTGGACTTGAGAAC CAGCTT	(+)1478 - (+)1500	b
R4Af	**CCGGAATTC**GATGGCTGCACC**ATG**AG CGTC	(-)12 - (+)9	c
R4Ar	**CCGCTCGAG**ACGGAA**TTA**GTGGAGCT TCTTGAG	(+)1513 - (+)1536	c

Table 4.3: Details of oligonucleotide primers used for isolation of full-length koala and rat *CYP4A1* and *CYP4A15* cDNAs.
Restriction sites and start/stop codon are shown in bold. A*: accession numbers: a, AF252263, koala CYP4A15 mRNA [8]; b, AF463456, koala liver CYP4A15 (Ngo *et al.*, direct submission); c, M14972, rat CYP4A1 [51]

and the reaction mixtures were heated at 70^0C for 10 minutes. After extraction once with hot phenol at 70^0C, twice with phenol/chloroform (1:1), and once with chloroform, the DNA was precipitated with ethanol and 3M sodium acetate (pH 5.2). The DNA solutions were centrifuged at 4^0C for 10 minutes. The DNA pellet was rinsed briefly with 70% ethanol and resuspended in an appropriate amount of sterile water. The PCR products were ligated into pGEM-T vector as described in Section 2.13.2, transformed into XL-1 Blue competent cells according to Section 2.13.3. The circular map of pGEM-T vector and its multiple cloning sites is shown in Figure 4.4. Several colonies were inoculated in 5ml LB containing ampicillin and incubated overnight at 37^0C. Plasmid DNA was purified using alkaline lysis and Qiaprep miniprep methods according to Section 2.14.1 and then analysed by restriction digest as per Sections 2.15.1 and 2.15.2. Plasmid DNA with the correct size inserts was sequenced using M13 universal (M13) and M13 reverse (M13r) sequencing primers (Table 2.5) as described in Section 2.16.

Amplification of koala *CYP4A15* 1517- and 1509-bp cDNAs by RT-PCR: Three gene-specific primers, designated K4Af1, K4Af2 and K4Ar (Table 4.3) derived

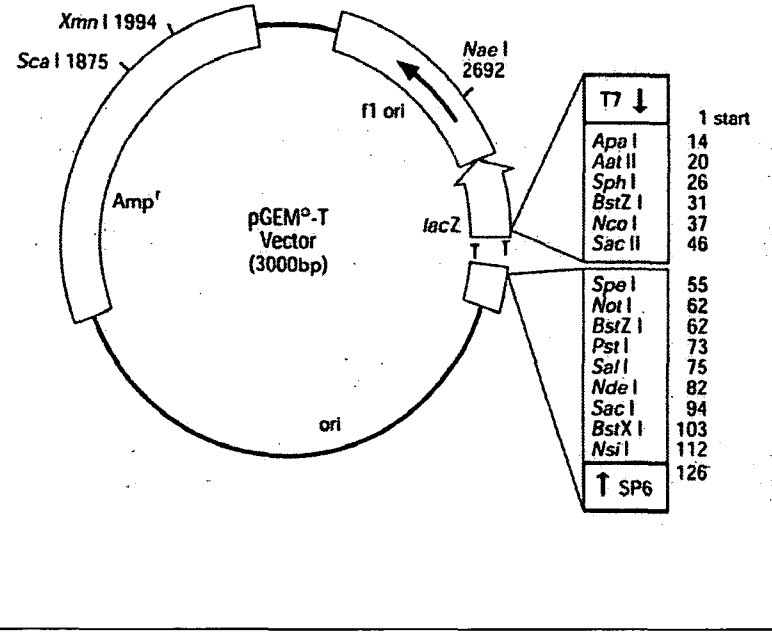

The pGEM-T vector Sequence Reference Points:

1. **Size:** 3000-bp
2. **T7 and SP6 RNA Polymerase promoters:** -17 to +3.
3. **M13 Forward Sequencing Primer:** 2941 to 2957.
4. **M13 Reverse Sequencing Primer:**161 to 177.
5. **Multiple cloning sites:** Multiple cloning sites are located between base pairs 10 to 113
6. **Eukaryotic selection:** Amp^r Stable selection of clones is made possible by the presence of the β-lactamase (Amp^r) coding region (1322 to 2182).

Figure 4.4: Circular map of pGEM-T vector and its multiple cloning sites. (Modified from Promega catalogue 1999).

from the 5' sequence obtained by RACE and the 3' end of the koala partial *CYP4A15* [8], were used for RT-PCR amplification of koala *CYP4A15* cDNAs, using koala first-strand cDNA as the template. Restriction sites, *EcoR* 1 and *Xho* 1, were included at the 5' end of the forward and reverse primers, respectively, to facilitate subsequent directional cloning into the pCMV-Script XR mammalian expression vector. K4Af1 and K4Ar primers amplify a 1517 base pair cDNA fragment. In comparison with other CYP4A sequence, this cDNA fragment corresponds to the entire coding region of CYP4A enzyme, except the last 11 (relative to CYP4A enzymes from rat, mouse and rabbit) or 20 (relative to human CYP4A) amino acid residues before the stop codon and contains the first 17 base pairs of the 5'-untranslated region (*5'-UTR*). K4Af2 and K4Ar primers amplify a 1509-bp cDNA fragment, including the first 9 base pairs *5'-UTR*. The cloning strategy for isolation of koala liver *CYP4A15* cDNA is summarised in Figure 4.5.

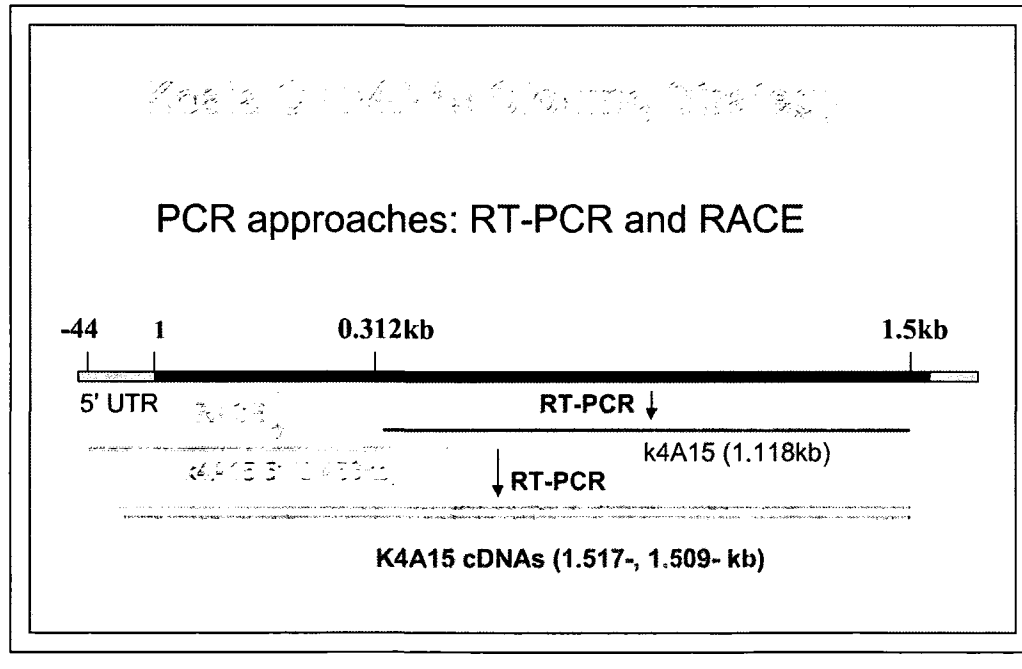

Figure 4.5: Schematic diagram of the cloning strategy for koala *CYP4A15* cDNAs.

The solid blue box represents the coding region of koala *CYP4A15* and the green boxes depict the 5' and 3' non coding regions. Single lines represent koala *CYP4A15* cDNAs: 5' cDNA amplified fragment obtained by RACE is red, and the koala partial *CYP4A15* isolated previously [8] is purple, koala 1517- and 1509-bp *CYP4A15* cDNAs are green.

PCR reactions were set up as described in Section 2.21.2. PCR reactions were cycled for 35 cycles of 94^{0}C for 30 seconds, 65^{0}C for 30 seconds and 72^{0}C for 2 minutes, followed by a final 10 minute extension at 72^{0}C.

PCR reactions were separated on 0.7% w/v low melt agarose gels, excised from the gels and then purified using a QIAEX II Gel Extraction Kit according to Sections 2.15.2. and 2.15.3. Purified PCR products were digested with *EcoR* 1 and *Xho* 1 as described in Section 2.15.1, ligated into pCMV-Script XR pre-digested vector according to Section 2.13.2 and transformed into *E. coli* strain XL1- Blue competent cells as per Section 2.13.3. Plasmid DNA from selected white colonies was extracted and screened by restriction digest with *EcoR* 1 and *Xho* 1 according to Sections 2.14.1 and 2.15.1. Plasmid DNA with correct size inserts was then sequenced in both forward and reverse directions using T3, T7 primers (Table 2.5) and derived internal primers (Table 2.5) as described in Section 2.16 .

4.2.2 Amplification of rat *CYP4A1* complete cDNA:

A full-length rat *CYP4A1* cDNA was isolated by RT-PCR essentially as described for the isolation of koala *CYP4A15* cDNA, using R4Af and R4Ar primers (Table 4.3), derived from rat *CYP4A1* published sequence [51]. The amplified clone was ligated into pCMV-Script XR pre-digested vector, transformed into XL 1-Blue competent cells, purified and sequenced as described for the cloning of the koala *CYP4A15* cDNA.

4.2.3 Expression of koala liver CYP4A15 and rat CYP4A1 in Cos-7 cells

Expression of koala liver CYP4A15 and rat CYP4A1 clones in pCMV-Script XR vector in Cos-7 cells was performed essentially as described in Section 2.21.4. Cos-7 cells are able to amplify and over express the transfected cDNA under the control of the SV40 large T promoter (for example cDNA clone in pCMV-Script XR vector). The koala *CYP4A* cDNA does not contain a stop codon, thus it was presumed that the product expressed in Cos-7 cells would have had an artefactual C-terminus derived from reading through the primer-derived sequence into the vector. The circle map and general features of pCMV-Script vector are shown in Figure 4.6.

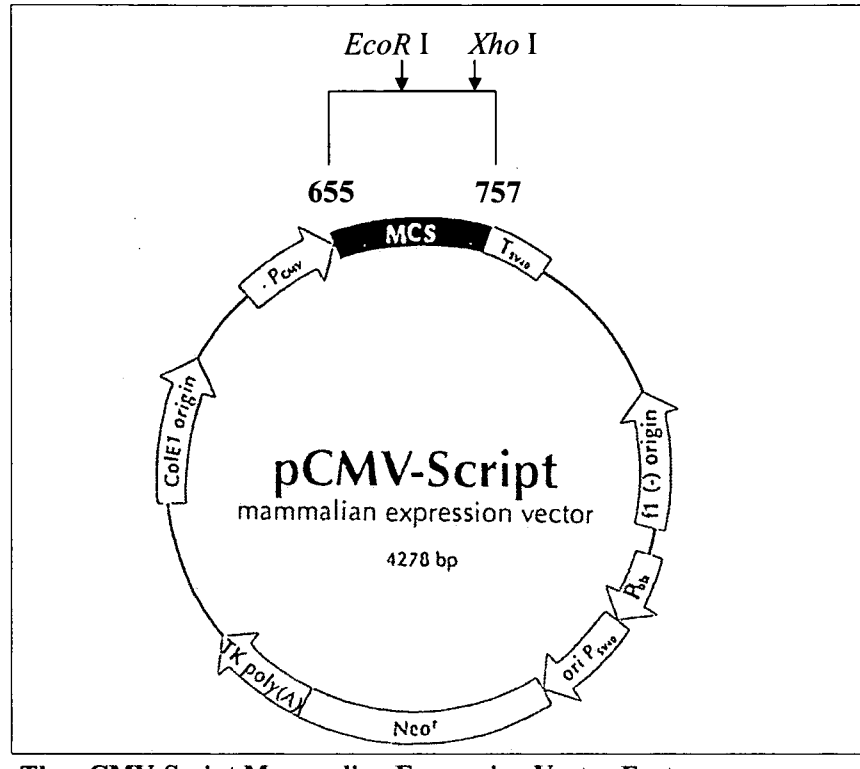

The pCMV-Script Mammalian Expression Vector Features:

1. **Size:** 4278-bp
2. **CMV promoter:** (1-602 bp) Eukaryotic expression driven by the CMV immediate early promoter.
3. **SV40 poly (A):** (811-1194)The SV40 polyadenylation sequence provides signals required for termination of transcription and polyadenylation.
4. **Kozac sequence:** Does not contain an ATG initiation codon
5. **Cloning sites:** Multiple cloning sites are located between base pair 655-757
6. **Eukaryotic selection:** Neo^r = G418 Stable selection of clones is made possible by the presence of the neomycin- and kanamycin-resistance gene (2180-2961)

Figure 4.6: Circle map of pCMV-Script vector and its features. (Modified from Stratagene catalogue 1998). The positions of *EcoR* I and *Xho* I cloning sites are shown.

4.2.4 Immunoblot analysis of cDNA-expressed koala and rat CYP4A enzymes and hepatic microsomes

Immunoblot analysis of cDNA expressed koala CYP4A15 and rat CYP4A1 enzymes (50 μg/lane) and of liver microsomes (50μg/lane) from koala and rat was performed essentially as described in Section 2.10. Sheep anti-rat CYP4A polyclonal antibody (1:200) and HRP-conjugated rabbit-anti-sheep IgG (1:2000) were used as primary and secondary antibodies, respectively.

4.2.5 Determination of total P450 content from cDNA-expressed koala and rat CYP4A enzymes in Cos-7 cell lysates

Total cytochrome P450 was determined by the method of Omura and Sato [29] using an absorption coefficient for the difference spectrum (450 to 490 nm) of 91 mM^{-1} cm^{-1}. Reduced-CO bound vs reduced difference spectra were determined after bubbling the sample cuvette with carbon monoxide.

4.2.6 Lauric acid hydroxylase activity of cDNA-expressed koala and rat CYP4A proteins

Lauric acid hydroxylase activity was determined using a modification of the method of Parker and Orton [233] as described in Section 3.2.4.

4.2.7 Microsomal preparations and protein assay

Preparation of hepatic microsomes was performed as described in Section 2.9.1 and the protein concentration of microsomes and Cos-7 cell lysates was determined by the method of Lowry *et al.* [229].

4.2.8 Analysis of CYP4A mRNA by Northern blotting

Isolation of total RNA from liver tissues and subsequent purification of mRNA was performed as described in Sections 2.19.2 and 2.19.3. Four to 10 μg of mRNA was separated on a 1% formaldehyde gel and then blotted onto a nylon membrane according to Sections 2.20.1 and 2.20.2. Prehybridisation, hybridisation, washing and

subsequent processing of the filter was performed according to Sections 2.20.3, using a koala *CYP4A15* 417-bp cDNA probe isolated by RT-PCR. The koala *CYP4A15* cDNA probe (corresponding to nucleotide 954-1371 in the CYP4A15 nucleotide sequence) contains the CYP4A highly conserved sequence and part of the P450 signature motif and shares approximately 73% nucleotide sequence identity to other CYP4A cDNA sequences. The koala *CYP4A15* probe was labelled with α-[^{32}P]-dCTP using the Gigaprime DNA labelling kit as described in Section 2.17. To assess relative mRNA loading, the filter was stripped and re-probed with a β-actin cDNA probe (Ambion International, TX, USA).

4.2.9 Analysis of the *CYP4A* gene by Southern blotting

Genomic DNA was extracted according to Section 2.18.1. DNA fragments were separated by gel electrophoresis through a 0.7% agarose gel and blotted onto a nylon membrane in 10 X SSC overnight as described in Sections 2.18.2 and 2.18.3. Prehybridisation, hybridisation, washing and developing of the filter was performed essentially as described for Northern blot analysis, except that 6 X SSC was used instead of 5 X SSC.

4.2.10 Comparative modelling and CYP4A15 3-D structure prediction

The 3-D structure of the koala CYP4A15 enzyme was modelled based on the empirically determined 3-D structure of CYP2C5 and amino acid sequence alignment of CYP4A15 with this rabbit CYP2C5 structure. In this procedure, the backbone of CYP4A15 sequence was arranged identically to CYP2C5 template to generate a homology model of the koala CYP4A15. The procedure was performed using Swiss PDB Viewer 3 programme. The amino acid sequence alignment of CYP4A15 with other CYP4A proteins was accomplished in an attempt to examine the active site residues that are involved in substrate recognition sites. The rabbit CYP2C5 crystal structure is currently the only mammalian P450 crystal structure available and is most homologous structure for modelling mammalian P450s [44]. The amino acid sequence of the koala CYP4A15 was submitted into the Protein Data Bank (PDB) [265] and a homology model of CYP4A15 was generated based on the 3-D structure

of this CYP2C5.

4.3 RESULTS

4.3.1 Cloning and sequencing of koala hepatic *CYP4A15* cDNA

Amplification of koala *CYP4A15* cDNA by Rapid Amplification of cDNA Ends (RACE): A partial koala *CYP4A15* cDNA of 1188-bp has been previously isolated in this laboratory [8]. In this chapter, the 5'-end of the koala *CYP4A15* cDNA was isolated by RACE. UPM and K4A5'r primers (Tables 2.5 and 4.3) amplified 850-bp and 500-bp 5'-RACE fragments as shown in Figure 4.7.

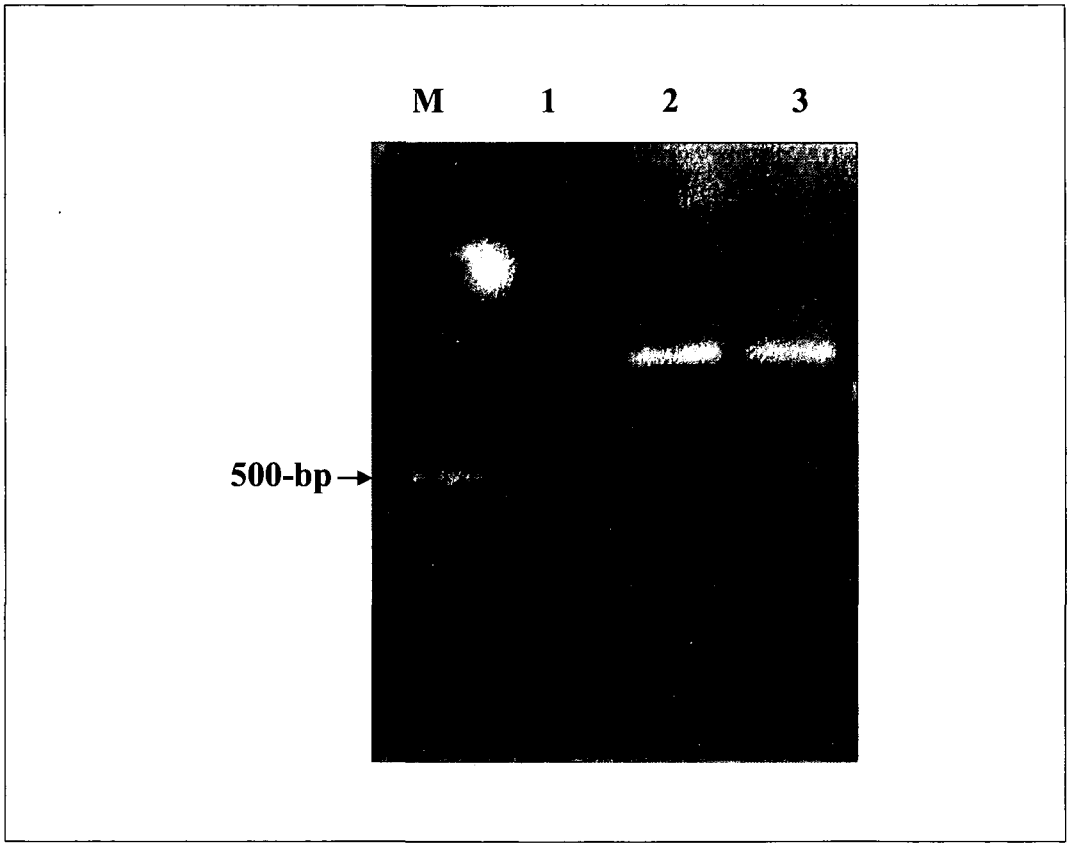

Figure 4.7: Agarose gel analysis of PCR products generated from koala liver 5'RACE-ready cDNA using UPM and K4A5'r primers.
Lanes 2 and 3: PCR reactions using UPM and K4A5'r primers. Lane 1: negative control (PCR reaction with no DNA template). Lane M: 100bp DNA ladder

The amplified PCR products were purified and subcloned into the pGEM-T vector (Sections 2.13.2 and 2.13.3). Several clones were sequenced to confirm their identity (Section 2.16). These 5' end cDNA sequences are identical and encode the first

105 amino acids of the koala CYP4A15 enzyme and contain 43-bp *5'-UTR*. The 5'-fragments also contains approximately 100-bp overlapping sequence with the koala partial *CYP4A15* cDNA isolated previously [8]. Other RACE products of size between 500- to 850-bp were also amplified, evident by the presence of a DNA smear in the gel electrophoresis of RACE products (Lane 3, Figure 4.7). The presence of multiple size DNA fragments may reflect several different size *CYP4A15* cDNA fragments in the RACE ready cDNA template.

Amplification of koala near full-length *CYP4A15* cDNAs by polymerase chain reaction: To confirm the presence of functional CYP4A15 in the koala liver, a koala liver *CYP4A15* cDNA including start codon was isolated and the enzymatic activity of cDNA-expressed koala CYP4A15 was examined. Utilising two forward primers K4Af1 and K4Af2 and a reverse primer K4Ar (Table 4.3), PCR fragments of size approximately 1.5-kb were visualised in the PCR samples generated from koala liver first-strand cDNA (Figure 4.8, Lane 2 and 3). This size was the expected size for these primer combinations. PCR fragments of the same size were amplified from rat liver first-strand cDNA (Figure 4.8, Lane 4 and 5), using R4Af and R4Ar primers (Table 4.3). Fig 4.9 shows the PCR products generated from large scale amplifications of koala liver first-strand cDNA (Lane 2-3), using forward K4Af1 and K4Af2 and reverse K4Ar primers.

The cDNAs were subcloned initially into the pGEM-T vector (Section 2.13.2 and 2.13.3) and sequenced in both forward and reverse direction to confirm their identity (Section 2.16). Two koala liver *CYP4A15* cDNAs of sizes 1517- and 1509-bp were amplified. The sequences of the two koala *CYP4A15* cDNAs were found to be identical. The previously cloned *CYP4A15* partial cDNA displays 100% sequence identity to the new 1517- and 1509-bp cDNA sequences [8]. By comparison with CYP4A subfamilies from other species, the koala *CYP4A15* cDNA has a 1500 base pair open reading frame and presumably encodes the entire coding region of CYP4A except the last 11 (relative to CYP4A enzymes from rat, mouse and rabbit) or 20 amino acids (relative to human CYP4A enzymes) before the stop codon. The nucleotide and deduced amino acid sequence of the koala CYP4A are shown in Figure 4.10. Its 43-bp 5'-*UTR* was also included.

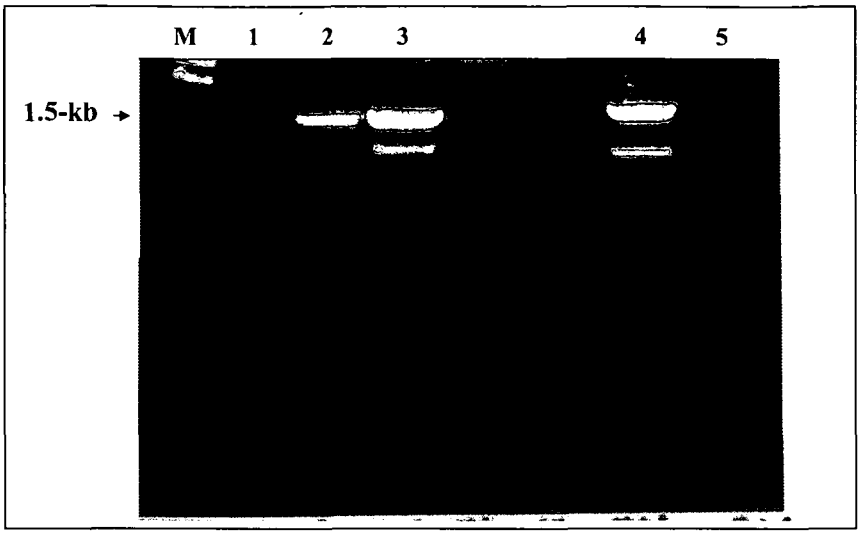

Figure 4.8: Agarose gel analysis of PCR products generated from koala first-strand cDNA
Lane 2: PCR reaction using forward K4Af1 and reverse K4Ar primers. Lane 3: PCR reaction using forward K4Af2 and reverse K4Ar primers. Lane 1: negative control (PCR reaction with no DNA template). Lane M: DNA markers, 100bp DNA ladder and λ DNA restricted with *Hind III*. Lane 4, 5: PCR products generated from different rat liver first-strand cDNAs, using R4Af and R4Ar primers.

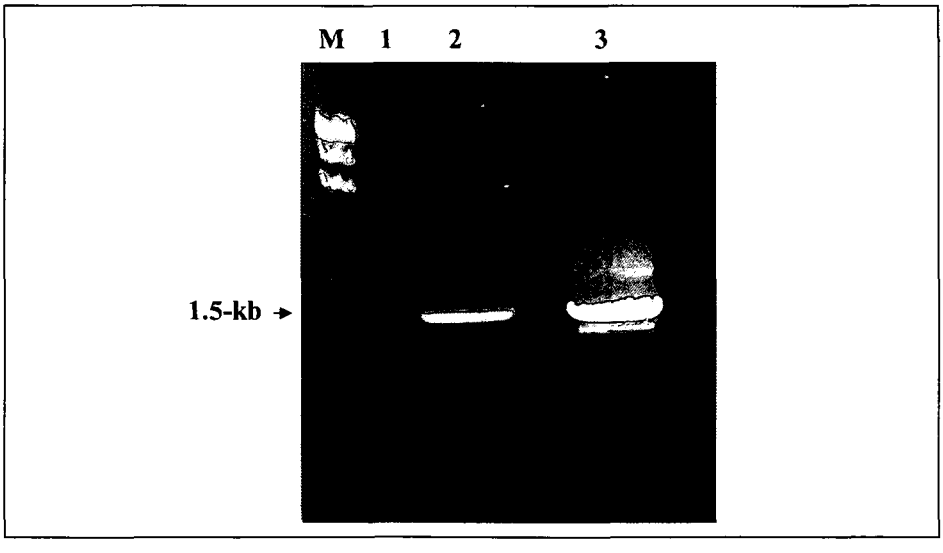

Figure 4.9: Agarose gel analysis of PCR products generated from koala first-strand cDNA (Large-scale PCR amplification).
Lane 2: PCR reaction using forward K4Af1 and reverse K4Ar primers. Lane 3: PCR reaction using K4Af2 and K4Ar primers. Lane 1: negative control (PCR reaction with no DNA template). Lane M: λ DNA restricted with *Hind III*.

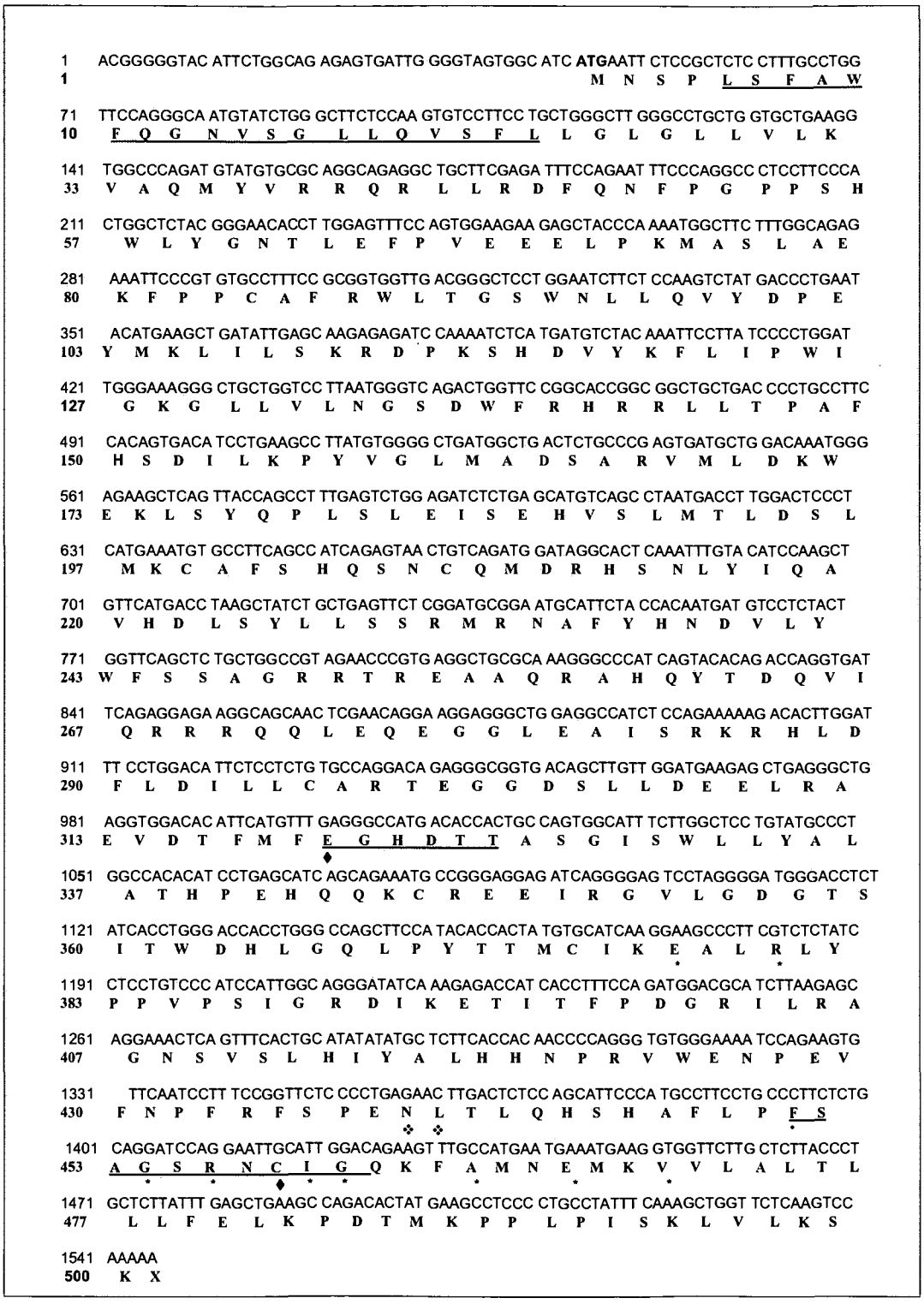

Figure 4.10: cDNA and deduced amino acid sequence of CYP4A15 from koala liver.

Figure 4.10 (continued): cDNA and deduced amino acid sequence of cytochrome P450 CYP4A15 cloned from koala liver. Nucleotides and the corresponding amino acids, shown by single-letter codes, are numbered as indicated at the left hand side of the figure. The ATG start codon is bolded at position 44. The sequence consists of an open reading frame encoding 500 amino acids and contains two extra amino acid residues, asparagine (N) and leucine (L), indicated by the four dot diamonds, as compared with the deduced amino acid sequences from other published *CYP4A* cDNAs. Underlined amino acid sequences correspond to a) The hydrophobic amino acid sequence of 20 residues (5 through 23) in the N-terminal which represents a transmembrane anchor, a fundamentally conserved amino acid structure core of all eukaryote cytochrome P450 enzymes, b) The CYP4A family highly conserved EGHDTT sequence in the I-helix, which contains the conserved glutamic acid residue present only in the CYP4A family, and c) The highly conserved P450 signature motif containing the haem-binding cysteine residue. The invariant cysteine residue and the CYP4A specific conserved glutamic acid residue are indicated by diamonds. Other highly conserved residues of significance are indicated by the asterisk. In comparison with CYP4A subfamilies from other species, the koala *CYP4A15* cDNA presumably encodes the entire coding region of CYP4A except the last 11 (relative to CYP4A enzymes from rat, mouse and rabbit) or 20 amino acids (relative to human CYP4A enzymes) before the stop codon.

The cloned koala *CYP4A15* cDNA exhibits highest sequence identity with the human *CYP4A11* cDNA, displaying 69% overall nucleotide identity. The deduced protein shares 65% amino acid identity with the human enzyme. The koala CYP4A also has several features in common with other cytochromes P450 however it contains two extra amino acid residues. These common features include the P450 signature motif of 10 residues and the hydrophobic sequence of about 19 residues in the N-terminal of eukaryotic P450. The P450 signature motif contains the absolutely conserved cysteine residue that ligates the heme iron while the N-terminal was reported to represent a transmembrane anchor. The two other invariant residues are glutamic acid (E) and arginine (R) (Figure 4.10). The cDNA sequence was submitted to GenBank (Bethesda, Maryland USA) and has been assigned the accession number AF463456.

4.3.2 Expression of CYP4A protein in Cos-7 cells and immunoblot analysis of cDNA-expressed CYP4A proteins

For transfection of Cos-7 cells, the koala *CYP4A15* was inserted into the pCMV-Script XR mammalian expression vector. Before transfection, several clones were sequenced in both directions to confirm their identity. A restriction map of *CYP4A15* was generated to ensure that the restriction sites selected for sub-cloning did not cut within the coding region (Figure A.1, Appendix A). The koala *CYP4A15* cDNA does not contain a *Xho* 1 restriction site. Since *EcoR* 1 occurs once after amino acid residue 1, the koala *CYP4A15* cDNA clones utilised in transfection studies does not contain the start codon methionine (Section 4.3.1). Another methionine codon was found at position 37 (Figure 4.10). While the second methionine codon does not appear to have a Kozac sequence positioned appropriately, it appears to function in the Cos-7 cell expression system (Figure 4.11).

The koala *CYP4A15* cDNA was digested with *EcoR* 1 and *Xho* 1 and then ligated into *EcoR* 1 and *Xho* 1 pre-digested pCMV-Script XR vector. For functional comparison, the rat *CYP4A1* cDNA was amplified by RT-PCR, inserted into the pCMV-Script XR vector and transfected into Cos-7 cells. The cells were harvested three days after transfection. Transfections with either no DNA or no LipofectAMINE were used as negative controls.

cDNA-expressed koala and rat CYP4A proteins were then detected by immunoblot analysis. Figure 4.11 shows an immunoblot of cDNA-expressed koala and rat CYP4A

proteins. CYP4A immunoreactive bands of mass 54-kDa were detected in both cDNA-expressed koala CYP4A15 and rat CYP4A1 proteins. No immunoreactive band of mass 54-kDa was observed for untransfected Cos-7 cell lysate. The expression of CYP4A proteins in the koala as compared to human, rat, and wallaby liver microsomes was also examined. Figure 4.12 shows a CYP4A immunoreactive band of greater intensity in koala microsomes as compared to other species studied.

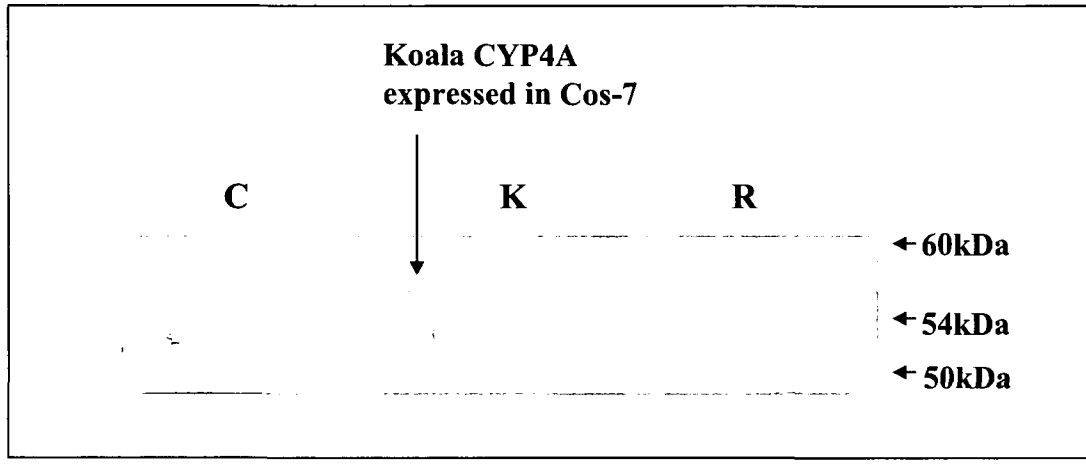

Figure 4.11: Immunoblot analysis of cDNA-expressed koala and rat CYP4A.
Lane 1: negative control (C), untransfected Cos-7 cell lysate, Lane 2: cDNA-expressed koala CYP4A protein (K) (50 μg/lane), Lane 3: positive control, cDNA-expressed rat CYP4A1 protein (R) (50 μg/lane). The blot shows that transfection of Cos-7 cells with koala and rat *CYP4A* cDNAs resulted in the expression of proteins of the mass approximately 54-kDa, recognised by a sheep anti-rat CYP4A polyclonal antibody. This immunoreactive band was not detected in untransfected Cos-7 cell lysate.

4.3.3 Determination of total CYP content from CYP4A protein expressed in Cos-7 cells

Total CYP contents were determined in Cos-7 cells transfected with koala and rat *CYP4A* cDNA clones. Microsomal samples from koala and rat livers were included as positive controls. The results are summarised in Table 4.4. Total CYP contents for cDNA-expressed koala CYP4A15 and rat CYP4A1 proteins in Cos-7 cells were comparable. A negligible reading was obtained for untransfected Cos-7 cell lysate.

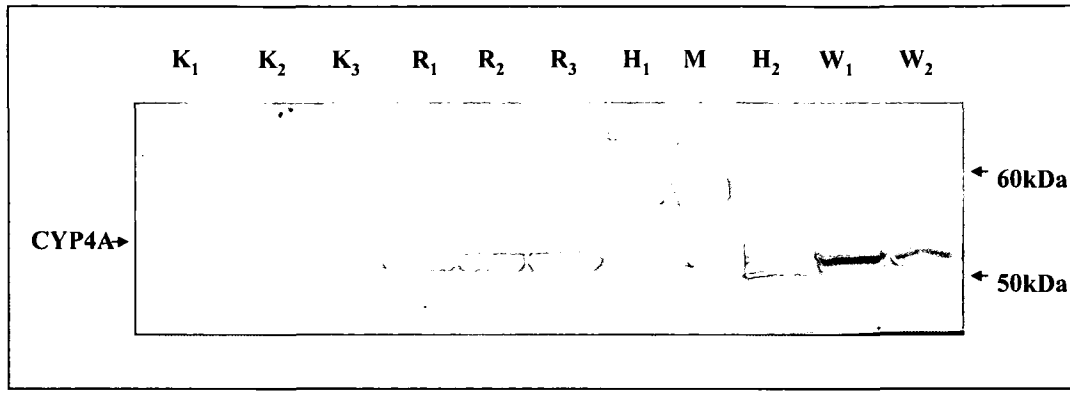

Figure 4.12: Immunoblot analysis of CYP4A proteins in koala liver microsomes as compared to human, rat, and wallaby.
Protein (50 μg/lane) from koala (K), rat (R), human (H), and wallaby (W) hepatic microsomal samples were used for immunoblot analysis, utilising sheep anti-rat CYP4A polyclonal antibody. The blot detected CYP4A immunoreactive protein of mass 54-kDa in koala, rat and wallaby liver microsomes. Immunoreactive protein of mass 52-kDa was detected in the human liver microsomes. Immunoreactive protein of mass 48-kD was also detected in the koala liver microsomes. For the wallaby samples, the band detected was very pronounced.

Samples	CYP450 content (nmole/mg protein)
Cos-7 cell Control (C)	Negligible
Transfection Control (T)	Negligible
Koala liver microsomes	1.250 ± 0.050
Rat liver microsomes	0.350 ± 0.011
cDNA-expressed koala CYP4A15 [a]	0.094 ± 0.001
cDNA-expressed koala CYP4A15[b]	0.326 ± 0.001
cDNA-expressed rat CYP4A1[a]	0.068 ± 0.005
cDNA-expressed rat CYP4A1[b]	0.130 ± 0.011

Table 4.4: Total P450 content determined in Cos-7 cells transfected with koala and rat *CYP4A* cDNA and in koala and rat microsomes.
Data are expressed as mean ± SD from triplicate determinations, each transfection was performed in duplicate. [a] Cell lysates from small-scale transfections. [b] Cell lysates from large-scale transfections. C: Cos-7 cell control. T: Transfection control, transfection with no LipofectAMINE.

A second larger scale transfection study was also performed. Total CYP contents for expressed koala CYP4A15 and rat CYP4A1 proteins in Cos-7 cells in this study were found to be higher than those observed for the first experiment (Table 4.4)

4.3.4 Determination of lauric acid hydroxylase activity of cDNA-expressed koala CYP4A15 protein

Lauric acid hydroxylase activity was examined for cDNA-expressed koala CYP4A15 and compared to that observed for cDNA-expressed rat CYP4A1. Samples from koala and rat liver microsomes were included as positive controls. The results are summarised in Table 4.5. Statistically significant higher levels of lauric acid hydroxylase activity were detected for both cDNA-expressed koala and rat CYP4A proteins, as compared to untransfected Cos-7 cell lysates ($p<0.025$). Lauric acid hydroxylase activity for cDNA-expressed koala CYP4A15 was similar to that for cDNA-expressed rat CYP4A1 (0.45 ± 0.18 and 0.55 ± 0.08 nmole/min/mg protein, respectively, mean $\pm$ SD). When expressed as nmole/min/nmole CYP, the rates of lauric acid hydroxylation for cDNA-expressed koala CYP4A15 are lower than that of cDNA-expressed rat CYP4A1 ($4.79\pm$ 1.91 versus 8.09 ± 1.17 nmole/min/nmole CYP respectively, mean $\pm$ SD, Table 4.5).

The results for lauric acid hydroxylase activity for cDNA-expressed koala CYP4A15 and rat CYP4A1 determined from the second large-scale transfection experiment are also summarised in Table 4.5. The activities per CYP content (nmole/min/nmole CYP) for both koala and rat CYP4A cDNA-expressed proteins are lower than that of the first experiment.

4.3.5 Northern blot analysis of CYP4A mRNA in koala liver and other hepatic tissues

Liver mRNA from two male koalas was analysed by Northern blot analysis using a koala *CYP4A15* 417-bp cDNA probe. Messenger RNA samples from rat, human, wallaby and possum livers were included for comparison. Equal loading between lanes was confirmed by ethidium bromide staining of the gel (Section 2.19.4) and spec-

Samples	LA (nmole/min/ mg protein)	LA (nmole/min/ nmole CYP)
Cos-7 cell control	0.06 ± 0.03	nd
Transfection control	0.02 ± 0.01	nd
Koala liver microsomes	7.18 ± 0.15	nd
Rat liver microsomes	4.13 ± 0.04	nd
cDNA-expressed koala CYP4A15 [a]	0.45 ± 0.18	4.79 ± 1.91
cDNA-expressed koala CYP4A15 [b]	0.90 ± 0.02	2.76 ± 0.06
cDNA-expressed rat CYP4A1 [a]	0.55 ± 0.08	8.09 ± 1.17
cDNA-expressed rat CYP4A1 [b]	0.50 ± 0.18	3.85 ± 1.38

Table 4.5: Lauric acid hydroxylase activity catalysed by cDNA-expressed koala and rat CYP4A proteins and in koala and rat microsomes.
Data are expressed as mean ± SD from triplicate determinations, each transfection was performed in duplicate. LA: lauric acid. [a] Cell lysates from small-scale transfections. [b] Cell lysates from large-scale transfections. C: Cos-7 cell control. T: Transfection control, transfection with no LipofectAMINE. nd: not determined.

trophotometric quantification of mRNA (Section 2.15.4). After stripping, the blot was hybridised with the housekeeping gene β-actin as an additional loading control. Northern blot of CYP4A mRNA in koala, rat, human and possum liver is shown in Figure 4.13. Messenger RNA hybridising with the koala *CYP4A15* cDNA probe was detected in all samples studied, except for the wallaby (not shown). More intense mRNA bands of size approximately 2.6-kb was detected in the koala livers as compared to other species examined.

4.3.6 Southern blot analysis of *CYP4A* genes in koala liver and other hepatic tissues

EcoR 1-digested liver genomic DNA from five male koalas was analysed by Southern blot analysis, using the koala *CYP4A15* 417-bp cDNA probe. Genomic DNA from male rat, wallaby, possum, and bandicoot livers was included for comparison. Southern blot analysis of *CYP4A* genes in these species is shown in Figure 4.14. Most genomic DNA samples showed distinct hybridisation bands with the koala *CYP4A15* cDNA probe. *EcoR* 1-digestion of genomic DNA produced *CYP4A* gene fragments

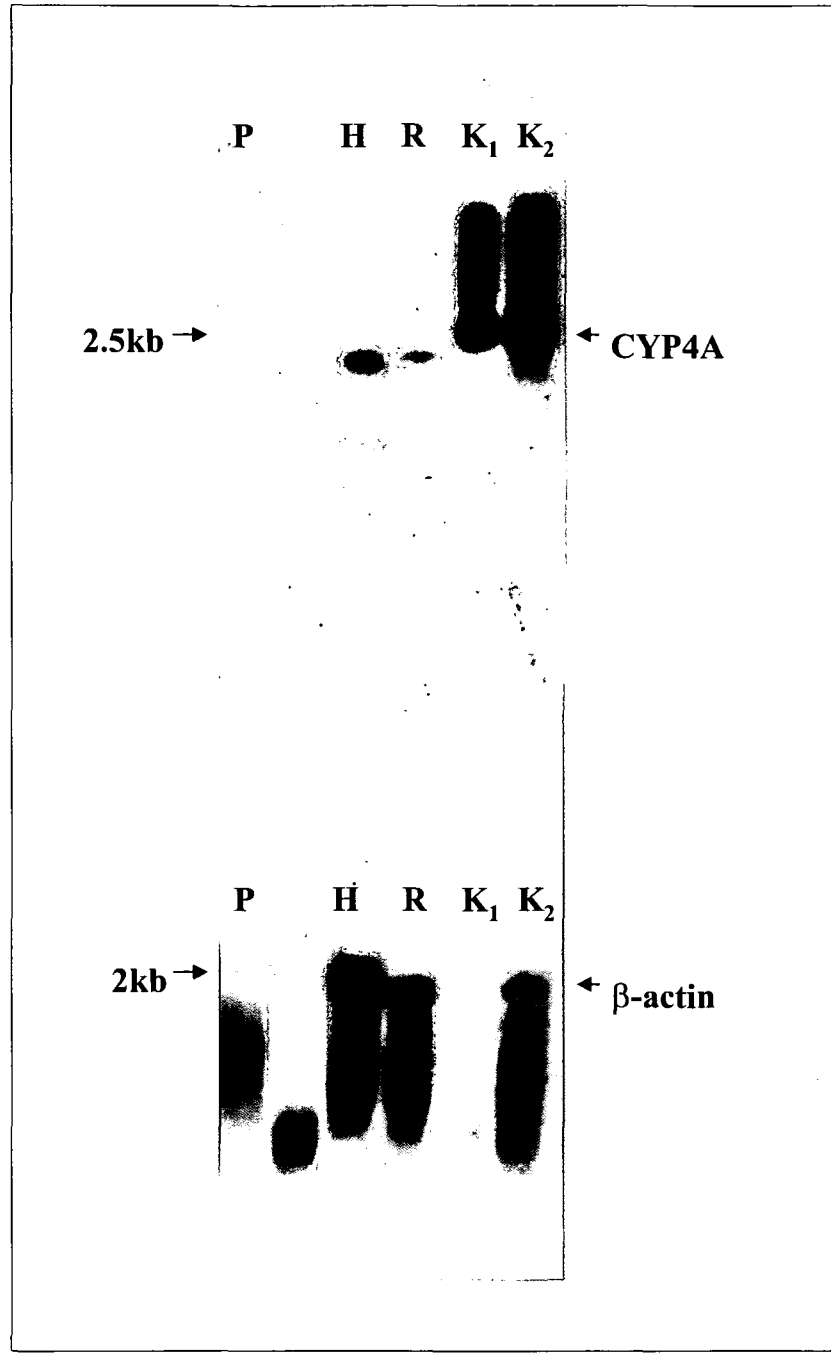

Figure 4.13: Northern blot of hepatic CYP4A mRNA.
Messenger RNA (10 μg, except koala K_1 (4 μg)) was purified from two koala (Lanes K_1 and K_2), possum (Lane P), human (Lane H) and rat (Lane R) liver samples and hybridised with a koala *CYP4A15* 417-bp cDNA probe,^{32}P-labelled (upper panel, between P and H samples: a degraded possum mRNA sample). Lower panel (B): Hybridisation with mouse β-actin. The blot shows more intense mRNA signals in koala livers as compared to that of other species. When re-probed with β-actin, a mRNA species of size 2-kb (correct size) was observed for all species studied, with significant differences in the intensity of the band detected across species.

of different sizes in the species examined.

4.3.7 Comparative modelling of the koala CYP4A15

The 3-D structure of the koala CYP4A15 enzyme was predicted using comparative modelling. Figure 4.15 shows a homology model of CYP4A15 based on the 3-D crystallised structure of the rabbit CYP2C5 enzyme. The heme, the I-helix and the four active site residues that form the substrate recognition site are shown. The position of the two extra amino acid residues asparagine (439) and leucine (440) versus the substrate recognition site regions is shown in figure 4.16.

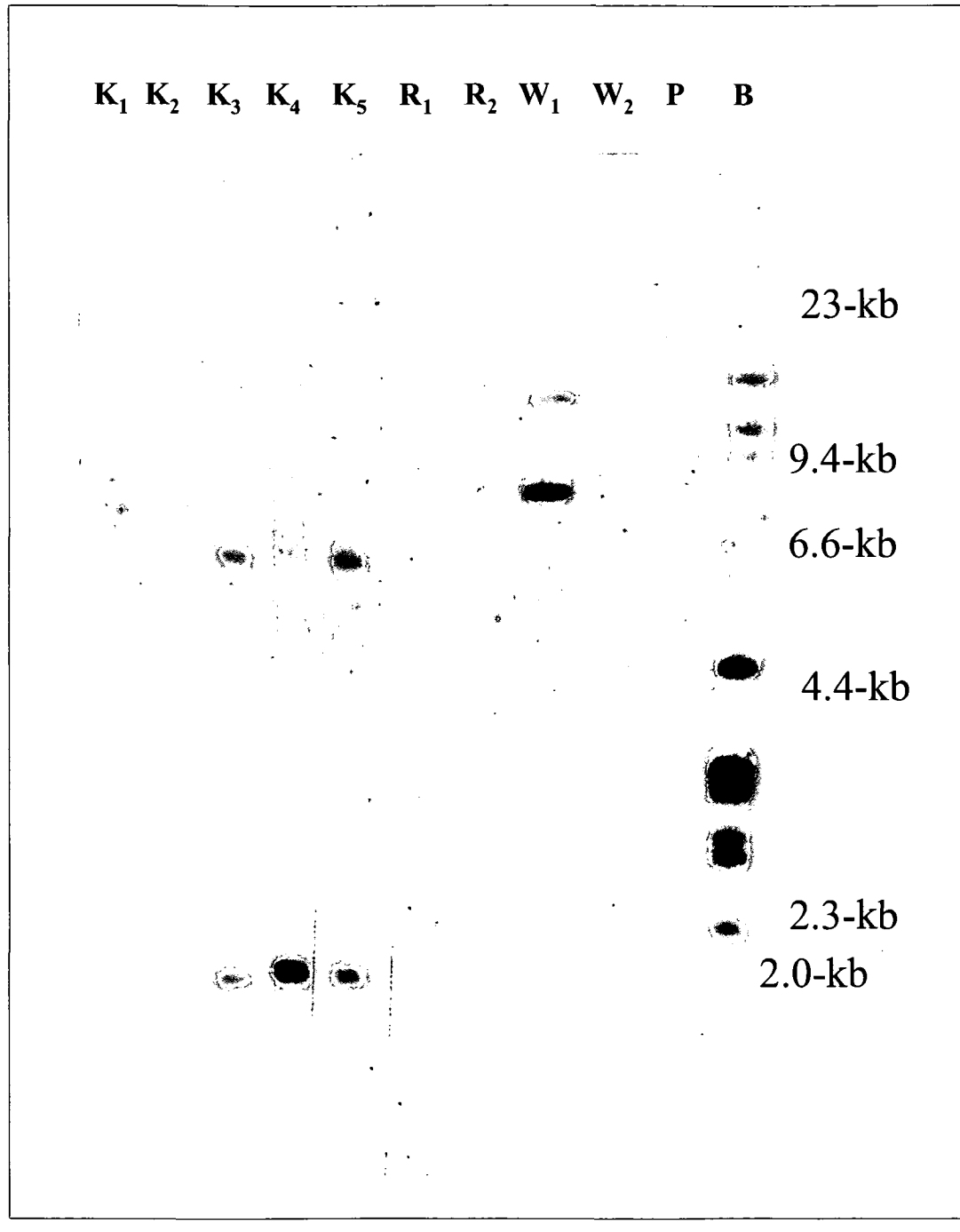

Figure 4.14: Southern blot analysis of the *CYP4A* gene.
Genomic DNA was extracted from five koala (Lane K_1-K_5), two rat (Lane R_1-R_2), two wallaby (Lane W_1-W_2), one possum (Lane P), and one bandicoot (Lane B) liver samples, digested with *EcoR* 1 and hybridised with a koala *CYP4A15* 417-bp cDNA probe (^{32}P-labelled). *CYP4A* gene fragments of different sizes were observed for the koala and other species studied.

4.4 DISCUSSION

The present study has utilised RT-PCR approaches to isolate and express the koala *CYP4A15* in Cos-7 cells. While koala CYP4A15 clone selected for protein expression and activity analysis has N- and C-terminally truncated due to *EcoRI* restriction digest (for N-terminal), both enzymatic assay and immunoblot analysis of the cDNA-expressed CYP4A15 protein clearly demonstrate that the *CYP4A15* cDNA-expressed protein appears functional, exhibiting similar capacity to metabolite lauric acid as cDNA-expressed rat CYP4A1. While N-terminal truncation may affect coupling of CYP4A15 enzyme with the reductase, C-terminal truncation and modification may or may not predictable effects. Future experiments looking at the activity of intact CYP4A15 protein will confirm the role of the N- and C-terminus in the catalytic function of the enzyme. The results of the present studies show higher CYP4A protein and mRNA levels in koala liver than in rat, human and wallaby liver. Higher hepatic microsomal lauric acid hydroxylase activity and CYP content in the koala is therefore likely to be a result of higher CYP4A expression. While the precise role of CYP4A enzymes in the oxidative metabolism of terpenes is not known, the possibility exists that *Eucalyptus* terpenes in the koala diet have an inducible effect on CYP4A protein and mRNA levels. In addition, the results of Chapter 3 have shown that a *Eucalyptus* diet modulates expression of other fatty acid metabolising enzymes such as acyl CoA Oxidase.

The cloned koala liver *CYP4A15* cDNA (3' truncated) has a 1500-bp open reading frame and contains a 44 base pair 5'-*UTR*. It encodes a protein of 500 amino acids. The size of the cloned *CYP4A15* cDNA is consistent with that of most mammalian *CYP4A* clones reported [51, 54, 55, 58, 61, 63, 64, 65]. When aligned with the available CYP4A deduced amino acid sequences from other species, the *CYP4A15* cDNA encodes the majority of the CYP4A protein with the exception of the last 11 (relative to rat, rabbit and mouse CYP4A1 enzymes) or 20 residues (relative to human CYP4A enzymes) prior to the stop codon (Figure B.1, Appendix B). It was interesting to observe that the koala *CYP4A15* cDNA contains six extra base pairs (two amino acid residues, asparagine–439 and leucine-440, Figure 4.10) and the N-terminus appears to be one codon shorter than those of other species. Another initiation codon, which appears to function in the Cos-7 cell expression system, was found at the position of amino acid residue 37 (Figure 4.10).

The koala CYP4A15 shows highest sequence identity to human CYP4A11. The cDNA sequence shares 69% nucleotide identity to human cDNA and the protein sequence exhibits 65% overall identity to the human enzyme (Table 4.6). It was obvious that the sequence identities between the various placental CYP4A enzymes are higher than any of the identities to the koala CYP4A15 sequence. This may reflects the divergence of the marsupial koala from the placental species.

The koala CYP4A15 protein shares several common features with other cytochrome P450 sequences. The initiator methionine is followed by a hydrophobic sequence of 20 residues in the N-terminal, residues 5 through 23 deduced from this cDNA (Figure 4.10). This N-terminal is thought to represent a transmembrane anchor, a fundamentally conserved structural core of amino acids seen in all other eukaryote cytochrome P450 enzymes identified to date[266]. As compared with most CYP4A subfamilies from other species, the N-terminal sequence of the koala CYP4A15 is shorter by one residue. Figure 4.17 shows the NH2-terminal amino acid sequence comparison between the koala CYP4A15 and CYP4A subfamilies from other species.

Studies of Hoch and colleagues (2000), who have generated chimeric forms in which the N-terminal region of CYP4A2 and CYP4A3 were switched, revealed that the first 119 amino acid residues determine the ratio of ω- and (ω-1) hydroxylation activity of these enzymes [70, 71]. The N-terminal of pig liver CYP4A21, a CYP4A enzyme without the capacity to hydroxylase lauric acid, was found to be shorter by six residues as compared to those of other species [65]. Given that the two bases immediately preceding the *EcoRI* site in pCMV-Script were not AT, the cDNA-expressed CYP4A15 protein has the capacity to hydroxylase lauric acid despite the absence of 36 single amino acid residues in the N-terminal sequence (Table 4.5). It would be of interest to express intact-CYP4A15 protein and examine its capacity to hydroxylase lauric acid. In most CYP4A subfamilies known to catalyse lauric acid predominantly at the ω-position, the N-terminal is also followed by a stretch of the hydrophobic amino acid, Leucine LGLLLLLL (Figure 4.17). In the koala CYP4A15, two of the leucine residues in these six consecutive leucine residues are replaced by glycine and valine. Amino acid substitutions at these positions were also found in rat CYP4A3, a CYP4A enzyme which metabolises lauric acid at both ω- and (ω-1) carbons [54, 55, 67]. It would be of interest to examine the role of CYP4A15 glycine and valine residues in the control of ω- and (ω-1) hydroxylation activity and in the process of integrating CYP4A15 into the endoplasmic reticulum membrane.

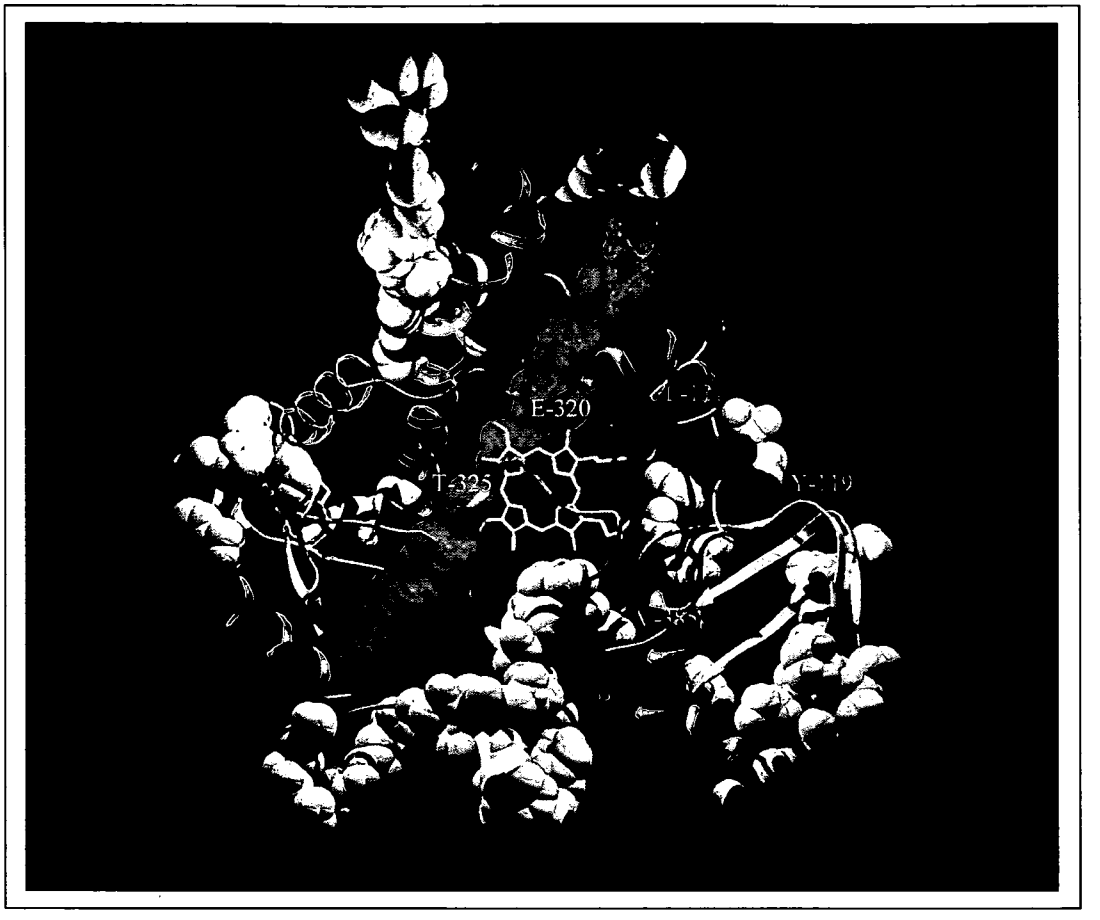

Figure 4.15: A homology model of CYP4A15 and its substrate recognition regions.

The homology model was generated based on the 3-D structure of rabbit CYP2C5. The red strands are α-helical structure and yellow strands are β-sheets. The heme (yellow) and the substrate recognition site (SRS) structures are highlighted. The structural elements involved in SRS include the absolutely conserved Glu-320 (E-320, green) on the I-helix (purple), and active site residues tyrosine (Y-119, blue), leucine (L-131, blue), threonine (T-324, blue) and valine (V-385, blue, also on the I-helix).



Figure 4.16: A homology model of CYP4A15 showing the position of the two extra amino acid residues versus the substrate recognition site (SRS) regions.

The two extra amino acid residues are asparagine and leucine, N-439 and L-440 (light green structure). The red strands are α-helical structure and yellow strands are β-sheets. The heme (yellow) and the substrate recognition site structure are highlighted. The structural elements involved in SRS include the absolutely conserved glutamic acid-320 (E-320, green) on the I-helix (purple), and active site residues tyrosine (Y-119, blue), leucine (L-131, blue), threonine (T-324, blue) and valine (V-385, blue, also on the I-helix).

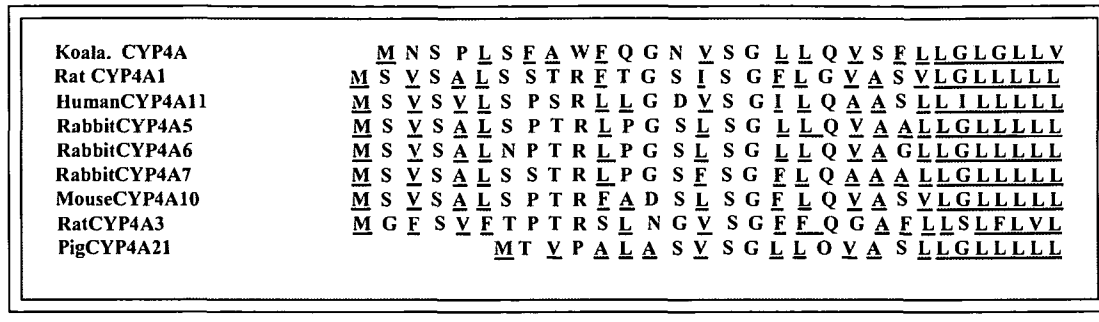

Figure 4.17: The NH2-terminal amino acid sequence comparison between the koala CYP4A and CYP4A subfamilies from other species.
In most CYP4A subfamilies known to catalyse lauric acid predominantly at the ω-position, the N-terminal is also followed by a stretch of the hydrophobic amino acid, Leucine LGLLLLLL (underlined).

Another highly conserved feature of P450s is the P450 signature motif of approximately 10 residues. This motif contains the invariant cysteine residue that ligates the heme iron [16] and is located towards the carboxyl terminus of the protein around residues 450 ± 15 [48]. In koala CYP4A15, the CYP signature is located at residues 451-460 and the absolutely conserved cysteine is at residue 458 (Figure 4.10). In this region, similar to other CYP4A enzymes, the cysteine is always followed by a hydrophobic residue, isoleucine, and a glycine. In addition, the positions -2, -4 and -7 upstream from the cysteine residue usually contain arginine, glycine and phenylalanine [58, 61, 63, 65]. A highly conserved EGHDTT sequence that contains the conserved glutamic acid residue was also observed in the CYP4A15 deduced amino acid sequence (Figure 4.10). This sequence is not present in known CYP families outside of the CYP4A family [262]. Another motif of significance is the highly conserved glutamine-377 and arginine-380 residues in the K-helix, generated by modelling with three soluble, crystallised cytochrome CYPs, namely P-450_{cam}, P-450_{BM-P} and $P450_{terp}$ [47]. The three residues alanine-464, glutamic acid-467 and valine-470 residues are other conserved residues among CYP4A subfamilies (Figure 4.10) [51, 58, 61, 63, 64, 65].

Expression of the koala and rat CYP4A enzymes in Cos-7 cells and subsequent functional analysis confirmed that the cloned koala *CYP4A15* cDNA encodes a protein of identical molecular weight to expressed rat CYP4A1 protein. Figure 4.11 shows that cDNA-expressed koala and rat CYP4A proteins of molecular mass approximately 54-kDa were detected by sheep anti-rat CYP4A polyclonal antibody. No CYP4A

CYP4A Subfamily	Koala CYP 4A15	Rat CYP 4A1	Rat CYP 4A3	Rabbit CYP 4A5	Rabbit CYP 4A7	Mouse CYP 4A10	Human CYP 4A11
CYP4A15[a]	100 100	66 61	65 58	68 62	67 63	66 61	69 65
CYP4A1[b]		100 100	78 77	79 79	78 77	93 93	81 81
CYP4A3[c]			100 100	78 77	77 76	79 78	79 77
CYP4A5[d]				100 100	91 86	80 79	87 84
CYP4A7[e]					100 100	77 76	84 82
CYP4A10[f]						100 100	81 81
CYP4A11[g]							100 100

Table 4.6: Nucleotide and amino acid sequence identities between koala liver CYP4A15 and CYP4A subfamily members from other species.
Percentage nucleotide identities were calculated from the koala *CYP4A15* cDNA and cDNAs from other CYP4A forms. Percentage amino acid identities (second row value) were calculated from the deduced amino acid sequence of the koala *CYP4A15* cDNA clone and deduced amino acid sequences from other *CYP4A* forms. The ClustalW alignment function in MacVector (Version 6.0) computer programme (Oxford Molecular, 1997) was used for alignment. [a]Koala liver CYP4A15, GenBank accession number AF463456 (Ngo *et al*, direct submission). [b]Rat CYP4A1, GenBank accession number M14972 [51]. [c] Rat CYP4A3, GenBank accession number M33936 [54]. [d] Rabbit CYP4A5, GenBank accession number M28655 [58]. [e] Rabbit CYP4A7, GenBank accession number M29530 [61]. [f] Mouse CYP4A10, GenBank accession number X69296 [64]. [g] Human CYP4A11, GenBank accession number L04751 [267].

immuno-reactive proteins of the same size were detected in untransfected Cos-7 cell lysate. This was consistent with the results obtained by Johnson and co-workers (1990), who detected no CYP4A immunoreactive bands when protein from untransfected Cos-1 cells was subjected to immunoblot analysis [58].

As expected, the CYP contents for cDNA-expressed koala and rat CYP4A proteins in Cos-7 cell lysates were lower than those obtained for koala and rat liver microsomes (Table 4.4). This was attributed to low CYP expression in the Cos-7 cell system. The total CYP content determined in rat microsomes were comparable to that reported by others [5], and similar to that obtained previously [94]. High CYP content observed in koala liver microsomes was also consistent with results reported previously [94].

When expressed as nmole/min/mg of protein, lauric acid hydroxylase activities detected for cDNA-expressed koala and rat CYP4A proteins were approximately 8-fold lower than that for koala and rat microsomes (Table 4.5). This was due to low protein expression of Cos-7 cell system. The result was consistent with that reported for expression of other CYP4A subfamilies in Cos-1 and Cos-7 cells [58, 268, 269]. The activity for cDNA-expressed rat CYP4A1 protein was comparable to those reported for rabbit CYP4A5, CYP4A6 and CYP4A7 expressed in Cos-1 cells [58]. The activity (expressed as nmole/nmole CYP/minute) for cDNA-expressed rat CYP4A1 protein was also similar to that of rat CYP4A subfamilies expressed in other expression systems [73]. The lauric acid hydroxylase activity determined in rat microsomes was comparable to that obtained by others [5] and similar to that detected previously [8]. The high lauric acid hydroxylase activity observed for the koala liver microsomes was consistent with that reported previously [8]. Lysates prepared from untransfected Cos-7 cells exhibited negligible capacity to metabolise lauric acid. In the second transfection, an approximate 2-fold lower activities were observed for both koala and rat CYP4A cDNA-expressed enzymes, as compared to the results of thefirst transfection. This finding was unexpected in that, because the second transfection gave much larger yield of CYP (nmol/mg protein) than the first transfection, CYP4A cDNA-expressed protein would be expected to be a larger fraction of total CYP in the second transfection, therefore higher activity would be observed. This could be due to the differences in the two transfection experimental conditions which may affect the activity of the cDNA-expressed protein or possibly due to the differences in the availability of the substrate since more enzyme were present. The finding may also be due to the differences in the ratio of CYP to endogenous reductase in the two

transfection experimental conditions.

From the results of the activity assays, no significant differences was observed between the rate of lauric acid hydroxylation catalysed by rat cDNA-expressed CYP4A1 and the koala truncated CYP4A15 enzymes. Future experiment looking at the activity of koala cDNA-expressed intact CYP4A15 enzyme would be of interest in order to compare the capacity to hydroxylate lauric acid of CYP4A15 enzyme with those observed from other species. Since koala liver was found to have higher liver CYP4A hydroxylase activity and CYP content [8], the characterisation of CYP4A expression at both protein and mRNA is essential in understanding this observation. As shown in Figure 4.12, a thick diffuse CYP4A immunoreactive band (54-kDa) was observed in koala microsomes as compared to rat microsomes appeared to be due to higher expression of CYP4A protein. Another immunoreactive band of lower molecular weight, approximately 48-kDa, was also observed in koala microsomes. This may represent either a closely related CYP4A enzyme or a post-translationally modified koala CYP4A enzyme. Since multiple CYP4A isoforms have been identified in the liver of other mammals, such as human, rat, rabbit and mouse [51, 54, 55, 59, 63, 64, 67], more than one CYP4A isoform may be expressed in the koala liver. The presence of two immunoreactive bands in rat microsomal samples of apparent molecular mass 53- and 54-kDa, most likely reflects the most abundant rat liver CYP4A isoforms, CYP4A1 and CYP4A3 [270].

From the Northern blot analysis, the results of the β-actin blot showed different intensity in the various species when the same amount of mRNA (10μg) was loaded for each sample (except for koala K_1, 4μg was loaded). This could be due to degradation of RNA sample during the process of analysis and needs to be considered when interpreting the expression of CYP4A. Given that the amount of intact mRNA from the koala samples was less than those from human, rat and possum (in comparison to sample K_1) as indicated by the β-actin blot, probing with CYP4A cDNA probe detected more intense bands in koala mRNA samples than was seen in human, rat and possum mRNA samples. This is due to higher CYP4A mRNA level in koala liver (Figure 4.13). The size of the rat and human CYP4A mRNA species is consistent with that reported by others [51, 63]. In addition, the size of CYP4A mRNA species in the koala and possum, marsupial species, is larger than human and rat, eutherian species. This suggests that the koala CYP4A15 may have longer 5'- and 3'-*UTR* than those of rat and humans.

The *CYP4A* gene has been reported to be a complex cluster consisting of many genes in rat and mouse [51, 64]. The complexity of the koala *CYP4A* gene was examined by Southern blot analysis. The blot suggested degradation of some genomic DNA samples, however more than one genomic DNA samples were analysed for most species and at least one genomic DNA sample from each species exhibited strong interactive bands with the CYP4A cDNA probe. The total lengths of hybridising fragments observed were less than 15-kb for three of the five koala genomic DNA samples (Figure 4.14). This may suggest that only a single gene exists in the koala liver *CYP4A* subfamily. It was noted that two distinct CYP4A-immunoreactive bands were detected in the all koala microsome samples representing either a closely related CYP4A enzyme or a post-translationally modified koala CYP4A enzyme. Given the results from the Southern blot analysis and from the RT-PCR cloning of the koala CYP4A, it is likely that the second immunoreactive band observed in the koala liver microsomes represents a post-translationally modified koala CYP4A enzyme. It was observed that no bands were detected in rats samples. This could be due to degradation of rat genomic DNA samples. It is unlikely to be due to the specificity of the koala CYP4A15 cDNA probe (Section 4.2.8) since this probe was found to detect rat CYP4A mRNAs from the Northern analysis. It was interesting that multiple intense bands were detected in the bandicoot, suggesting multiple CYP4A genes present in this species.

Knowledge of 3-D structure of P450s provides valuable insights into their function. In an attempt to understand the structure-function relationship of CYP4A15, the 3-D structure of the koala CYP4A15 protein was generated by comparative modelling, using a single 3-D structure template approach. The known 3-D template structure used in this approach, rabbit CYP2C5, is the most homologous mammalian 3-D structure available. Extensive studies into the active site residues of the CYP4A enzymes have been conducted [70, 71, 262]. Four amino acid residues have been identified to be active site residues that determine the regiospecificity of CYP4A subfamily [262]. On the koala CYP4A15 model, these residues are Tyr-119, Leu-131, Thr-324, and Val-385 [262]. The CYP4 family possesses a highly conserved glutamic acid residue that plays an essential role in heme binding. This residue is glutamic acid 320 in the koala CYP4A15. The two extra amino acid residues were found not to be in the substrate recognition site structure. Future experiments to re-generate a CYP4A15 model which does not include these two residue will provide useful information on the role of these two extra residues in the overall CYP4A15 protein structure. The gener-

ated homology model of CYP4A15 is useful in providing valuable insights into where the alpha carbons of key residues sit in the folded CYP4A15 protein. This model provides a useful guide for mutagenesis experiments or hypotheses about structure-function relationships.

Collectively, the results of this chapter suggest that the higher liver lauric acid hydroxylase activity and CYP content in the koala relative to other species studied is due to higher expression of both CYP4A protein and mRNA. This chapter provides the primary molecular data to confirm the presence of functional CYP4A15 enzyme in the koala liver. In addition, generation of a homology model of the koala CYP4A15 enzyme provides an important tool for further studies on the structure-function of CYP4A15.

Chapter 5

KOALA LIVER FATTY ACYL-COA OXIDASE

5.1 INTRODUCTION

Peroxisomes are cytoplasmic organelles, which are present in all eukaryotic cells. While these organelles contain more than fifty identified enzymes, more than half of these are responsible for lipid metabolism [105]. The most well characterised process occurring in peroxisomes is fatty acid β-oxidation.

Based on the substrate specificity of the participating enzymes, the peroxisomal β-oxidation system is divided into two inter-connected pathways [106, 115, 116, 117, 118]. They are the L-hydroxy specific classical pathway and the D-hydroxy specific pathway. The same four reaction cascade occurs in both the D- and the L-hydroxy specific pathways, however, the enzymes involved in each step are different with very distinct substrate specificity [114, 118] (Section 1.3.3, Figure 1.7). The enzymes responsible for the L-pathway consist of straight chain acyl-CoA oxidase (AOX), L-enoyl-CoA hydratase/3-hydoxyacyl-CoA dehydrogenase multifunctional enzyme, and 3-keto-CoA thiolase (PTL), whereas those for the D-pathway are branch chain AOX, D- multifunctional enzyme, and sterol carrier protein X (SCP-X). The straight chain AOX is also known as fatty acyl-CoA oxidase. While straight long chain fatty acyl-CoAs are oxidised predominantly by the L-hydroxy specific β-oxidation pathway, straight very long chain fatty acyl-CoAs are oxidised by the D-hydroxy specific β-oxidation pathway. Straight very long chain fatty acyl-CoAs are also oxidised by fatty acyl-CoA oxidase and thiolase of the L-hydroxy specific β-oxidation system

[106, 116, 117, 118]. In general, the L-hydroxy specific pathway acts predominantly on straight chain saturated fatty acyl-CoAs, whereas the D-hydroxy-specific pathway utilises branched chain acyl-CoAs as substrates. Of these two β-oxidation systems, the enzymes of the L-hydroxy specific classical pathway are markedly induced in the liver of rats and mice by a diverse group of chemicals, collectively termed peroxisome proliferators.

Among the inducible enzymes of the peroxisomal β-oxidation pathway, fatty acyl CoA oxidase is the first and rate-limiting enzyme. This enzyme is critical for completion of straight chain fatty acid β-oxidation. It has been reported that enzymes immediately downstream of fatty acyl CoA oxidase are not essential for the completion of the straight chain fatty acid β-oxidation [118]. This is also because after straight chain acyl-CoA esters are converted to enoyl-CoAs, the metabolites can also be processed further by the D-multifunctional enzyme of the second peroxisomal β-oxidation system or even by mitochondrial β-oxidation system [118].

Fatty acyl CoA oxidase (AOX) is a FAD containing oxidase. AOX transfers electrons directly to oxygen to generate hydrogen peroxide while converting acyl CoA esters to the 2-trans-enoyl-CoA esters. Acyl CoA oxidase was first identified in peroxisomes from castor bean endosperm, as part of the fatty acid metabolising system [120]. Subsequently, it has been described from other sources, including yeasts [124, 125], several germinating fat seeds, other higher plants [126, 127, 128] and animal tissues [121, 122, 123].

Deficiencies of the enzymes of the classical peroxisomal β-oxidation spiral have been identified as important causes of severe fatty acid metabolism disorders. In these diseases, accumulation of plasma and tissue very long-chain fatty acids, dicarboxylic acids and bile acid intermediates may be observed [271, 272, 273]. In human AOX deficiency, termed pseudodoneonatal adrenoleukodystrophy, varying degrees of dysmorphic features, hypotonia, and psychomotor retardation are manifested in the neonatal period. Death may occur by 4 to 5 years of age [114, 273]. In AOX knock-out mice, accumulation of unmetabolised acyl CoAs derived from very long chain fatty acids, dicarboxylic acid and other substrates of AOX were observed. Since AOX substrates may act as peroxisome proliferator activated receptor-alpha (PPAR-α) ligands (Section 1.3), their accumulation leads to sustained elevation of CYP4A enzyme expression. Excess production of toxic dicarboxylic acids and very long chain fatty

acids, which are products of CYP4A ω-hydroxylation and can not be processed further in the absence of AOX, causes microvesicular liver steatosis and steatohepatitis in the liver of AOX knock-out mice. These observations demonstrate the indispensable function of AOX in the physiological regulation of fatty acid metabolism as well as regulation of PPAR-α [136]. Deficiency of peroxisomal L-multifunctional enzyme (L-PBE) genes has been shown not to affect the oxidative metabolism of straight chain fatty acids. L-PBE knock-out mice exhibit no liver steatosis and fail to induce peroxisome proliferation [118, 136]. This is because after acyl-CoA esters of straight chain fatty acid are converted to enoyl-CoAs, the metabolites can be further processed by D-bifunctional enzyme or by the mitochondrial β-oxidation system [114, 118].

It is well established that induction of the β-oxidation enzymes, in particular the first and rate limiting enzyme, AOX, by peroxisome proliferators is often associated with induction of the CYP4A subfamily [118]. The results of studies reported in this thesis using a possum model demonstrate that monoterpenes elevate liver β-oxidation enzyme activity and the level of AOX mRNA. No significant changes in microsomal CYP4A expression were seen. In the koala livers, while higher levels of both CYP4A protein and mRNA were detected, peroxisomal β-oxidation activity was absent [8].

The absence of β-oxidation suggests that one or more enzymes of the L-specific β-oxidation system are not expressed in koala liver tissue. The biochemical and molecular characterisation of β-oxidation enzymes is important in assessing the ability of the koala to cope with fatty acid metabolism without an obvious β-oxidation system. This chapter reports studies which aimed to isolate two types of cDNAs of koala liver fatty acyl CoA oxidase (AOX), the first and rate limiting enzyme of the L-specific β-oxidation system. These studies also determined the activity of AOX in koala liver homogenates as well as the activity of cDNA-expressed koala AOX enzymes. The research strategy involved isolation of the two new *AOX* full-length cDNAs using RT-PCR approaches, expression of these *AOX* cDNAs in Cos-7 cells, and subsequent kinetic studies using fluorescent assays.

5.2 METHODS

5.2.1 Isolation of koala liver fatty acyl CoA oxidase cDNAs by RT-PCR approaches

The cloning strategy for the isolation of koala liver fatty acyl CoA oxidase (*AOX*) full-length cDNAs involved amplification of three new *AOX* partial cDNAs using reverse transcription-polymerase chain reaction (RT-PCR) and rapid amplification of cDNA ends (RACE). Degenerate primers were designed from the alignment of AOX nucleotide sequences from multiple species. Full-length *AOX* cDNAs were then isolated using gene specific primers derived from the three partial *AOX* cDNAs. The isolation of the two *AOX* cDNAs was accomplished by restriction digests of several selected clones and sequencing analysis. The AOX cloning strategy is depicted schematically in Figure 5.1.

Amplification of AOX partial cDNAs by RT-PCR: The isolation of total RNA, purification of mRNA from total RNA samples and synthesis of first-strand cDNA were performed as described previously in Section 4.2.1. Several degenerate primers were derived from the alignment of *AOX* cDNA sequences from other species in the GenBank database (Table 5.1).

Initial PCR reactions were set up using several primer pairs, designed from different highly conserved regions evident in the alignment of AOX from human, rat and mouse [133, 274, 275]. Optimisation of PCR amplifications was accomplished using a range of temperatures from 45^0C to 65^0C and also different $MgCl_2$ concentrations from 1.5mM to 4mM. KAOXf2 and kAOXr2 primers amplify a 1161-bp cDNA fragment (corresponding to position 479 - 1640 within the coding region of the human *AOX* cDNA). KAOX3'r and gene-specific forward primer kAOX3'f amplify a 3'-end 550-bp cDNA fragment (corresponding to position 1532 - 2040 within the coding region of the human *AOX* cDNA) including the stop codon TGA. The kAOX3'f primer was derived from the 1161-bp *AOX* cDNA sequence. PCR reactions were set up as described in Section 2.21.2. The conditions for PCR amplifications of the 1161-bp cDNA fragment were: denaturation at 94^0C for 5 minutes; then 30 cycles of 94^0C for 45 seconds, 55^0C for 45seconds, and 72^0C for 1 minutes; final extension at 72^0C for 10 minutes. The cycling conditions for amplification of the 3'-end were similar to that of the 1161-bp *AOX* cDNA fragment except that annealing temperatures were varied

from 55^{0}C to 65^{0}C. PCR reactions were repeated with Q solution included into the PCR reaction samples. In addition, the gene-specific forward primer kAOX3'f was added to the PCR reactions after the reaction mixtures were cycled for 5 cycles of 94^{0}C for 45 seconds, 55^{0}C for 45seconds, and 72^{0}C for 1 minute to enhance yield and specificity.

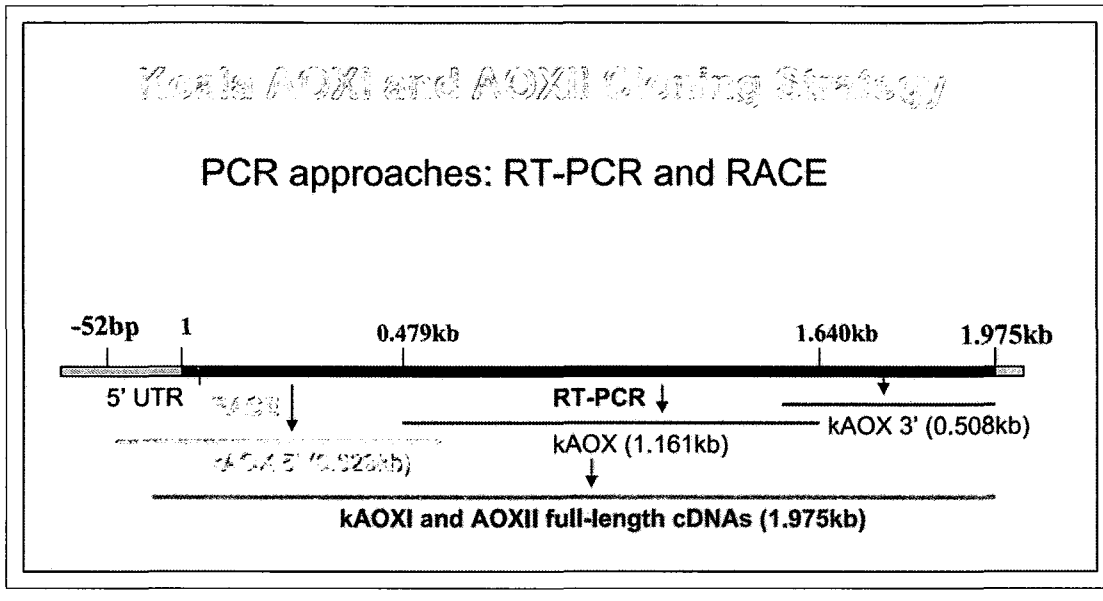

Figure 5.1: Schematic diagram of the cloning strategy for koala *AOX* cDNAs.
The solid blue box represents the coding region of koala AOXs and the green boxes depict the 5' and 3' non coding regions. Single lines represent koala AOX cDNAs: 5' cDNA amplified fragment obtained by RACE is red, koala 1517- and 1509-bp *AOX* cDNAs are green.

Amplification of *AOX* 5'end cDNAs by RACE: The 5'-ends of the koala AOX cDNAs were amplified by RACE using a SMART RACE cDNA Amplification kit as described in Section 4.2.1 protocol. The RACE reactions were set up as described in section 2.21.3 Koala 5'-end *AOX* cDNA fragments were amplified utilising Universal Primer Mix (UPM)(Table 2.6) and a gene-specific reverse primer, designated kAOX5'r (Table 5.1), based on the koala 1161-bp *AOX* cDNA sequence. An *EcoR* 1 restriction site was added to the 5' end of the anti-sense primer to facilitate screening by restriction digest analysis. Touchdown PCR conditions for RACE reactions were as follows: 5 cycles of 94^{0}C for 5 seconds and 72^{0}C for 2 minutes; 5 cycles of 94^{0}C for 5 seconds, 70^{0}C for 10 seconds and 72^{0}C for 2 minutes, and 32 cycles of 94^{0}C for

5 seconds, 68^{0}C for 10 seconds and 72^{0}C for 2 minutes. Two 5' cDNA fragments of sizes 850-bp and 650-bp were amplified.

Amplified RACE fragments were analysed by gel electrophoresis as described in Section 2.15.2. For subsequent cloning into pGEM-T vector, polymerase was removed from the RACE reactions as described in Section 4.2.1 The PCR products were ligated into pGEM-T vector as described in Section 2.13.2 and transformed into XL-1 Blue competent cells according to Section 2.13.3. The circular map of pGEM-T and its multiple cloning sites is shown in Figure 4.4. Several colonies were inoculated in 5ml LB containing ampicillin and incubated overnight at 37^{0}C. Plasmid DNA was purified using alkaline lysis and Qiaprepp miniprep methods, as described in Section 2.14.1 and analysed by restriction digest as per Sections 2.15.1 and 2.15.2. Plasmid DNAs with the correct size inserts were sequenced using M13 universal (M13) and M13 reverse (M13r) sequencing primers (Table 2.5) as described in Section 2.16.

Name	Sequences (5'-3')	Origin	A*
kAOXf2	**GAATTC**ACGGAACTCATCTTCGAGG	(+)479 - (+)498	a
kAOXr2	**GAATTC**GTGCCTCACTTGCTCGAACA	(+)1621 - (+)1640	a
kAOX3'f	CGAGCAGCCCGATTAGTAGA	(+)1532 - (+)1551	b
kAOX3'r	CTTCAGAGCTTCGACTGCAG	(+)2021 - (+)2040	a
kAOX5'r	GGTTTTCCCAAGTCCACCAG	(+)588 - (+)607	b
kAOXf	**CCGCTCGAG**TTCTGATCGTCGTCAC CTTCTGC	(-)41 - (-)18	b
kAOXr	**AAAAAGGAAAAGCGGCCGC**CTTC ACAGCTTAGACTGCAG	(+)1969 - (+)1988	b
rAOXf	**CCGCTCGAGCATG**AACCCCGACCTG CGCAA	(+)1 - (+)20	c
rAOXr	**AAAAGGAAAAGCGGCCGC**CCAGG GAAACTTCAAAGCT	(-)1978 - (+)1997	c

Table 5.1: Details of oligonucleotide primers used for isolation of full-length koala and rat *acyl CoA oxidase* cDNAs
Restriction sites and the start codon are shown in bold. A*: accession numbers: a, UO7866, human fatty AOX mRNA [276], degenerate primers were derived from the alignment of *AOX* cDNAs from rat, human and mouse with the origin relative to human *AOX* cDNA; b, AF463453, koala AOX mRNA (Ngo et al. 2001, direct submission); c, J02752, rat AOX mRNA [133].

Amplification of full-length *AOX* cDNAs by RT-PCR: Nucleotide sequences of two types of *AOX* full-length cDNAs were obtained by sequence analysis of the partial *AOX* cDNAs isolated by RT-PCR and RACE. Two gene-specific primers, forward primer kAOXf and reverse primer kAOXr (Table 5.1) were derived from the koala *AOX* 5' and 3' sequences. Koala *AOX* cDNAs were then amplified by RT-PCR, using these two primers and koala first-strand cDNA as the template. Restriction sites, *Xho* 1 and *Not* 1, were included at the 5' and 3' ends of the forward and reverse primers respectively, to facilitate subsequent directional cloning into the pCI Neo expression vector. KAOXf and kAOXr primers amplified 2039-bp fragments corresponding to the entire coding region of the koala AOX, including the start and stop codons and the 51-bp 5'-*UTR*. PCR reactions were set up as described in Section 2.21.2. PCR reactions were cycled for 35 cycles of 94^0C for 30 seconds, 65^0C for 30 seconds and 72^0C for 2 minutes, followed by a final 10 minutes extension at 72^0C.

PCR reaction products were separated on 0.7% w/v low melt agarose gels, excised from the gels and then purified using a QIAEX II Gel Extraction Kit as described in Sections 2.15.2. and 2.15.3. Purified PCR products were digested with *Xhol* 1 and *Not* 1 as described in Section 2.15.1. The purified koala 2039-bp *AOX* cDNA fragment was ligated into the pCI-neo expression vector (pre-digested with *Xhol* 1 and *Not* 1) according to Section 2.13.2, and then transfected into E. coli strain DH-5α competent cells as per Section 2.13.3. Plasmid DNA was isolated from approximately 100 selected colonies using a modified alkaline lysis miniprep procedure and screened for the presence of the 2039-bp inserts. Screening was performed by restriction digest with *Xhol* 1 and *Not* 1 according to Sections 2.14.1 and 2.15.1. Plasmid DNAs with the correct size inserts were then purified using the Qiaquick Spin Miniprep kit, according to Section 2.14.1, and subsequently sequenced in both forward and reverse directions as described in Section 2.16, using T3, $T7_{PCI}$ primers (Table 2.5) and internal primers (derived from the sequencing data obtained utilising T3, $T7_{PCI}$ primers).

5.2.2 Isolation of rat full-length *AOX* cDNAs

For control studies, two full-length rat *AOX* cDNAs, designated r*AOX*1 and r*AOX*2, were isolated by RT-PCR using rAOXf and rAOXr primers, derived from published rat *AOX* cDNA sequences (Table 5.1). These two cDNAs are identical to those previously cloned and designated rat *ACO*-I and *ACO*-II [277]. Amplification, subcloning

into pCI-neo vector, screening and sequencing of rat *AOX*1 and *AOX*2 cDNAs was performed essentially as described above for koala *AOX* cDNAs.

5.2.3 Expression of koala and rat *AOX* cDNAs in Cos-7 cells

The growth and maintenance of Cos-7 cells was performed as described in Section 4.2.3. Plasmid DNAs were then isolated using the QIAfilter Midiprep Spin kit as described in Section 2.14.3. Just prior to transfection, the cells were washed gently with DMEM with no serum and the media removed. Full-length koala *AOX* cDNAs cloned in pCI-Neo vector were transfected into Cos-7 cells using LipofectAMINE as described in Section 4.2.3. A circle map of pCI-Neo vector is shown in Figure 5.2. Cells were harvested as described in Section 4.2.3 and the cell lysates were used directly for protein determination and AOX activity assay.

5.2.4 Preparation of liver homogenates

Liver homogenates 10% (wv-1) were prepared at 40^0C, 15 min prior to commencing the AOX activity incubations. Livers were homogenised in cold homogenisation medium (0.25M sucrose, 5 mM 3-(N-Morpholino) propane-sulfonic acid (MOPS, pH 7.5) and 1mM ethylene diamine tetraacetic acid (EDTA), pH 7.5) using a Teflon probe. The liver homogenates were then filtered through cotton gauze and stored on ice until needed. Protein concentrations were determined by the method of Lowry *et al.* [229] .

5.2.5 Determination of palmitoyl-CoA oxidase (AOX) activity

Palmitoyl-CoA oxidase (a measure of the activity of the first rate limiting enzyme acyl-CoA oxidase) activity was determined using a modification of the method described by Veldhoven (1995) using palmitoyl-CoA as the substrate [235]. AOX activity was measured via the formation of H_2O_2 coupled to the dimerisation of homovanillic acid into a fluorescent product, catalysed by peroxidase in the presence of the generated H_2O_2 [235]. Test and blank incubations were performed for each individual liver sample with no substrate palmitoyl-CoA in the blank incubations. For deter-

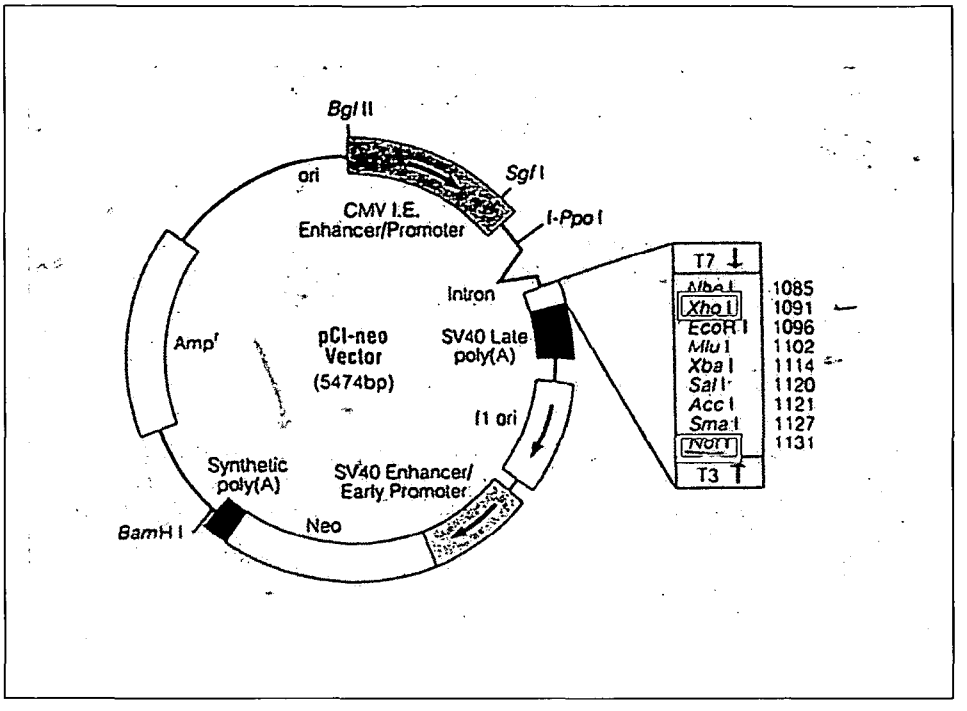

The pCI-neo Mammalian Expression Vector Sequence Reference Points:

1. **Size:** 5474-bp
2. **CMV enhancer/ promoter:** (1-659/669-750) Eukaryotic expression driven by the CMV immediate early enhancer/ promoter.
3. **SV40 late poly (A):** (1167-1388) The SV40 late polyadenylation sequence provides signals required for termination of transcription and polyadenylation.
4. **T7 and T3 promoters:** (1067-1085 and 1137-1158, respectively)
5. **Cloning sites:** Multiple cloning sites are located between base pair 1085-1137
6. **Eukaryotic selection:** Amp^r Stable selection of clones is made possible by the presence of the β-lactamase (Amp^r) coding region (3783-4642), Neomycin selectable marker also present.

Figure 5.2: Circle map of pCI-neo vector and its features.
(Modified from Promega catalogue 1996). *Xho* 1 and *Not* 1 cloning sites are highlighted.

mination of total palmitoyl-CoA oxidase activity, test and blank reaction mixtures contained 160μl of diluted liver homogenate (Section 5.2.4, 1 in 10 dilution) and 40 μl of pre-incubation mixture containing 25mM NaN_3 and 25mM FAD. The assay mixtures were pre-incubated for 10 minutes on ice in order to inhibit catalase activity and to saturate the oxidase with its cofactor FAD. The reaction was initiated by adding 800 μl of appropriate pre-warmed test reaction mixture to the test incubations and 800 μl of blank reaction mixture to the blank incubations and placing the preparations in a shaking water bath at 37°C. The test and blank reaction mixtures contained 50mM K-phosphate buffer (pH 8.0), 0.1mg/ml peroxidase, 0.15% (w/v) defatted BSA, 125mM palmitoyl-CoA and 0.75mM HVA, except that palmitoyl-CoA was not included in the blank incubation mixture. After 8, 16, 24 and 32 minute incubation, 200 μl of each test and blank incubated samples were then removed, transferred into a new tube and to these 200 μl withdrawal samples were added 80 μl of stop buffer (8% (w/v) $HClO_4$) to terminate the reaction. The resultant mixtures were centrifuged, followed by alkalinisation of the supernatant with 2.8ml of 0.5M sodium carbonate and 10mM EDTA buffer, pH 10.7 and fluorescence was then read after 10 minutes. Fluorescence was standardised using uric acid and urate oxidases, essentially as described by Veldhoven 1995 [235]. For determination of palmitoyl-CoA oxidase activity of cDNA-expressed AOX proteins, crude cell homogenates were used.

5.2.6 Northern analysis of hepatic acyl CoA oxidase mRNA

The isolation of total RNA from liver tissues and the purification of mRNA from total RNA were performed as described in Sections 2.19.2 and 2.19.3. Four to 10 μg of mRNA was separated on a 1% formaldehyde gel and then blotted onto a nylon membrane according to Sections 2.20.1 and 2.20.2. Prehybridisation, hybridisations, washing and subsequent processing of the filter were accomplished as described in Sections 2.20.3, using a 320-bp koala *AOX* cDNA probe isolated previously by RT-PCR. The probe cDNA is located 300-bp downstream from the start codon of the cloned koala AOX cDNAs. The koala *AOX* probe was labelled with α-[^{32}P]-dCTP using the Gigaprime DNA labelling kit as described in Section 2.17. To assess relative mRNA loading, the filter was stripped and re-probed with a α-[^{32}P]-dCTP labelled β-actin cDNA probe (Ambion International, TX, USA).

5.2.7 Southern analysis of hepatic genomic DNA

Genomic DNA was extracted as described in Section 2.18.1. DNA fragments were separated by gel electrophoresis through a 0.7% agarose gel and blotted onto a nylon membrane in 10 X SSC overnight as described in Sections 2.18.2 and 2.18.3. Pre-hybridisation, hybridisation with the koala *AOX* 320-bp cDNA probe, washing and developing of the filter were carried out essentially as described for Northern blot analysis, except that 6 X SSC was used instead of 5 X SSC.

5.3 RESULTS

5.3.1 Cloning of koala liver acyl CoA oxidase cDNAs

Amplification of koala AOX partial cDNAs by RT-PCR: Two partial koala *AOX* cDNAs were isolated by RT-PCR using koala cDNA as the template. KAOXf2 and kAOXr2r primers (Table 5.1) were the optimal primer pair which amplified a cDNA fragment of size approximately 1.2-kb and the optimal PCR amplification condition was described in Section 5.2.1. This was the expected size for this primer combination. Figure 5.3 shows the gel analysis of PCR products amplified by this primer combination. A gene-specific forward primer, designated kAOX3'f was then derived from the cDNA sequence of the 1.2-kb clone obtained. KAOX3'r and gene-specific forward primer kAOX3'f amplify a cDNA fragment of expected size of 550-bp as shown in Figure 5.4. Due to the presence of other non-specific PCR products, Q solution was added to the PCR reactions to increase both specificity and yield of the 550-bp products (Figure 5.4, Panel B).

The amplified PCR products were purified and subcloned into the pGEM-T vector (Sections 2.13.2 and 2.13.3). Several clones with correct size inserts were sequenced to confirm their identity (Section 2.16). A partial koala *AOX* cDNA of size 1161-bp and AOX 3' end of size 508-bp, containing the stop codon were obtained. These two partial cDNAs have an overlapping sequence of 108-bp.

Amplification of koala *AOX* 5' cDNA by RACE: The 5'-ends of two types of koala *AOX* cDNAs were isolated by RACE. UPM and kAOX5'r primers (Tables 2.5 and 5.1) amplified a 750-bp and a 900-bp 5'-RACE fragments as shown in Figure 5.5.

The amplified PCR products were purified and subcloned into the pGEM-T vector (Sections 2.13.2 and 2.13.3). Several clones with differing size inserts (from approximately 600- to 900-bp, result not shown) were sequenced to confirm their identity (Section 2.16). Two types of *AOX* 5' end cDNAs were obtained, designated *AOX I* 5' and *AOX II* 5'. *AOX I* 5' cDNA was 723-bp and included 170-bp 5'-*UTR* upstream of the start codon; *AOX II* 5' end cDNA was 70-bp shorter and included 100-bp 5'-*UTR*. The two 5' cDNAs both have 128-bp overlapping sequence with the koala partial AOX 1161-bp cDNA isolated by RT-PCR as described above. The 5'-*UTR* sequences of the two RACE products were identical. *AOX I* 5' and *AOX II* 5' cDNAs differed in exon three only, the coding region between nucleotides 269 - 429.

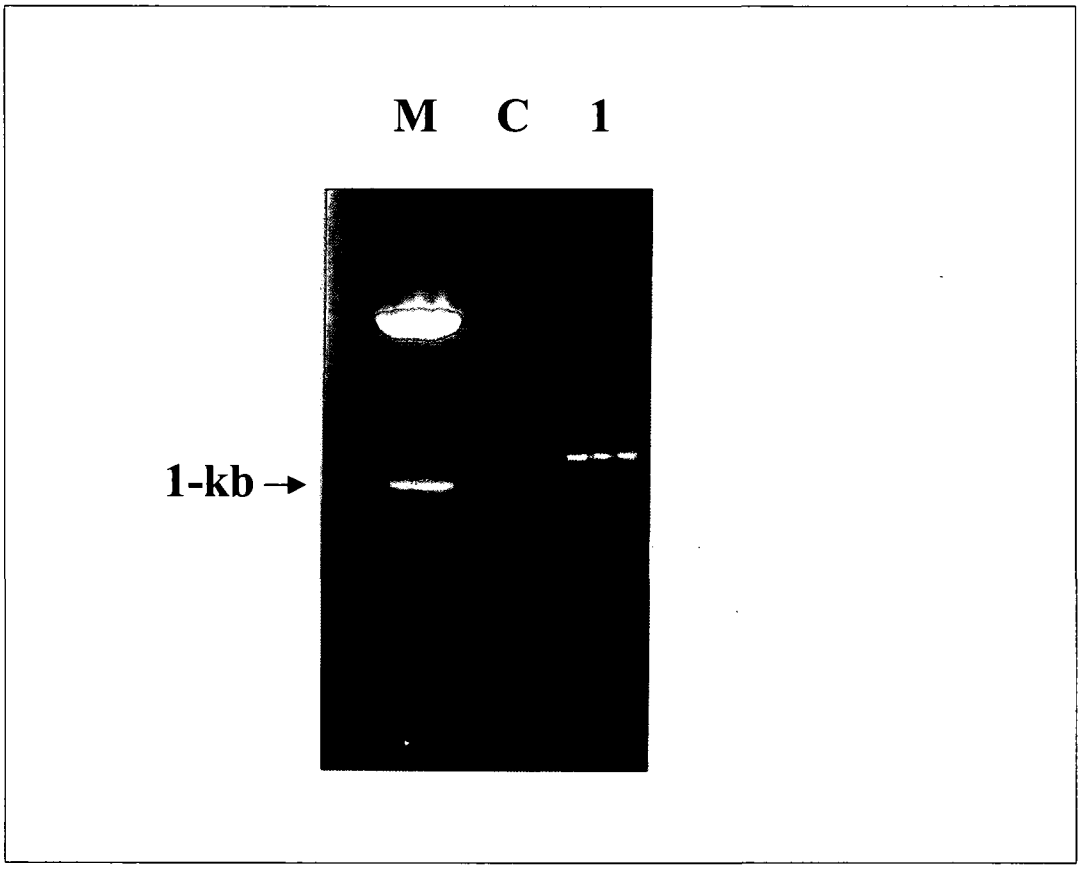

Figure 5.3: Agarose gel analysis of PCR product generated from koala liver cDNA using kAOXf2 and kAOXr2 primers.
A cDNA fragment of size approximately 1.2-kb was amplified (Lane 1). Lane C: negative control (PCR reaction with no DNA template). Lane M: DNA molecular weight marker

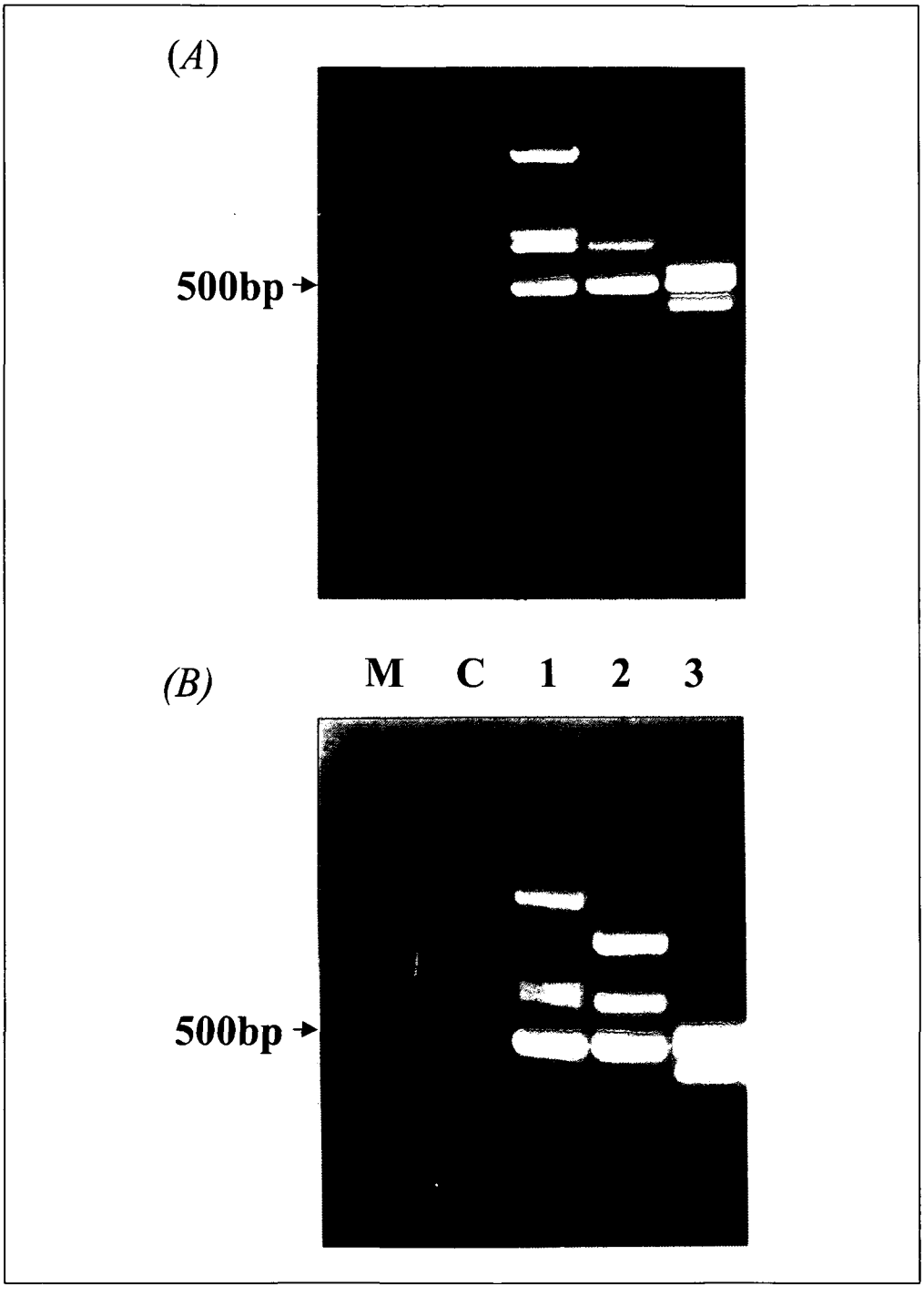

Figure 5.4: Agarose gel analysis of PCR products generated from koala liver cDNA template using kAOX'3f and kAOX'3r primers at different annealing temperatures.

A cDNA fragment of expected size of 550-bp was amplified (Lane 1: 55^0C, Lane 2: 60^0C, Lane 3: 65^0C). Lane C: negative control (PCR reaction with no DNA template). Lane M: DNA molecular weight marker. Panel (A): PCR reactions without Q solution; Panel(B): PCR reactions with Q solution.

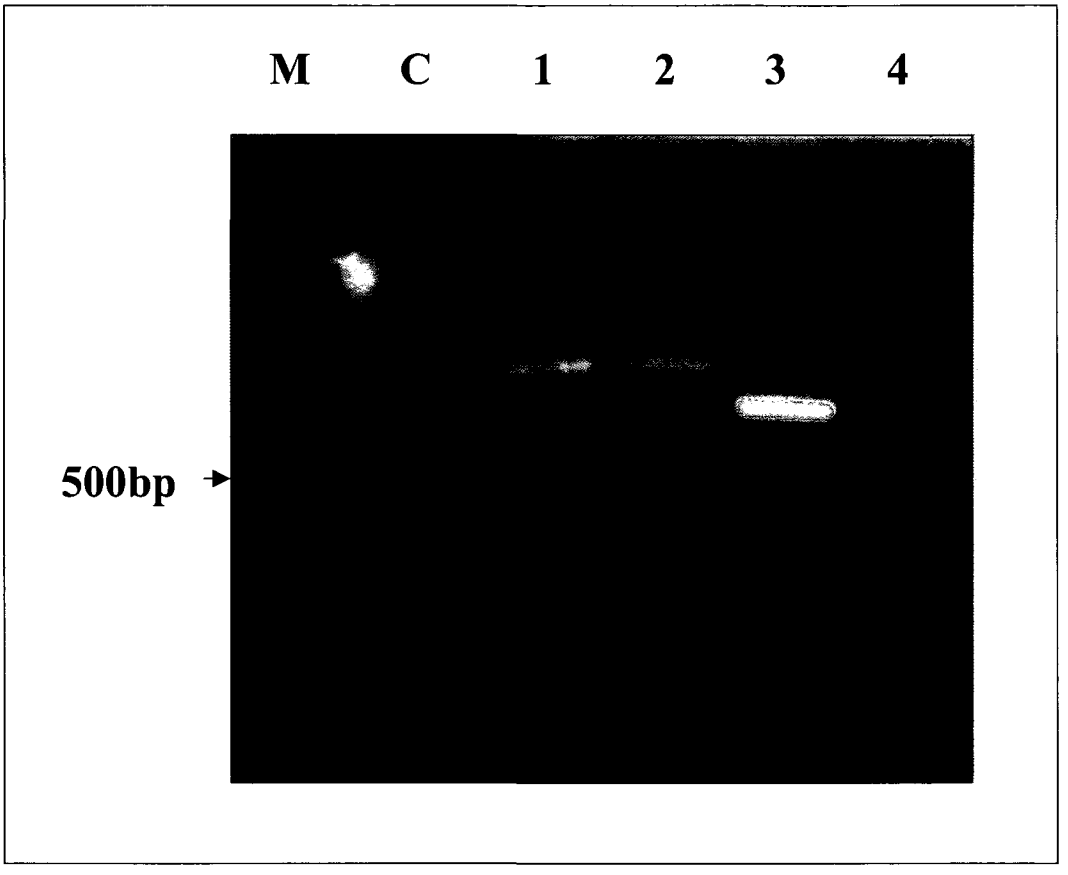

Figure 5.5: Agarose gel analysis of PCR products generated from koala liver 5' RACE-ready cDNA template using UPM and kAOX5'r primers. RACE products of sizes 750-bp(Lane 3) and 900-bp (Lane 4) were amplified. Lane C: negative control (PCR reaction with no DNA template). Lane M: DNA molecular weight marker. (Lanes 1,2 : RACE products for cloning of koala CYP4A15, Chapter 4)

Amplification of two types of koala *AOX* cDNAs by RT-PCR: To investigate the functional significance of the existence of two types of *AOX* cDNAs, both full-length *AOX* cDNAs were isolated and the enzymatic properties of the cDNA-expressed proteins examined. Gene-specific primers kAOXf and kAOXr (Table 5.1) amplified a fragment of size approximately 2.2-kb from koala 5'RACE-ready cDNA template (Figures 5.6, Lane 1). Predominant PCR products of size approximately 2-kb were amplified from koala liver cDNA template (Figure 5.7, Panel A, Lane 2-3). PCR products of size 2.2-kb was also amplified. PCR fragments of the same size were amplified from rat liver first-strand cDNA (Figure 5.7, Panel B, Lane 2), using R4Af and R4Ar primers (Table 5.1). The expected size of this primer combination is 2039-bp. Fig 5.7 (Panel B, Lane 3-5) shows the PCR products generated from large scale amplifications of koala liver *AOX* cDNAs, using kAOXf and kAOXr primers.

PCR products were initially subcloned into the pGEM-T vector (Section 2.13.2 and 2.13.3) and several clones were selected to screen for the two types of koala AOX cDNA. Screening was accomplished by restriction digest using several restriction enzymes (Result not shown) and sequence analysis according to Sections 2.15.1, 2.15.2 and 2.16. Two new full-length koala AOX cDNAs, of size 2039-bp, were isolated using kAOXf and kAOXr primers. They were designated *AOX I* and *AOX II*. These differ in a small area of the coding region, between nucleotides 269 - 429. Each cDNA has an open reading frame of 1988-bp, which encodes a protein of 662 aa, and both contain a 51-bp 5'-*UTR*. Both koala *AOX I* and *AOX II* cDNAs exhibit high nucleotide sequence identities with the reported human and rat *AOX* cDNA sequences (Table 5.2). The nucleotide and deduced amino acid sequences of the koala AOX I and AOX II are shown in Figures 5.8 and 5.9. The koala *AOX I* and *AOX II* cDNA nucleotide sequences were submitted to GenBank (Bethesda, Maryland USA) and their accession numbers are AF463453 and AF463454 respectively.

5.3.2 Determination of palmitoyl-CoA oxidase (AOX) activity in koala liver homogenates

To determine the AOX activity present in koala liver, total palmitoyl-CoA oxidase and AOX-dependent palmitoyl-CoA oxidase activities were determined for koala liver homogenates. Activities were also determined for rat and human liver homogenates. Results of these assays are shown in Table 5.3. As shown in Table 5.3, total palmitoyl-

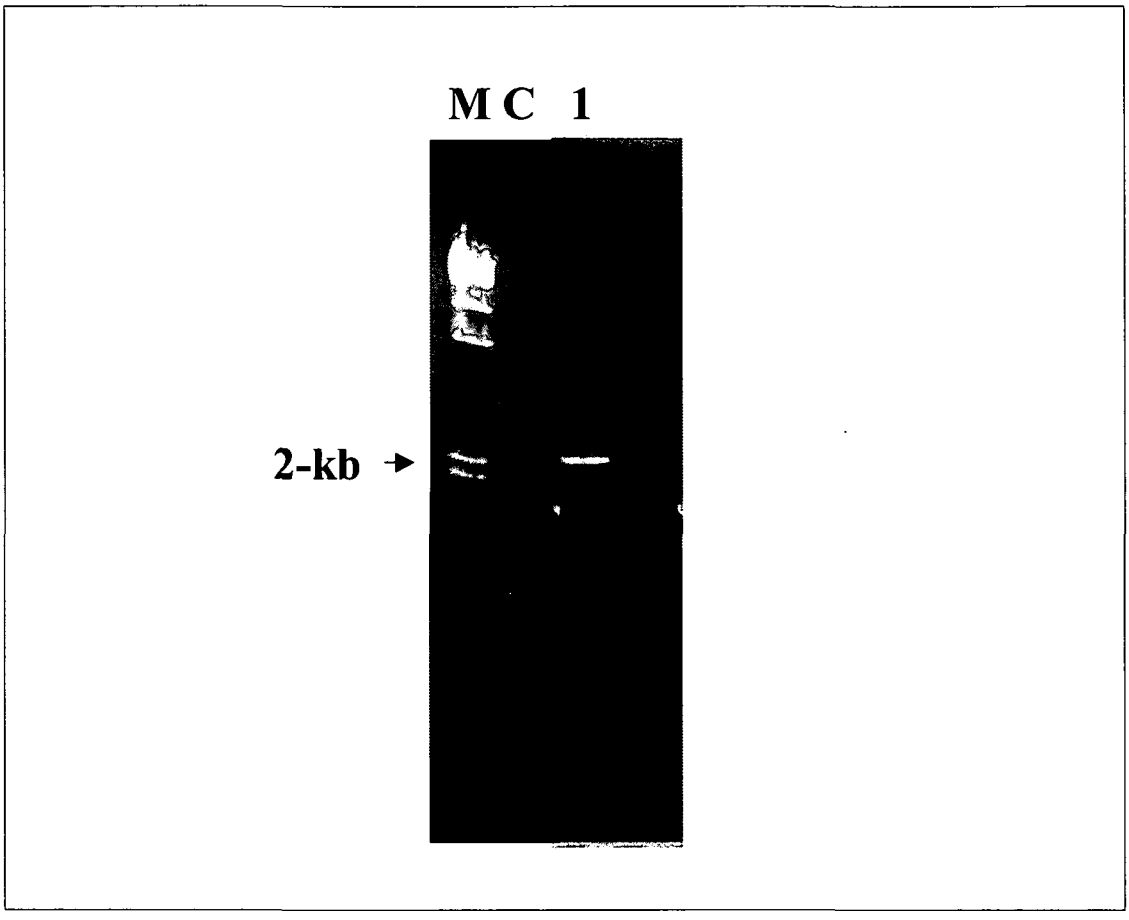

Figure 5.6: Agarose gel analysis of PCR products generated from koala 5'RACE-ready cDNA template using forward kAOXf and reverse kAOXr primers

Lane 1: PCR reaction using forward kAOXf and reverse kAOXr primers. Lane C: negative control (PCR reaction with no DNA template). Lane M: DNA molecular weight marker.

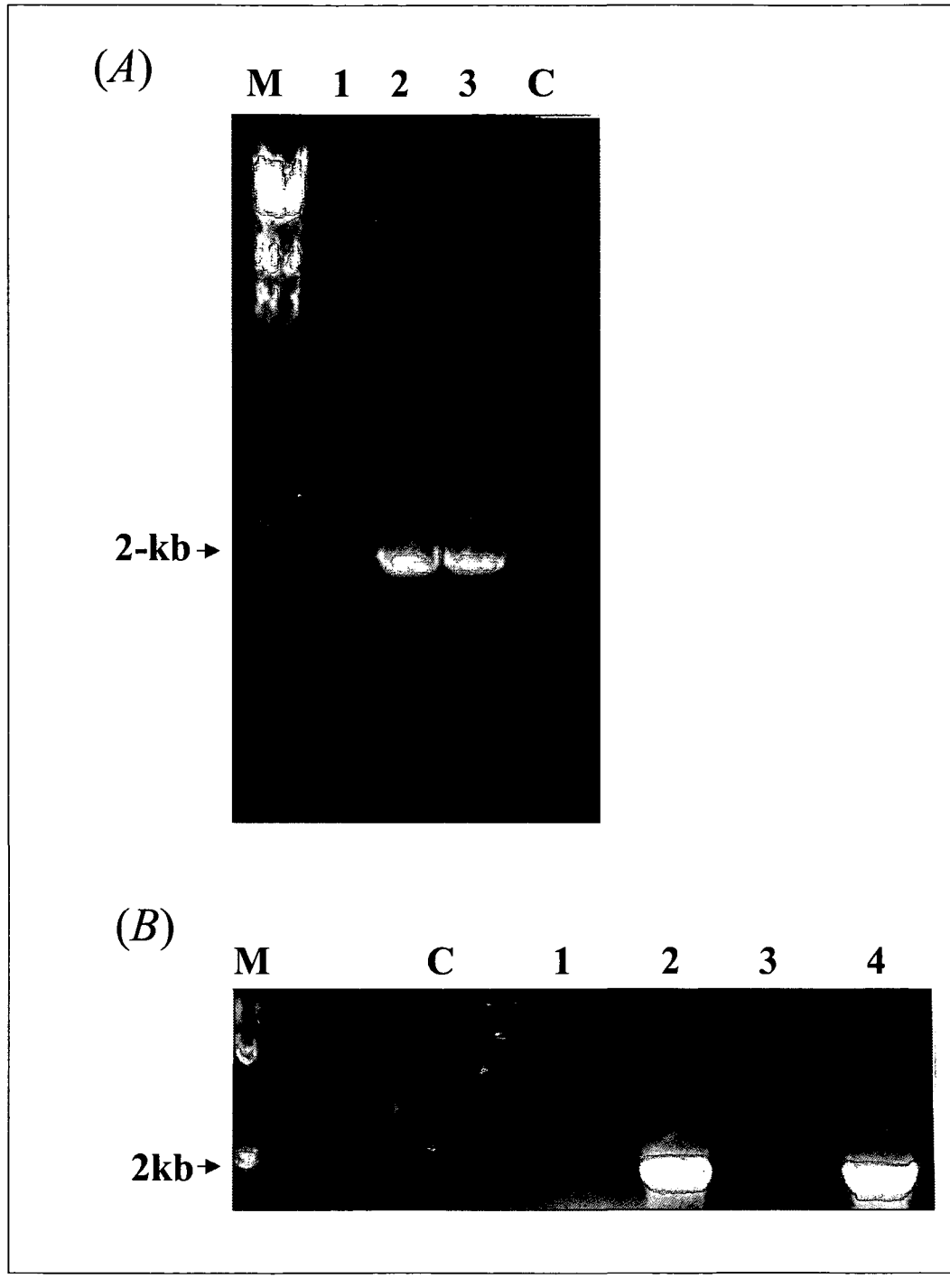

Figure 5.7: Agarose gel analysis of PCR products generated from koala liver cDNA template, using forward kAOXf and reverse kAOXr primers. Panel A: Lane 1-3: PCR products generated using koala cDNA template 1-3 (Lane 1-3). Panel B: PCR products generated using koala cDNA template 1-3 (Lane 3-5, Large-scale PCR amplification), using rat cDNA (Lane 2). Lane C: negative control (PCR reaction with no DNA template). Lane M: DNA molecular weight marker.

CoA and AOX-dependent palmitoyl-CoA activities detected in liver homogenates revealed that total palmitoyl-CoA activity of koala livers is about 12-fold and relatively 5-fold less than those seen in rat and human homogenates, respectively.

5.3.3 Expression of koala *AOXI* and *AOXII* in Cos-7 cells and determination of palmitoyl-CoA oxidase (AOX) activity

To confirm that the cloned koala *AOX* cDNAs encode functional enzymes, koala *AOX I* and *AOX II* cDNAs were cloned into the pCI-neo vector and transfected into Cos-7 cells. For transfection of Cos-7 cells, the koala *AOX I* and *AOX II* cDNAs were subcloned into the pCI-neo mammalian expression vector. Restriction maps of the two koala AOXs were generated (Figure A.2, Appendix A). The maps reveal the presence of two *EcoR* 1 sites within the coding regions of both koala *AOX I* and *AOX II*. *EcoR* 1 and *Xho* 1 pre-digested pCMV-Script XR vector was therefore not suitable for cloning. The koala *AOX I* and *AOX II* cDNAs do not contain *Xho* 1 and *Not* 1 sites, therefore these were selected for cloning. Approximately 100 colonies were screened for the two *AOX* cDNAs. Several clones containing *AOX I* or *AOX II* cDNA were sequenced in both directions to confirm their identity.

	AOX I[a]	AOX II[b]	hAOX1[c]	hAOX2[d]	rAOX[e]	mAOX[f]
AOX I[a]	100 100	96 80	83 88	81 84	78 81	77 80
AOX II[b]		100 100	80 84	83 86	80 83	79 82
hAOX1[c]			100 100	96 96	82 85	81 83
hAOX2[d]				100 100	85 88	83 86
rAOX[e]					100 100	93 95
mAOX[f]						100 100

Table 5.2: Nucleotide and deduced amino acid sequence identities between the koala *AOX I* and *AOX II* cDNAs and *AOX* cDNAs from other species. Percentage nucleotide identities were calculated from the koala *AOX* cDNA clone and other *AOX* cDNAs. Percentage amino acid identities (second row value) were calculated from the deduced amino acid sequence of the koala *AOX* cDNA clone and deduced amino acid sequences from other *AOX* cDNAs. The ClustalW alignment function in MacVector (Version 6.0) computer programme (Oxford Molecular, 1997) was used for alignments. [a]Koala liver fatty *AOX* cDNA type 1 nucleotide and deduced amino acid sequences, GenBank accession number AF463453 (Ngo *et al.*, direct submission). [b]Koala liver fatty *AOX* cDNA type 2 nucleotide and deduced amino acid sequences, GenBank accession number AF463454 (Ngo *et al.*, direct submission). [c] Human fatty *AOX* cDNA type 1 nucleotide and deduced amino acid sequences, GenBank accession number UO7866 [274]. [d]dHuman fatty *AOX* cDNA type 2 nucleotide and deduced amino acid sequences, GenBank accession number UO7866 [274]. [e] Rat fatty *AOX* cDNA nucleotide and deduced amino acid sequences, GenBank accession number J02752 [133]. [f] Mouse fatty *AOX* cDNA nucleotide and deduced amino acid sequences, GenBank accession number AF006688 [275].

```
   1  GGGGGGGGAC TTCTGATCGT CGTCACCTTC TGCCCCATCG CCGCCTTTAC CATGAACCCA
   1                                                          M  N  P
  61  GACTTGCGCA GGGAGCGGGA CGCTGCCAGC TTCGATGCGG AAAAACTCAC TTACATCCTG
   4   D  L  R  R  E  R  D  A  A  S  F  D  A  E  K  L  T  Y  I  L
 121  GATGGGGGCT CCGAGAGGAC CCGGCGCCGC CGGGAGATCG AGAACCTGAT TCTGAATGAT
  24   D  G  G  S  E  R  T  R  R  R  R  E  I  E  N  L  I  L  N  D
 181  CCGGACTTTA AGCATGAAGA CTTGAATTTC CTTACCCGGA GCGAGCGCTA TGAGATAGCT
  44   P  D  F  K  H  E  D  L  N  F  L  T  R  S  E  R  Y  E  I  A
 241  GTCAGAAAGA GTGCCACAAT GGTGAAGAAG ATGCGAGATT TTGGCATTGC TGATCCTGAA
  64   V  R  K  S  A  T  M  V  K  K  M  R  D  F  G  I  A  D  P  E
 301  GAGATCATGT GGTTTAAAAA CTTTGTGCAT CGTGGGCGTC CTGAGCCTTT GGACCTTCAC
  84   E  I  M  W  F  K  N  F  V  H  R  G  R  P  E  P  L  D  L  H
 361  TTGGGTATGT TTCTGCCCAC ATTACTTCAC CAGGCAACCC AGGAGCAGCA GGAACGCTTC
 104   L  G  M  F  L  P  T  L  L  H  Q  A  T  Q  E  Q  Q  E  R  F
 421  TTCATACCAG CCTGGAACCT GGAGATTATT GGCACTTATG CCCAGACAGA AATGGGCCAT
 124   F  I  P  A  W  N  L  E  I  I  G  T  Y  A  Q  T  E  M  G  H
 481  GGAACTCACC TTCGAGGCCT AGAAACCACA GCAACTTATG ACCCTAAAAC ACAGGAGTTT
 144   G  T  H  L  R  G  L  E  T  T  A  T  Y  D  P  K  T  Q  E  F
 541  ATTCTTAACA GCCCTACTGT TACTTCCATT AAGTGGTGGC CTGGTGGACT TGGGAAAACC
 164   I  L  N  S  P  T  V  T  S  I  K  W  W  P  G  G  L  G  K  T
 601  TCAAATCATG CCATAGTTCT GGCTCAGCTC TACACTAAGG GAGAGTGCTA TGGATTGCAT
 184   S  N  H  A  I  V  L  A  Q  L  Y  T  K  G  E  C  Y  G  L  H
 661  GCCTTCATTG TACCTATTCG AGAAATGGGA ACCCACAAAC CTTTTCCAGG CATTATCGTG
 204   A  F  I  V  P  I  R  E  M  G  T  H  K  P  F  P  G  I  I  V
 721  GGAGACATCG GGCCCAAGTT TGGCTATGAT GAAATGGATA ATGGTTATCT AAAGATGGAC
 224   G  D  I  G  P  K  F  G  Y  D  E  M  D  N  G  Y  L  K  M  D
 781  AACTATCGAA TTCCTCGGGA AAATATGCTG ATGAAGTACG CCCAGGTCAA ACCTGATGGC
 244   N  Y  R  I  P  R  E  N  M  L  M  K  Y  A  Q  V  K  P  D  G
 841  ACATATGTGA AGCCTTTAAG TAACAAACTG ACTTATGGAA CCATGGTGTT TGTCAGATCC
 264   T  Y  V  K  P  L  S  N  K  L  T  Y  G  T  M  V  F  V  R  S
 901  TTTCTTGTGG GAGAGGCAGC TCGATCATTG TCTAAAGCTT GCACTATTGC TATCCGCTAC
 284   F  L  V  G  E  A  A  R  S  L  S  K  A  C  T  I  A  I  R  Y
 961  AGTTTAATAA GGCACCAGTC TGAAATCCAG CCAGGTGATC CTGAACCCCA GATCTTGGAT
 304   S  L  I  R  H  Q  S  E  I  R  P  G  D  P  E  P  Q  I  L  D
1021  TTTCAGACCC AGCAATATAA ACTTTTTCCT CTCTTGGCCA CTGCCTATGC CTTTCAATTT
 324   F  Q  T  Q  Q  Y  K  L  F  P  L  L  A  T  A  Y  A  F  Q  F
1081  GTGGGAGCCT ACATGAAGGA AACCTATCAT CGCATTAATG TGGACATCAG CCAAGGGAAC
 344   V  G  A  Y  M  K  E  T  Y  H  R  I  N  V  D  I  S  Q  G  N
1141  CTGAATGAAC TACCTGAGCT TCATGCACTG ACAGCTGGGC TTAAGGCTTT CACCTCTTGG
 364   L  N  E  L  P  E  L  H  A  L  T  A  G  L  K  A  F  T  S  W
1201  ACAACTAATT CTGGCATTGA AGCCTGCCGG ATGGCTTGTG GTGGGCATGG ATACTCCCAC
 384   T  T  N  S  G  I  E  A  C  R  M  A  C  G  G  H  G  Y  S  H
1261  TGCAGTGGCC TCCCAAACAT TTATGTCACT TTTACCCCCA CCTGCACCTT TGAAGGCGAA
 404   C  S  G  L  P  N  I  Y  V  T  F  T  P  T  C  T  F  E  G  E
1321  AACACTGTGA TGATGCTCCA GACAGCTCGG TTTTTGATGA AAAGCTATGA TCAGGTTCAC
 424   N  T  V  M  M  L  Q  T  A  R  F  L  M  K  S  Y  D  Q  V  H
1381  TCAGGAAAGT TGGTGGGTGG CATGGTGTCC TACTTGAATG ACCTGCCTAG TCAGCGCATC
 444   S  G  K  L  V  G  G  M  V  S  Y  L  N  D  L  P  S  Q  R  I
1441  CAGCCACAGC AGGTGGCAGC TTGGCCAGCG ATGGTGGATA TCAACAACCC AGACAGCCTC
 464   Q  P  Q  Q  V  A  A  W  P  A  M  V  D  I  N  N  P  D  S  L
1501  ACAGAAGCCT ATAAACATCG AGCAGCCCGA TTAGTAGAAG CTGCAGCAAG GAACCTTCAA
 484   T  E  A  Y  K  H  R  A  A  R  L  V  E  A  A  A  R  N  L  Q
1561  GCCGAAATGA AGCACAGAAA AAGCAAAGAG ATAGCATGGA ACTTCACCTC GGTGGACCTT
 504   A  E  M  K  H  R  K  S  K  E  I  A  W  N  F  T  S  V  D  L
1621  GTTCGAGCAA GTGAGGCTCA TTGTCACTAT GTGGTAGTAA AGCTCTTTTC TGGAAATCTC
 524   V  R  A  S  E  A  H  C  H  Y  V  V  V  K  L  F  S  G  N  L
1681  TCTAAAATTG ATGACAAACCCATTCAGGCA GTCCTGACGA ATTTGTGTCT CTTATATGCC
 544   G  I  S  S  K  I  D  D  K  P  I  Q  A  V  L  T  N  L  C  L
1741  CTGTATGGAA TCAGTCAGAA TTCTGGGGAC TTTCTACAGG GGGGCATCTT GACAGAGTCC
 564   L  Y  A  L  Y  Q  N  S  G  D  F  L  Q  G  G  I  L  T  E  S
1801  CAACTTACCC AAGTGAACCA GCGGGTGAAG GAGCTCCTGA CACTGATCCG CCCCGAATCT
 584   Q  L  T  Q  V  N  Q  R  V  K  E  L  L  T  L  I  R  P  E  S
1861  GCTGCTTTAG TGGATGCATT TGATTTTCAA GATGTTTCAC TTGGCTCTGT GCTTGGCCGC
 604   A  A  L  V  D  A  F  D  F  Q  D  V  S  L  G  S  V  L  G  R
 121  TATGATGGCA ATATTTATGA AAATATGTTT GAATGGGCCA AGAAATCTCC ACTGAATAAA
 624   Y  D  G  N  I  Y  E  N  M  F  E  W  A  K  K  S  P  L  N  K
1981  TCAGAGGTCC ATGAATCTTA TCACAAACAC CTGAAGCCAC TGCAGTCTAA GCTGTGAAG
 644   S  E  V  H  E  S  Y  H  K  H  L  K  P  L  Q  S  K  L  X
```

Figure 5.8: Nucleotide and deduced amino acid sequences of the fatty acyl-CoA oxidase (*AOX*) type I full-length cDNA isolated from koala liver.

Figure 5.8 (continued): Nucleotide and deduced amino acid sequences of the fatty acyl-CoA oxidase (*AOX*) type I full-length cDNA isolated from koala liver. Nucleotides and the corresponding amino acids, shown by single-letter codes, are numbered as indicated at the left hand side of the figure. The ATG start codon is boxed at position 51. The sequence consists of an open reading frame encoding 662 amino acids. Underlined amino acid sequences are: a) The conserved unique fatty acyl CoA oxidase motif KWWPGG found at residues 174 - 180, b) The FAD binding motif CGGHGY located at residues 396 - 400 and c) The C-terminus containing an SKL motif, which was proposed to be an import signal present in several peroxisomal matrix proteins. The koala *AOX I* sequence has been submitted to GenBank and its accession number is AF463453.

```
AOXI
317 AACTTTGTGCAT CGTGGGCGTC CTGAGCCTTT GGACCTTCAC TTGGGTATGT TTCTGCCCAC
 89   N  F  V  H  R  G  R  P  E  P  L  D  L  H  L  G  M  F  L  P  T
379 ATTACTTCAC CAGGCAACCC AGGAGCAGCA GGAACGCTTC TTCATACCAG CCTGGAACCT
110   L  L  H  Q  A  T  Q  E  Q  Q  E  R  F  F  I  P  A  W  N  L
439 GGAGATTATT GGCACTTATG CCCAGACAGA AATGGGCCAT
130   E  I  I  G  T  Y  A  Q  T  E  M  G  H

AOXII
317 AAACCACAGTTG ATCAATTTTG TGGAACCGGT TGGCCTCACT TACTCCATGT TTATCCCTAC
 89   K  P  Q  L  I  N  F  V  E  P  V  G  L  T  Y  S  M  F  I  P  T
379 CTTGCTGGAT CAGGGCACCA CTGCTCAGCA ACAGAAATGG CTGCCTCCAA CCCAAGGACT
110   L  L  D  Q  G  T  T  A  Q  Q  Q  K  W  L  P  P  T  Q  G  L
439 CCAGATAATT GGCACCTACG CCCAGACCGA GATGGGGCAC
130   Q  I  I  G  T  Y  A  Q  T  E  M  G  H
```

Figure 5.9: Koala liver *AOX I* and *AOX II* cDNA and deduced amino acid sequences in the coding region located between nucleotides 269-429 (exon 3), where sequence differences were identified.
The accession number of koala *AOX II* is AF463454.

The koala *AOX* cDNAs were digested with *Not* 1 and *Xho* 1 and then ligated into *Not* 1 and *Xho* 1 digested pCI-neo vector. For functional comparison, rat *AOX*1 and *AOX*2 cDNAs were amplified by RT-PCR, inserted into the pCI-neo vector, and transfected into Cos-7 cells. The cells were harvested three days after transfection. Transfections with either no DNA or no LipofectAMINE were used as negative controls.

The palmitoyl-CoA oxidase activity of the expressed koala AOXI and AOXII proteins was determined and compared to that of the expressed rat AOX 1 and AOX 2. Koala, human and rat liver homogenate samples (n=1 for each) were included as control samples. Palmitoyl-CoA activities for expressed koala and rat AOXI and AOXII enzymes are shown in Table 5.4. Each reported activity of cDNA-expressed proteins represents the average of two transfection experiments.

Kinetic analysis was performed for both cDNA-expressed koala AOXI and AOXII enzymes using palmitoyl-CoA substrate concentrations ranging from 25 to 175μM, as previously described by Veldhoven and colleagues [131, 278, 235]. The apparent K_m and V_{max} values obtained for expressed koala AOXI and AOXII proteins were 28- and 38-μM, respectively and those for rat and human liver homogenates were 78- and 70-μM, respectively (Table 5.4).

Samples	Total palmitoyl-CoA oxidase activity	AOX-dependent palmitoyl-CoA oxidase activity
Koala (n=6)	389.4 ± 192.7	292.5 ± 100.7
Rat (n=3)	4323.9 ± 191.6	3515± 508.5
Human (n=1)	1881.7	nd

Table 5.3: Total palmitoyl-CoA and acyl-CoA oxidase-dependent palmitoyl-CoA oxidase activities determined in koala and rat liver homogenates.
Values are expressed as mean± SD. Activity is expressed as nmole/g protein/ minute. nd: not determined.

Samples	Palmitoyl-CoA oxidase activity (nmole/min/g protein)	Km (μM)	Vmax [a]
Expressed koala AOX I	1472.70	28	1499.10
Expressed koala AOX II	543.30	38	677.00
Expressed rat AOX1	n.d.	-	-
Expressed rat AOX2	471.65	-	-
Rat liver homogenate	4643.95	-	-
Koala liver homogenate	375.90	78	610.40
Human liver homogenate	1883.65	70	2600.85

Table 5.4: Palmitoyl-CoA activity catalysed by cDNA-expressed koala and rat AOX enzymes.
Data are derived from multiple time points and expressed as a mean of duplicate determinations (Section 5.2.5). [a] Vmax was expressed as nmole/min/g protein. n.d.: No activity detected. -: Enzyme kinetic parameters not determined. No activity was detected in untransfected Cos-7 cell lysates.

5.3.4 Northern analysis of acyl CoA oxidase mRNA

Northern blot analysis of AOX mRNA from koala, rat and human livers is shown in Figure 5.10. The koala *AOX* cDNA probe recognised a mRNA species in all mRNA samples studied. In koala, a single band corresponding to a mRNA species of approximately 5-kb was observed in all livers studied. A single band of lower intensity was also detected in rat and human liver mRNA samples, of approximately 4-kb and 3-kb, respectively.

5.3.5 Southern analysis of the *AOX* gene

Southern blot analysis of EcoR1-digested genomic DNA from male koala, rat, wallaby, possum, and bandicoot liver is shown in Figure 5.11. From this blot, it is apparent that *EcoR* 1-digestion of genomic DNA produced only one *AOX* gene fragment of size less than 14-kb for koala, wallaby and rat samples.

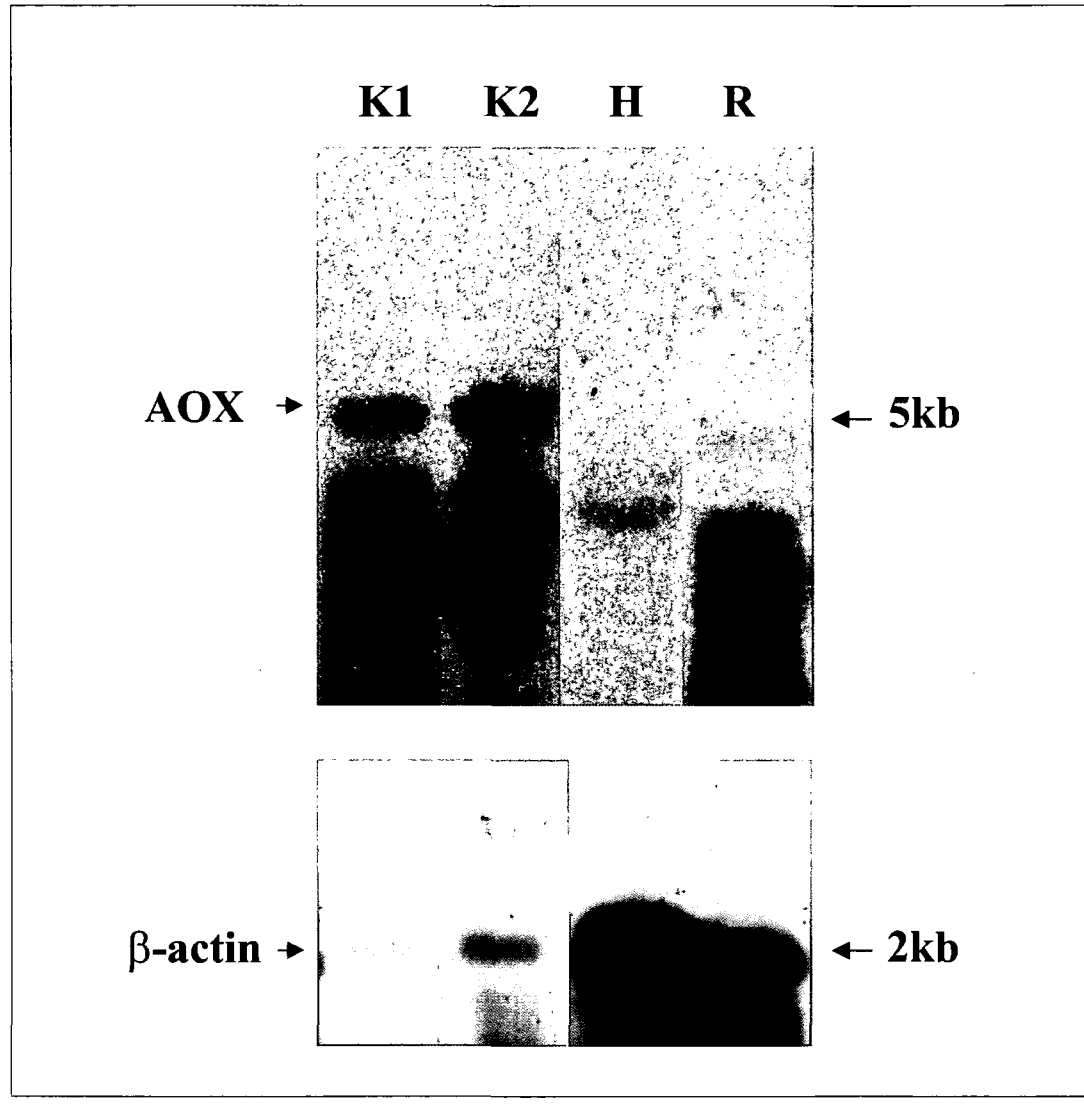

Figure 5.10: Northern blot analysis of hepatic AOX mRNA. Messenger RNA (10 μg, except koala K_1 (4 μg)) was purified from two koala (Lanes K_1-K_2), human (Lane H), and rat (Lane R) liver samples and hybridised with a 320-bp koala *AOX* cDNA probe (^{32}P-labelled). Panel (A): Hybridisation with the 320-bp koala *AOX* cDNA probe. Panel (B): Hybridisation with mouse β-actin.

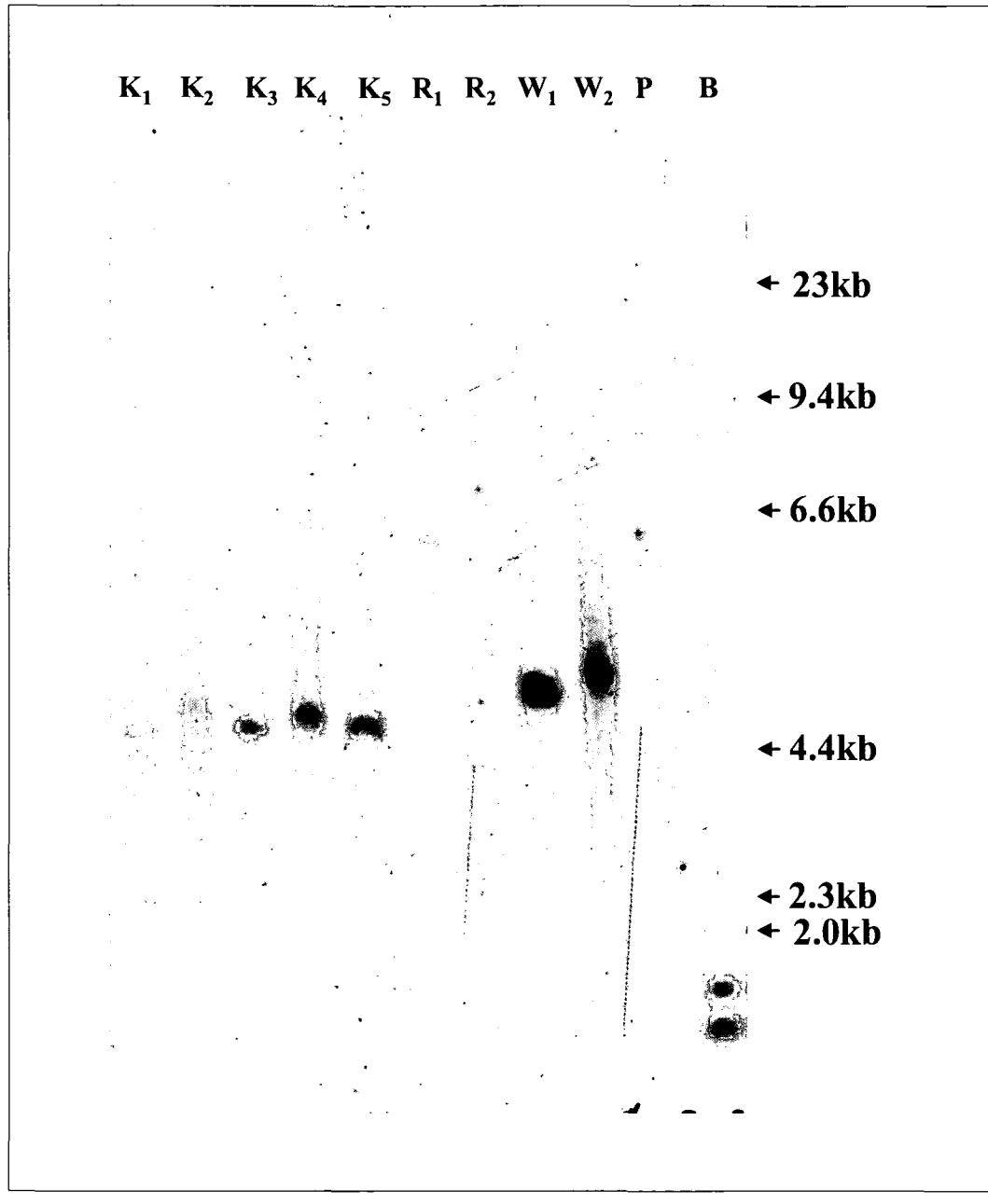

Figure 5.11: Southern blot analysis of the *AOX* gene.
Genomic DNA was extracted from five koala (Lanes K_1-K_5), two rat (Lanes R_1-R_2), two wallaby (Lanes W_1-W_2), one possum (Lane P), and one bandicoot (Lane B) liver sample and hybridised with a 320-bp koala *AOX* cDNA probe (^{32}P-labelled). A single *AOX* gene fragment of size less than 14-kb was observed for the koala and other species examined with the exception of the bandicoot where 2 distinct bands were observed.

5.4 DISCUSSION

Previous work by this laboratory had demonstrated an absence of peroxisomal cyanide-insensitive palmitoyl-CoA oxidation, a measure of overall peroxisomal β-oxidation activity, in the koala liver [8]. This chapter focussed on the molecular characterisation of the first and rate-limiting enzyme in this pathway, fatty acyl-CoA oxidase (AOX).

Two 2039-bp koala *AOX* cDNAs were isolated from koala liver utilising PCR based approaches and were designated *AOX I* and *AOX II*. These differ in a small area of the coding region, between nucleotides 269 - 429 (Figure 5.9). This finding is consistent with results reported in both the rat and in humans [133, 279]. In each species, a single *AOX* gene was identified which gives rise to alternative mRNA species via differential splicing [133, 279]. Two *AOX* cDNAs have also been described in the yeast, *Candida tropicalis* [280].

Each koala *AOX* cDNA has an open reading frame of 1988-bp, which encodes a protein of 662-aa, and both contain a 51-bp 5' UTR. Both koala *AOX I* and *AOX II* cDNAs exhibit high nucleotide sequence identity to the reported human and rat *AOX* cDNA sequences (Table 5.2). The nucleotide and deduced amino acid sequences of koala *AOX I* and *AOX II* are shown in Figures 5.8 and 5.9. The koala *AOX I* and *AOX II* cDNA sequences were submitted to GenBank (Bethesda, Maryland USA) and have been assigned the accession numbers AF463453 and AF463454, respectively.

As shown in Figures 5.8 and 5.9, the koala *AOX I* and *AOX II* cDNAs share several common features with other *AOX* sequences: the conserved unique fatty acyl CoA oxidase sequence KWWPGG found at residues 174 - 180 [281], the FAD binding motif CGGHGY located at residues 396 - 400 [281], and the C-terminus containing an SKL motif which has been proposed to be an import signal present in several peroxisomal matrix proteins (Figure 5.8) [275]. The alignment of the deduced amino acid sequences of koala AOX I and AOX II with other AOX proteins is shown in Figures B.2 and B.2 (Appendix B).

The total palmitoyl-CoA activity of koala livers was about 12- and 5- fold less than that in rat and human liver homogenates. This finding suggests that the level of functional AOX protein in koala liver is significantly lower than in rat and human liver. The acyl-CoA oxidase activity of rat liver homogenate determined in our study

is consistent with that reported by Veldhoven (1994) [278].

Expression of koala AOX I and AOX II in Cos-7 cells and determination of palmitoyl-CoA oxidase activity confirms that the cloned koala *AOX* cDNAs encode functional enzymes. Based on sequence alignments, koala AOX I displays higher sequence identity with rat AOX2 (ACO-II). The activity of cDNA-expressed koala AOX I was higher than that observed with cDNA-expressed rat AOX2 (1472.70 versus 471.65 nmole/min/g protein, respectively). The activity of cDNA-expressed koala AOX II was lower (543.3) while no activity was observed for cDNA-expressed rat AOX1. Each reported activity for cDNA-expressed proteins represents the average of two experiments and it is unlikely that no activity observed for cDNA-expressed rat AOX1 was due to experimental errors. While the apparent K_m values for cDNA-expressed koala AOXI and AOX II were lower than that of koala liver homogenate (28 μM and 38 μM versus 78 μM, respectively), these K_m values for cDNA-expressed koala AOXI and AOX II are within the order of magnitude reported for that of purified rat and human AOX1 enzymes (10 μM) [111, 282]. The apparent K_m for human liver homogenate observed in our study is comparable to that reported by others [282]. Decreases in palmitoyl-CoA oxidase activity of cDNA-expressed koala and rat AOX enzymes as well as liver homogenates were also observed with substrate concentrations just above the V_{max} values as reported for activity measurements of rat purified AOX1 by others [131, 277, 283].

As is clear from Northern blot analysis of hepatic mRNAs from koala, rat and human, the intensity of AOX signal detected for the koala was much stronger. This suggests higher expression of koala liver AOX mRNA. The size of human and rat AOX mRNAs detected in the present study compare with previously reported values of 3.2-kb and 3.8-kb, respectively [274]. Our studies also show higher expression of rat AOX mRNA as compared to human which is consistent with previous studies [274]. Analysis of liver genomic DNA suggests the existence of a single *AOX* gene in all species studied.

In summary, two koala *AOX* cDNAs have been isolated which differ only in a small area of the coding region, between nucleotides 269 - 429. This finding is consistent with results reported in both the rat and in humans. Expression of koala AOX I and AOX II in Cos-7 cells and kinetic analysis confirms that the cloned koala *AOX* cDNAs encode functional enzymes with palmitoyl-CoA oxidase activity. The results of these studies suggest that the absence of peroxisomal cyanide-insensitive palmitoyl-

CoA oxidation, a measure of the overall peroxisomal β-oxidation activity, in the koala liver, is possibly due to deficiencies of one or more enzymes downstream of fatty acyl-CoA oxidase and/or deficiencies of mitochondrial β-oxidation enzymes. The enzymes downstream of fatty acyl-CoA oxidase include enoyl-CoA hydratase/3-hydroxyacyl-CoA dehydrogenase bifunctional enzyme and 3-ketoacyl-CoA thiolase.

Chapter 6

KOALA LIVER PPAR-α

6.1 INTRODUCTION

Peroxisome proliferator activated receptor-alpha (PPAR-α) is a member of the nuclear receptor gene superfamily. PPAR-α is activated by a structurally diverse group of xenobiotics collectively termed peroxisome proliferators and also by several endogenous substrates. In susceptible rodents, peroxisome proliferators cause marked peroxisome proliferation and an increase in liver size. Induction of peroxisomal β-oxidation enzymes [172, 173, 284] and microsomal CYP4A [174, 285] often occurs concurrently with peroxisome proliferation. These profound effects are highly tissue-specific and occur predominantly in the liver parenchymal cells [161]. A more detailed discussion on peroxisome proliferators, their induction of peroxisome proliferation and the regulatory role of PPAR-α is found in Sections 1.4.2, 1.4.3 and 1.4.5

In humans, rat and other species studied, PPAR-α mediates the effects of peroxisome proliferators via transcriptional activation of target genes including members of the *CYP4A* subfamily and the peroxisomal β-oxidation enzyme, acyl CoA oxidase [166, 167, 204, 286]. PPAR-α binds to a specific binding sequence, the peroxisome proliferator responsive element (PPRE), in the promoter region of these target genes and trans-activates gene expression. Evidence for the direct binding of PPAR-α to PPRE has been reported [147, 148]. The function of PPAR-α in trans-activating PPRE derived from either rat AOX or rabbit CYP4A6 in the presence of RXR has been confirmed in several species including humans, guinea-pigs, mice and rats[149, 152, 155, 163]. Transgenic mice with disruption of the PPAR-α gene were found to exhibit no liver enzyme induction, no peroxisome proliferation, altered constitutive expression of fatty acid metabolising enzymes and no increase in liver

size after treatment with peroxisome proliferators [105, 159].

In humans, rat, mouse and other species studied, the PPAR-α gene comprises six coding exons [139, 152, 164]. One exon codes for the N-terminal domain which contains a variable A/B region, displaying a ligand-independent transactivation function (AF-1 domain). The central DNA binding domain (DBD) is encoded by two exons and forms two fingers. They are responsible for sequence-specific DNA recognition and dimerisation. The C-terminal is subdivided into D, E and F regions with one exon encoding each region and these function as the ligand binding domains (LDB). The E LDB is highly conserved and also acts as a ligand-dependent transactivation domain (AF-2 domain). The C-terminal F domain is essential for the interaction of the nuclear receptor with nuclear receptor coactivators and co-repressors [114, 139, 164]). The general structure of PPAR-α is shown in figure 6.1

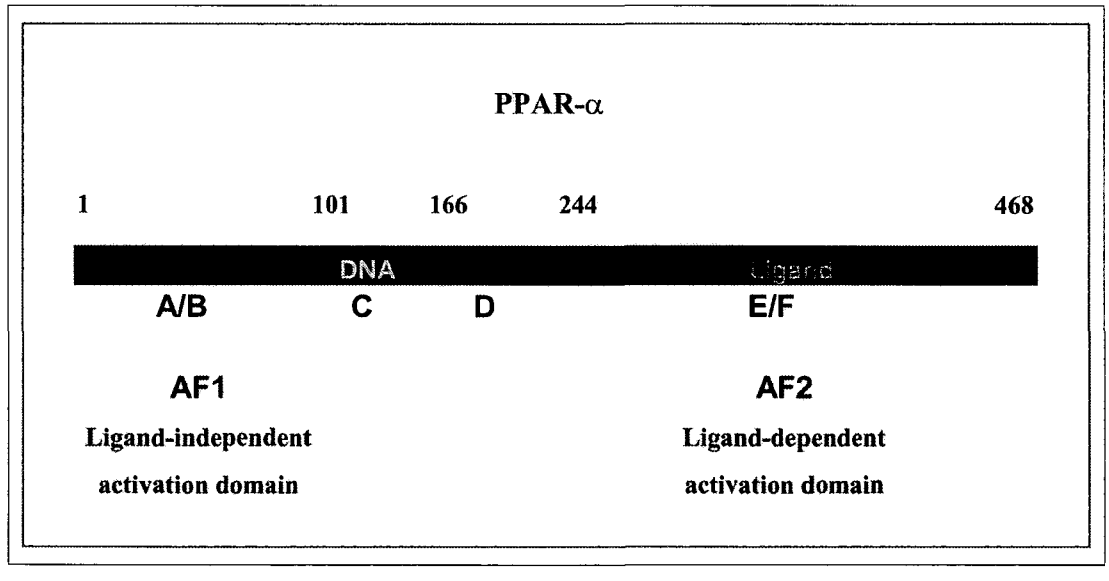

Figure 6.1: A schematic diagram depicting the nuclear receptor PPAR-α structure.
The structure is based on human PPAR-α. The scheme shows the four domain structure of PPAR-*alpha* which is the same as for other members of the nuclear receptor superfamily. AF1 and AF2 are the activation function 1 and activation function 2 domain.

PPAR-α is critically important in mediating key transcriptional responses involved in lipid homeostasis. Fatty acids and non metabolisable fatty acids have been identified as potent activators of PPAR-α [152, 163]. Chapters 4 and 5 have described

the biochemical and molecular characterisation of microsomal CYP4A15 and peroxisomal β-oxidation fatty acyl CoA oxidase in the koala liver. The following overview demonstrates the important role of PPAR-α in mediating the expression of these lipid metabolising enzymes (Figure 1.1).

Significance species differences in responses to peroxisome proliferators have been reported [62, 185, 186, 187, 188]. Rats and mice are highly responsive whereas humans, rhesus monkeys, dogs, guinea pigs and marmosets are weakly or nonresponsive. These species differences appear to be due to marked variations in the abundance of liver PPAR-α and variation in gene specific effects involving other transcriptional regulatory factors [202, 203, 287]. In the majority of species studied, PPAR-α is most abundant in liver, kidney, heart and muscle. While PPAR-α is highly expressed in rat and mouse livers, both PPAR-α mRNA and protein levels are much less abundant in human and guinea pig livers[149]. For example, the level of PPAR-α protein expression in human liver was found to be approximately 10-fold less than that observed in rats. This low level of PPAR-α protein is probably insufficient for competing effectively with other proteins to bind to PPRE [205]. The weak or nonresponsive nature of some species has also been hypothesised to be due to fundamental deficiencies in PPAR-α [200].

The results of studies reported in Chapters 3, 4 and 5 indicate a higher level of liver CYP4A and AOX mRNA in the koala as compared to other species and suggest a moderately responsive nature of marsupials to peroxisome proliferator monoterpenes. To date, no studies on PPAR-α have been reported from the koala or any other marsupial species. *PPAR-α* cDNA was first isolated from mouse liver [152] and subsequently cloned from livers of Xenopus [162], rat [163], human [155] and guinea-pig [149]. Studies described in this chapter aimed to confirm the presence of a functional *PPAR-α* gene in the koala and to provide the first primary molecular data for further study on the regulatory role of PPAR-α in koala livers. The study also provided insight into PPAR-α mRNA and protein levels in the koala liver and investigated the organisation of the *PPAR-α* gene across species using Southern blot analysis.

6.2 METHODS

6.2.1 Isolation of koala liver peroxisome proliferator activated receptor-alpha *PPAR-α* cDNA by RT-PCR approaches

A similar cloning strategy as was described for the isolation of koala liver *AOX* cDNAs in Section 5.2.1 was employed for the isolation of a full-length koala liver *PPAR-α* cDNA. As the *PPAR-α* cDNA is approximately 500-bp shorter than the *AOX* cDNAs, the method involved amplification of only two partial *PPAR-α* cDNAs using RT-PCR and RACE. Degenerate primers were derived from the alignment of known *PPAR-α* nucleotide sequences from other species. A full-length *PPAR-α* cDNA was then isolated using gene-specific primers derived from the two partial cDNAs. The PPAR-α cloning strategy is detailed in Figure 6.2.

RT-PCR amplification of koala liver *PPAR-α* cDNA: The isolation of total RNA, purification of mRNA from total RNA samples and synthesis of first-strand cDNA were performed as described previously in Section 4.2.1. Reactions for RT-PCR amplification were set up as described in Section 2.21.2. Degenerate primers, designated kGPf and kGPr, were derived from *PPAR-α* cDNA sequences from other species in the GenBank database (Table 6.1). The optimal conditions for PCR amplification were: denaturation at 94^0C for 3 minutes; then 30 cycles of 94^0C for 45 seconds, 55^0C for 45 seconds, and 72^0C for 1 minute; final extension at 72^0C for 10 minutes.

RACE amplification of koala 5' end PPAR-α cDNA: The 5'-end of koala PPAR-α cDNA was amplified using SMART RACE cDNA Amplification kit as described in section 4.2.1. Koala 5'-end *PPAR-α* cDNA fragments were amplified utilising Universal Primer Mix (UPM) (Table 2.6) and gene specific reverse primer kPP5', based on the koala 1051-bp *PPAR-α* cDNA sequence (Table 6.1). RACE amplification reactions were set up as described in section 2.21.3. Touchdown PCR conditions for RACE reactions were as follows: 5 cycles of 94^0C for 5 seconds and 72^0C for 2 minutes; 5 cycles of 94^0C for 5 seconds, 70^0C for 10 seconds and 72^0C for 2 minutes, and 32 cycles of 94^0C for 5 seconds, 68^0C for 10 seconds and 72^0C for 2 minutes. Several 5' cDNA fragments of different sizes from 500- to 800-bp were amplified. Amplified DNA fragments were separated and excised from agarose gel as per Sections 2.15.2 and 2.15.3 and sub-cloned into pGEM-T vector as described in Sections 2.13.1, 2.13.2

and 2.13.3. The clones were subsequently sequenced using M13 universal (M13) and M13 reverse (M13r) sequencing primers as per Section 2.16.2. The 5' cDNA fragment obtained contains a 141-bp overlapping DNA fragment with the koala 1051-bp *PPAR-α* cDNA clone and also includes a 107-bp 5' untranslated region (5'*UTR*).

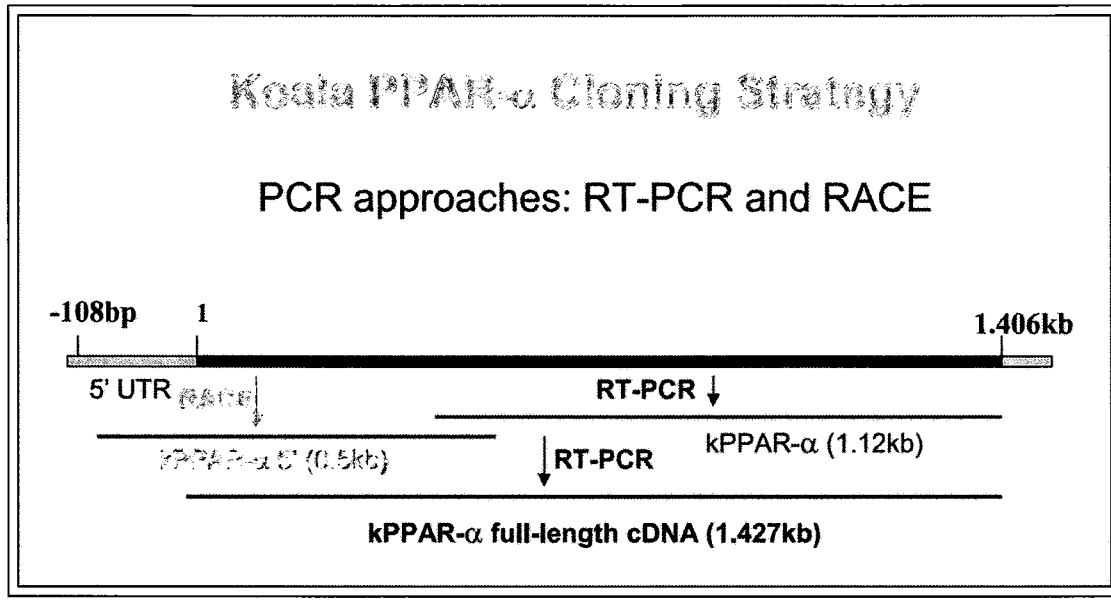

Figure 6.2: Schematic diagram of the cloning strategy to obtain a full–length *PPAR-α* cDNA from koala liver.
The solid blue box represents the coding region of koala PPAR-α and the green boxes depict the 5' and 3' non coding regions. Single lines represent koala *PPAR-α* cDNAs: 5' cDNA amplified fragment obtained by RACE is red, koala partial *PPAR-α* cDNA is purple, koala liver 1427-bp *PPAR-α* cDNA is green.

RT-PCR amplification of koala and rat liver *PPAR-α* cDNA:
Full-length koala *PPAR-α* cDNA was then amplified by RT-PCR using kPPfF and kPPfR primers (Table 6.1), derived from the 5' and 3' sequences obtained, and koala first-strand cDNA as a template. Restriction sites *EcoR* 1 and *Xho* 1 were included at the 5' and 3' ends of the forward and reverse primers respectively, to facilitate subsequent directional cloning into the pCMV-Script vector. KPPfF and kPPfR primers amplified a cDNA fragment corresponding to the entire coding region of the koala *PPAR-α* including the start and stop codons (Table 6.1). PCR reactions were set up as described in Section 2.21.2 and were cycled for 30 cycles of 94^{0}C for 30 seconds, 55^{0}C for 30 seconds and 72^{0}C for 2 minutes followed by a final 10 minute extension at 72^{0}C. PCR reaction products were separated on 0.7% w/v low melt agarose gels

Name	Sequences (5'-3')	Origin	A*
kGPf	**GAATTC**GAAGGCTGCAAGGGCTTCTT	(+)357 - (+)377	b
kGPr	**GAATTC**CTCAGTACATGTCCCTGTAGAT	(+)1385 - (+)1407	b
kPP5'	**ATTCCA**ACTGAAAGGCACTTCTGGAA ACGGCAA	(+)465 - (+)498	b
kPPfF	**GAATTC**ACCGGCTGTGCCTTATCAAG	(-)20 - (+)1	c
kPPfR	**CCGCTCGAGC TCA**GTACATGTCCCT GTAGAT	(+)1385 - (+)1407	c
rPPfF	**GAATTC**CCACAACCATTCAAC**ATG**GTG	(-)15 - (+)6	d
rPPfR	**CCGCTCGAGCTCA**GTACATGTCCCT GTAGAT	(+)1358 - (+)1407	d

Table 6.1: Details of oligonucleotide primers for PCR amplification of koala *PPAR-α* cDNA.
Restriction sites and start and stop codons are shown in bold. Origin: Corresponding to the position of the nucleotides relative to the start codon (designated +1). A*: accession numbers: b: NM 011144, mouse *PPAR-α* cDNA [152]; c: AF463455, koala liver *PPAR-α* cDNA (Ngo *et al*, direct submission); d: NM 013196, rat *PPAR-α* cDNA [163].

as described in Section 2.15.2, excised and purified as described in Section 2.15.3. After digestion with *EcoR* 1 and *Xho 1* as described per Section 2.15.1, the purified koala *PPAR-α* cDNA fragment was ligated into pCMV-Script XR pre-digested vector and transfected into *E. coli* strain XL1-Blue competent cells as described in Sections 2.13.1, 2.13.2, and 2.13.3. Plasmid DNA was isolated from selected white colonies using a modified alkaline lysis miniprep procedure and screened for the presence of correctly-sized inserts by restriction digest as described in Section 2.15.1. Plasmid DNAs with correct size inserts were then purified using the Qiaquick Spin Miniprep kit as described in Section 2.14.1 and subsequently sequenced in both forward and reverse directions using T3, T7 primers (Table 2.5) and derived internal primers.

For control studies, full-length rat *PPAR-α* cDNA was isolated by RT-PCR using rPPfF and rPPfR primers, derived from published rat *PPAR-α* cDNA sequence (Table 6.1). The rat *PPAR-α* cDNA is identical to those previously cloned and characterised [163]. The amplification, subcloning into the pCMV-Script XR vector, screening and sequencing of rat *PPAR-α* cDNA were performed essentially as described above for koala *PPAR-α* cDNA.

6.2.2 Expression of koala liver *PPAR*-α cDNA in Cos-7 cells

The growth and maintenance of Cos-7 cells was performed as described in Section 4.2.3. Plasmid DNAs were isolated using the QIAfilter Midiprep Spin kit as described in Section 2.14.3. Just prior to transfection, the cells were washed gently with DMEM with no serum and the media was then removed. Koala and rat *PPAR*-α cDNAs subcloned into the pCMV-Script XR vector were transfected into Cos-7 cells using LipofectAMINE reagent as per Section 4.2.3. Cells were harvested as described in Section 4.2.3 and the crude cell lysates were used directly for immunoblot analysis.

6.2.3 Preparation of liver cytosol and nuclear extracts

Preparation of hepatic cytosol and nuclear extracts was performed as described in Sections 2.9.1 and 2.9.3. Protein concentrations of various subcellular fractions were determined by the method of Lowry *et al.* 1951.

6.2.4 Immunoblot analysis

Immunodetection of PPAR-α in cytosolic and nuclear extracts from koala, rat, possum and wallaby livers was performed as described in Section 2.10, using a rabbit anti-human polyclonal PPAR-α antibody (1:200 dilution) and a mouse-anti-rabbit (1:2000 dilution) IgG (Santa Cruz, Germany) as primary and secondary antibodies, respectively. For immunodetection of cDNA-expressed koala and rat PPAR-α proteins, crude Cos-7 cell lysates were used.

6.2.5 Analysis of PPAR-α mRNA

Northern analysis was performed using the koala liver α-[^{32}P]-dCTP labelled *PPAR*-α 1051-bp cDNA probe. Electrophoresis of mRNA through formaldehyde gels and blotting were performed as described in Section 2.19.1 and Section 2.19.2. The integrity of mRNA was assessed by visualisation with ethidium bromide. To assess mRNA loading, the filter was stripped and reprobed with α-[^{32}P]-dCTP labelled β-*actin* cDNA probe.

6.2.6 Southern analysis of hepatic genomic DNA

Genomic DNA was extracted as per Section 2.20.1 and digested with *EcoR* 1 at 37^0C overnight. A second aliquot of *EcoR* 1 was added to the reaction mixture and the digestion was continued for another 6 hours to ensure complete digestion. DNA fragments were separated by gel electrophoresis and transferred to a nylon membrane as described per Section 2.20.2 and Section 2.20.3. Prehybridisation and hybridisation with α-[^{32}P]-dCTP labelled koala *PPAR-α* 1051-bp cDNA probe were performed at 42^0C in a hybridisation solution containing 50% formamide as per Section 2.20.4. The blot was exposed to X-ray film with intensifying screens at -80^0C for several days.

6.3 RESULTS

6.3.1 Cloning of koala liver *PPAR-α* cDNA

RT-PCR of koala liver *PPAR-α* partial cDNA: A koala 1051-bp *PPAR-α* cDNA including the stop codon was amplified by RT-PCR using kGPf and kGPr degenerate primers. Initial PCR reactions were established using several primer pairs, designed from different highly conserved regions from the alignment of *PPAR-α* from human, rat and mouse [163, 152, 155]. Optimisation of PCR amplifications was accomplished using a range of annealing temperatures from 45^0C to 65^0C and also varying $MgCl_2$ concentrations from 1.5mM to 4mM. KGPf and kGPr primers (Table 6.1) were the optimal primer pair which amplified a correct insert of approximately 1.05-kb with the optimal PCR amplification conditions as described in Section 6.2.1. Figure 6.3 shows agarose gel electrophoresis of the initial PCR products generated by different primer pairs at a range of temperatures from 45^0C to 60^0C. To reduce non-specific binding and increase the yield of the 1.05-kb fragment, Q solution was included into PCR reactions and the annealing temperatures were kept at 50^0C to 60^0C. To decrease non-specific binding further, reverse primer kGPr was added into the reaction separately after 5 PCR cycles. Figure 6.4 shows the analysis of the gel electrophoresis of PCR products generated by kGPf and kGPr primers under different optimising conditions.

RACE amplification of koala 5' end *PPAR-α* cDNA: The 5'-end of the koala *PPAR-α* cDNA was isolated by RACE using UPM and kPP5' primers (Table 6.1). UPM and kPP5' primers amplified a smear of DNA fragments of sizes from 200- to 900-bp. The optimisation of RACE reactions was performed essentially as described previously for RT-PCR of koala liver *PPAR-α* 1.05-kb partial cDNA. Figure 6.5 shows an agarose gel electrophoresis of RACE products generated by UPM and kPP5' primers, using range of $MgCl_2$ concentrations from 2mM to 4mM. A series of PCR products sizes approximately 250- to 850-bp were seen, suggesting non-specific amplification under these conditions.

Amplified PCR products were purified and subcloned into the pGEM-T vector (Sections 2.13.2 and 2.13.3). Several clones with different size inserts from 500- to 850-bp were sequenced to confirm their identity (Section 2.16). A koala *PPAR-α* 5' end cDNA of size 605-bp was obtained. The 5' *PPAR-α* cDNA has 141-bp overlapping sequence with the koala partial *PPAR-α* 1051-bp cDNA and contains 107-bp 5'-*UTR*.

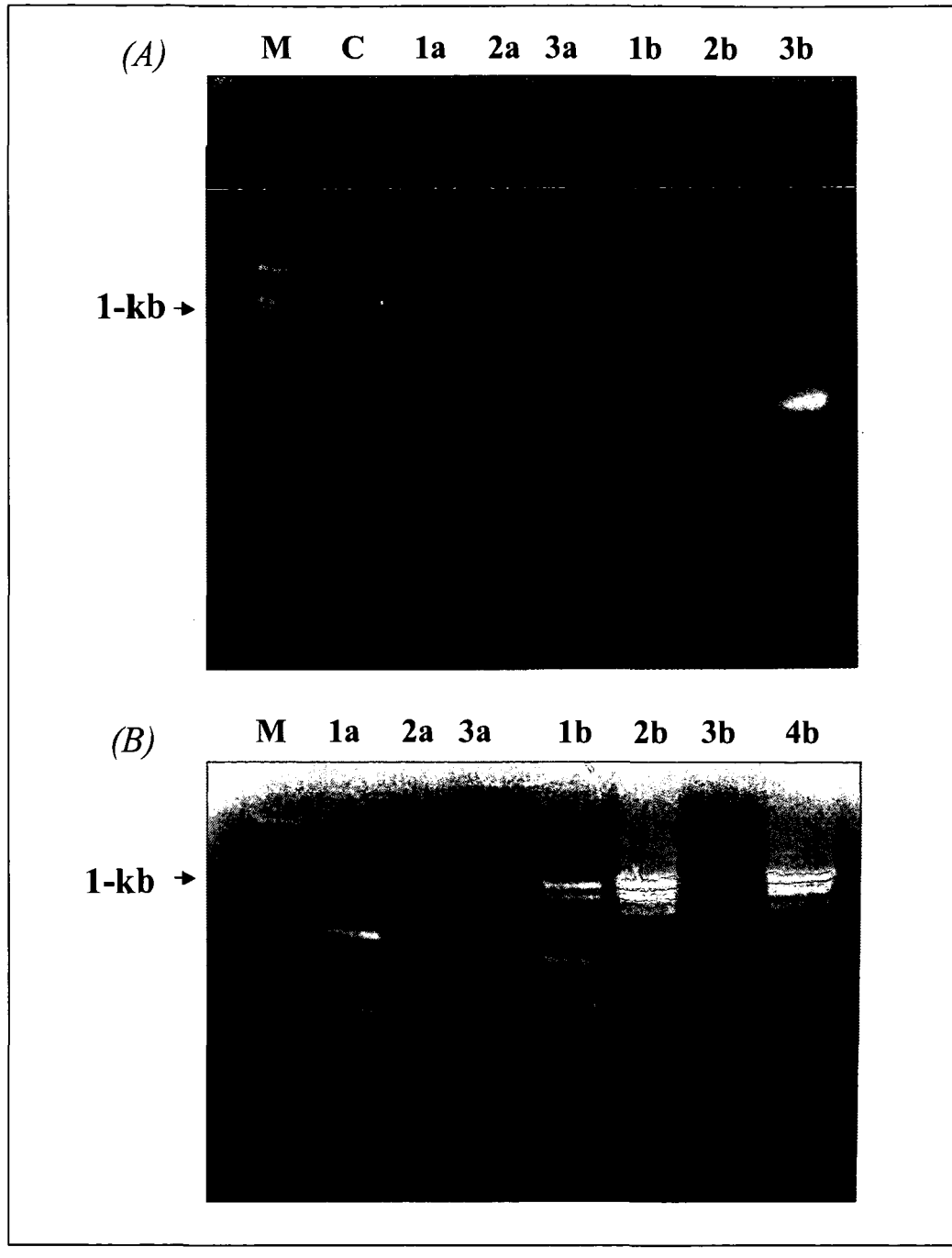

Figure 6.3: Agarose gel analysis of PCR products amplified by KGPf and KGPr primers using koala liver cDNA template.
Panel A, lanes 1b-3b: PCR products generated at annealing temperatures 45^{0}C, 50^{0}C and 55^{0}C, respectively. Panel B: Reamplification of PCR products from panel A using KGPf and KGPr primers at the same corresponding temperatures (lanes 1b-3b), lane 4b: at 60^{0}C with 2b template. Expected 1.05-kb products were amplified. Lanes 1a-3a: products amplified by other primers at the same corresponding temperatures. Lane C: Negative control (PCR reaction with no DNA template). Lane M: DNA molecular weight marker.

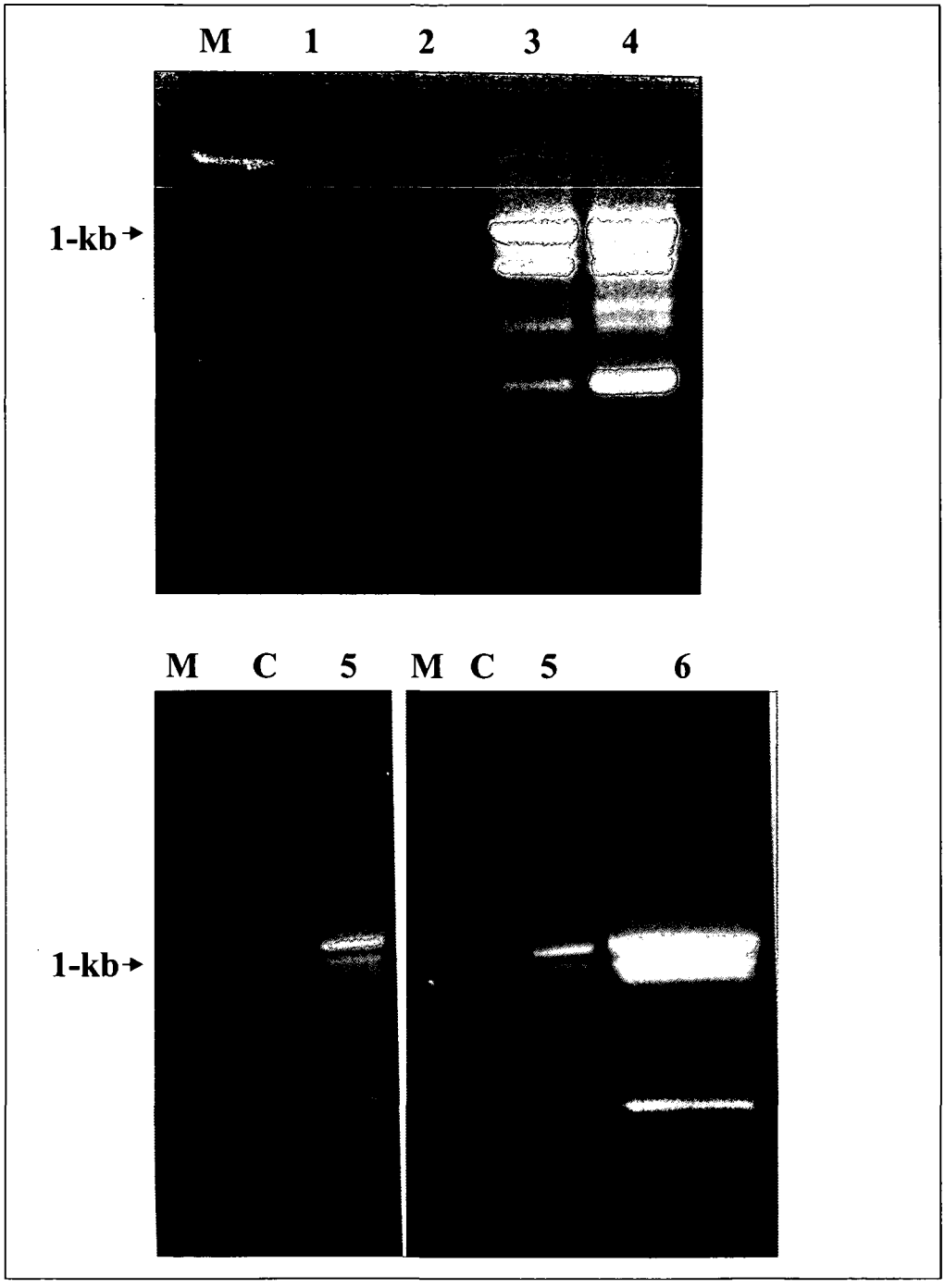

Figure 6.4: Agarose gel analysis of PCR products amplified by KGPf and KGPr primers from koala liver cDNA template with Q solution.
Lanes 1, 2: at annealing temperatures 55^0C and 60^0C (Template 1). Lane 3, 4: at 55^0C and 60^0C (Template 2). Lane 5: at 55^0C and KGPr primer was added separately after 5 PCR cycles (Template 2). Lane 6: Large scale amplification of PCR reaction from lane 5. Expected 1.05-kb products were amplified. Lane C: negative control (PCR reaction with no DNA template). Lane M: DNA molecular weight marker. Lower panel: different sections of the same photo

RT-PCR isolation of koala complete *PPAR-α* cDNA: Several gene-specific primers were derived based on the sequences obtained for the two partial *PPAR-α* cDNA clones. Forward primer KPPfF and reverse primer kPPfR (Table 6.1) were found to be the optimal primer pair, which amplified a PCR fragment of approximately 1.45-kb using koala liver first-strand cDNA template as shown in Figure 6.6 (Panel A, Lanes 2, 4 and 5). This size was the expected size for the primer combination. Figure 6.6 also shows a large scale amplification of this product using kPPfF and kPPfR primers (Panel B, Lane 3). PCR fragments of the same size were amplified from rat liver first-strand cDNA (Figure 6.6, Panel B, Lane 1 and 2), using rPPfF and rPPlR primers (Table 6.1).

PCR products were subcloned initially into the pGEM-T vector (Sections 2.13.2 and 2.13.3) and sequenced in both forward and reverse directions to confirm their identity (Section 2.16). A full-length koala liver *PPAR-α* cDNA of 1428-bp was amplified. The koala *PPAR-α* cDNA has an open reading frame of 1408-bp and encodes a protein of 468-aa. The nucleotide and deduced amino acid sequence of the koala *PPAR-α* are shown in Figure 6.7. Its 107-bp 5'-*UTR* was also included.

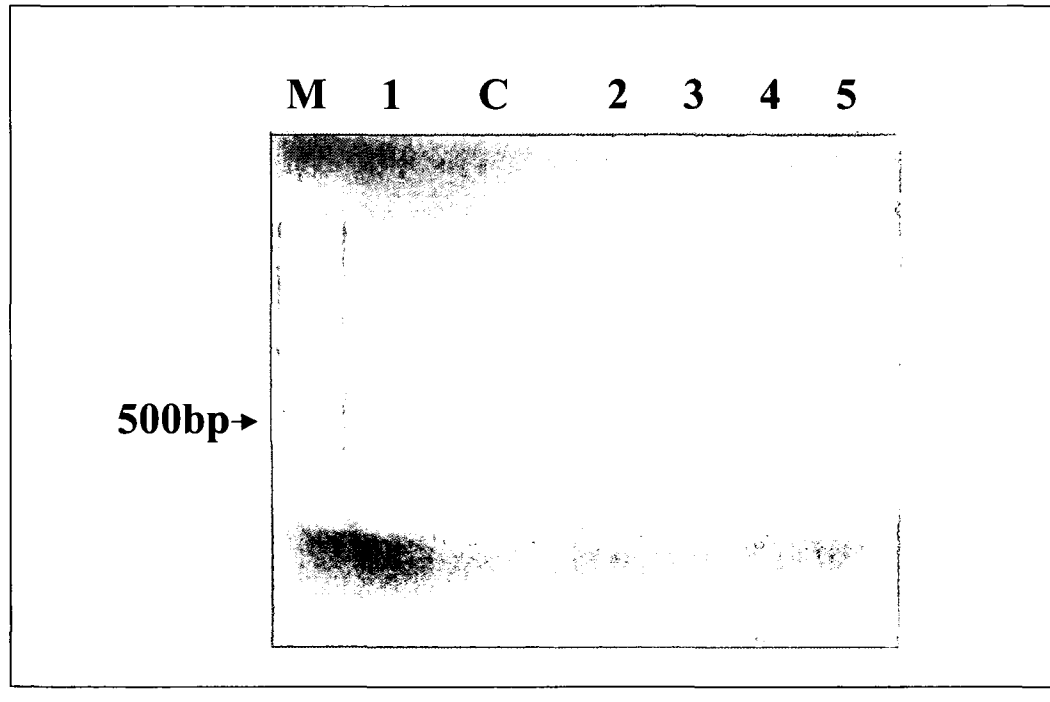

Figure 6.5: Agarose gel analysis of PCR products amplified from koala liver 5'RACE-ready cDNA using UPM and kPP5' primers.
Lane 1-5: at $MgCl_2$ concentration of 2mM, 2.5mM, 3mM, 3.5mM and 4mM respectively. A smear of RACE products from 250-bp to 900-bp were amplified. Lane C: negative control (PCR reaction with no DNA template). Lane M: DNA molecular weight marker.

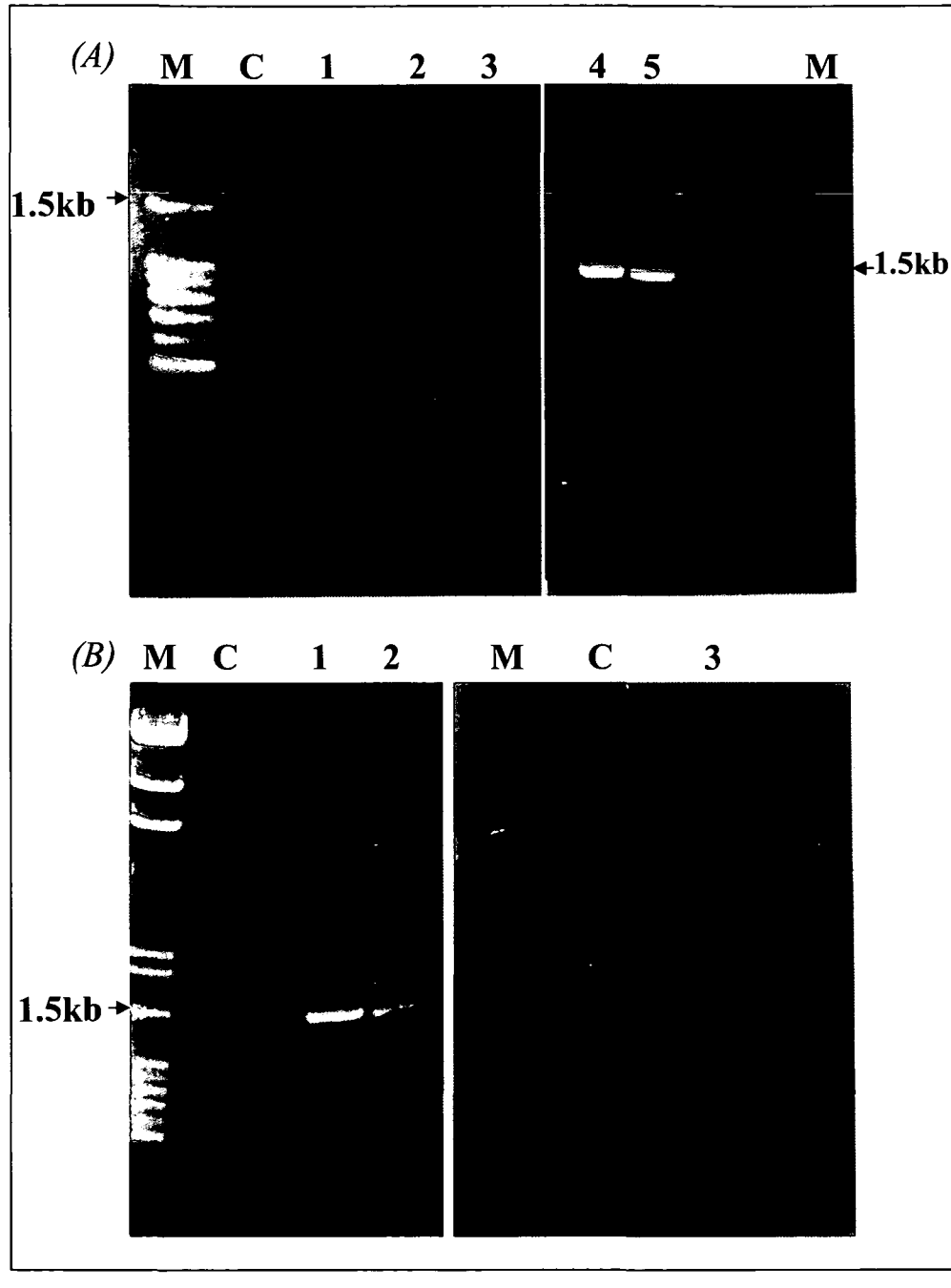

Figure 6.6: Agarose gel analysis of PCR products amplified from koala liver cDNA using kPPfF and kPPfR primers.
Panel A: Lanes 2, 4 and 5 PCR reactions using kPPfF and kPPfR primers with different templates, Lanes 1 and 3: PCR reaction using other primer pairs. Panel B: Lane 3: Large scale amplification of PCR product generated from koala liver cDNA using kPPfF and kPPfR primers. Lanes 1 and 2: PCR product amplified from rat liver cDNA using rPPfF and rPPfR primers. DNA fragments of approximately 1.5-kb were amplified. Lane C: negative control (PCR reaction with no DNA template). Lane M: DNA molecular weight marker.

```
   1GGAGCCGGAG CCCGGGCCGC GAGCAGGCAG CAGTGGCGGC GGCTTCACGA GGGACGCGAC
  61 ACGCGGAGCT TAAAGACCTT TAAGGGGACC GGCTGTGCCT TATCAAGATG GTAGACACCG
   1                                                   M  V  D  T
 121 AGAGCCAGAT CTGCCCCCTT TCTCCCTTCG GTGATGATGA TCTGGAAAGC CCACTCTCAG
   5 E  S  Q  I  C  P  L  S  P  F  G  D  D  D  L  E  S  P  L  S
 181 AAGAGTTTCT CCAAGAGATG GGGAGCATCC AGGAAATCTC TCCATCCATT GGCGATGACA
  25 E  E  F  L  Q  E  M  G  S  I  Q  E  I  S  P  S  I  G  D  D
 241 GCTCGGGCAC CTT TGCTTTT GCAGAGTATC GCTGTTTGGG AAGTGGTCCA GGCTCAGACG
  46 S  S  G  T  F  A  F  A  E  Y  R  C  L  G  S  G  P  G  S  D
 301 GCTCCATCAT T  ACAGACACT CTGTCCCCAG CGTCCAGTCC TTCGTCTGTG AGTTACACCC
  65 G  S  I  I  T  D  T  L  S  P  A  S  S  P  S  S  V  S  Y  T
 361 CAATCGCAGG CAGTGCTGAT GACTCTTCCA GTGCTACCTT AAACATAGAG TGCAGAATTT
  85 P  I  A  G  S  A  D  D  S  S  S  A  T  L  N  I  E  C  R  I
 421 GTGGGGACAA AGCCTCTGGC TACCATTATG GTGTGCATGC CTGTGAAGGT TGCAAGGGCT
 105 C  G  D  K  A  S  G  Y  H  Y  G  V  H  A  C  E  G  C  K  G
 481 TTTTCCGGAG GACTATTCGC CTTAAGCTTG CCTATGACAA GTGTGACCGC AGCTGTAAAA
 125 F  F  R  R  T  I  R  L  K  L  A  Y  D  K  C  D  R  S  C  K
 541 TTCAAAAAAA GAATCGTAAC AAGTGTCAAT ATTGCCGTTT CCAGAAGTGC CTTTCAGATG
 145 I  Q  K  K  N  R  N  K  C  Q  Y  C  R  F  Q  K  C  L  S  D
 601 GAATGTCACA CAATGCCATC CGTTTTGGGA GAATGCCAAG ATCTGAAAAA GCAAAATTAA
 165 G  M  S  H  N  A  I  R  F  G  R  M  P  R  S  E  K  A  K  L
 661 AAGCAGAGAT TCTTACATGT GAACACGATT TAGAAGATTC AGAAGTTGCA GATCTCAAGT
 185 K  A  E  I  L  T  C  E  H  D  L  E  D  S  E  V  A  D  L  K
 721 CTCTTGCCAA ACGCATTTAT GAAGCCTACC TGAAAAACTT TAACATGAAC AAGATCAAGG
 205 S  L  A  K  R  I  Y  E  A  Y  L  K  N  F  N  M  N  K  I  K
 781 CCAGAATCAT CCTGGCAGGG AAGGCCAGCA ACAACCCACC TTTTGTCATC CACGACATGG
 225 A  R  I  I  L  A  G  K  A  S  N  N  P  P  F  V  I  H  D  M
 841 AGACCCTGTG CATGGCAGAG AAGACACTTG TGGCCAAGCT GGTGGCCAAT GGGATCCAGA
 245 E  T  L  C  M  A  E  K  T  L  V  A  K  L  V  A  N  G  I  Q
 901 ACAAGGAGGC TGAGGTGCGG ATATTCCACT GCTGCCAATG TACCTCGGTA GAGACTGTCA
 265 N  K  E  A  E  V  R  I  F  H  C  C  Q  C  T  S  V  E  T  V
 961 CGGAGCTGAC AGAGTTCGCT AAATCGATCC CTGGCTTCTC GAATCTAAAC CTGAATGATC
 285 T  E  L  T  E  F  A  K  S  I  P  G  F  S  N  L  N  L  N  D
1021 AGGTGACTTT GTTAAAGTAT GGGGTCTATG AAGCAATATT TGCAATGTTG TCATCAGTAA
 305 Q  V  T  L  L  K  Y  G  V  Y  E  A  I  F  A  M  L  S  S  V
1081 TGAACAAAGA TGGCATGTTG GTGGCCTACG GAAACGGTTT CATAACCCGC GAGTTTCTGA
 325 M  N  K  D  G  M  L  V  A  Y  G  N  G  F  I  T  R  E  F  L
1141 AAAGTTTAAG AAAACCATTT TGTGACATCA TGGAACCTAA ATTTGATTTT GCAATGAAAT
 345 K  S  L  R  K  P  F  C  D  I  M  E  P  K  F  D  F  A  M  K
1201 TCAATGCCTT GGAACTGGAT GATAGCGACA TTTCCCTTTT TGTGGCTGCT ATAATCTGCT
 365 F  N  A  L  E  L  D  D  S  D  I  S  L  F  V  A  A  I  I  C
1261 GTGGAGATCG GCCCGGCCTC TTGAACGTGG GACACATTGA GAGAATGCAG GAGAGCATCG
 385 C  G  D  R  P  G  L  L  N  V  G  H  I  E  R  M  Q  E  S  I
1321 TGCACGTGCT CCAGCTTCAC CTGCAAAACA ACCACCCTGA TGATGTCTTC CTTTTCCCCA
 405 V  H  V  L  Q  L  H  L  Q  N  N  H  P  D  D  V  F  L  F  P
1381 AGTTGCTCCA GAAGATGGCG GACCTTCGGC AGCTGGTCAC GGAGCACGCT CAGCTGGTGC
 425 K  L  L  Q  K  M  A  D  L  R  Q  L  V  T  E  H  A  Q  L  V
1441 AAGTCATCAA AAAGACTGAA TCTGATGCTG CCCTGCATCC TTTGCTGCAA GAAATCTACA
 445 Q  V  I  K  K  T  E  S  D  A  A  L  H  P  L  L  Q  E  I  Y
1501 GGGACATGTA CTGAG
 465 R  D  M  Y  X
```

Figure 6.7: Nucleotide and deduced amino acid sequences of the full-length koala *PPAR-α* cDNA isolated from liver.

Figure 6.7 (continued): Nucleotide and deduced amino acid sequences of the full-length koala *PPAR*-α cDNA isolated from liver. Nucleotides and the corresponding amino acids, shown by single-letter codes, are numbered as indicated at the left hand side of the figure. The ATG start codon and TGA stop codon are at nucleotide 108 and 1512, respectively. The sequence consists of an open reading frame encoding 468 amino acids. Underlined amino acid sequences correspond to the absolute conserved sequence CEGCKG located in the DNA binding domain (DBD) and the ligand binding domain (LBD). The DBD domain is important for sequence-specific DNA binding in receptors and recognises the TGACCT motif located in the PPRE of target genes [152]. The LBD is highly conserved among all nuclear receptors studied [145]. The koala *PPAR*-α cDNA sequence has been submitted to GenBank and its accession number is AF463455.

6.3.2 Expression of koala and rat PPAR-α in Cos-7 cells and immunoblot analysis of cDNA-expressed PPAR-α

For transfection of Cos-7 cells, the koala *PPAR-α* cDNA was subcloned into the pCMV-Script XR vector. Several clones selected for transfection were sequenced in both directions to confirm their identity. A restriction map of *PPAR-α* was generated to ensure that the restriction sites selected for sub-cloning do not cut within the coding region (Figure A.3, Appendix A). The koala *PPAR-α* cDNA does not contain *Xho* 1 and *EcoR* 1 restriction sites.

Two koala *PPAR-α* cDNA-pCMV-Script XR vector clones were selected for transfection studies. Sequence analysis confirmed that the two clones both contained start and stop codons and had 100% sequence identity. Transfection of the koala *PPAR-α* cDNA into Cos-7 cells resulted in the expression of a protein of mass approximately 52-kD, which was recognised by an anti-human PPAR-α polyclonal antibody. No immunoreactive bands were observed in untransfected Cos-7 cell lysates. Immunoblot analysis of cDNA-expressed koala PPAR-α is shown in Figure 6.8.

6.3.3 Immunoblot analysis of PPAR-α in cytosol and nuclear extracts

Expression of PPAR-α was examined in cytosolic and nuclear extracts from koala, wallaby, possum and rat livers. Figure 6.9 shows that PPAR-α is expressed in both cytosolic and nuclear extracts of these species. PPARα proteins detected in the rat cytosol and nuclear extract were approximately 54-kDa and those in koala and wallaby samples were approximately 52-kDa. Mouse PPARα was previously reported to be approximately 53-kDa [228].

6.3.4 Northern analysis of PPAR-α mRNA

The expression of PPAR-α mRNA was examined in koala, human, rat and possum livers as shown in Figure 6.10. The koala *PPAR-α* cDNA probe recognised a single band corresponding to a mRNA species of approximately 8-kb in koala mRNA sample. While no band at the corresponding size was observed for human, rat and possum mRNA samples, there appears to be some hybridisation of the probe to a lower molecular weight smear in all samples.

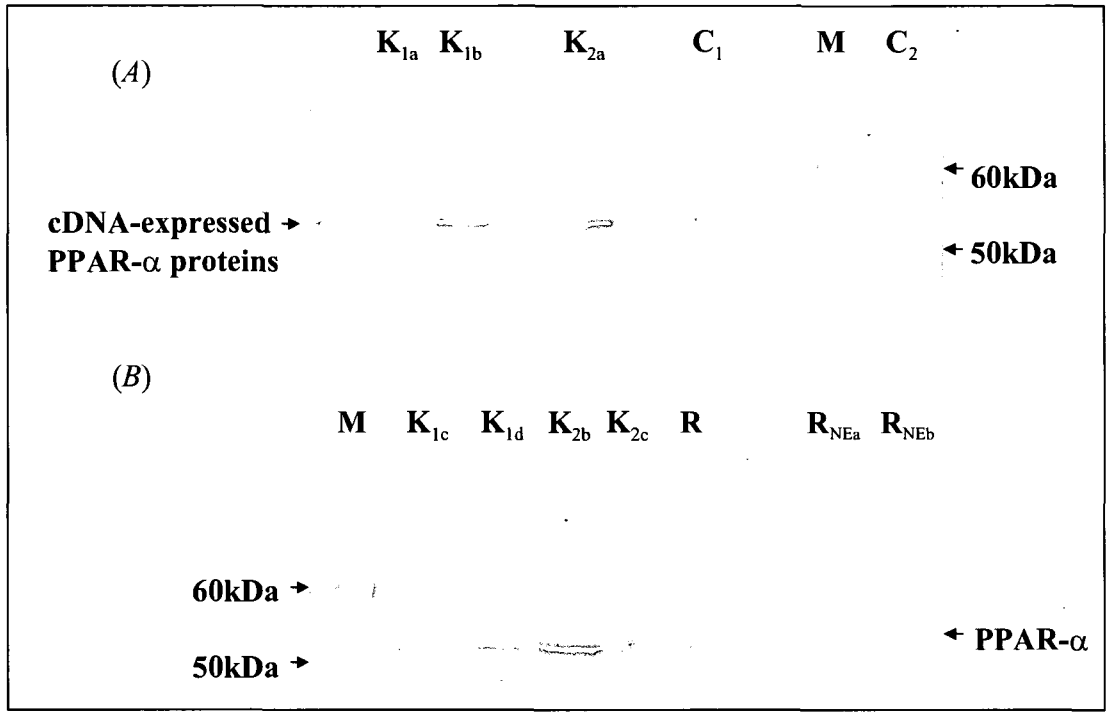

Figure 6.8: Immunoblot analysis of cDNA-expressed koala and rat PPAR-α using sheep anti-human PPAR-α polyclonal antibody.
The blots show that koala and rat PPAR-α cDNAs transfected into Cos-7 cells result in the expression of proteins recognised by this PPAR-α polyclonal antibody, with no immunoreactive bands detected in untransfected Cos-7 cell lysates.
Panels (A) and (B): Lane K_{1a}- K_{1d}: cDNA-expressed koala PPAR-α proteins from 4 different transfection experiments using clone 1. Lane K_{2a}- K_{2c}: cDNA-expressed koala PPAR-α proteins from 3 different transfection experiments using clone 2. Lane C_1-C_2: negative controls, untransfected Cos-7 cell lysates. Lane R: positive control, cDNA-expressed rat PPAR-α proteins. Lane R_{NEa}-R_{NEb}: positive controls, rat nuclear extracts. Lanes M: pre-stained protein ladder.

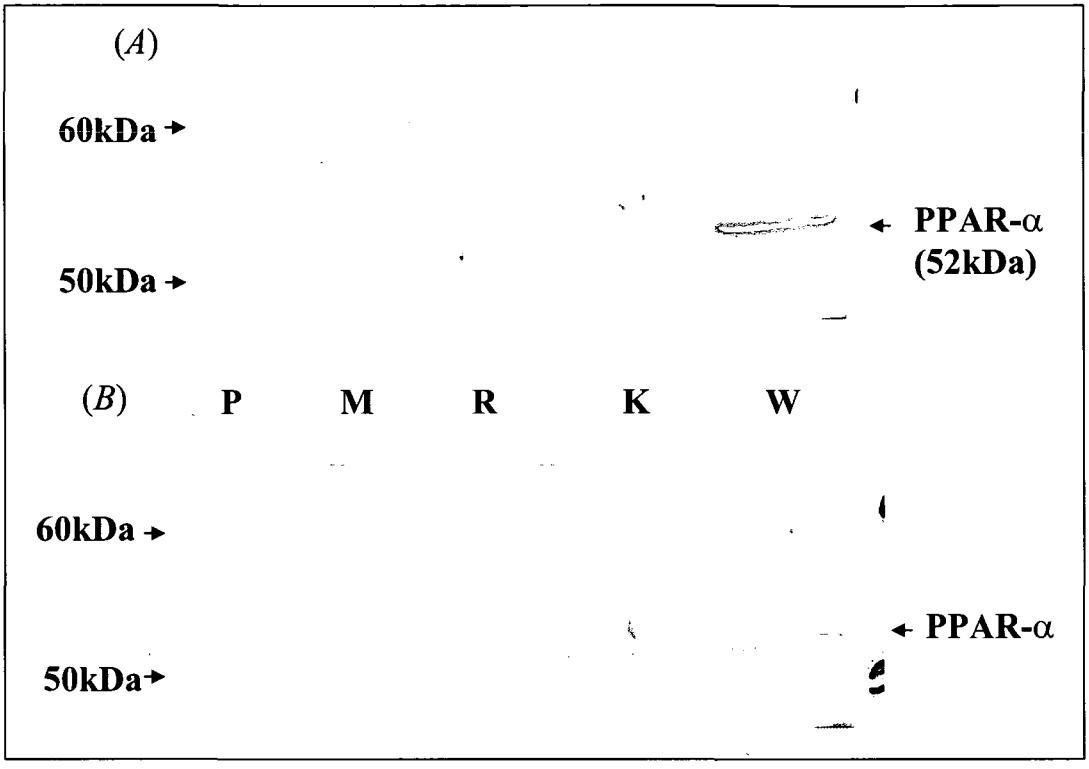

Figure 6.9: Immunoblot analysis of PPAR-α proteins in nuclear and cytosolic extracts utilising sheep anti-human PPAR-α polyclonal antibody. Protein (50 μg/lane) from koala (K), wallaby(W), possum (P) and rat (R), Lane M: pre-stained protein ladder. Panel A: nuclear extracts. Panel B: cytosol.

6.3.5 Southern analysis of the *PPAR-α* gene

Southern blot analysis of *EcoR* 1-digested genomic DNA from male koala, rat, wallaby, possum, and bandicoot livers is shown in Figure 6.11. From this blot, it was apparent that *EcoR* 1-digestion of genomic DNA produced only one *PPAR-α* gene fragment of size less than 4.4-kb for koala and rat samples, and two *PPAR-α* gene fragments of sizes from 4.5- to 10-kb for wallaby, possum and bandicoot samples.

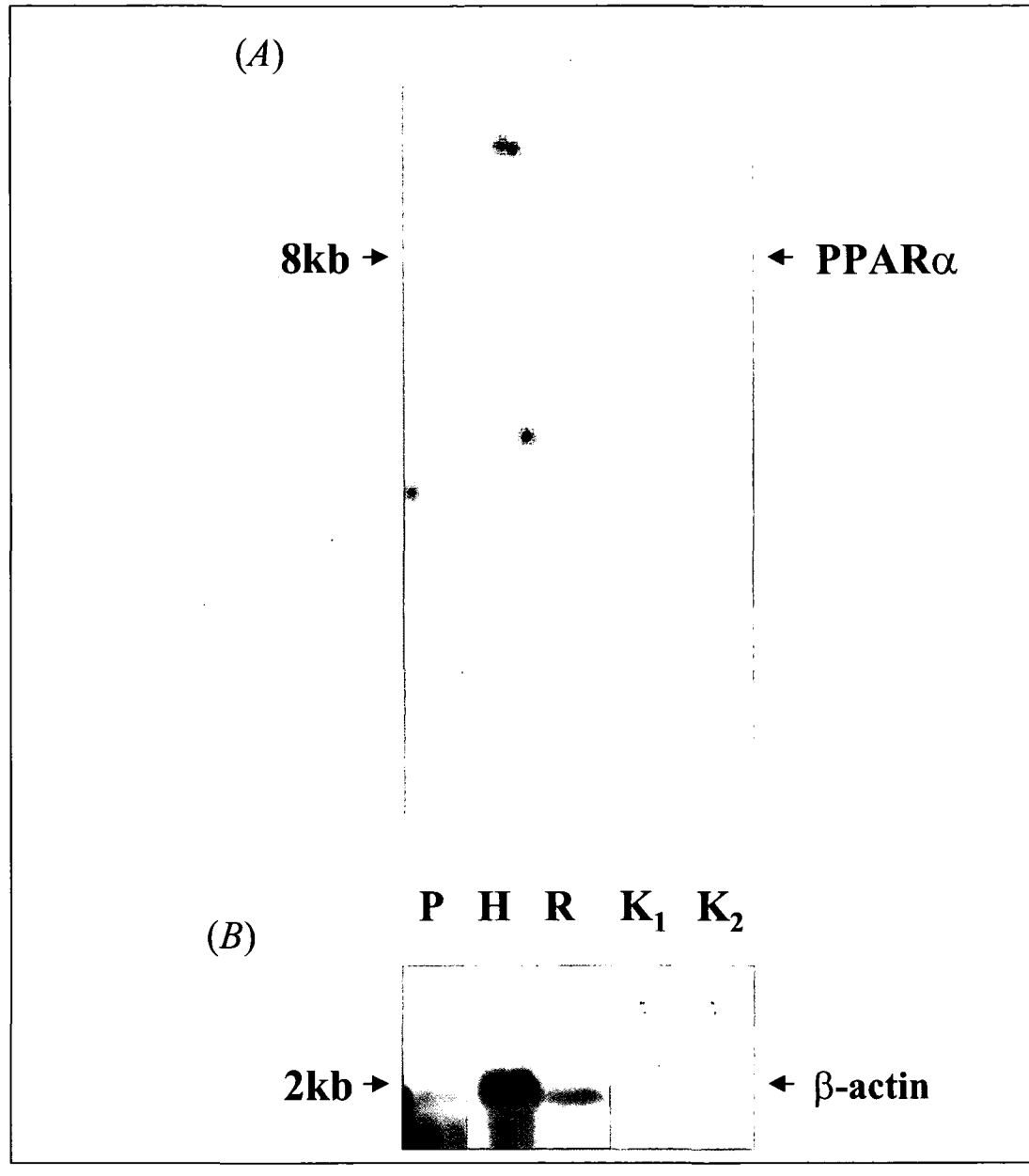

Figure 6.10: Northern blot analysis of hepatic PPAR-α mRNAs. Messenger RNAs (10 μg, except koala K_1, 4 μg) were purified from two koala (Lanes K_1-K_2), human (Lane H) and rat (Lane R) liver samples and hybridised with a koala *PPAR-α* 1051-bp cDNA probe (^{32}P-labelled). Panel (A): Hybridisation with koala *PPAR-α* 1051-bp cDNA probe. Panel (B): Hybridisation with mouse β-actin.

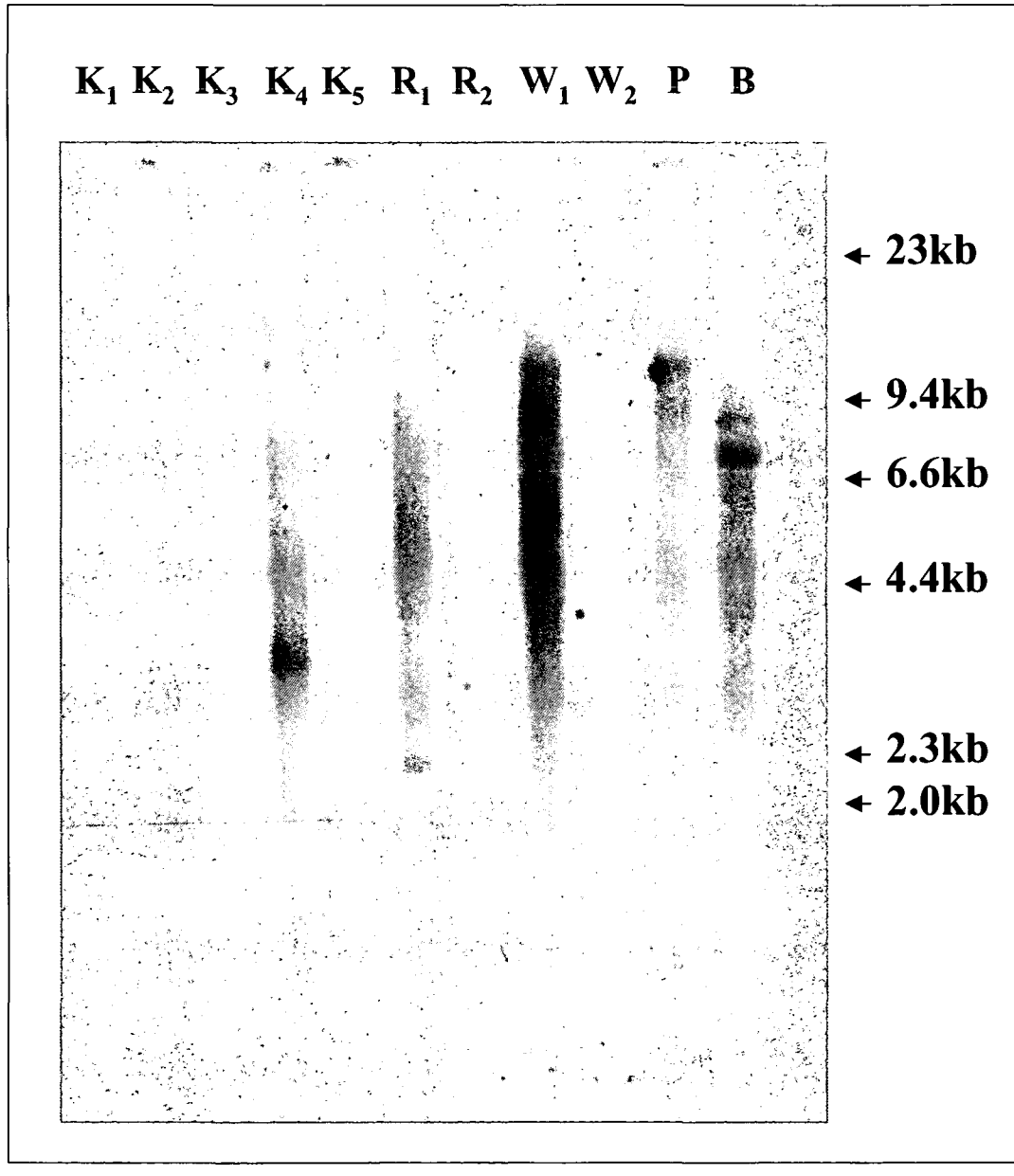

Figure 6.11: Southern blot analysis of the PPAR-α gene.
Genomic DNAs were extracted from five koala (Lane K−1-K_5), two rat (Lane R_1-R_2), two wallaby (Lane W_1-$W2$), one possum (Lane P), and one bandicoot (Lane B) liver samples and hybridised with a koala *PPAR-α* 1051-bp cDNA probe (^{32}P-labelled).

6.4 DISCUSSION

In the present study, the molecular characterisation and cloning of PPAR-α was accomplished using RT-PCR cloning approaches, an expression study and Northern and Southern blot analyses. In humans, rat and other species studied, the receptor has been reported to mediate expression of genes encoding microsomal CYP4A and peroxisomal AOX enzymes. This study confirmed the presence of a *PPAR-α* gene which encodes the entire coding region of the receptor in the koala liver.

A 1515-bp full-length *PPAR-α* cDNA was isolated from koala liver and designated *kPPAR-α*. The *kPPAR-α* cDNA exhibits high nucleotide sequence identity to the reported human, rat and mouse *PPAR-α* cDNA sequences (Table 6.2). Figure 6.12 shows the deduced amino acid sequences of kPPAR-α aligned with the published human, rat and mouse receptors .

As shown in Figure 6.7, the *kPPAR-α* cDNA shares the following common features with *PPAR-α* cDNAs from other species. The N terminal domain encodes the first 69 aa, corresponding to exon 3. The DNA binding domain (DBD) contains the absolutly conserved sequence CEGCKG (underlined). This domain encodes the 2 Zinc fingers, aa 70-123 and aa 124-169, corresponding to exon 4 and 5. The putative ligand binding domain (LBD) encodes aa 170-237, which is highly conserved among all nuclear receptors studied, corresponding to exon 6. The C terminal domain encodes aa 238-468, corresponding to exon 7 and 8.

When the kPPAR-α deduced amino acid sequence was aligned with the published human, rat and mouse receptors, it was apparent that the putative DBD contains highly conserved sequence across species and the putative LBD was very highly conserved between these four receptors studied (Figure 6.12). In addition, there was a higher degree of consensus toward the C terminal domain between these four PPAR-α proteins. This highlights the putative functional significance of this region in transcriptional activation, protein-protein interactions and ligand binding [149]. While the N terminal sequence is highly conserved between human, rat and mouse, the deduced amino acid sequence of kPPAR-α exhibits a number of significant differences with amino acid substitutions in this region. In human, rat and mouse PPAR-α, leucine-glutamate-alanine were found at position 14-17 whereas in the kPPAR-α, these were substituted by phenylalanine-glycine-aspartic acids.

	kPPAR-α	hPPAR-α	rPPAR-α	mPPAR-α
kPPAR-α[a]	100 100	79 90	77 88	78 87
hPPAR-α[b]		100 100	85 92	85 92
rPPAR-α[c]			100 100	94 98
mPPAR-α[d]				100 100

Table 6.2: Nucleotide and amino acid sequence identities between the koala liver kPPAR-α and PPAR-α from other species.
Percentage nucleotide identities were calculated from the koala *PPAR-α* cDNA and *PPAR-α* cDNAs from other species. Percentage amino acid identities (second row value) were calculated from the deduced amino acid sequence of the koala *PPAR-α* cDNA clone and deduced amino acid sequences from other species. The ClustalW alignment function in MacVector (Version 6.0) computer programme (Oxford Molecular, 1997) was used for alignment. [a] Koala liver PPAR-α, GenBank accession number AF463455 (Ngo *et al.*, direct submission). [b] Human liver PPAR-α, accession number NM 005036 [155]. [c] Rat liver PPAR-α, accession number NM 013196 [163]. [d] Mouse liver PPAR-α, accession number NM 011144 [152].

At positions 7, 33, 39, 56 of human, rat and mouse receptors, there are proline, asparagine, glutamine and tyrosine, respectively. In kPPAR-α, these were replaced by glutamine, serine, proline and cysteine, respectively (Figure 6.12). While in the DBD, human, rat and mouse PPAR-α cDNAs all encode proline at positions 84, 87, 94, and alanine at position 97, in the kPPAR-α cDNA, threonine, alanine, serine and threonine were found at these positions, respectively (Figure 6.12, underlined aa). Glycine at position 60 was also a non-conservative substitution found in the kPPAR-α. Other positions in which amino acid substitutions occur include position 200 in the LBD and positions 301 and 403 in the C-terminal domain, where threonine, aspartic acid and glycine in human, rat and mouse were replaced by valine, asparagine and serine, respectively in kPPAR-α (Figure 6.12).

Transfection of the koala *PPAR-α* cDNA into Cos-7 cells resulted in the expression of a protein of mass approximately 52-kD recognised by an anti-human PPAR-α polyclonal antibody. PPAR-α proteins detected in the rat cytosol and nuclear extract were approximately 54-kDa and those in koala, possum and wallaby samples were approximately 52-kDa. Mouse PPAR-α was reported to be approximately 53-kDa [228]. Other extra immunoreactive bands were also visible in both cytosol and nuclear extract from each of the species, representing either related PPAR isotypes, PPAR-β and PPAR-γ, which share significant sequence identity with PPAR-α or other related proteins. The results from the blot also suggested the non-specificity of the anti-human PPAR-α polyclonal antibody.

The absence of PPAR-α mRNA species in rat tissue was consistent with that reported by Sterchele and colleagues, who found that the level of PPAR-α mRNA in rat liver was quite low for detection by Northern blot analysis [252]. The level of hepatic human PPAR-α mRNA was reported to be even lower than that in rat [149]. While only two animals were assessed for the koala and the band detected in the koala sample was hardly visible, the results in this chapter may suggest a higher level of koala PPAR-α mRNA as compared to humans, rat, and possums. Southern blot analysis of *EcoR* 1-digested genomic DNA suggests the existence of a single *PPAR-α* gene in all species studied.

In summary, a full-length *PPAR-α* cDNA was isolated from the koala liver which shares several common features with human, rat and mouse receptors. Expression of koala *PPAR-α* cDNAs in Cos-7 cells and subsequent immunoblot analysis confirmed the presence of a functional koala *PPAR-α* gene that was able to express a protein recognised by anti-human PPAR-α antibody. The results of this chapter also suggested higher expression of hepatic PPAR-α mRNA in the koala, whose diet is restricted to *Eucalyptus* leaves, than is seen in humans, rat, and possums, species which do not ingest Eucalyptus leaves as food. The study provided the first primary molecular data for further study into the regulatory role of PPAR-α in the expression of microsomal CYP4A and fatty acid β-oxidation enzymes in the koala liver.



Figure 6.12: Multiple sequence alignment of PPAR-α proteins from koala, human, rat and mouse.

Underlined are the N-terminal sequence, the ligand binding domain (LBD) which is highly conserved between these four receptors studied and the conserved C terminus.

Chapter 7

VISUALISATION OF PEROXISOMES IN KOALA LIVER

7.1 INTRODUCTION

Peroxisomes are membrane bound cytoplasmic organelles which are present in nearly all eukaryotic cells. In most animal cells, peroxisomes are widely distributed and their number as well as volume and density remain relatively constant under various physiological conditions [126, 288]. In rats, mice and most other mammals, peroxisomes in the liver parenchymal cells occupy less than two percent of the cytoplasmic volume [289]. Liver peroxisomes in most species can be identified due to the presence of a crystalloid core containing urate oxidase. While urate oxidase is specific for the liver in most mammals, human liver peroxisomes lack this distinct core structure as a result of their silenced urate oxidase gene (reviewed in [142]). A brief historical background of peroxisomes and a current understanding of morphological and biochemical characteristics of peroxisomes follows.

7.1.1 Historical background

In 1954, a single-membrane limited cytoplasmic organelle containing a finely granular matrix was identified in the proximal tubular epithelium of the mouse kidney and was termed "microbody" [290]. In 1956, microbodies were found in the parenchymal cells of rat liver [291]. Subsequently, several studies in the 1960s revealed the presence of microbodies with some variation in size and shape in various vertebrate liver and kidney cells [292, 293, 294]. These microbodies were also found to have different kinds of nucleoid or crystalline core. Subsequent biochemical studies led to

the characterisation of urate oxidase, D-amino acid oxidase, and catalase in rat liver microbodies [288, 295, 296, 297]. The term "peroxisome" was introduced in 1965 to emphasise the biochemical property of the microbody enzymes to generate hydrogen peroxide. In 1968, the development of a histochemical assay to identify the enzyme catalase initiated the identification of certain peroxisomes in various cell types [298]. It was subsequently established that peroxisomes are present in all eukaryotic cells as well as plant cells [298, 299, 300].

7.1.2 Morphological characteristics

Peroxisomes are morphologically characterised by a single membrane, a finely granular electron-dense matrix and a crystal core that signifies the presence of urate oxidase. The presence of crystalloid core structures in peroxisomes and their single membrane bound appearance distinguish them from mitochondria. Peroxisomes can be distinguished from lysosomes by a smaller size, uniformity of their appearance and the matrix containing crystalloid core structure. Peroxisomes are also distinguished from lysosomes by a close arrangement with the smooth endoplasmic reticulum and the absence of other structures normally found in lysosomes such as vacuoles, lipid droplets, myelin features and ferritin [294]. In liver parenchymal cells, peroxisomes are approximately 0.3 to 1.0 μm in diameter [158].

7.1.3 Biochemical characteristics

In rat liver, important enzymes found in peroxisomes include enzymes of the fatty acid β-oxidation system, five different oxidases, acyl transferase and catalase. While the marker enzyme of peroxisomes, catalase, is a constant component of peroxisomes derived from various tissues, the hydrogen peroxide-generating flavin oxidases present in peroxisomes are likely to vary in number and specificity depending on the tissue. Peroxisomal fatty acid β-oxidation enzymes are significantly different from the mitochondrial enzymes in terms of molecular aspects and catalytic properties [126, 301, 302]. For example, the peroxisomal β-oxidation does not require carnitine and is insensitive to potassium cyanide (KCN) whereas mitochondrial β-oxidation requires carnitine and is inhibited by KCN. The enzymes of the β-oxidation pathway are discussed in Section 1.3.4.

7.1.4 Function of peroxisomes

At present, more than fifty proteins have been identified in peroxisomes and more than half of these are involved in lipid metabolism. Peroxisomes are also involved in several other functions including respiration, gluconeogenesis, thermogenesis and purine catabolism [234]. The presence of fatty acid β-oxidation enzymes in peroxisomes validates the observation that xenobiotic-induced peroxisome proliferation is related to fatty acid metabolism [115, 300, 301]. In susceptible rodents such as rats and mice, several structurally diverse compounds with hypolipidemic properties have been found to cause a marked increase in number and size of peroxisomes in liver parenchymal cells and an increase in liver weight. This profound peroxisome proliferation often occurs in conjunction with induction of lipid metabolising enzymes, in particular microsomal CYP4A and peroxisomal β-oxidation fatty acyl CoA oxidase.

In rat livers, *Eucalyptus* terpenes such as citral have been shown to induce CYP4A and peroxisomal β-oxidation enzymes and to increase liver weight. No morphological studies of hepatic tissues examining peroxisome proliferation have been reported in koala or any other eucalypt feeders. This study aimed to examine the association between higher lipid metabolising enzyme expression and peroxisome proliferation in the koala liver.

7.2 METHODOLOGY OUTLINE

7.2.1 Visualisation of peroxisomes by cytochemical localisation of catalase

Peroxisomes are visualised by transmission electron microscopy (TEM) with a reaction for catalase activity, the marker enzyme present in peroxisomes [303, 304]. The reagent used is 3',3'-diaminobenzidine (DAB). DAB has four reactive amino groups and acts as a hydrogen donor for the oxidative reaction catalysed by catalase. When oxidised, these amino groups link DAB molecules and form an insoluble polymer that is precipitated and is brown in colour [305]. The chemical reaction involved in the oxidative polymerisation of DAB is shown in Figure 7.1. The catalytic activity of catalase in the oxidative polymerisation of DAB is enhanced by prior fixation in aldehydes. In addition, the stability of DAB in aqueous solution is sufficient for most times of incubation. Since the DAB polymer is strongly osmiophilic, when treated with osmium tetroxide it takes up approximately 0.8 atoms of osmium for each molecule of DAB polymerised, leading to increased electron density and improved visibility of peroxisomes in electron microscopy [305]. A general overview of the procedure of electron microscopy and its utilisation is found in Appendix C.

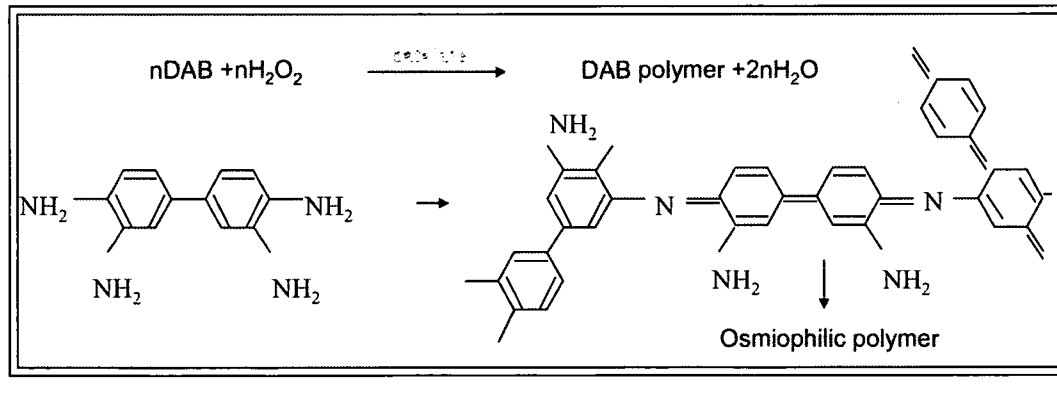

Figure 7.1: The catalase reaction for visualisation of peroxisomes using DAB reagent.

7.2.2 Specimen preparation

Marsupial liver sections were obtained from three mature male koalas and a bandicoot and details of these tissues are shown in Section 2.3. Male Hooded Wistar rats

were used as a source of rat livers. Morphological examination of liver peroxisomes in the koala, an eucalypt feeder, was accomplished using livers of rat and bandicoot, non eucalypt feeders, as control samples. All liver sections for light and electron microscopy were dissected within a few minutes after sacrifice of the animals and immersed immediately in glutaraldehyde solution.

7.2.3 Fixation and DAB staining

Pre-fixation in glutaraldehyde: Fresh tissues were cut into small blocks with a razor blade and fixed by immersion in at least 10 x volumes of cold 2.5% (v/v) glutaraldehyde in 0.1 M sodium cacodylate buffer (pH 7.4) for 18 to 24 hours at 4^0C. The fixed tissues were rinsed twice in cacodylate buffer (each 10 minutes) with constant rotation and then stored in the same buffer overnight or for several days until required at 4^0C.

DAB staining: The glutaraldehyde pre-fixed blocks were stained for catalase by incubating in at least 10x volumes of a freshly prepared solution, containing 0.05% (w/v) DAB in 0.1M Tris-HCl buffer (pH 8.5) and 0.02% (v/v) hydrogen peroxide, for 30 to 60 minutes at 37^0C with gentle agitation. Blocks were then rinsed in cacodylate buffer several times each of 10 minutes with constant rotation.

Post-fixation in osmium tetroxide: DAB stained blocks were post-fixed for 1 to 1 and a half hours at room temperature in 1% solution of osmium tetroxide in 0.05 M sodium cacodylate buffer (pH 7.4).

7.2.4 Dehydration

Prior to dehydration, osmium fixed blocks were rinsed twice in cacodylate buffer (each 10 minutes) and then washed with distilled water several times (each 10 minutes). Dehydration of the sections was accomplished in a graded series of ethanol in distilled water on a rotor as follows:

(i) 50% ethanol in water for 10 minutes
(ii) 70% ethanol in water for 10 minutes, then stored overnight
(iii) Two changes of 70% ethanol in water each of 10 minutes

(iv) Two changes of 90% ethanol in water each of 10 minutes
(v) Absolute ethanol for 10 minutes
(vi) Absolute ethanol for 1 hour

7.2.5 Infiltration and embedding

The epoxy resin Durcupan ACM mixtures number 1 and 2 were used throughout the procedure of infiltration and embedding. The Durcupan mixtures were prepared as described by the manufacturer (Section 2.1, Table 2.1).

Infiltration was performed on a rotor by gradual and continuous replacement of the dehydrating agent with an embedding medium as follows:
(i) 50% Durcupan mixture 1 in absolute ethanol for 1 hour at room temperature
(ii) 75% Durcupan mixture 1 in absolute ethanol for 1 hour at room temperature
(iii) 100% Durcupan mixture 1 at 50^0C for 1 hour or overnight
(iv) 50% Durcupan mixture 2 in Durcupan mixture 1 at 50^0C for 1 hour
Tissue blocks were then placed in small embedding capsules in Durcupan mixture 2 and polymerised at 60^0C for 18 to 48 hours. After polymerisation, the blocks were allowed to cool for 2 to 4 hours and the plastic capsule was removed.

7.2.6 Sectioning

Prior to sectioning, blocks were trimmed and sections were cut using a glass knife. Semi-thin sections of 0.5 to 1 μm were stained with a solution of 10% toluidine blue in 5% aqueous borax and examined by light microscopy. Morphology studies were performed using a transmission electron microscope. Ultra thin sections of approximately 70 to 100nm (pale gold interference colour) were obtained. This enables adequate penetration of the electron beam for reasonable resolution and contrast.

7.3 RESULTS

7.3.1 Visualisation of peroxisomes in the koala livers

Visualisation of peroxisomes was accomplished on liver specimens from three koalas, two rats and a single bandicoot. Rat and bandicoot livers were used for comparative purposes. For each animal tissue, several tissue blocks were dissected and subjected to the procedure of EM. Blocks without staining with DAB from each animal were used as negative controls. Typical electron micrographs of hepatocytes from both negative and DAB stained sections for koala, rat and bandicoot livers are shown in Figures 7.2, 7.3, 7.4 and 7.5. Numerous catalase positive peroxisomes, dark globular structures surrounded by a single membrane, were observed in hepatocytes from all koala tissue specimens. For rat and bandicoot liver samples, these dark globular structures were less abundant.

Figure 7.2: DAB cytochemical visualisation of peroxisomes in koala liver by transmission electron microscopy. Upper panel: Test ultra-thin section of koala liver stained with diaminobenzidine (DAB). Section features numerous peroxisomes which clearly stand out by their black single-membrane globular structures (original magnification x 10500).

Lower panel: Test ultra-thin section of koala liver stained with diaminobenzidine (DAB). Four peroxisomes are enlarged photographically, featuring striation within peroxisomes. The striation is clearly visible in the peroxisome located in the lower centre (the middle one in the group of three peroxisomes below the mitochondrion) (original magnification x 4 x 10500).

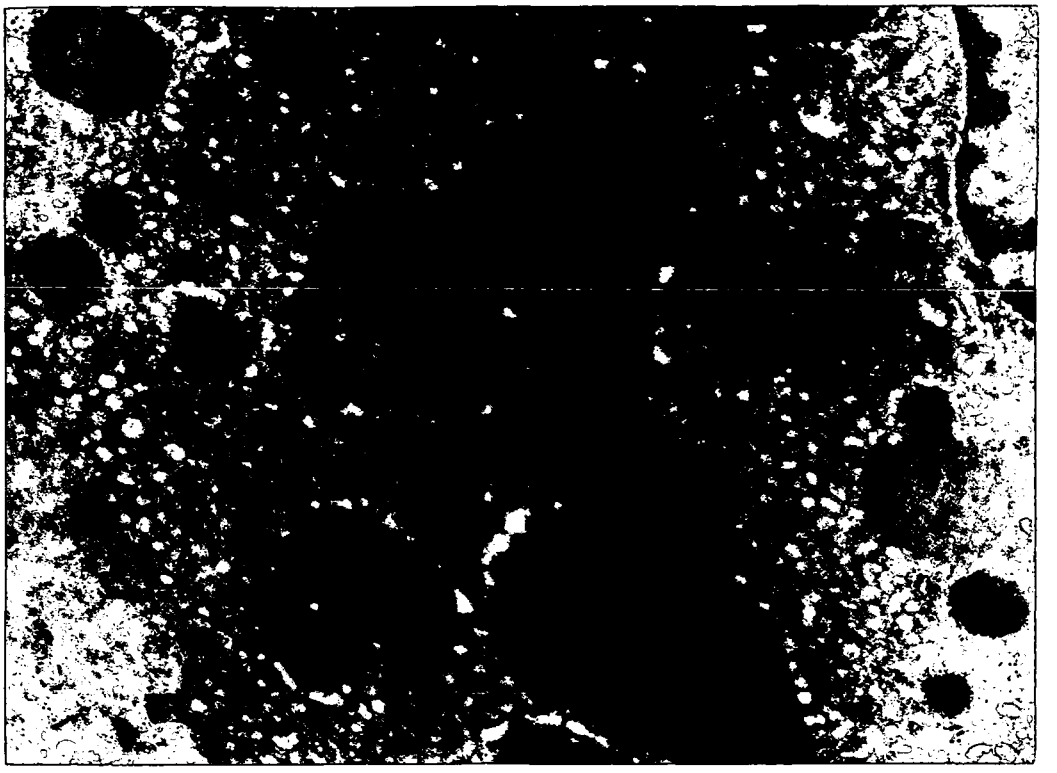

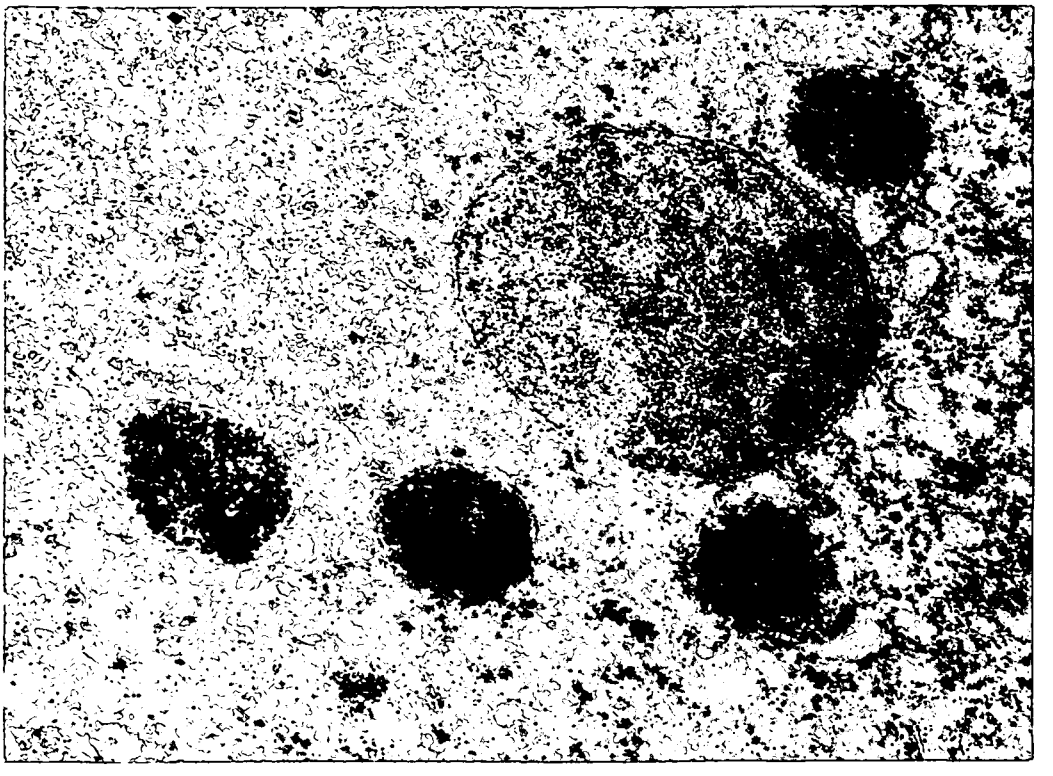

Figure 7.3: DAB cytochemical visualisation of peroxisomes in koala liver by transmission electron microscopy showing the presence of dark bodies within the hepatocyte. Upper panel: Test ultra-thin section of koala liver stained with diaminobenzidine (DAB). Section features a dark particle (very dark structure, located in the centre of the lower area) and numerous peroxisomes standing out clearly as dark single-membrane bound globular structures (original magnification x 10500)

Lower panel: Control ultra-thin section of koala liver. (Section was not stained with diaminobenzidine (DAB), original magnification x 10500).

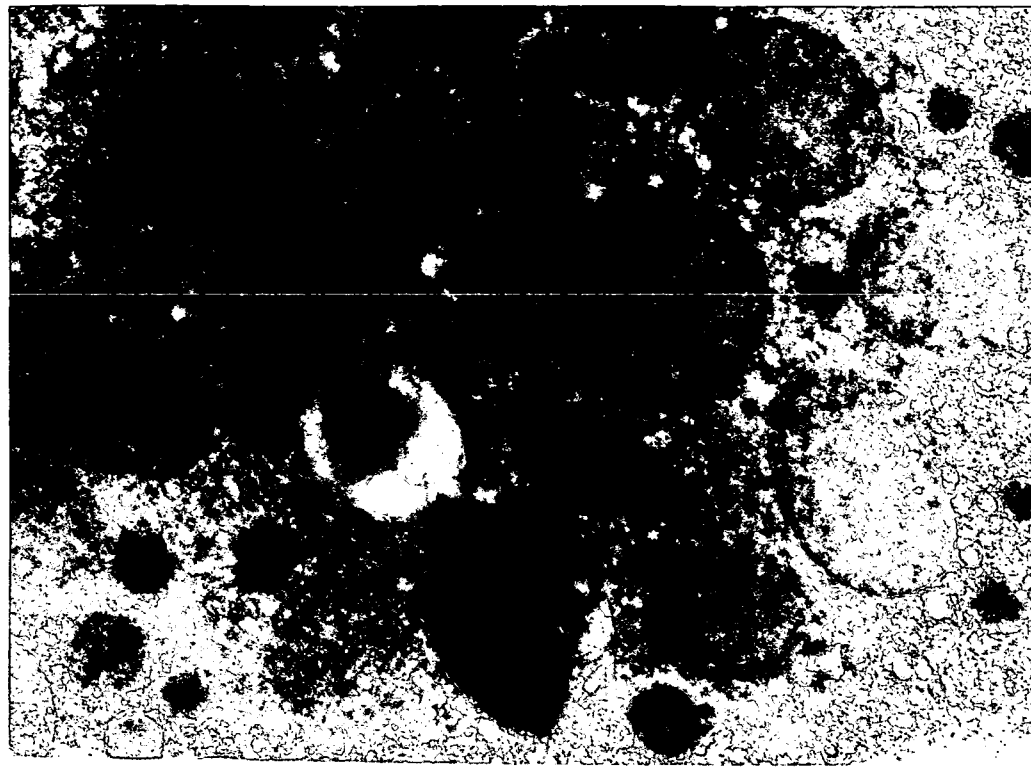

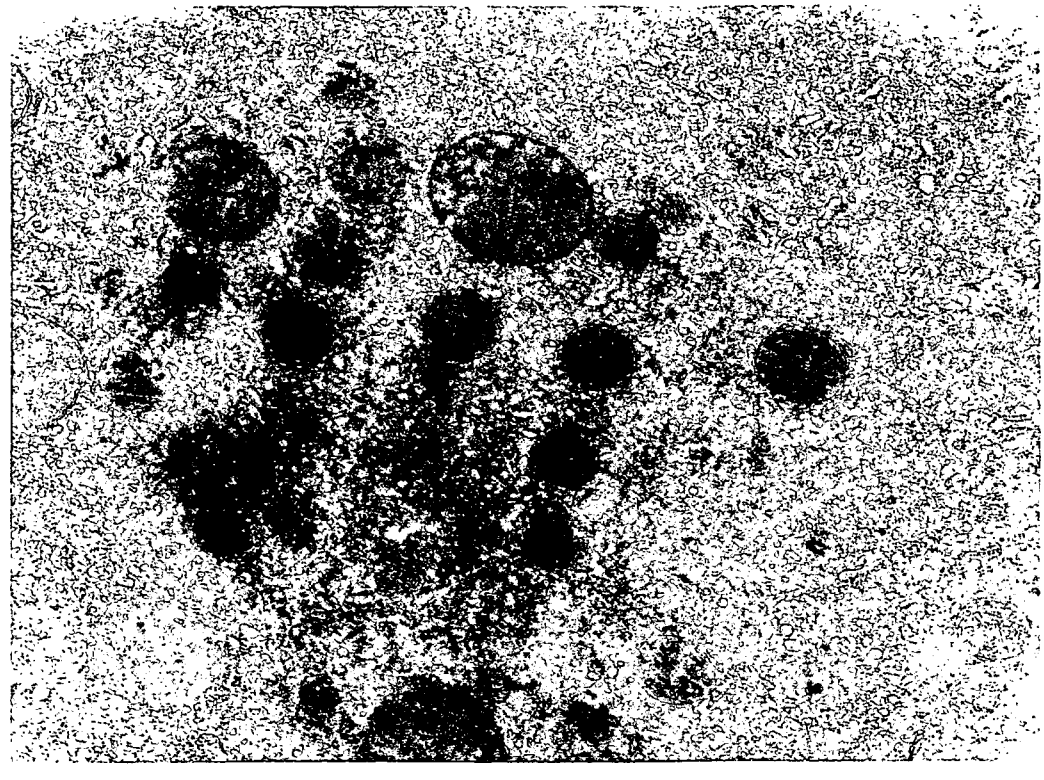

Figure 7.4: DAB cytochemical visualisation of peroxisomes in rat liver by transmission electron microscopy. Upper panel: Test ultra-thin section of rat liver stained with diaminobenzidine (DAB). Section features peroxisomes which clearly stand out as dark single-membrane bound globular structures (original magnification x 10500).

Lower panel: Control ultra-thin section of rat liver. (Section was not stained with diaminobenzidine (DAB), original magnification x 10500).

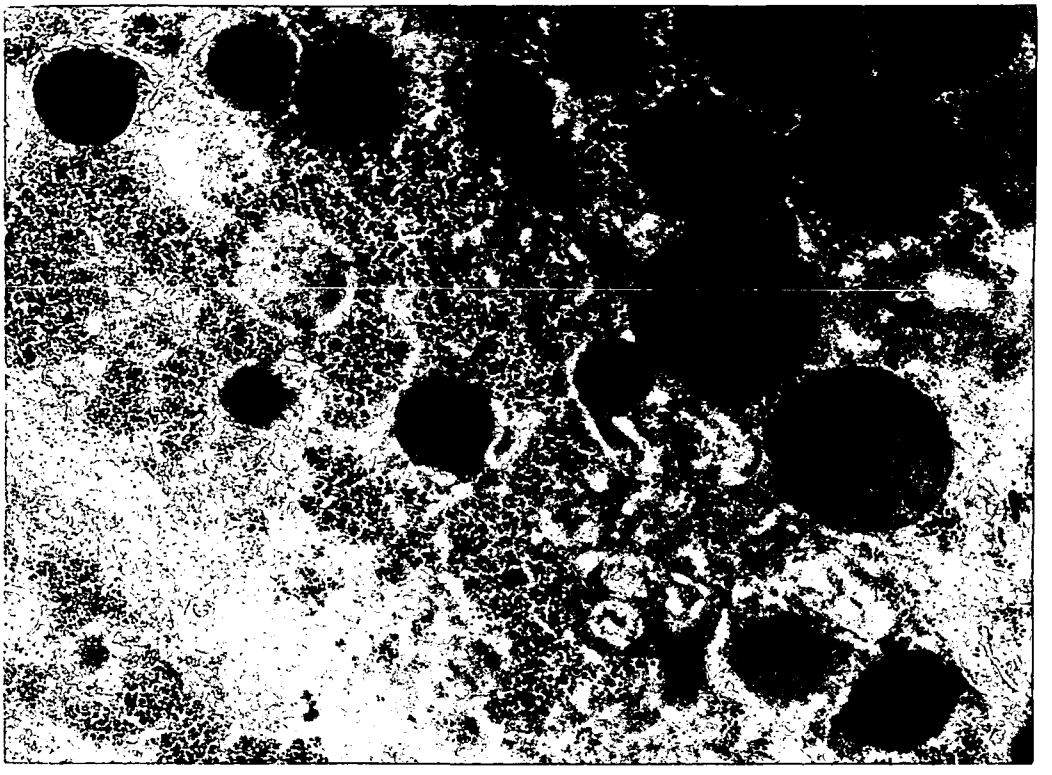

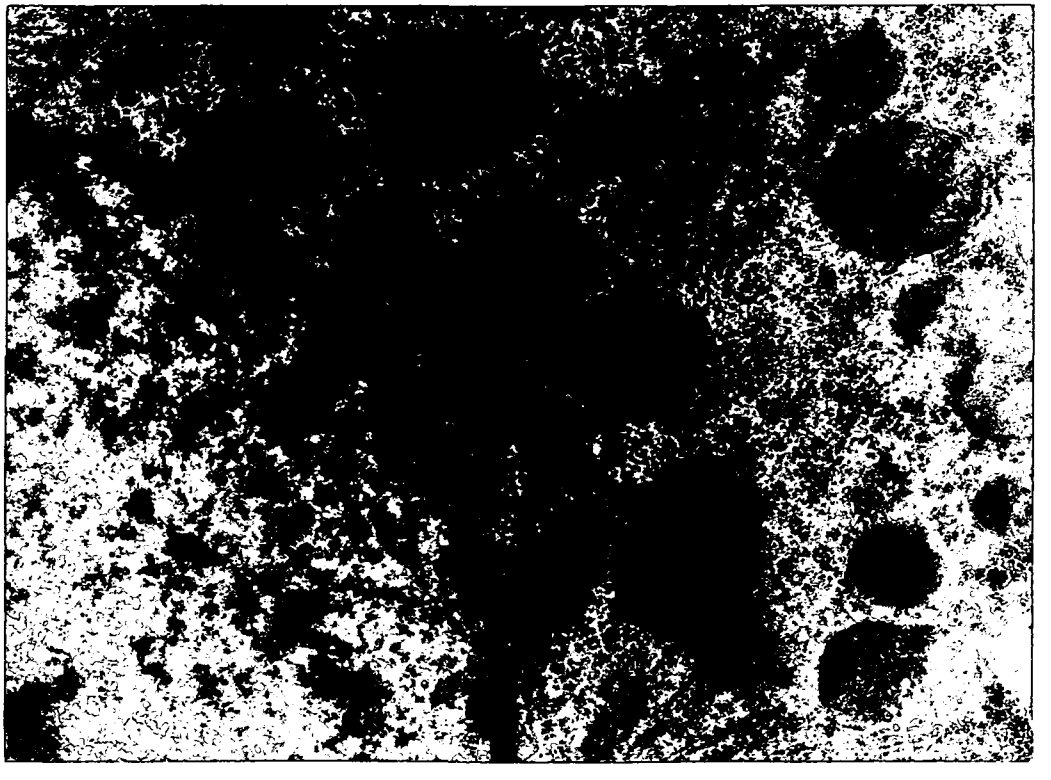

Figure 7.5: DAB cytochemical visualisation of peroxisomes in bandicoot liver by transmission electron microscopy. Upper panel: Test ultra-thin section of bandicoot liver stained with diaminobenzidine (DAB). Peroxisomes do not clearly stand out in the ultra-thin section, however are still visible by their single membrane structures. It appeared that catalase activity was lost due to prolonged storage of the tissue in cacodylate buffer prior to DAB staining (original magnification x 10500).

Lower panel: Control ultra-thin section of bandicoot liver. (Section was not stained with diaminobenzidine (DAB), original magnification x 10500).

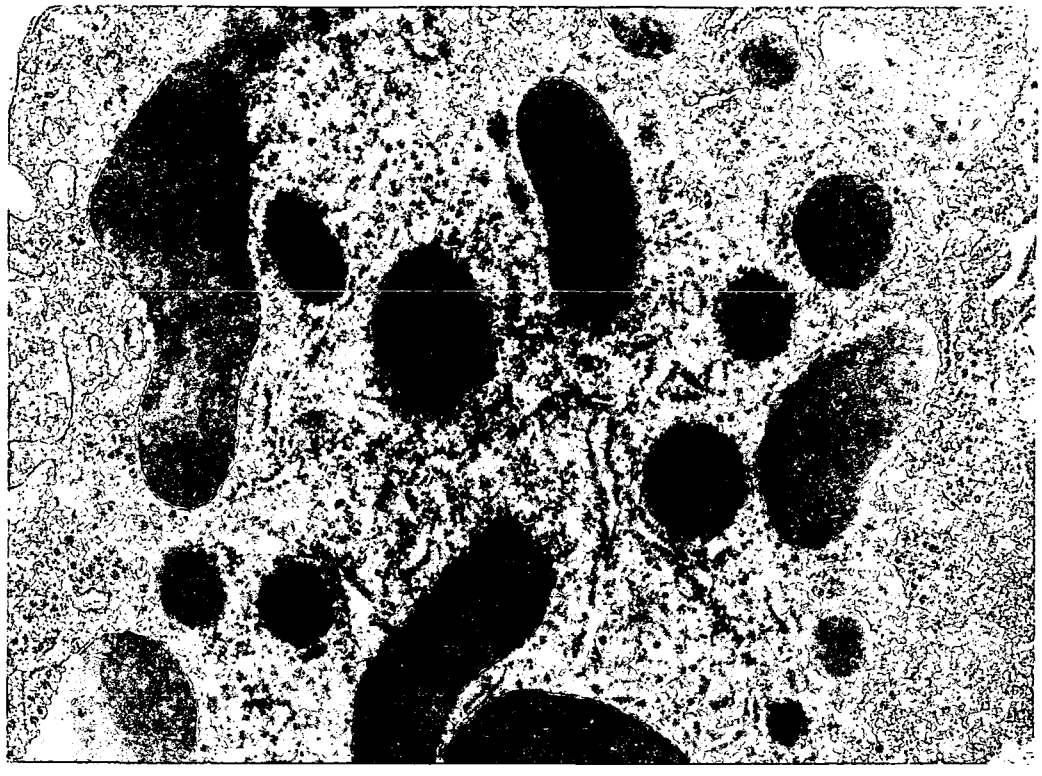

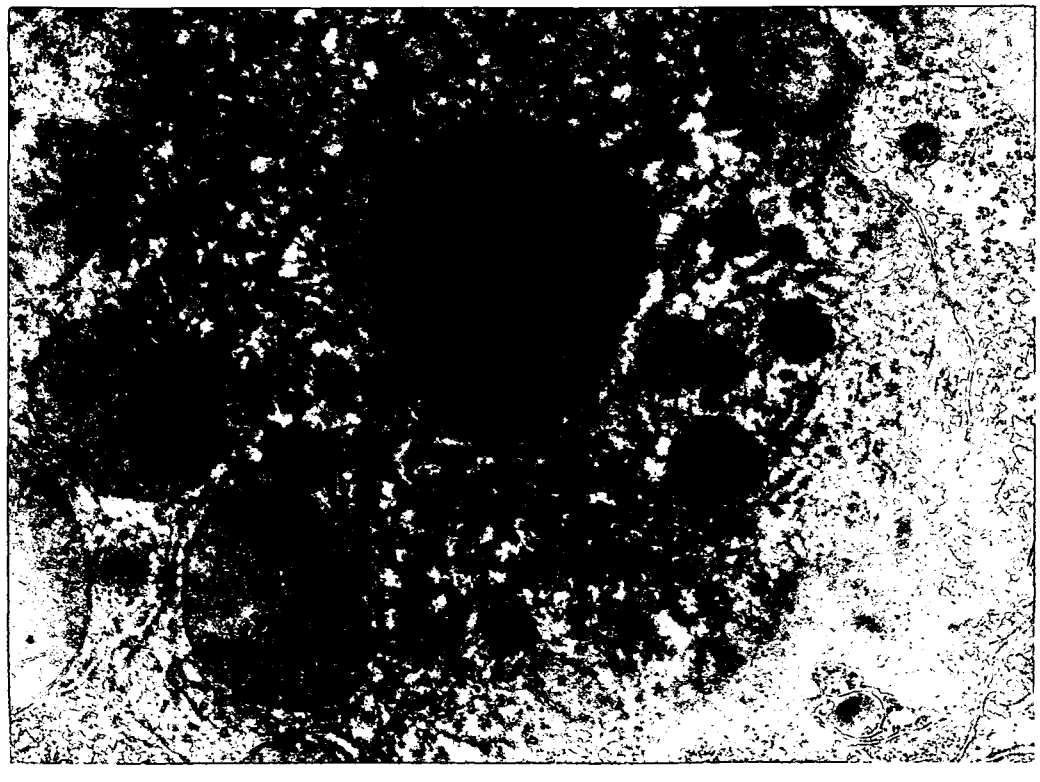

7.3.2 Quantification of peroxisomes

Many ultra-thin sections were cut from several tissue blocks for quantification and measurement of peroxisomes. For each individual animal, counting of peroxisomes was performed on at least 50 hepatocytes. The measurement of the size of peroxisomes was performed on approximately 40 peroxisomes from many different hepatocytes. The average number of peroxisomes per hepatocyte and the average size of peroxisomes for each species are shown in Table 7.1.

Sample	Number of peroxisomes per hepatocyte	Size (μm)
Koala (n=3)	20± 2	0.403±0.032
Rat (n=2)	11	0.504
Bandicoot (n=1)	9	0.375

Table 7.1: Quantification and measurement of peroxisomes in koala, rat and bandicoot livers.
For koala, values were expressed as mean ± SD. Results for rat were expressed as a mean for two animals, and those for bandicoot were from a single animal.

7.4 DISCUSSION

The present work presents the first morphological study examining peroxisomes in koala liver. In the electron micrographs of the koala and rat liver ultra-thin sections stained with DAB, peroxisomes clearly stand out as black globular structures throughout the hepatocytes. This is due to the formation of precipitated DAB polymer, catalysed by peroxisomal marker enzyme catalase, leading to increased electron density and improved visibility of peroxisomes in ultra-thin sections stained with DAB [305]. It is obvious that peroxisomes do not stand out in the electron micrographs of the negative ultra-thin sections, which were not incubated with DAB (Figure 7.2, 7.3 and 7.5). For the bandicoot liver DAB stained sections, the reaction for catalase was not clearly evident (Figure 7.5, Panel A). It appeared that catalase activity was lost during prolonged storage of the tissue in cacodylate buffer before staining with DAB. Variation in the sizes and shape of peroxisomes within the same hepatocyte was also observed. This was consistent with that reported in the literature for rat and human liver peroxisomes [142]. Apart from the catalase activity, it was obvious on the electron micrographs that peroxisomes are clearly distinguished from mitochondria by their apparent single membrane-bound structures. These globular structures surrounded by a single membrane were also clearly present in the electron micrographs of rat and to a lesser extent of bandicoot (Figure 7.5).

The most striking structural component of the liver peroxisomes is the dense core. This core or nucleoid has often been described as crystalline, semi-crystalline, crystalloid, or muti-lamellated [288]. A typical image of such a core structure observed for the koala liver peroxisomes is shown in Figure 7.3 (a very regular striation within peroxisomes). Although this core structure was not seen in all peroxisome particles, it is likely to be present in all. This is because its volume was reported to be distinctly smaller than that of the whole particle [288] and as a result, it may not always be included in the sections. In most ultra-thin sections from koala liver, dark cytoplasmic particles with irregular shapes were also observed. A representative image of such structures is shown in Figure 7.3 (upper panel). These black cytoplasmic particles were not seen in rat or bandicoot.

The average size of peroxisomes for koala, rat and bandicoot livers was 0.403 ± 0.032 μm, 0.504 μm, and 0.375 μm, respectively. These values are within the range of values reported for peroxisomes in most species studied (0.3 to 1 μm) [158]. While no

significant species differences in the average size of peroxisomes were observed, the average number of peroxisomes per hepatocyte for the koala, an obligate *Eucalyptus* feeder, is obviously higher than those from rat and bandicoot, non-*Eucalyptus*-feeders (Table 7.1). Since the density of peroxisome often varies with the zone distribution of the hepatocytes, in the present study, several tissue blocks from each species were cut randomly from different parts of the liver and many ultra thin sections from each block were examined. It is unlikely that the zone variation in the density of peroxisome has a significant implication in the interpretation of the results of this chapter. An increase in number of peroxisomes in hepatocytes is one of the indications of peroxisome proliferation due to exposure to peroxisome proliferators. The results of this study suggest that the marsupial koala is responsive to peroxisome proliferators given that the numbers of peroxisomes are the sole important criterion.

In summary, morphological examination of liver tissues reveal the presence of more peroxisomes in hepatocytes of the koala, an *Eucalyptus* feeder, than those of rat and bandicoot, non- *Eucalyptus* feeding species. No differences in the sizes of peroxisomes were observed. While rats and human have been reported to be highly responsive and nonresponsive species to peroxisome proliferators, respectively, marsupial koalas show higher numbers of peroxisomes per hepatocyte, suggesting that the koala is a responsive species.

Chapter 8

GENERAL DISCUSSION

The characterisation of cytochrome P450 CYP4A and peroxisomal β-oxidation enzymes has focussed and continues to focus significant research in laboratories worldwide. In human, rat and most species studied, microsomal ω-hydroxylation and peroxisomal β-oxidation cooperate smoothly to control lipid homeostasis in the liver. This process occurs in both normal physiological conditions and in conditions where there is a fatty acid overload. In these species, the expression of CYP4A and peroxisomal β-oxidation enzymes is mediated by the nuclear receptor, PPAR-α, via transcriptional activation of target genes. In susceptible rodents, induction of CYP4A due to exposure to a structurally divergent group of xenobiotics has been reported to be associated with induction of peroxisomal β-oxidation enzymes. It has also been established that this induction occurs concurrently with peroxisome proliferation and an increase in liver weight. From the results of the present studies in marsupials, relative to eutherian species, the Australian marsupial koala displays several significant differences in lipid-metabolising enzymes at both the biochemical and molecular level.

Marsupials are unique and significant Australian fauna. Like humans and other mammalian species, marsupials are exposed to xenobiotics from a diverse range of sources including diet and other environmental exposures. Since marsupials differ from eutherian mammals in many aspects of their development and in their mode of reproduction, this may alter their ability to metabolise environmental chemicals. Relative to eutherians, marsupial neonates are exposed to environmental chemicals earlier in life and therefore are more vulnerable to environmental chemical exposures. It is postulated that the detoxifying enzyme system of marsupials may have evolved differently from that of placental mammals [1]. While most of the current information on the oxidative metabolism of environmental chemicals in the literature derives from stud-

ies on rats, mice, rabbits and humans, few studies examining the metabolism of these chemicals in Australian marsupials have been reported, especially at the molecular level of the enzymes involved (reviewed in [3]).

The diet of the koala is restricted to *Eucalyptus* leaves, which contain a high proportion of toxic plant secondary metabolites, phenolics and terpenoids. The induction of some drug metabolising enzymes due to exposure to terpenoids and essential oils has been established, in particular, the microsomal CYP4A enzymes. Significant findings prior to the commencement of these studies were a 3-fold higher mean cytochrome P450 content and a 3.5 fold higher CYP4A activity observed with koala liver microsomes relative to rat and humans [8]. While in susceptible rodents, induction of CYP4A enzymes is often associated with induction of peroxisomal β-oxidation enzymes, the activity of the later was absent in koala liver. Further biochemical and molecular studies of CYP4A, peroxisomal β-oxidation enzymes and PPAR-α were critically important in identifying the significance of these initial observations and in understanding the adaptation of marsupial folivores to their unique *Eucalyptus* diet.

In the present studies, the brush tail possum model provided a useful marsupial model for investigating the effects of *Eucalyptus* terpenes on the expression of lipid-metabolising enzymes. While the koala and other marsupials, including the greater glider and the ring tail possums, only eat *Eucalyptus* leaves, the brush tail possum is not an obligate *Eucalypt* feeder. Its diet also contains fruits, vegetables and cereal. Protein and mRNA levels of CYP4A, peroxisomal AOX and PPAR-α were examined in livers of a terpene-treated group of possums and compared to an appropriate control group. The control group (4 possums) were given an artificial diet of fruit and cereal for ten days. The terpene-treated group (4 possums) were given the same artificial diet in which a mixture of monoterpenes including 1,8-cineole, α-pinene, *d*-limonene and *p*-cymene was added for the same number of days. The induction protocol has previously been reported to cause maximum induction of P450 enzymes [6]. This model clearly demonstrated that *Eucalyptus* monoterpenes cause an increase in expression of acyl CoA oxidase, the first and rate limiting enzyme that is essential for completion of peroxisomal straight chain fatty acid β-oxidation.

To isolate several different full-length *CYP4A15*, *AOX*, and *PPAR-α* cDNAs from koala liver, a specific cloning strategy was designed for the isolation of each full-length cDNA. While the cloning strategies for all involved mainly RT-PCR and RACE ap-

proaches and degenerate primers from other species, a thorough literature review was conducted prior to each experiment. Although the potential for PCR-induced errors may occur during the RT-PCR amplification of the cDNA clones, this is not the case for the isolation of *CYP4A15*, *AOX*, and *PPAR-α* cDNA clones. The fact that the 5' end of the cDNA was amplified and sequenced multiple times with the same result gives cofidence that the sequence was actually correct. The present studies have provided successful cloning approaches for the isolation of an almost full-length *CYP4A15* cDNA, full-length *AOX* and *PPAR-α* cDNAs using RT-PCR approaches. Based on the almost full-length *CYP4A15* cDNA obtained, future cloning experiment using 3'RACE to obtain the 3'end CYP4A15 cDNA will enable the isolation and expression full-length *CYP4A15* cDNA.

The isolation of *CYP4A15* cDNA and subsequent functional analysis of cDNA-expressed CYP4A15 clearly indicates that the koala CYP4A15 cDNA encode a functional CYP4A15 enzyme. A near full-length koala liver *CYP4A* cDNA, of size 1544-bp, was isolated and designated *CYP4A15*. The cDNA shares highest nucleotide and deduced amino acid sequence identity to human CYP4A11. The cDNA-expressed koala CYP4A15 enzyme was recognised by a sheep anti-rat CYP4A polyclonal antibody. Although CYP4A15 protein was expressed from 5' and 3' truncated CYP4A15 cDNA, no differences in the rate of lauric acid hydroxylation was seen between this protein and cDNA-expressed rat CYP4A1. This finding provides essential information for future studies to assess the function of the 3- and 5-end terminus of CYP4A15 enzyme in fatty acid (lauric acid) hydroxylation. This can be achieved by isolation of full-length CYP4A15 and functional expression of a more native CYP4A15 enzyme. Protein and mRNA levels of CYP4A were examined in the livers of koala and compared to human and rat. The results from this study does suggest higher levels of CYP4A protein and mRNA for koala liver, as compared to that of non-*Eucalyptus* feeders including human, rat and other marsupials. However, in the conducted study, there were limitations that makes it difficult to draw solid conclusion. These limitations were arisen from the small numbers of animals used for comparison across species and from the process of mRNA normalisation of the Northern blot. Future studies using larger sample size and more integrity mRNA samples will overcome these limitations and firm conclusion can be drawn. Southern analysis of *CYP4A* genomic DNA revealed different *CYP4A* gene organization across species. In conclusion, it appears that higher lauric acid hydroxylation activity and CYP content in koala liver are due to higher levels of CYP4A protein and mRNA.

From studies reported in this thesis, it is apparent that koala liver *acyl CoA oxidase* cDNAs produce active proteins with palmitoyl-CoA oxidation activity. Two 2039-bp koala liver *AOX* full-length cDNAs, designated *AOX I* and *AOX II*, were cloned and differ only in a small coding region from amino acid residues 89 to 130. This finding was consistent with results reported for humans, rat and other species studied. Kinetic studies of cDNA-expressed AOX I and AOX II demonstrates that these enzymes possess palmitoyl-CoA oxidase activity with apparent K_m values of 28μM and 38μM, respectively. These values are within the order of magnitude reported for rat and human purified AOX enzymes. While no significant differences in the activity of acyl CoA oxidase were detected between liver homogenates from koalas and rats, a more intense AOX mRNA band was detected in koala liver as compared to rat and human livers. Southern blot analysis of liver genomic DNA samples revealed a single *AOX* gene. From these results, it is apparent that the absence of total peroxisomal β-oxidation activity in koala liver is possibly due to deficiencies of one or more enzymes downstream of acyl-CoA oxidase and/or deficiencies of mitochondrial β-oxidation enzymes.

Given the limitations of the present studies as discussed previously in each related chapter, both CYP4A15 and peroxisomal AOX mRNA levels appeared to be higher in koala liver than were seen in rat and humans. While koala liver microsomes exhibit higher CYP4A activity than those from rat and human livers, AOX activity was lower for koala liver homogenate than that for rat liver. It appears that the level of active AOX protein in koala liver is lower than that in rat liver. While in the rats, humans and other species studied, the expression of CYP4A and AOX has been shown to be mediated by the nuclear receptor PPAR-α, studies on PPAR-α have not been reported in any marsupial species. This work therefore represents the first biochemical and molecular studies of PPAR-α in Australian marsupials. A koala liver full-length *PPAR-α* cDNA of size 1515-bp was successfully isolated. Subsequent immunoblot analysis of cDNA-expressed koala PPAR-α confirmed the presence of a *PPAR-α* gene which encodes the coding region of the receptor in koala liver. The expression of *PPAR-α* protein was detected in both koala liver cytosolic and nuclear extracts by immunoblot analysis. Koala liver PPARα mRNA species detected by Northern analysis was of size approximately 8-kb. Analysis of koala and other species liver genomic DNA clearly demonstrated different *PPAR-α* gene organization across species.

Studies reported here also include the first cytochemical localisation of peroxisomes in koala liver using transmission electron microscopy. This morphological study reveals relatively more peroxisomes in koala liver as compared to non-*Eucalyptus* feeders such as bandicoot and rat. No significant difference in the average size of peroxisomes was observed.

Collectively, the contributions made by the present studies principally comprise:

(i). isolation of four new cDNA nucleotide sequences that have been published in the GenBank DNA database. These data provide the first molecular information for the entire coding region of koala hepatic *CYP4A*, *AOX I*, *AOX II* and *PPARα*.

(ii). expression of these cDNAs confirming the presence of functional *CYP4A15*, *AOXI*, *AOXII*, and *PPAR-α* genes in koala liver. *CYP4A15* and *AOX* genes produced active proteins with lauric acid hydroxylase and palmitoyl-CoA oxidase activity, respectively.

(iii). study in control and terpene-treated possums demonstrating that dietary *Eucalyptus* terpenes significantly elevate AOX at both activity and mRNA levels.

(iv). histological visualisation of peroxisomes in hepatic tissues from koala and other animals suggesting a moderately responsive nature of the koala to peroxisome proliferators such as monoterpenes.

The present studies provide primary molecular data and insights for future research into marsupial microsomal and peroxisomal fatty acid metabolism. These studies also provide a useful tool for further studies on the transcriptional regulatory role of *PPAR-α* gene in the expression of lipid metabolising enzymes in Australian marsupials, in particular CYP4A and Acyl CoA Oxidase. Future studies of interest include:

(i). PPAR-α receptor activation study to examine the function of the koala liver PPAR-α and to confirm whether it is able to be activated by peroxisome proliferators. This study can be performed by co-transfection and reporter gene assay using the full-length CYP4A15 and PPAR-α cDNAs and potent PPs candidate such as Wy14643. The study also requires rat or human CYP4A 5' promoter region containing PPRE

and RXR (PPAR-α partner) which are available in other laboratories. Alternately, cloning of koala CYP4A and AOX 5' promoter region containing PPRE PPAR-α would be one of the first experiments for this proposed study. The proposed study will also establish whether koala is a highly responsive species to peroxisome proliferators such as rodents or weakly responsive species such as human and non-human primates.

(ii) studies to confirm the hypotheses generated from this project that *Eucalyptus terpenes* are PPAR-α ligands and high expression of CYP4A protein and CYP4A and AOX mRNA is due to activation of PPAR-α by *Eucalyptus terpenes.* These studies can be conducted using a koala cell line or assay using a transgenic construct containing full-length CYP4A15, AOX, PPAR-α, rat or human CYP4A or AOX 5' promoter region containing PPRE, and RXR. The proposed studies will also confirm whether the PPAR-α mediated expression and induction of both CYP4A and AOX in koala liver have the same or two separate mechanisms involved.

APPENDIX A

Restriction maps.

A.1 The restriction map of the koala *CYP4A15*

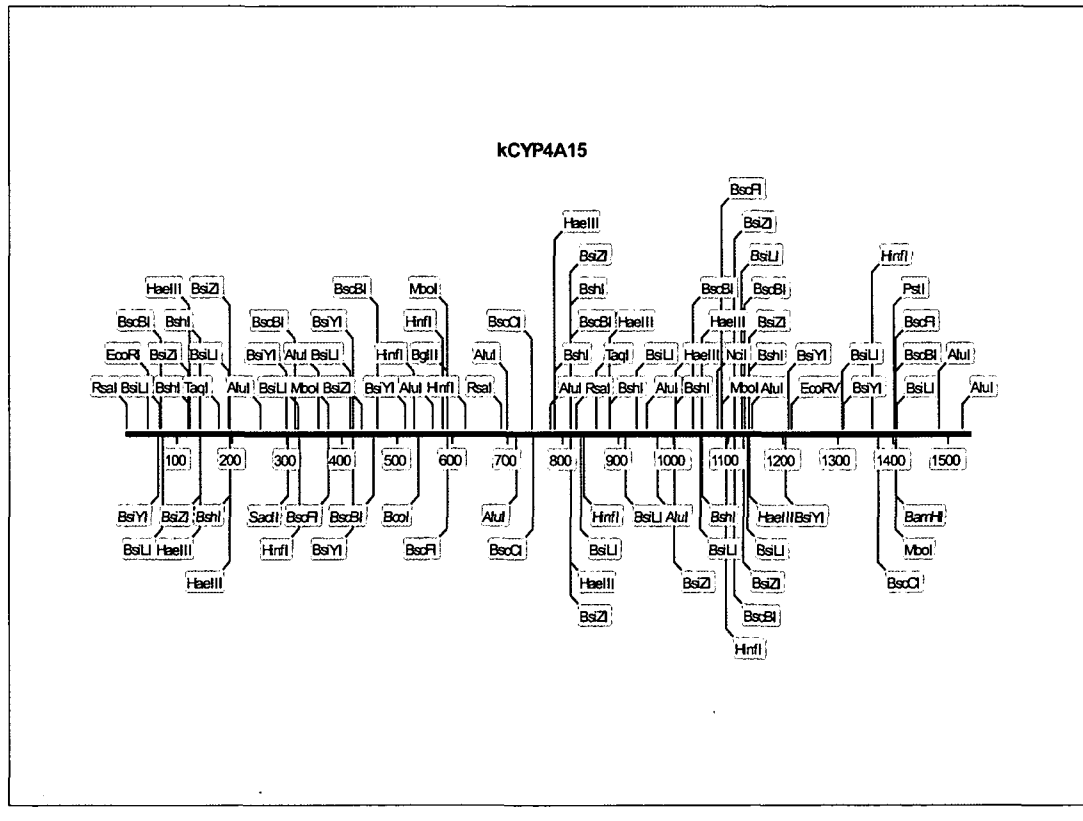

Figure A.1: The restriction map of the koala CYP4A15.

A.2 The restriction maps of the koala *AOX I* and *AOX II*

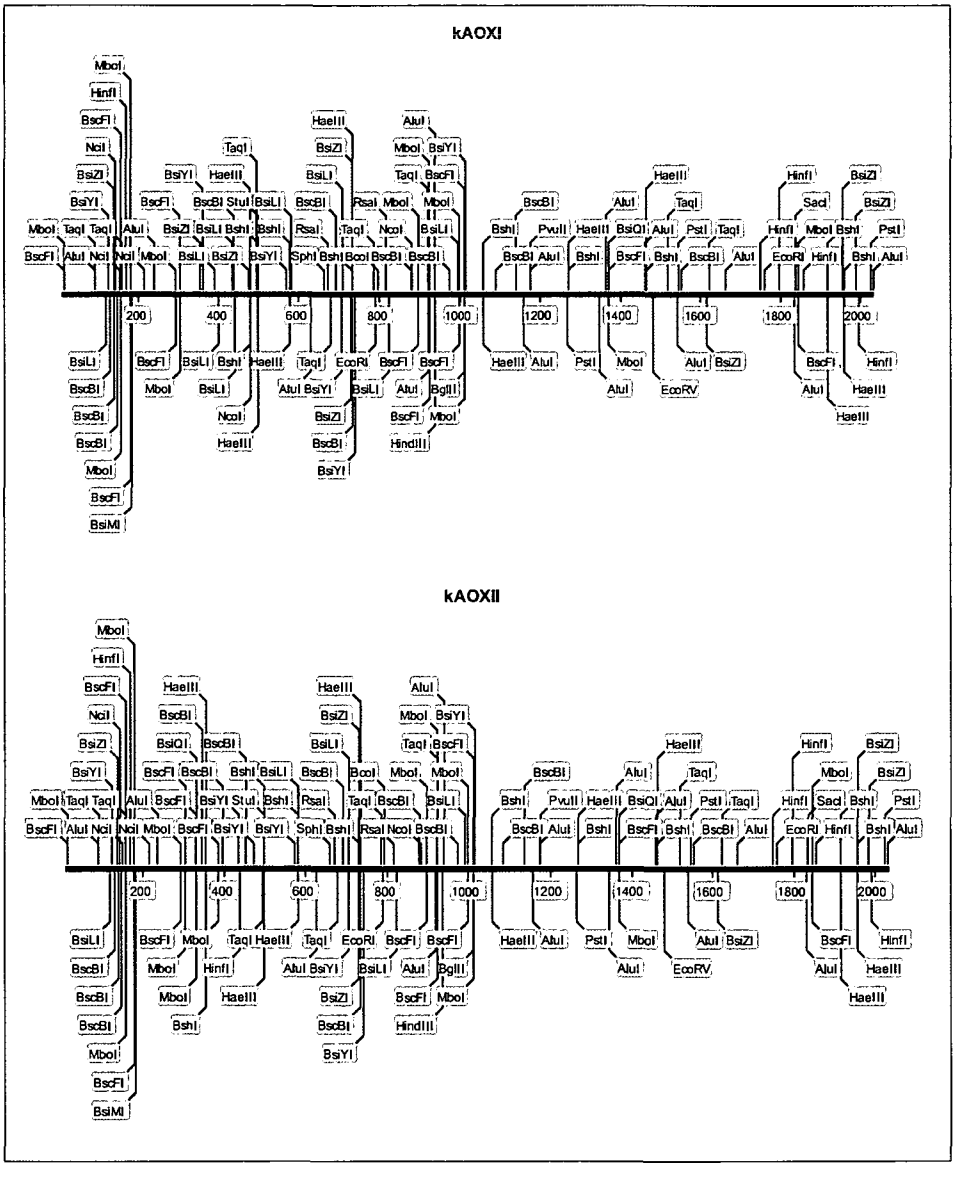

Figure A.2: The restriction maps of the koala *AOX I* and *AOX* II.

A.3 The restriction map of the koala *PPAR-α*

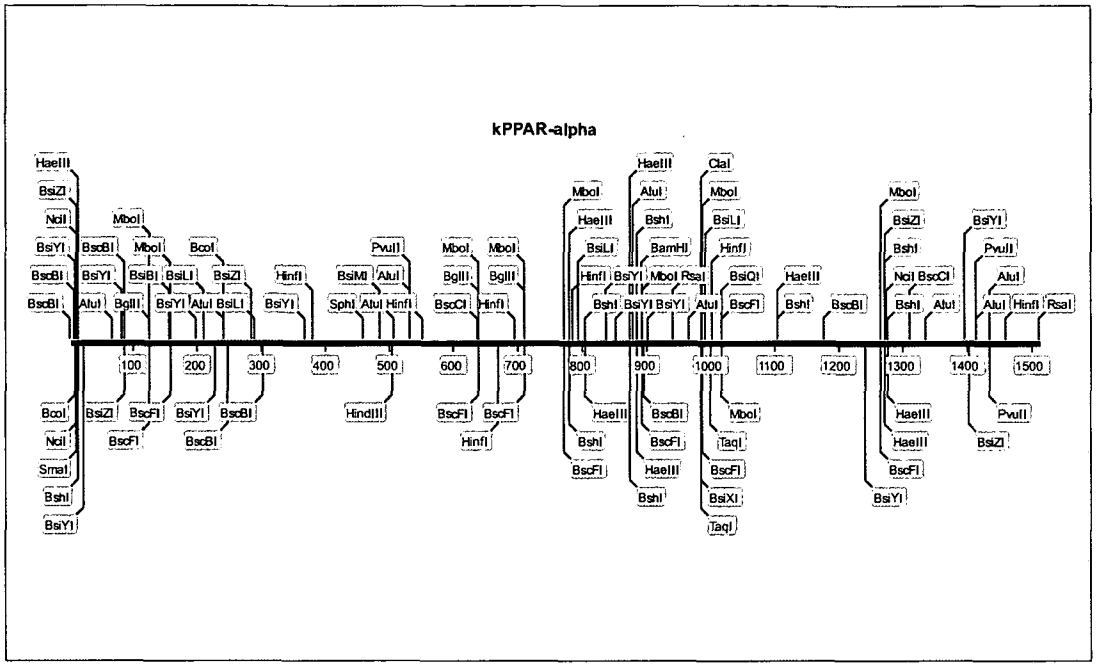

Figure A.3: The restriction map of the koala *PPAR-α*.

APPENDIX B

Deduced amino acid sequence alignment.

B.1 Alignment of the deduced amino acid sequences of the koala CYP4A15 with other CYP4A proteins

B.2 Alignment of the deduced amino acid sequences of the koala AOX I and AOX II with other AOX proteins



Figure B.1: Alignment of the deduced amino acid sequence of the koala *CYPA415* clone with other CYP4A proteins.

Conserved amino acid residues are indicated by the asterisks and amino acid residues having similar function are indicated by the dots.

```
CYP4A15 RHLD FLD I LLCART EGGDSLLDE ELRAEV DTFMFE GHDTTASG I SW LLYA 335
CYP4A11 RHLD FLD I LLLAKMENGS ILS DKDLRAEV DTFMFE GHDTTASG I SW I LYA 336
CYP4A1  RRLD FLD I LLLARMENGDSLS DKDLRAEV DTFMFE GHDTTASG VSW I FYA 335
CYP4A3  RHLD FLD I LLFAKMEDGKSLS DEDLRAEV DTFMFE GHDTTASG I SWVFYA 333
CYP4A5  RRLD FLD VLLFAKMENGSSLS DQDLRAEV DTFMFE GHDTTASG V SW IFYA 337
CYP4A7  RRLD FLD VLLFAKMENGSSLS DQDLRAEV DTFMFE GHDTTASG I SW IFYA 337
CYP4A10 RRLD FLD I LLFARMENGDSMSD KDLRAEVDTFMFE GHDTTASG V SW I FYA 336
        *.*****.** *.  * *  .  * .******************** **. **

CYP4A15 LATHPEHQQKCREE I RGVLGDGTS I TWD HLGQL PYTTMC I KE AL RL YP PV 385
CYP4A11 LATHPKHQERCREE I HS LLGDGAS I TWN HLDQMPYTTMC I KEAL RL YP PV 386
CYP4A1  LATHPKHQQRCREEVQSV LGDGSS I TWD HLDQ I PYTTMC I KE A LRL YP PV 385
CYP4A3  LATHPEHQERCREE VQS I LGDGTSV TWD HLDQ I PYTTMC I KE A LRLYP PV 383
CYP4A5  LATHP EHQHRCREE IQGLLGDGAS I TWE HLDQMPYTTMC I KE AMRLYP PV 387
CYP4A7  LATHP EHQHRCREE IQGLLGDGAS I TWE HLD KMPYTTMC I KE A LRLYP PV 387
CYP4A10 LATHPDHQQRCREE VQSLLGDGSS ITWD HLD Q I PYTTMC I KE A LRLYP PV 386
        ******* . **** .. .****.* .** ** ..  **********.******

CYP4A15 PS I G RDIKET I TF PDGR I LRAG N SVSLHIYALHHNP RVWE NPEVFN PF RF 435
CYP4A11 PGI G RELSTPV TF PDGR S LPKG I MVLLSIYGLHHNP KVWP NPEVFD PF RF 436
CYP4A1  P G I VRELSTSV TF PDGR S LPKG I QVT LSIYGLHHNP KVWP NPEVFD PS RF 435
CYP4A3  P S V SRELSSPV TF PDGR S I PKG I T TT I LIYGLHHNP SYWP NPKVFD PS RF 433
CYP4A5  P A I S RDLSSPVTF PDGR S  LPKG FTV TLSIYGLHHNP NVWPNPEV FD PGRF 437
CYP4A7  P GV GRQLSSPVTF PDGR S LPKG  I I T LSIYGLHHNP KVWPNPEV FD PS RF 437
CYP4A10 PG I V RELSTS VTF PDGR S LPKGVQV T LSIYGLHHNP KVWPNPEV FD PS RF 436
        *  . *  .  .****** .  *  .  ** ***** * ** ** * **

CYP4A15 SPENLTLQHSHA FLP FS AG SRNC IGQKFAMNEMKVVLALTLLLFELKPDT 485
CYP4A11 APG- -SAQHSHAFLP FS G G SRNC IGKQFAMNELKVATALTLLRFELLPDP 484
CYP4A1  APD- -SP RHSHS FLP FS GG ARNC IGKQFAMSEMKVIVALTLLRFELLPDP 483
CYP4A3  SP D- - S P RHSHAYLP FS GGARNC IGKQFAMNELKVAVALTLLRFELLPDP 481
CYP4A5  TPG – S A R HSHAFLP FS GGARNC IGKQFAMNELKVAVALTLVRFELLPDP 485
CYP4A7  APG – S A RHSHAFLP FS GG SRNC IGKQFAMNELKVAVALTL LRFELLPDP 485
CYP4A10 AP D- - S P RHSHS FLP FS GGARNC IGKQFAMS ELKV IVALTL LRFELLPDP 484
        .*  . . ***. . **** *. *****.. *** *. **  ****. *** **

CYP4A15 MKPPLP I S KLVLKSK                                    500
CYP4A11 TR I P I PIA RLVLKSKNGIHLRLRRLPNPCEDKDQL              519
CYP4A1  TKVP I PLP RLVLKSKNGIYLYLKKLH                         509
CYP4A3  TR I PVPMARLVLKSKNGIHLRLKKLR                          508
CYP4A5  TR I PKP TARLVLKSNNGIHLRLRKLQ                         511
CYP4A7  TRVP I P IT RLVLKSKNGIHLRLRKLH                        511
CYP4A10 TRVPMPLARLVLKSKNGIYLHLKKLH                            510
          . * * .*****
```

Figure B.1 (continued): Alignment of the deduced amino acid sequence of the koala *CYP4A15* lone with other CYP4A proteins. The CYP4A family highly conserved EGHDTT sequence and the conserved P450 signature motif containing the heme-binding cysteine residue are shown in bold.

```
kAOXI   1 MNPDLRRERDAAS FDAEKLTYI LDGGS ERTRRRREIEN L  ILNDPDF K HED
kAOXII  1 MNPDLRRERDAAS FDAEKLTYI LDGGS ERTRRRREIEN L  ILNDPDF K HED
hAOXI   1 MNPDLRRERDS AS FNP ELLTHI LDGSP EK TRRRREIEN M ILNDPDF Q HED
hAOXII  1 MNPDLRRERDS AS FNP ELLTHI LDGSP EK TRRRREIEN M ILNDPDF Q HED
rAOXI   1 MNPDLRKERASAT FNP ELI THI LDGSP EN TRRRREIEN L  ILNDPDF Q HED
mAOX    1 MNPDLRKERAAAT FNP EL ITHVLDGSP EN TRRRREIEN L  ILNDPDF Q HED
          ******.**  . *. *  *  . *  . * ** * *********. *******.***

kAOXI  51 LNFLTRS ERYE IA  VR KSA TMVKKMR DF GI ADPEEIMWFK  NFVHRGRPEP L
kAOXII 51 LNFLTRS ERYE IA  VR KSA TMVKKMR DF GI ADPEEIMWFK  KPQLINFV  EPV
hAOXI  51 LNFLTRS QRYEVA VR KSA IMVKKMR EF GI ADPDEIMWFK NFVHRGRP EPL
hAOXII 51 LNFLTRS QRYEVA VR KSA IMVKKMR EF GI ADPDEIMWFK KLHLVNFVEPV
rAOXI  51 YNFLTRS QRYEVA VK KSA TMVKKMR EY GI SDPEEIMWFK  KLYLANFV EPV
mAOX   51 YNFLTRS QRYE VA VKKSA TMVKKMR EF GI ADPEEIMWFK KLHMVNFV EPV
          ******. ***. * *. *** ******* .. **. **.******       .  **.

kAOXI  101 DLHLGMF  L PTLL HQ ATQE QQERFF IPAW N  LE I IGTYAQ TEM GHGT H LRGL
kAOXII 101 GLTYSMF  I PTLL DQ GTTA QQQKW LPPTQG  LQ I IGTYAQ TEM GHGT HLRGL
hAOXI  101 DLHLGMF  L PTLL HQ ATAE QQ ERFFMPAWN LE I IGTYAQ TEM GHGT H LRGL
hAOXII 101 GLNYSMF  I PTLL NQ GTTA Q K EKWLLSSKG LQ I IGTYAQ TEM GHGT H LRGL
rAOXI  101 GLNYSMF  I PTLL NQ GTTA QQ EKWMRPSQE LQ I IGTYAQ TEM GHGT H LRGL
mAOX   101 GLNYSMF  I PTLL NQ GTTA QQ EKWMHPSQE LQ I IGTYAQ TEM GHGT H LRGL
             *    **  .**** *  *    *  . . .  .      *.******************

kAOXI  151 ETTATYDP KTQEF I LN SPTVTS I KWW PGG L GKT SN HA I VLAQL YTKG ECY
kAOXII 151 ETTATYDP KTQEF I LN SPTVTS I KWW PGG L GKT SN HA I VLAQL YTKG ECY
hAOXI  151 ETTATYDP ETQEF I LN SPTVTS I KWW PGG L GKT SN HA I VLAQL I TKG KCY
hAOXII 151 ETTATYDP ETQEF I LN SPTVTS I KWW PGG L GKT SN HA I VLAQL I TKG KCY
rAOXI  151 ETTATYDP KTQEF I LN  SPTVTS I KWW PGG L GKT SN HA I VLAQL I TQG ECY
mAOX   151 ETTATYDP KTQEF I LN SPTVTS I KWW PGG L GKT SN HA I VLAQL I TRG ECY
          ******** ********************************** *. *  **

kAOXI  201 GLHAF IVP IRE MG THKP FPGI I VGD I GPKFGY DE MDNGYLKMDN Y R I P RE
kAOXII 201 GLHAF IVP IRE MG THKP FPGI I VGD I GPKFGY DE MDNGYLKMDN Y R I P RE
hAOXI  201 GLHAF IVP IRE N R THKP LPGI TVGD I GPKFGY DE  I DNGYLKMDN H R I P RE
hAOXII 201 GLHAF IVP IRE N R THKP LPGI TVGD I GPKFGY DE  I DNGYLKMDN H R I P RE
rAOXI  201 GLHAF  VVPIRE I G  THKP LPGI TVGD I GPKFGY EE MDNGYLKMDN Y R I P RE
mAOX   201 GLHAF  VVP IRE I G THKP LPGI TVGD I GPKFGY EE M DNGYLKMDN YR I  PRE
          ***** .*****  **** *** **********.*  . ********* *****

kAOXI  251 NMLMKYAQVKPDG T YVKPLSNKLTYG TMV FVRSFLVGEAARS  L SKACT I A
kAOXII 251 NMLMKYAQVKPDG T YVKPLSNKLTYG TMV FVRSFLVGEAARS  L SKACT I A
hAOXI  251 NMLMKYAQVKPDG P YVKPLSNKLTYG TMV FVRSFLVGEAARA L SKACT I  A
hAOXII 251 NMLMKYAQVKPDG P YVKPLSNKLTYG TMV FVRSFLVGEAARA L SKACT I  A
rAOXI  251 NMLMKYAQVKPDG T YVKPLSNKLTYG  TMV FVRSFLVGNAAQS L SKACT I  A
mAOX   251 NMLMKYAQVKPDG T YVKPLSNKLTYG XMX FVRSFLVGSAA QS L SKACT I  A
          ************ ************  ******** **.. ********

kAOXI  301 I RYS L I  RHQSE IQPGD PEPQ I LDFQTQQY K L FPL LA T AYA F Q FV GAYMKE
kAOXII 301 I RYS L I  RHQSE IRPGD PEPQ I LDFQTQQY K LFPL LA T AYA F  Q FV GAYMKE
hAOXI  301 I RYS AV RHQSE IKPGE  PEPQ I LDFQTQQY K LFPL LA T AYA F Q FV GAYMKE
hAOXII 301 I RYS AV RHQSE IKPGE  PEPQ I LDFQTQQY K LFPL LA T AYA F Q FV GAYMKE
rAOXI  301 I RYS AV RR QSE IKQSE  PEPQ I LDFQTQQY K LFPL LA T AYA  F H FV GRYMKE
mAOX   301 I RYS AV RR QSE IKRSE  PEPQ I LDFQTQQY K LFPL LA T AYA  F H F L GRY I KE
          **** . * .****  .  .************************.*. * * .**
```

Figure B.2: Alignment of the deduced amino acid sequences of the koala *AOX I* and *AOX II* clones with other AOX proteins.

The conserved unique fatty acyl CoA oxidase sequence KWWPGG [281] is shown in bold. Conserved amino acid residues are indicated by the asterisks and amino acid residues having similar function are indicated by the dots.

```
kAOXI  351 TY HR I N VD IS QGNLN ELPELHAL TAGLKAFT SW TTNS  G I E ACRMACGGHG
kAOXII 351 TY HR I N VD IN QGNLNELPELHAL AAGLKAFT SW TTNS  G I E ACRMACGGHG
hAOXI  351 TY HR I N EG IG QGDL S ELPELHAL TAGLKAFT SW TANT G I E ACRMACGGHG
hAOXII 351 TY HR I N EG IG QGDLS ELPELHAL  TAGLKAFT SW TANT G I E ACRMACGGHG
rAOXI  351 TY  LR I N ES  IG QGDLS ELPELHAL  TAGLKAFT TW TANA GI E ECRMACGGHG
mAOX   351 TY MR I N ES IG QGDLS ELPE LHAL TAGLKAFT TW TANA GI E  ECRMACGGHG
           **  ***   * ** * ********.*******.** .* .*** **** *****


kAOXI  401 YSHC SG LPN I YVTFTP TCTFEGEN TVMM LQTARF LMK S YDQV HSGKLV GG
kAOXII 401 YSHC SG LPN I YVTFTP TCTFEGEN TVMM LQTARF LMK S YDQV HSGKLV GG
hAOXI  401 YSHC SG LPN I YVNFTP SCTFEGEN TVMM LQTARF LMK S YDQV HSGKLV CG
hAOXII 401 YSHC SG LPN I YVNFTP SCTFEGEN TVMM LQTARF LMK S YDQV HSGKLV CG
rAOXI  401 YSHS SG I PN I YVTFTP ACTFEGEN TVMM LQTARF LMK  I YDQV RSGKLV GG
mAOX   401 YSHS SG I PN I YVTFTP ACTFEGEN TVMM LQTARF LMK I YDQV QSGKLV GG
           ***. **.***** .***.******************** **** .***** *


kAOXI  451 MVSYLNDLPSQR I Q P Q QV A AWP AMVD I NNPDSLTEAYK HRAARLVEAAAR
kAOXII 451 MVSYLNDLPSQR I Q P Q QV A AWP AMVD I NNPDSLTEAYK HRAARLVEAAAR
hAOXI  451 MVSYLNDLPSQR I Q P Q QV A VWP TMVD I NSPES LTEAYK  LRAARLVE I AAK
hAOXII 451 MVSYLNDLPSQR I Q P Q QV A VWP TMVD I NSPES LTEAYK  LRAARLVE I AAK
rAOXI  451 MVSYLNDLPSQR I Q P Q QV A  VWP TMVD I NSLEGLTEAYK  LRAARLVE I AAK
mAOX   451 MVSYLNDLPSQR I Q P Q QV A VWP TL VD I NSLDS LTEAYK  LRAARLVE I AAK
           ******************** ** . . **** .  ****** ******* **.


kAOXI  501 NLQAE MK HRKSKE I AWN FTSVDLV  RAS  E AH C HYVV VKLFSGN LSKIDDKP
kAOXII 501 NLQAE MK HRKSKE I AWN FTSVDLV  RAS  G AHC HYVV VKLFSGN LSKIDDKP
hAOXI  501 NLQKE V I  HRKSKE V AWN LTSVDLV RAS  E AH LHYGL VKL FSEK LLKIQDKA
hAOXII 501 NLQKE V I  HRKSKE V AWN LTSVDLV RAS E AH L HYGL V KLFSEK LLKIQDKA
rAOXI  501 NLQTH V S HRKSKE V AWN LTSVDLV RAS E AH C HYVV V KVFSDKLPKIQDKA
mAOX   501 NLQAQ V S HRKSKE V AWN LTSVDLV RAS E AH C HYVT V KVFADKLPKIQDRA
           ***  .   ******.*** ********* **  **  ** .*. * ** * .


kAOXI  551 I QAVLT N LCLLYAL YG I SQ NS  GDFL QGG I L TES  QLT QVNQ RVK ELLTL  IR
kAOXII 551 I QAVLT N LCLLYAP YG I SQ NS  GDFL QGG I L TES  QLT QVNQ RVK ELLTL  IR
hAOXI  551 I QAVLR S LCLLY SL YG I SQ NA GDFL QGS  I MTEP  Q IT QVNQ RVK ELLTL  IR
hAOXII 551 I QAVLR S LCLLY SL YG I SQ NA GDFL QGS  I MTEP  Q IT QVNQ RVK ELLTL  IR
rAOXI  551 V QAVLR NLCLLYSL YG I SQ KG  GDFL EGS  I  I TGA QLS  QVNA R I L ELLTL  IR
mAOX   551 V QAVLR NLCLLYSL YGI SQ KG  GDFL  EGN I  I TGA QMS QVNS R I L ELLTV TR
           .**** ***** . *****  **** .*  *. *  *  . .*** * .  **** . *


kAOXI  601 PESA ALVDA FDFQDVS LGSVLGRYDGN I YEN MFEWAK K SPLN K S EVH E SY
kAOXII 601 PESA ALVDA FDFQDVS LGSVLGRYDGN I YEN MFEWAK K SPLN K S EVH E SY
hAOXI  601 SDAV ALVDA FDFQDVTLGSVLGRYDGN VYEN L FEWAK N SPLN K A EVH E SY
hAOXII 601 SDAV ALVDAFDFQDVT LGSVLGRYDGN VYEN L FEWAK N SPLN K A EVH E SY
rAOXI  601 PNAV ALVDA FDFKDMTLGSVLGRYDGN VYEN L FEWAK K SPLN K T  EVH E SY
mAOX   601 PNAV ALVDA FDFKDVTLGSVLGRYDGN VYEN L FEWAK K SPLN K T  EVH Q SY
           .     ********.*. ***********.***. *****  ***** .***  . **


kAOXI  651 HKHLK P LQ SKLX
kAOXII 651 HKHLK P LQ SKLX
hAOXI  651 - KHLK S LQ SKLX
hAOXII 651 - KHLK S LQ SKLX
rAOXI  651 H KHLK P LQ SKLX
mAOX   651 Y KHLK P LQ SKLX
           **** *****
```

Figure B.2 (continued): Alignment of the deduced amino acid sequences of the koala *AOX I* and *AOX II* clones with other AOX proteins. The FAD binding motif CGGHGY[281] and the SKL motif, an import signal present in several peroxisomal matrix proteins, are shown in bold.

APPENDIX C

Transmission electron microscopy.

Morphological study of most biological specimens can be examined in the form of ultra-thin section using transmission electron microscopy (EM). Since adequate penetration of the electron beam and resolution is optimal if ultra-thin section are less than 0.1μm, this study utilised ultra-thin sections of size approximately 50nm. For selective staining of peroxisomes, the peroxidatic reaction of catalase is widely used. A more detailed analysis of the catalase reaction for visualisation of peroxisomes is found in Section 7.2.1. The following is a general overview of the procedure of electron microscopy, its rationale and utilisation.

Chemical fixation is the most widely used method to preserve biological materials for electron microscopy. The goals include the adequate preservation of cell structure with minimum alteration from the living state, minimum loss of many cellular components including enzymes, the clarity of structural details shown by electron micrographs and protection of specimens against subsequent treatments. Two types of commonly used fixatives include coagulant and non-coagulant fixatives. Non-coagulant fixatives produce stabilisation of proteins without much structural distortion from the original state and can render some proteins non-coagulable by subsequently used coagulant reagents such as ethanol. Glutaraldehyde is the most widely used due to its capacity to stabilise most protein components and other cell constituents. Other commonly used fixatives include osmium tetroxide, acrolein and formaldehyde. A double fixation with glutaraldehyde followed by osmium tetroxide is considered the most effective fixation method since they together stabilise the maximum number of different types of cell components [306].

After being fixed, biological materials should be rinsed to prevent reaction between

the fixatives and the dehydration agent. In general, two to three quick rinses in the buffer for a total of 10 to 20 minutes is adequate for most specimens [306]. For embedding in water-immiscible epoxy resins, dehydration is achieved by passing the specimens through a series of ascending concentrations of ethanol or acetone [306]. For satisfactory sectioning, complete and uniform penetration of tissue specimen is essential. This is achieved infiltrating small blocks of tissue ($1mm^3$) with a series of ascending concentrations of embedding medium prior to polymerisation. While infiltration involves a gradual replacement of the dehydration agent with the embedding medium, embedding is a complete impregnation of the interstices of a tissue specimen with the medium [306].

Bibliography

[1] R. M. Bolton and J. T. Ahokas. Review: detoxication in Australian marsupials. Ecotoxicological implications. *Aust. J. Eco.*, 1:85–98, 1995.

[2] C. H. Tyndale-Biscoe. *Life of Marsupials.* Adward Arnold, London, UK, 1973.

[3] I. Stupans, B. Jones, and R. A. McKinnon. Xenobiotic metabolism in Australian marsupials. *Comp. Biochem. Physiol.*, 128(C):367–376, 2001.

[4] S. McLean and W. J. Foley. Metabolism of Eucalyptus terpenes by herbivorous marsupials. *Drug Metab. Rev.*, 29:213–218, 1997.

[5] S. J. Roffey, R. Walker, and G. Gibson. Hepatic peroxisomal and microsomal enzyme induction by citral and linalool in rats. *Fd. Chem. Toxic.*, 28:403–408, 1990.

[6] J. G. Pass, S. McLean, and I. Stupans. Induction of xenobiotic metabolising enzymes in the common brushtail possum, *Trichosurus vulpecula*, by *Eucalyptus* terpenes. . *Comp. Biochem. Physiol.*, 124(C):239–246, 1999.

[7] J. G. Pass, S. Mclean, I. Stupans, and N. Davies N. Microsomal metabolism of the terpene 1,8-cineole in the common brushtail possum *Trichosurus vulpecular*, koala *Phascolarctos cinereus*, rat and human. *Xenobiotica*, pages 205–221, 2001.

[8] S. N. T. Ngo, S. Kong, A. Kirlich, R. A. McKinnon, and I. Stupans. Cytochrome P450 4A, peroxisomal enzymes and nicotinamide cofactors in koala liver. *Comp. Biochem. Physiol.*, 127(C):327–334, 2000.

[9] I. Fleming. Cytochrome P450 enzymes in vascular homeostasis. *Cir. Res.*, 89:753–762, 2001.

[10] Http. http://www.icgeb.org/p450srv. 18-10-2003.

[11] T. L. Poulos, B. C. Finzel, I. C. Gunsalus, G. C. Wagner, and J. Kraut. The 2.6-A crystal structure of *Pseudomonas putida* cytochrome p-450. *J. Biol. Chem.*, 260:16122–16130, 1985.

[12] G. A. Roberts, G. Grogan, A. Greter, S. L. Flitsch, and N. J. Turner. Identification of a new class of cytochrome P450 from a *Rhodococcus sp. J. Bacteriol.*, 184 (14):3898–3908, 2002.

[13] C. S. Miles, T. W. B. Ost, M. A. Noble, A. W. Munro, and S. K. Chapman. Protein engineering of cytochrome P450. *Biochem. Biophys. Acta*, 1954:383–407, 2000.

[14] Http. http://drnelson.utmem.edu/homepage.html. 19-10-2003.

[15] Http. http://drnelson.utmem.edu/homepage.html. 02-11-2002.

[16] D. R. Nelson, L. Koymans, T. Kamataki, J. J. Stegeman, R. Feyereisen, D. J. Waxman andM. R. Waterman, O. Gotoh, M. J. Coon, R. W. Estabrook, I. C. Gunsalus, and D. W. Nebert. P450 superfamily: update on new sequences, gene mapping, accession numbers and nomenclature. *Pharmacogenetics*, 6:1–42, 1996.

[17] D. W. Nebert and D. R. Nelson DR. In Cytochrome P450. Methods enzymology, M. R. Waterman and E. F. Johson (eds). 206:3–11, 1991.

[18] B. K. Park, M. Pirmohamed, and N. R. KJitteringham. The role of cytochrome P450 enzymes in hepatic and extrahepatic human drug toxicity. *Pharmaco. Ther.*, 68:385–424, 1995.

[19] T. D. Porter and M. Coon. Cytochrome p-450. Multiplicity of isoforms, substrates, and catalytic and regulatory mechanisms. *J. Biol. Chem.*, 266:10019–10022, 1991.

[20] R. T. Williams. The metabolism of drugs and toxic substances. *Annu. Rev. Biochem.*, 20:441–464, 1951.

[21] S. Lieberman and K. Dobriner. Biochemistry of steroid. *Annu. Rev. Biochem.*, 20:227–264, 1951.

[22] B. B. Brodie, J. R. Gillette, and B. N. La Du. Enzymatic metabolism of drugs and other foreign compounds. *Annu. Rev. Biochem.*, 27:427–454, 1958.

[23] E. C. Miller and J. A. Miller. Biochemistry of carcinogenesis. *Annu. Rev. Biochem.*, 28:291–320, 1959.

[24] B. Priess and K. Bloch. ω-oxidation of long chain fatty acid in rat liver. *J. Biol. Chem.*, 239:85–88, 1964.

[25] O. Hayaishi, M. Katagiri, and S. Rothberg. Mechanism of the pyrocatechase reaction. *J. Am. Chem. Soc.*, 77:5450–5451, 1955.

[26] H. S. Mason, W. L. Fowlks, and E. Peterson. Oxygen transfer and electron transport by the phenolase complex. *J. Am. Chem. Soc.*, 77:2914–2915, 1955.

[27] M. Klingenberg. Pigments of rat liver microsomes. *Arch. Biochem. Biophys.*, 75:376–386, 1958.

[28] T. Omura and R. Sato. A new cytochrome in liver microsomes. *J. Biol. Chem.*, 237:1375–1376, 1962.

[29] T. Omura and R. Sato. The carbon monoxide-binding pigment of liver microsomes. I. evidence for its hemprotein nature. *J. Biol. Chem.*, 239:2370–2378, 1964.

[30] T. Omura and R. Sato. The carbon monoxide-binding pigment of liver microsomes. II. solubilisation, purification and properties. *J. Biol. Chem.*, 239:2379–2385, 1964.

[31] A. Y. H. Lu and M. J. Coon. Role of hemoprotein P450 in fatty acid omega-hydroxylation min a soluble enzyme system from liver microsomes. *J. Biol. Chem.*, 243:1331–1332, 1968.

[32] A. Y. H. Lu, K. W. Junk, and M. J. Coon. Resolution of the cytochrome P450 containing omega-hydroxylation system of liver microsomes into three components. *J. Biol. Chem.*, 244:3714–3721, 1969.

[33] D. K. Ro, J. Ehlting, and C. J. Douglas. Cloning, functional expression, and subcellular localisation of multiple NADPH-cytochrome P450 reductases from hybrid poplar. *Plant. Physiol.*, 130(4):1837–1851, 2002.

[34] A. E. Simpson. The cytochrome P450 4 (CYP4) family. *Gen. Pharmacol.*, 28:351–359, 1997.

[35] D. W. Nebert, M. Adesnik, M. J. Coon, R. W. Estabrook, F. J. Gonzalez, F. P. Guengerich, I. C. Gunsalus, E. F. Johson, B. Kemper, W. Levin, I. R. Phillips, R. Sato, and M R. Waterman. The P450 superfamily: recommended nomenclature. *DNA*, 6:1–11, 1987.

[36] K. R. Korzekwa and J. P. Jones. Predicting the cytochrome P450 mediated metabolism of xenobiotics. *Pharmacogenetics*, 3:1–18, 1993.

[37] D. A. Williams. *In Principles of Medicinal Chemistry*, chapter Drug metabolism, W. O. Foye and T. L. Lemke and D. A. Williams (Eds). Williams and Wilkins, PA, USA, 1995.

[38] S. Graham-Lorence and J. A. Peterson. How similar are P450s and what can their differences teach us. Minireview. *Arch. Biochem. Biophys.*, 369:24–29, 1999.

[39] K. G. Ravichandran, S. S. Boddupalli, C. A. Hasemann, J. A. Peterson, and J. Deisenhofer. Crystal structure of hemoprotein domain of P450BM-3, a prototype for microsomal P450's. *Science*, 261:731–736, 1993.

[40] C. A. Hasemann, K. G. Ravichandran J. A. Peterson, and J. Deisenhofer. Crystal structure and refinement of cytochrome $P450_{terp}$ at 2.3 A^o resolution. *J. Mol. Biol.*, 263:1169–1185, 1994.

[41] J. R. Cupp-Vickery and T. L. Poulos. Structure of cytochrome P450eryF: substrate, inhibitors, and model compounds bound in the active site. *Steroids*, 62(1):112–116, 1997.

[42] S. Y. Park, H. Shimizu, S. Adachi, A. Nakagawa, I. Tanaka, K. Nakahara, H. Shoun, E.Obayashi, H. Nakamura, T. Iizuka, and Y. Shiro. Crystal structure of nitric oxide reductase from denitrifying fungus Fusarium oxysporum. *Nature Struct. Biol.*, 4:827–832, 1997.

[43] P. N. Palma, I. Moura, J. LeGall, J. Van Beeumen, J. E. Wampler, and J. J. Moura. Evidence for a ternary complex formed between flavodoxin and cytochrome c3: 1H-NMR and molecular modelling studies. *Biochemistry*, 33:6394–6407, 1994.

[44] S. B. Kirton, C. A. Baxter, and M. J. Sutcliffe. Comparative modelling of cytochrome P450. *Advanced Drug Delivery Reviews*, 54:385–406, 2002.

[45] C. A. Hasemann, R. C. Kurumbail, S. S. Boddupalli, J. A. Peterson, and J. Deisenhofer. Structure and function of cytochrome P450: A comparative analysis of three crystal structures. *Structure*, 3:41–62, 1995.

[46] T. L. Poulos, B. C. Finzel, and A. J. Howard. Coon. High-resolution crystal structure of cytochrome $P450_{cam}$. *J. Biol. Chem.*, 195:687–700, 1987.

[47] S. Graham-Lorence and J. A. Peterson. Serial review. P450: structural similarities and functional differences. *The FASEB Journal*, 10:206–214, 1996.

[48] G. G. Gibson. Comparative aspects of the mammalian cytochrome P450 IVA gene family. *Xenobiotica*, 19:1123–1148, 1989.

[49] L. A. LeBrun, U. Hoch, and P. R. Ortiz de Montellano. Autocatalytic Mechanism and consequences of covalent heme attachment in the cytochrome P4504A family. *J. Biol. Chem.*, 277:12755–12761, 2002.

[50] D. W. Nebert and F. J. Gonzalez. Cytochrome P450 gene expression and regulation. *Trends. Pharmaco. Sci.*, 6:160–164, 1985.

[51] J. P. Hardwick, B. Song, E. Huberman, and F. Gonzalez. Isolation, complementary DNA sequence, and regulation of rat hepatic lauric acid omeha-hydroxylase (cytochrome P450 LA-ω). Identification of a new cytochrome P450 gene family. *J. Biol. Chem.*, 262:801–810, 1987.

[52] S. Imaoka and Y. Funae. Purification and NH_2-terminal sequence of cytochrome-P450 from kidney microsomes of untreated male rat. *Biochem. Biophys. Res. Commun.*, 141:711–717, 1986.

[53] S. Imaoka, K. Nagashima, and Y. Funae. Characterisation of three cytochrome P450s purified from renal microsomes of untreated male rats and comparison with human renal cytochrome P450. *Arch. Biochem. Biophys.*, 276:473–480, 1990.

[54] S. Kimura, N. Hanioka, and F. J. Gonzalez. The rat clofibrate-inducible CYP4A subfamily II. Complete intron and exon sequence of the CYP4A1 and CYP4A2 genes, unique exon organisation, and identification of a conserved 19-bp upstream element. *DNA*, 8:503–516, 1989.

[55] S. Kimura, J. P. Hardwick, C. A. Kozak, and F. J. Gonzalez. The rat clofibrate-inducible CYP4A subfamily II. cDNA sequence of CYP4A3, mapping of the cyp4a locus to mouse chromosome 4, and coordinate and tissue-specific regulation of the CYP4A genes. *DNA*, 8:517–525, 1989.

[56] M. H. Wang, D. E. Stec, M. Balazy, V. Mastyugin, C. S. Yang, R. J. Roman, and M. L. Schwartzman. Cloning, sequencing, and DNA-directed expression of the rat renal CYP4A2: arachidonic acid ω-hydroxylation and 11, 12-epoxidation by CYP4A2 protein. *Arch. Biochem. Biophys*, 336:240–250, 1996.

[57] M. Yoshimoto, E. Kusunose, N. Yamamoto, M. Maekawa, and M. Kusunose. Purification and characterisation of two forms of cytochrome P450 from rat kidney cortex microsomes. *Biochem. Int.*, 13:749–755, 1986.

[58] E. F. Johnson, D. L. Walker, and K. J. Griffin. Cloning and expression of three rabbit kidney cDNAs encoding lauric acid omega-hydroxylase. *Biochemistry*, 29:873–879, 1990.

[59] Y. Kikuta, E. Kisunose, T. Okumoto, I. Kubota, and M. Kusunose. Purification and characterisation of two forms of cytochrome P450 with ω-hydroxylase activities toward prostaglandin A and fatty acids from rat liver microsomes. *J. Bioochem.*, 107:260–286, 1990.

[60] E. Kusunose, A. Sawamura, H. Kawashima, I. A. Kubota, and M. Kusunose. Isolation of a new from of cytochrome P450 with prostaglandin A and fatty acid ω-hydroxylase activities from rabbit kidney cortex microsomes. *J. Biochem.*, 106: 194-196, 1989.

[61] N. Yokotani, R. Bernhardt, K. Sogawa, E. Kusuno, O. Gotog, M. Kusuco, and Y. Fujii-Kuriyama. Two forms of omega-hydroxylase toward prostaglandin A and laurate. cDNA cloning and their expression. *J. Biol. Chem.*, 264:21665–21669, 1989.

[62] D. R. Bell, N. J. Plant, L. Na, C. G. Rider, S. Brown, I. Ateitalla, S. K. Acharya, M. H. Davies, E. Elias, N. A. Jenkins, D. J Gilbert, N. G. Copeland, and C. R. Elcombe. Species-specific induction of cytochrome P-450 4A RNAs: PCR cloning of partial guinea pig, human and mouse CYP4A cDNA. *Biochem. J.*, 294:173–180, 1993.

[63] H. Kawashima, E. Kusunose, Y. Kikuta, H. Kinoshita, S. Tanaka, S. Yamamoto, T. Kishimoto, and M. Kusunose. Purification and cDNA cloning of human liver CYP4A fatty acid omega-hydroxylase. *J. Biochem.*, 116:74–80, 1994.

[64] C. J. Henderson, T. Bammler, and C. R. Wolf. Deduced amino acid sequence of a murine cytochrome P-450 cyp4a protein: developmental and hormonal regulation in liver and kidney. *Biochimica et Biophysica Acta*, 1200:182–190, 1994.

[65] K. Lundell, R. Hansson, and K. Wikvall. Cloning and expression of a pig liver taurochenodeoxycholic acid 6α-hydroxylase (CYP4A21). A novel member of the CYP4A subfamily. *J. Biol. Chem.*, 276:9606–9612, 2001.

[66] J. P. Hardwick. *In Methods in Enzymology*, chapter CYP4A subfamily: functional analysis by immunohistochemistry and in situ hybridisation, M. R. Waterman R and E. F. Johson (Eds), pages 273–284. Academic Press, New York, 1991.

[67] R. T. Okita and J. R. Okita. Cytochrome P450 4A fatty acid -hydroxylases. *Current Drug Metabolism*, 2:265–281, 2001.

[68] S. K. Bains, S. M. Gardiner, K. Mannweiler, D. Gillet, and G. G. Gibson. Immunochemical study on the contribution of hypolipidaemic-induced P450 to the metabolism of lauric acid and arachidonic acid. *Biochem. Pharmac.*, 34:3221–3229, 1985.

[69] G. G. Gibson, T. C. Orton, and P. P. Tamburini. Cytochrome P450 induction by clofibrate. *Biochem. J.*, 203:161–168, 1982.

[70] U. Hoch, J. R. Falck, and P. R. Ortiz de Montellano. Molecular basis for the omega-regiospecificity of the CYP4A2 and CYP4A3 fatty acid hydroxylases. *J. Biol. Chem.*, 275:26952–26958, 2000.

[71] U. Hoch, Z. P. Zhang, D. L. Kroetz, and P. R. Ortiz de Montellano. Structural determination of the substrate specificities and regioselectivities of the rat and human fatty acid omega-hydroxylase. *Arch. Biochem. Biophys.*, 373:63–71, 2000.

[72] P. A. Loughran, L. J. Roman, A. E. AitkenR. T. Miller, and B. S. Masters. Identification of unique amino acids that modulate CYP4A7 activity. *Biochemistry*, 39:15110–15120, 2000.

[73] X. Nguyen, M. Wang, K. M. Reddy, J. R. Falck, and M. L. Schwartzman. Kinetic profile of the rat CYP4A isoforms: arachidonic acid metabolism and isoform-specific inhibitors. *Am. J. Physiol.*, 45:R1691–R1700, 1999.

[74] R. T. Okita, J. E. Clark, J. R. Okita, and B. S. S. Masters. *In Methods in Enzymology, M. R. Waterman and E. F. Johson (Eds)*, pages 432–440. Academic Press, New York, 1991.

[75] P. P. Tamburini, H. A. Masson, S. K. Bains, R. J. Makowski andB. Morris, and G. G. Gibson. Multiple forms of hepatic P450. Purification, characterisation and comparison of a novel clofibrate-induced isozyme with other major forms of cytochrome P450. *Eur. J. Biochem*, 139:247–252, 1984.

[76] J. H. Capdevila, J. R. Falck, and R. C. Harris. Cytochrome P450 and arachidonic acid bioactivation. Molecular and functional properties of arachidonate monooxygenase. *J. Lipid. Res.*, 41:163–181, 2000.

[77] J. D. Imig. Eicosanoid regulation of the renal vasculature. *Am. J. Physiol. Renal Physiol.*, 279:F965–981, 2000.

[78] J. C. McGiff and J. Quilley. *Am. J. Physiol.*, 277:R607–R623, 1999.

[79] R. K. Ockner, R. M. Kaikaus, and N. M. Bass. Fatty acid metabolism and the pathogenesis of hepatocellular carcinoma: review and hypothesis. *Hepatology.*, 18:669–676, 1993.

[80] R. T. Okita, J. E. Clark, J. R. Okita, and B. S. S. Masters. *In Peroxisome Proliferator: Unique Inducers of Drug-Metabolising Enzymes, D. E. Moody (Ed)*, pages 37–49. CRC Press, Boca Raton, 1994.

[81] A. Lange, D. Gebremedhin, J. Narayanan, and D. Harder. 20-Hydroxyeicosatetraenoic acid-induced vasoconstriction and inhibition of potasium current in cerebral vascular smooth muscle is dependent on activation of protein kinase C. *J. Biol. Chem.*, 272 (43):27345–27352, 1997.

[82] S. Nowicki, S. L. Chen, O. Aizman, X. J. Cheng, D. Li, C. Nowicki, A. Nairn, P. Greengard, and A. Aperia. 20-hydroxyeicosatetraenoic acid (20-HETE) activates protein kinase C. Role in regulation of rat renal Na^+, K^+-ATPase. *J. Clin. Invest.*, 99:1224–1230, 1997.

[83] M. M. Muthalif, I. F. Benter, N. Karzoun, S. Fatima, J. Harper, M. R. Uddin, and K. U. Malik. 20-hydroxyeicosatetraenoic acid mediates calcium/calmodulin-dependent protein kinase II-induced mitogen-activated protein kinase activation in vascular smooth muscle cells. *Natl. Acad. Sci.*, 95:12701–12706, 1998.

[84] M. R. Uddin, M. M. Muthalif, N. A. Karzoun, I. F. Benter, and K. U. Malik. Cytochrome P450 metabolites metadiate norepinephrine-induced mitogenic pathway. *Hypertension.*, 31 (2):242–247, 1998.

[85] M. Alonso-Galicia. 20-HETE agonists and antagonists in the renal circulation. *Am. J. Physiol.*, 277:F790–F796, 1999.

[86] K. D. Croft, J. C. McGiff, A. Sanchez-Mendoza, and M. A. Carroll. Angiotensin II release 20-HETE from rat renal microvessels. *Am. J. Physiol. Renal Physiol.*, 279:F544–F551, 2000.

[87] M. M. Muthalif, I. F. Benter, Z. Khandekar, L. Gaber, A. Estes, S. Malik, J. H. Parmentier, V. Manne, and K. U. Malik. Contribution of Ras GTPase/kinase and cytochrome P450 metabolite to deoxycorticosterone-salt-induced hypertension. *Hypertension.*, 35 (2):457–463, 2000.

[88] A. O. Oyekan and J. C. McGiff. Functional response of the rat kidney to inhibition of nitric oxide synthesis: role of cytochrome P450-derived arachidonate metabolites. *Br. J. Pharmacol.*, 125:1065–1073, 1998.

[89] A. O. Oyekan, K. McAdward, and J. C. McGiff. Renal functional effects of endothelins: dependency on cytochrome P450-derived arachidonate metabolites. *Biol. Res.*, 31:209–215, 1998.

[90] K. Omata, N. G. Abraham, B. Escalante, and M. Lanaido Schwartzman. Age related changes in renal cytochrome P450 arachidonic acid metabolism in spontaneously hypertensive rats. *Am. J.Physiol.*, 162:F8–F16, 1992.

[91] M. H. Wang, F. Zhang, J. Marji, B. A. Zand, A. Nasjletti, and M. L. Schwartzman. CYP4A1 antisense oligonucleotide reduces mesenteric vascular reactivity and blood pressure in SHR. *Am. J. Physiol. Regulatory Integrative Comp. Physiol.*, 280:R255–R261, 2001.

[92] R. A. J. Sharma, B. G. Lake, and G. G. Gibson. Microsomal cytochrome P452 and the peroxisomal fatty acid beta-oxidation pathway in the rat by clofibrate and di-(2-ehtylhexyl)phthalate. *Biochem. Pharmacol.*, 37:1193–1201, 1988.

[93] R. A. J. Sharma, B. G. Lake, and G. G. Gibson. Co-induction of microsomal cytochrome P-452 induction and the peroxisome proliferation by hypolipidaemic agents in rat liver. *Biochem. Pharmacol.*, 37:1203–1206, 1988.

[94] I. Stupans, S. Kong, A. Kirlich, M. Murray, E. L. Bailey, B. R. Jones, and R. A. McKinnon. Hepatic microsomal enzyme activity in the koala and tamma wallaby:

high 17beta-hydroxysteroid oxidoreductase activity in koala liver microsomes. *Comp. Biochem. Physiol.*, 123(C):67–73, 1999.

[95] C. Barnett, G. G. Gibson, C. R. Wolf, P. R. Flatt, and C. Joannides. Induction of cytochrome P4501 and P450IV family proteins in streptozotocin-induced diabetes. *Biochem. J.*, 268:765–769, 1990.

[96] C. E. Neat, M. S. Thomassen, and H. Osmundsen. Effect of high fat diets on hepatic fatty acid oxidation in the rat-isolation of rat liver peroxisomes by vertical rotor centrifugation by using a selt generated, iso-osmotic, percoll gradient. *Biochem. J.*, 196:149–159, 1981.

[97] H. Iber, M. B. Sewer, T. B. Barclay, S. R. Mitchell, T. Li, and E. T. Morgan. Modulation of drug metabolism in infectious and inflammatory diseases. *Drug. Metab. Rew.*, 31(1):29–41, 1999.

[98] G. G. Gibson and B. G. Lack BG. *In Cytochrome P450, Methods Enzymology, M. R. Waterman and E. F. Johson (Eds)*, volume 206, chapter Induction protocol for the cytochrome P450IVA subfamily in animals and primary hepatocyte cultures, pages 353–364. Orlando, Florida: Academic Press, 1991.

[99] D. L. Kroetz, P. Yook, P. Costet, P. Bianchi, and T. Pineau. Peroxisome proliferator activated receptor α controls the hepatic CYP4A induction adaptive response to starvation and diabetes. *J. Biol. Chem.*, 273 (47):31581–31589, 1998.

[100] P. A. RaM and D. J. Waxman. Dehydroepiandrosterone 3 beta-sulphate is an endogenous activator of the peroxisome proliferation pathway: induction of cytochrome P-4504A and Acyl CoA oxidase mRNAs in primary rat hepatocyte culture and inhibitory effects of Ca (+2)-channel blockers. *Biochem. J.*, 301:753–758, 1994.

[101] N. Ohishi, S. Imaoka, and Y. Funae. Changes in content of P450 isozymes in hepatic and renal microsomes of the male rat treated with cis-diamminechloroplatinum hydroxylase. *Xenobiotica.*, 24:873–880, 1994.

[102] E. Rekka, E. O. Ayalogu, D. F. V. Lewis, G. G. Gibson, and C. Ioannides. Induction of hepatic microsomal CYP4A activity and of peroxisomal beta-oxidation by two non-steroidal anti-inflammatory drugs. *Arch. Toxicol. Nutr.*, 68:73–78, 1994.

[103] M. B. Sewer, D. R. Koop, and E. T. Morgan. Endotoxemia in rats is associated with induction of the P4504A subfamily and suppression of several other forms of cytochrome P450. *Drug. Metab. Dispos.*, 24:401–407, 1996.

[104] M. B. Sewer, D. R. Koop, and E. T. Morgan. Differential inductive and suppressive effects of endotoxin and particulate irritants on hepatic and renal cytochrome P450 expression. *Pharmacol. Exp. Ther.*, 280(3):1445–1454, 1997.

[105] T. Aoyama, J. M. Peters, M. Iritani, T. NakaJima, K. Furihata, T. Hashimoto, and F. J. Gonzalez. Altered constitutive expression of fatty acid-metabolizing enzymes in mice lacking the peroxisome proliferator-activated receptor alpha (PPAR-α). *J Biol Chem.*, 273:5678–5684, 1998.

[106] T. Hashimoto, T. Fujita, N. Usuda, W. Cook, C. Qi, J. M. Peters, F. J. Gonzalez, A. V. Yeldandi, M. S. Rao, and J. K. Reddy. Peroxisomal and mitochondrial fatty acid β-oxidation in mice nullizygous for both peroxisome proliferator-activated receptor α and peroxisomal fatty acyl-CoA oxidase. *J. Biol. Biochem.*, 274:19228–19236, 1999.

[107] J. K. Reddy and G. P. Mannaerts. Peroxisome lipid metabolism. *Annu. Rev. Nutr.*, 14:343–470, 1994.

[108] P. R. Ortiz de Montellano. *Cytochrome P450, Structure, Mechanism, and Biochemistry, 2nd Ed.* Plenum Press, New York, USA, 1995.

[109] T. Hashimoto. Peroxisomal β-oxidation: enzymology and molecular biology. *Ann. N.Y. Acad. Sci*, 804:86–98, 1996.

[110] G. P. Mannaerts, P. P. Van Veldhoven, and M. Casteels. Peroxisomal lipid degradation via β- and α-oxidation in mammals. *Cell Biochem. Biophys.*, 32:73–87, 2000.

[111] R. Chu, N. Usuda, M. K. Reddy, C. Liu, T. Hashimoto, K. Alvares, M. S. Rao, and J. K. Reddy. Functional expression of rat peroxisomal acyl-CoA oxidase in *Spodoptera frugiperda* cells. *Biochem. Biophys. Res. Com.*, 200:178–186, 1995.

[112] A. Uchiyama, T. Aoyama, K. KamiJo, Y. Uchida, and N. Kondo. Molecular cloning of cDNA encoding rat very long chain acyl CoA synthetase. *J. Biol Chem.*, 271:30360–65.

[113] H. van den Bosch, R. B. Schutgens, R. J. Wanders, and J. M. Tager. Biochemistry of peroxisomes. *Annu. Rev. Biochem.*, 61:157–197, 1992.

[114] J. K. Reddy and T. Hashimoto. Peroxisomal β-oxidation and peroxisome proliferator-activated receptor alpha: an adaptive metabolic system. *Annu Rev Nutr*, 21:193–230, 2001.

[115] P. B. Lazarow and C. de Duve. A fatty acyl-CoA oxidation system in rat liver peroxisomes: enhancement by clofibrate, a hypolipidermic drug. *Proc. Natl. Acad. Sci.*, 73:2043–46, 1976.

[116] M. Baes, S. Huyghe, P. Carmeliet, P. E. P. E. Declercq, D. Collen, and et al. Inactivation of the peroxisomal multifunctional protein-2 in mice impedes the degradation of not only 2-methyl-branched fatty acids and bile acid intermediates but also very long-chain fatty acids. *J. Biol. Chem.*, 275:16329–16336, 2000.

[117] E. Baumgart, J. C. Vanhooren, H. D. Fransen, F. Van Leuven, H. D. Fahimi, P.P Van Veldhoven, and G. P. Mannaerts. Molecular cloning and further characterisation of rat peroxisomal trihydroxycoprostanoyl-CoA oxidase. *J. Biochem.*, 320:115–121, 1996.

[118] C. Qi, Y. Zhu Y., J. Pan, N. Usuda, N. Maeda, A. V. Yeldandi, M. S. Rao, and T. Hashimoto. Absence of spontaneous peroxisome proliferation in enoyl-CoAhydratase/L-3-hydroxyacyl-CoAdehydrogenase deficient mouse liver. Further support for the role of fatty acyl CoA oxidase in PPAR-α ligand metabolism. *J. Biol. Chem.*, 274:15775–80, 1999.

[119] Http. http://www.peroxisome.org/Scientist/Biochemistry/matrixenzymesumary.html-5k-. 18-08-2000.

[120] T. G. Cooper and H. Beevers. β-oxidation of glyoxysomes from castor bean endosperm. *J. Biol. Chem.*, 244:3514–20, 1969.

[121] N. C. Inestrosa, M. Bronfman, and F. Leighton. Detection of peroxisomal fatty acyl-coenzyme A oxidase activity. *J. Biochem.*, 182:779–788, 1979.

[122] T. Osumui, T. Hashimoto, and N. Ui. Purification and properties of acyl CoA oxidase from rat liver. *J. Biochem.*, 87:1735–1746, 1980.

[123] T. Osumui and T. Hashimoto. The inducible fatty acid oxidation system in mammalian peroxisomes. *Trends. Biochem. Sci.*, 9:317–319, 1984.

[124] A. Kawashima, S. Tsubtani, S. Seyama, Y. Yamakawa, T. Osumi, T. Hashimoto, T. Kikuchi Aand T. Ando, and S. Okuda. Stereochemistry of dehydrogenation catalysed by acyl CoA oxidase. *J. Biochem.*, 88:1481–1486, 1980.

[125] S. Shin, K. Yasui, Y. Tani, and H. Yamada. Acyl CoA oxidase from Candida tropicalis. *Biochem. Biophys. Res. Comm.*, 91:108–113, 1979.

[126] N. E. Tolbert. Metabolic pathways in peroxisomes and glyoxysomes. *Ann. Rew. Biochem.*, 50:133, 1981.

[127] B. Gerhardt. *Planta*, 159:238–246, 1983.

[128] B. Gerhardt. *Methods Enzymol.*, 148:517–525, 1987.

[129] L. Schepers, P. P. Van Veldhoven, M. Casteels, J. H. Eyssen, and G. P. Mannaerts. Presence of three acyl CoA oxidases in rat liver peroxisomes- an inducible fatty acyl CoA oxidase, a non-inducible fatty acyl CoA oxidase and a non-inducible trihydroxycoprostanoyl-CoA oxidase,. *J. Biol. Chem.*, 265:5242–5246, 1990.

[130] P. P. V. Van Veldhoven, G. Vanhove, F. Dacremont, H. J. Eyssen, and G. P. Mannaerts. Identification and purification of a branched chain fatty acyl-CoA oxidase. *J. Biol. Chem.*, 266:24676–24683, 1991.

[131] P. P. V. Van Veldhoven, G. Vanhove, S. Assselberghs, H. J. Eyssen, and G. P. Mannaerts. Substrate specificities of rat liver peroxisomal acyl-CoA oxidase (inducible acyl-CoA oxidase), pristanoyl-CoA trihydroxycoprostanoyl-CoA oxidase. *J. Biol. Chem.*, 267:20065–20074, 1992.

[132] S. Miura, M. Mori, M. Takiguchi anf M. Tatibana, S. Furuta, S. Miyazawa, and T. Hashimoto. Biosynthesis and intracellular transport of enzymes of peroxisomal β-oxidation. *J. Biol. Chem.*, 259:6397–6402, 1984.

[133] S. Miyazawa, H. Hayashi, M. Hijikata, N Ishii, S. Furuta, H. Kagamiyama, T. Osumi, and T. Hashimoto. Complete nucleotid sequence of cDNA and predicted amino acid sequence of rat acyl-CoA oxidase. *J. Biol. Chem.*, 262:8131–8137, 1987.

[134] T. Osumui. Structure and expression of the gene encoding peroxisomal β-oxidation enzymes. *Biochimie*, 75:243–250, 1993.

[135] S. Miyazawa, T. Osumi, T. Hashimoto, K. Ohno, S. Miura, and Y. Fujiki. Peroxisome targeting signal of rat liver acyl-coenzyme A oxidase resides at the carboxy terminus. *Mol. Cell. Chem.*, 9:83–91, 1989.

[136] C-Y. Fan, J. Pan, N. Usuda, A. V. Yeldandi, M. S. Rao, and J. K. Reddy. Steatohepatitis , spontaneous peroxisome proliferation and liver tumors in mice lacking peroxisomal fatty acyl-CoA oxidase. *J. Biol. Chem.*, 273:15639–45, 1998.

[137] F. J. Gonzalez, M. P. Peters, and C. C. Cattley. Mechanism of action of the nongenotoxic peroxisome proliferators: role of the peroxisome proliferator-activated receptor α. *J. National Cancer Institute*, 90(22):1702–1709, 1998.

[138] N. Latruffe and J. Vamecq. Peroxisome proliferatore and peroxisome proliferator activated receptors (PPARs) as regulators of lipid metabolism. *Biochimie.*, 79:81–94, 1997.

[139] B. Desvergne and W. Wahli. Peroxisome proliferator-activated receptors: |uppercaseNuclear control of metabolism. *Endocr. Rev.*, 20(5):649–688, 1999.

[140] N. J. McKenna, R. B. Lanz, and B. W. O'Malley. Nuclear receptor coregulators: cellular and molecular biology. *Endocr. Rev.*, 20:321–344, 1999.

[141] S. A. Kliewer, K. Umesono, D. J. Noonan, R. A. Heyman, and R. M. Evans. Convergence of 9-cis retinoic acid and peroxisome proliferator signalling pathways through heterodimer formation of their receptors. *Nature*, 358:771–774, 1992.

[142] J. K. Reddy and R. Chu. Peroxisome proliferator-induced pleiotropic responses: pursuit of a phenomenon. *Annu. N.Y. Acad. Sci.*, 804:176–201, 1996.

[143] J. J. Zhang, U. Vinkemeier, W. Gu, D. Chakravarti, C. M. Horvath, and Jr. J. E. Darnell. Two contact regions between Start1 and CBP/p300 in interferon γ signaling. *Proc. Natl. Acad. Sci. USA*, 93:15092–15096, 1996.

[144] K. Yu, W. Bayona, C. P. Kallen H. P. Harding, C. P. Ravera, and G. McMahon et al. Differential activation of peroxisome proliferators by eicosanoids. *J Biol. Chem.*, 270:23975–83, 1995.

[145] K. L. Gearing, A. Crickmore, and J. Å. Gustafson. Structure of mouse peroxisome proliferator activated receptor a gene. *Biochem. Biophys. Res. Commu.*, 199:255–263, 1994.

[146] J. A. Gustafsson. *In : Peroxisomes, Biology and role in toxicology and disease*, chapter Fatty acid signalling of peroxisome proliferator activated receptor, Aspen Co. Symposium.

[147] P. Dowell, V. J. Peterson, T. M. Zabriskie, and M. Leid. Ligand induced peroxisome proliferator activated receptor alpha conformational change. *J. Biol. Chem.*, 272:2013–2020, 1997.

[148] P. R. Devchand, H. Keller, J. M. Peters, M. Vazquez, F. J. Gonzalez, and W. Wahli. The ppar-α leukotrien B4 pathway to inflammation control. *Nature*, 384:39–43, 1996.

[149] J. D. Tugwood, P. R. Holden, N. H. James, R. A. Prince, and R. A. Roberts. A peroxisome proliferator activated receptor alpha (PPAR-α) cDNA cloned from guinea-pig liver encodes a protein with similar properties to the mouse PPAR-alpha: implications for species differences in resp[onses to peroxisome proliferators. *Arch. Toxicol.*, 72:169–177, 1998.

[150] C. De-Duve. Introductory remarks. *Ann. N.Y. Acad Sci.*, 168:211–213, 1969.

[151] C. De-Duve. Evolution of the peroxisome. *Ann. N.Y. Acad Sci.*, 168:369–381, 1969.

[152] I. Issemann and S. Green. Activation of a member of the steroid hormone receptor superfamily by peroxisome proliferators. *Nature*, 347:645–650, 1990.

[153] O. Sabzevari, M. Hatcher, M. O'Sullivan, P. Kentish, and G. Gibson. Comparative induction of cytochrome P450 in rat hepatocyte culture by peroxisome proliferators, bifonazole and clofibrate. *Xenobiotica*, 25(4):395–403, 1995.

[154] J. Shepherd. Fibrates and statins in the treatment of hyperlipidaemia: an appraisal of their efficacy and safety. *Eur. Heart J.*, 16:5–13, 1995.

[155] T. Sher, H. Yi, O. W. McBride, and F. Gonzalez. cDNA cloning, chromosomal mapping, and functional characterisation of the human peroxisome proliferator activated receptor. *Biochemistry.*, 32:5598–5604, 1993.

[156] E. D. Barber, B. D. Astill, E. J. Moran, B. F. Schneider, T. J. B. Gray, B. G. Lake, and J. G. Evans. Peroxisome induction studies on seven phthalate esters. *Toxicol. Ind. Health*, 3:130, 1987.

[157] C. R. Elcombe. Species differences in the carcinogenecity and peroxisome proliferation due to trichloroethylene; a biochemical human hazard assessent. *Arch. Toxicol. Suppl.*, 8:6–17, 1985.

[158] J. K. Reddy and N. D. Lalwani. Carcinogenesis by hepatic peroxisome proliferators. Evaluation of the risk of hepatocarcinogenic drugs and industrial plasticisers to humans. *Crit Rev Toxicol*, 12:1–58, 1983.

[159] S. S. T. Lee, T. Pineau, J. Drago, E. J. Lee, J. W. Owens, D. L. Kroetz, P. M. Fernandez-Salguero, H. Westphal, and F. J. Gonzalez. Targeted disruption of the alpha isoform of the peroxisome proliferator-activated receptor gene in mice results in abolishment of the pleiotropic effects of peroxisome proliferators. *Mol. Cell Biol.*, 15:3012–3022, 1995.

[160] G. G. Gibson and B. G. Lack BG. *In Toxicology and Medicine.*, chapter Peroxisomes: Bology and Importance in Toxicology and Medicine. Taylor and Francis, London, 1993.

[161] P. Grasso. *In Peroxisomes: biology and importance vin toxicology and medicine, G. Gibson and B. N. K. Lake (Eds.)*, chapter Hepatic changes associated with peroxisome proliferation. Taylor and Francis Ltd, 1993.

[162] C. Dreyer, G. Krey, H. Keller, F. Givel, G. Helftenbein, and W. Wahli. Control of peroxisome β-oxidation pathway by a novel family of nuclear hormone receptors. *Cell*, 68:879–887, 1992.

[163] M. Gottlicher, E. Widmark, Q. Li, and J. Å. Gustafson. Fatty acids activate a chimera of the clofibric acid-activated receptor and the glucocorticoid receptor. *Proc. Natl. Acad. Sci USA*, 89:4653–4657, 1992.

[164] C. Qi, Y. Zhu Y., and J. K. Reddy. Peroxisome proliferator activated receptors, coactivators, and dowstream targets. *Cell Biochem. Biophys.*, 32:1085–91, 2000.

[165] C. K. Glass. Differential regconition of target genes by nuclear receptor monomers, dimers, and heterodimers. *Endocr. Rev.*, 15:391–407, 1994.

[166] E. F. Johnson, C. N. Palmer, and M. H. Hsu. The peroxisome proliferator-activated receptor: transcriptional activation of the CYP4A6 gene. *Ann. N. Y. Acad. Sci.*, 84:373–386, 1996.

[167] M. H. Hsu, C. M. Palmer, K. J. Griffin, and E. F. Johson. A single amino acid change in the mouse peroxisome proliferator activated receptor alpha alters transcriptional responses to peroxisome proliferators. *Mol. Pharmacol.*, 48(3):559–67, 1995.

[168] T. Lemberger, B. Staels, R. Saladin, B. Desverger, J. Auwerx, and W. Wahli. Regulation of the peroxisome proliferator activated receptor α gene by glucocorticoids. *J. Biol. Chem.*, 269:24527–24530, 1994.

[169] H. H. Steineger, H. N. Sorensen, J. D. Tugwood, S. Skrede, O. Spydevold, and K. M. Gautvik. Dexamethasone and insulin demonstrate marked and opposite regulation of the steady state mrna level of the peroxisome proliferator activated receptor (PPAR) in hepatic cells-hormonal modulation of of fatty acid induced transcription. *Eur. J. Biochem.*, 225:967–974, 1994.

[170] J. Berger, M. D. Leibowitz, T. W. Doebber, A. Elbrecht, B. Zhang, G. Zhou, C. Biswas, C. A. Cullinan, N. S. Hayes, Y. Li, M. Tanen, J. Ventre, M. S. Wu, G. D. Berger, R. Mosley, R. Marquis, C. Santini, S. P. Sahoo, R. L. Tolman, R. G. Smith, and D. E. Moller. Novel peroxisome proliferator activated receptor (PPAR) γ and PPAR δ ligands produce distinct biological effects. *J. Bio. Chem.*, 274:6718–6725, 1999.

[171] T. M. Willson and W. Wahli. Peroxisome proliferator activated receptor (PPAR) agonists. *Curr. Opin. Chem. Biol.*, 1:235–241, 1997.

[172] T. Osumui, J. K. Wen, and T Hashimoto. Two cis-acting regulatory sequences in the peroxisome proliferators responsive enhancer region of rat acyl CoA oxidase gene. *Biochem. Biophys. Res. Commun*, 175:866–871, 1991.

[173] J. D. Tugwood, I. Issemann, R. G. Anderson, K. Bundell, W. Mc Pheat, and S. Green. The mouse peroxisome proliferator activated receptor recognises a response element in the 5' flanking sequence of the rat acyl CoA oxidase gene. *EMBO J.*, 11:433–439, 1992.

[174] A. S. Muerhoff, K. J. Griffin, and E. F. Johnson. The peroxisome proliferator-activated receptor mediates the induction of CYP4A6, a cytochrome P450 fatty acid ω-hydroxylase, by clofibric acid. *J. Biol. Chem.*, 267:19051–19053, 1992.

[175] C. K. Glass and M. G. Rosenfeld. The coregulator exchange in transcriptional functions of nuclear receptors. *Genes Dev.*, 14:121–141, 2000.

[176] Y. Zhu, C. Qi, M. S. Rao, and J. K. Reddy. Isolation and characterisation of PBPx1, a protein that interacts with peroxisome proliferator activated receptor. *J. Biol. Chem.*, 272 (25):500–506, 1997.

[177] T. Hashimoto, W. S. Cook, C. Qi, A. V. Yeldandi, J. K. Reddy, and M. S. Rao. Defect in peroxisome proliferator-activated receptor α-inducible fatty acid oxidation determines the severity of hepatic steatosis in response to fasting. *J. Biol. Chem.*, 275:28918–28, 2000.

[178] S. Kersten, J. Seydoux, J. M. Peters, F. J. Gonzalez, B. Desvergne, and W. Wagli. Peroxisome proliferator activated receptor alpha mediates the adaptive response to fasting. *J. Clin. Invest.*, 103:1489–98, 1999.

[179] T. C. Leone, C. J. Weinheimer, and nD. P. Kelly. A critical role for the peroxisome proliferator activated receptor α in the cellular fasting response: the PPAR-α null mouse as a model of fatty acid oxidation disorders. *Proc. Natl. Acad. Sci. USA*, 96:7473–78, 1999.

[180] G. Martin, K. Schoonjans, A. M. Lefebvre, B. Staels, and J. Auwerx. Coordinate regulation of the expression of the fatty acid transport protein and acyl CoA synthetase genes by PPAR-alpha and PPAR-gamma activators. *J. Biol. Chem.*, 272:28210–7, 1977.

[181] K. Motojima, P. Passilly, J. M. Peters, F. J. Gonzalez, and N. Latruffe. Expression of putative fatty acid transporter genes are regulated by peroxisome proliferator activated receptor alpha and gamma activators in a tissue- and inducer-specific manner. *J. Biol. Chem.*, 273:16710–4, 1998.

[182] N. VuDac, K. Schoonjans, V. Kosykh, J. Dallongeville, J. C. Fruchart, B. Staels, and J. Auwerx. Fibrates increase human apolipoprotein A-II expression through activation of the peroxisome proliferator activated receptor. *J. Clin. Invest.*, 96:741–750, 1995.

[183] J. M. Peters, R. C. Cattley, and F. J. Gonzalez. Role of PPAR-alpha in the mechanism of action of action of the nongenotoxic carcinogen and peroxisome proliferator Wy-14,643. *Carcinogenesis.*, 18:2029–33, 1997.

[184] B. Ren, A. P. Thelen, J. M. Peters, F. J. Gonzalez, and D. P. Jump. Polyunsaturated fatty acid suppression of hepatic fatty acid synthetase and S14 gene expression does not require peroxisome proliferator activated receptor alpha. *J. Biol. Chem.*, 272:26827–32, 1997.

[185] D. R. Bell, R. Savory, N. J. Horley, A. I. Choudhury, M. Dickins, T. J. B. Gray, A. M. Salter, and D. R. Bell. Molecular basis of non-responsiveness to peroxisome proliferators: the guinea pig PPAR-α is functional and mediates peroxisome proliferator-induced hypolipidaemia. *Biochem. J.*, 332:689–693, 1998.

[186] M. H. Frick, O. Elo, K. Haapa, and O. P. Cytochrome P450 enzymes in vascular homeostasis. *Circulation Research*, 89:753–762, 2001.

[187] B. G. Lake, J. G. Evans, T. J. B. Gray, S. A. Korosi, and C. J. North. Comparative studies on nafenopin induced hepatic hepatic peroxisome proliferation in the rat, Syrian hamster, guinea pig and marmoset. *Toxicol. Appl. Pharmacol.*, 99:148–160, 1989.

[188] D. A. Stringer. *Monograph no.17 Hepatic peroxisome proliferation.* Brussels, Belgium, 1992.

[189] B. J. Blaauboer, C. W. van Holstein, R. Bleumink, W. C. Mennes, F. N. van Peit, S. H. Yap, J. F. van Pelt, A. A. van Iersel, A. Timmerman, and B. P. Schmidt. The effects of beclobric acid and clofibric acid on peroxisomal β-oxidation and peroxisome proliferation in primary culotures of rat, monkey, and human hepatocytes. *Biochem. Pharmacol.*., 40:521–528, 1990.

[190] C. R. Elcombe. Peroxisome proliferators: species differences in response of primary hepatocyte cultures. *Ann. N. Y. Acad. Sci.*, 804:628–35, 1996.

[191] M. F. Oliver. Strategy of reducing coronary risk and the use of drugs. *J. Cardiovasc. Pharmacol.*, 6 Suppl:S880–S887, 1984.

[192] E. Chinje, P. Kentish, B. Jarnot, M. George, and G. Gibson. Induction of CYP4A subfamily by perfluorodecanoic acid: the rat and the guinea-pig as susceptible and non-susceptible species. *Toxicol. Lett.*, 71:69–75, 1994.

[193] J. M. Makowska, G. G. Gibson, and F. Bonner. Species differences in ciprofibrate induction of hepatic cytochrome P450 CYP4A1 and peroxisome proliferation. *J. Biochem. Toxicol.*, 7:183–191, 1992.

[194] C. Pacot, M. Petit, M. Rollin, N. Behechti, M. Moisant, P. Deslex, J. Althoff, J. C. LOLhuguenot, and N. Latruffe. Differences between guinea-pig and rat in the liver

peroxisomal response to equivalent plasmatic level of ciprofibrate. *Arch. Biochem. Biophys.*, 327:181–188, 1996.

[195] J. A. Styles, M. Kelly, N. R. Pritchard, and C. R. Elcombe. A species comparison of acute hyperplasia induced by peroxisome proliferator methylclofenapate: involvement of the binucleated hepatocyte. *Carcinogenesis.*, 9:1647–1655, 1988.

[196] H. A. Dirvan, P. H. van den Broek, M. C. Peeters, J. G. Peters, W. C. Mennes, B. J. Blaauboer, J. Noordhoek, and F. J. Jongeneelen. Effects of the peroxisome proliferator mono(2-ethylhexyl)phthalate in primary hepatocyte cultures derived from rat, guinea-pig, rabbit and monkey. Relationship between interspecies differences in biotransformation and peroxisome proliferating potencies. *Biochem. Pharmacol.*, 45:2425–2434, 1993.

[197] N. D. Lalwani, M. K. Reddy, S. Ghosh, S. D. Barnard, J. A. Mollelo, and J. K. Reddy. Induction of fatty acid beta-oxidation and peroxisome proliferation in the liver of rhesus monkeys by DL-040, a new hypolipidemic agent. *Biochem. Pharmacol.*, 34:3473–82, 1985.

[198] J. K. Reddy, N. D. Lalwani, S. A. Qureshi, M. K. Reddy, and C. M. Moehle. Induction of hepatic peroxisome proliferation in non-rodent species, including primates. *Am. J. Pathol.*, 114:171–83, 1984.

[199] M. S. Rao and J. K. Reddy. Peroxisomal β-oxidation and Steatohepatitis. *Seminars in Liver Disease*, 21 (1):43–55, 2001.

[200] J. Ashby, A. Brady, C. R. Elcombe, B. M. Elliott, J. Ishmael, and J. Odum et al. Mechanistically-based human hazard assessment of peroxisome proliferator induced hepatocarcinogenesis. *Hum. Exp. Toxicol.*, 13:Suppl 2:S1–117, 1994.

[201] R. Mukherjee, L. Jow, D. Noonan, and D. P. McDonnell. Human and rat peroxisome proliferator activated receptors (PPARs) demonstrate similar tissue distribution but differences responsiveness to PPAR activator. *J. Steroid Biochem. Mol. Biol.*, 51:157–66, 1994.

[202] C. N. Palmer, M. H. Hsu, K. J. Griffin, J. L. Raucy, and E. F. Johnson. Peroxisome proliferator activated receptor-alpha expression in human liver. *Mol. Pharmacol.*, 53:14–22, 1998.

[203] J. D. Tugwood, T. C. Aldridge, K. G. Lambe, and N. Mcdonald N. J. Woodyatt. Peroxisome proliferator activated receptors: structure and function. *Ann. N. Y. Acad. Sci.*, 804:252–65, 1996.

[204] U. Varanasi, R. Chu, Q. Huang, R. Castellon, and A. Yeldandi. Identification of a peroxisome proliferator-responsive element upstream of the human peroxisomal fatty acid acyl-coenzyme A oxidase gene. *J. Biol. Chem.*, 271:2147–2155, 1996.

[205] N. J. Woodyatt, K. G. Lambe K. A. Myers, and J. D. Tugwood. The peroxisome proliferator (PP) response element upstream of the human acyl CoA oxidase gene is inactive among a sample human population: significance for species differences in response to PPs. *Carcinogenesis*, 20(3):369–72, 1999.

[206] A. Choudhury, S. Chahal, A. R. Bell, S. R. Tomlinson, R. A. Roberts, A. M. Salter, and D. R. Bell. Species differences in peroxisome proliferation; mechanisms and relevance. *Mutation Research*, 448:201–212, 2000.

[207] E. L. Ghisalberti. Bioactive acylphloroglucinol derivatives from Eucalyptus species. *Phytochemistry*, 41:7–22, 1996.

[208] I. D. Hum. *Digestive Physiology and Nutrition of Marsupials (Monographs on Marsupial Biology.* Cambridge University Press, Cambridge, UK, 1982.

[209] W. J. Foley. Digestion and metabolism in a small arboreal marsupial, the greater glider, (*Petauroides volans*) fed high terpene *Eucalyptus* foliage. *J. Comp. Physiol.*, B 157:355–362, 1987.

[210] S. Patel and J. Wiggins. Eucalyptus oil poisoning. *Arch. Dis. Child.*, 55:405–406, 1980.

[211] D. G. Spoerke, S. A. Vandenberg, S. C. Smolinske, K. Kulig, and B. H. Rumack. Eucalyptus oil: 14 cases of exposure. *Vet. Hum. Toxicol.*, 31:166–168, 1989.

[212] N. J. Webb and W. R. Pitt. *Eucalyptus* oil poisoning in childhood: 41 cases in southeast queenland. *J. Paediatr. Child. Health*, 29:368–371, 1993.

[213] M. E. McManus and K. F. Ilett. Mixed function oxidase activity in a marsupial, the quokka (*Setinix brachyrus*). *Drug Metabolism and Disposition*, 4:199–202, 1976.

[214] M. E. McManus and K. F. Ilett KF. Microsomal xenobiotic metabolism in marsupials. *Drug Metabolism and Disposition*, 5:503–509, 1977.

[215] R. M. Bolton and J. T. Ahokas. Mixed function oxidases in an Australian marsupials, the brush tail possum (*Trichosurus vulpecula*). *Arch. Environ. Contam. Toxicol.*, 33:83–89, 1997.

[216] R. M. Bolton and J. T. Ahokas. Ontogenic expression of detoxication enzymes in an Australian marsupials, the brush tail possum (*Trichosurus vulpecula*). *Comp. Biochem. Physiol. B Biochem. Mol. Biol.*, 118:239–347, 1997.

[217] A. Chadha and M. K. Madhava. Metabolism of geraniol and linalool in the rat and effects on liver and lung microsomal enzymes. *Xenobiotica*, 14:365–374, 1984.

[218] J. Jarvisalo and H. Vainio. Enhancement of hepatic drug biotransformation by a short-term intermittent turpentine exposure in the rat. *Acta. Pharmacol. Toxicol. Copenh.*, 46:32–36, 1980.

[219] H. J. Lich and C. J. Coscia CJ. Cytochrome P-450LM2 mediated hydroxylation of monoterpene alcohols. *Biochemistry*, 17:5638–5645, 1978.

[220] R. Boyle, S. McLean, W. J. Foley, and N. W. Davies. Comparative metabolism of the dietary terpene, p-cymene, in generalist and specialist folivorous marsupials. *J. Chem. Ecol.*, 26:2109–2126, 1999.

[221] R. V. Baudinette, J. F. Wheldrake, S. Hewitt, and D. Hawke. The metabolism of [C-14] phenol by native Australian rodents and marsupials. *Aust. J. Zool.*, 28:511–520, 1980.

[222] S. McLean, H. Galloway, S. Butleer, D. Whittle, and S. C. Nicol. Acetylation of sulphanilamide in four marsupials and a montreme. *Xenobiotica.*, 13:81–85, 1983.

[223] M. Miyazawa, M. Shindosumi, and T. Shimada. Oxidation of 1,8-cineole, the monoterpene cyclic ether originated from *Eucalyptus polybractea*, by the cytochrome **P450 3A** enzymes in rat and human liver microsomes. *Drug Metabolism and Disposition*, 29:200–205, 2001.

[224] P. Liapis, J. G. Pass, R. A. McKinnon, and I. Stupans. Characterisation of tolbutamide hydroxylase activity in the common brushtail possum, (Trichosurus vulpecula) and koala (Phascolarctos cinereus): inhibition by the eucalyptus terpene 1,8-cineole. *Comp. Biochem. Physiol.*, 127(C):351–357, 2000.

[225] B. Mojarrabi and P. I. MacKenzie. Characterisation of two UDP glucuronosyl transferases that are predominantly expressed in human colon. *Biochem. Biophy. Res. Comm.*, 247:704–709, 1998.

[226] S. Kong, R. A. McKinnon, B. Mojarrabi, and I. Stupans. Absence of type 1 11beta-hydroxysteroid dehydrogenase enzyme in koala liver. *Comp. Biochem. Physiol.*, 131(C):39–50, 2002.

[227] R. A. McKinnon, P. D. L. M. Hall, L. C. Quattrochi, R. H. Tukey, and M. E. McManus. Localisation of CYP1A1 and CYP1A2 messenger RNA in normal human liver and in hepatocellular carcinoma by in situ hybridisation. *Hepatology*, 14:848–856, 1991.

[228] A. M. Gebel and F. Oesch. Induction of peroxisome proliferator activated receptor by fenofibrate in rat liver. *FEBS, Lett*, 309:37–40, 1992.

[229] O. H. Lowry, N. J. Rosenbrough, A. L. Far, and R. J. Randall. Protein measurement with the Folin phenol reagent. *J Biol Chem.*, 193:265–75, 1951.

[230] U. K. Laemmli. Cleavage of structural protein during the assembly of the head of bacteriophage T4. *Nature*, 227:680–685, 1970.

[231] H. Towbin and J. Gordon. Immunoblotting and dot blotting: current status and outlook. *J. Immunol. Method.*, 72:331–349, 1984.

[232] M. Klingenberg. *In Methods of Enzymatic Analysis vol. 4, H. U. Bergmeyer (Ed.)*, chapter Nicotinamide-adenine dinucleotides (NAD, NADP, NADH. NADPH): spectrophotometric and fluorimetric methods, pages 2045–2059 and 2298–2299. Verlag Chemie, New York, 1974.

[233] G. L. Parker and T. C. Orton. *In Biochemistry, Biophysics and Regulation of Cytochrome P-450.*

[234] P. B. Lazarow. *In Methods in Enzymology, Lipids, vol. 72, J. J. Lowenstein (Ed.)*, chapter Assay of peroxisomal β-oxidation of fatty acids, pages 315–319. Academic Press Inc, New York, 1981.

[235] P. P. van Veldhoven. Activity measurements of acyl-CoA oxidases in human liver. *J. Inher. Metab. Dis.*, 18, Suppl. 1:125–134, 1995.

[236] P. Chomcynski and N. Sacchi. Single step method for RNA isolation by acid guanidinium thiocyanate-phenol-chloroform extraction. *Anal. Biochem*, 162:156–159, 1987.

[237] G. Lehrach, D. Diamond, J. M. Wozney, and H. Boedtker. RNA molecular weight determinations by gel electrophoresis under denaturing conditions, a critical reexamination. *J. Biol. Chem.*, 16:4743–4748, 1977.

[238] D. A. Goldgerg. Isolation and partial characterisation of drosophilia alcohol dehydrogenase gene. *Proceedings of the National Academy of Science of the United States of America*, 77:5794–5798, 1980.

[239] B. Seed. *In Genetic Engineering: Principles and Methods*, volume 4, chapter Attachment of nucleic acids to nitrocellulose and diazonium substituted supports. Plenum Publishing, New York, USA, 1982.

[240] J. Sambrook, E. F. Fritsch, and T. Miniatis. *Molecular Cloning: A lab manual, Vol 1, 2 and 3, 2nd Ed.* Cold Spring Habour Laboratory Press, New York, USA, 1989.

[241] S. J. Cork and W. J. Foley. *In Marsupial Biology, Recent Research, New Perspectives, N. K. Saunders and uppercaseL. A. Hinds (Eds.)*, chapter Digestive and metabolic adaptations of arboreal marsupxials for dealing with plant antinutrients and toxins, pages 204–226. UNSW Press, Sydney, 1997.

[242] D. Corrigan. *In Adverse Effect of Herbal Drugs, P. A. G. M. De Smet, R. Keller, R. Hansel and R. F. Chandler (Eds.)*, pages 125–133. Springer, Berlin, 1992.

[243] W. J. Freeland and H. Janzen. Strategies in herbivory by mammals: the role of plant secondary compounds. *Am. Nat.*, 108:269–87, 1974.

[244] D. V. Parker and H. Rahman. The effects of some terpenoids and other dietary anutrients on hepatic drug-metabolising enzymes. *J. Biochem.*, page 12, 1969.

[245] A. Jori, A. Bianchetti, and P. E. Prestini. Effects of essential oils on drug metabolism. *Biochem. Pharmacol.*, 18:2081–2085, 1969.

[246] A. Jori and G. Briatico. Short communication: Effects of eucalyptol on microsomal enzyme activity of foetal and newborn rats. *Biochem. Pharmacol.*, 22:543–544, 1973.

[247] T. Hiroi, Y. Miyazaki, Y. Kobayashi, S. Imaoka, and Y. Funae. Induction of hepatic P450s in rat by essential wood and leaf oils. *Xenobiotica*, 25:457–67, 1995.

[248] A. C. A. X. De-Oliveira, L. F. Ribeiro-Pinto, S. S. Otto, A. Goncalves, and F. J. R. Paumgartten. Induction of liver monoxygenases by β-myrcene. *Toxicology*, 124:135–140, 1997.

[249] M. Shin, N. Iwamoto, M. Yamashita, K. Sano, and C. Umezawa. Pyridine nucleotide levels in the liver of rats fed clofibrate- or pyrazinamide-containing diets. *Biochem. Pharmacol.*, 55:367–371, 1998.

[250] M. Shin, M. Ohnishi, S. Iguchi, and C. Umezawa. Peroxisome-proliferator regulates key enzymes of the tryptophan-NAD+ pathway. *Toxicol. Appl. Pharmacol.*, 158:71–80, 1999.

[251] F. Labrie, V. Luu-The, S. X. Lin, C. Labrrie, J. Simard, R. Breton, and A. Belanger. The key role of 17 beta-hydroxysteroid dehydrogenases in sex steroid biology. *Steroids*, 62:148–158, 1997.

[252] P. F. Sterchele, H. Sun, R. E. Peterson, and J. P. V. Heuvel. Regulation of peroxisome proliferator-activated receptor alpha mRNA in rat liver. *Arch. Biochem. Biophy.*, 326:281–289, 1996.

[253] M. A. Correia. *In Cytochrome P450: Structure, Mechanism, and Biochemistry, Ortiz de Montellano (Ed).* Appendix B: Rat and Human Liver Cytochrome P450. Substrate and Inhibitor Specificities and Functional Markers. Plenum Press, New York, USA, 1995.

[254] S. E. Clarke, S. J. Baldwin, J. C. Bloomer, A. D. Ayrton, R S. Sozio, and R. J. Chenery. Lauric acid as a model substrate for the stimultaneous determination of cytochrome P450 2E1 and 4A in hepatic microsomes. *Chem. Res. Toxicol.*, 7: 836-842, 1994.

[255] J. L. Boucher, M. Delaforge, J. P. Salaun, F. Pinot, F. Durst, P. Pflieger, and C. Mioskowski. In vitro hydroxylation and epoxidation of some isomeric lauric acid analogs by rat liver microsomes. Identification of metabolites and and effects of clofibrate or phenobarbital pretreatment. *Drug Metab. Dispo.*, 24:462–468, 1996.

[256] D. R. Bell, R. G. Bars, G. G. Gibson, and C. R. Elcombe. Localisation and differential induction of cytochrome-p450iva and acyl-coa oxidase in rat liver. *Biochem. J.*, 275:247–252, 1991.

[257] D. R. Bell and C. R. Elcombe. Induction of acyl-CoA oxidase and cytochrome-P4504A1 RNA in rat primary hepatocyte culture by peroxisome proliferators. *Biochem. J.*, 280:249–253, 1991.

[258] R.G. Bars, D.R. Bell, and C.R. Elcombe. Induction of cytochrome P450 and peroxisomal enzymes by clofibric acid in vivo and in vitro. *Biochem. Pharmacol.*, 45:2045–2053, 1993.

[259] T. F. Kalhorn, K. E. Thummel, S. D. Nelson, and J. T. Slattery. Analysis of oxidised and reduced pyridine dinucleotides in rat liver by high-performance liquid chromatography. *Anal. Biochem.*, 151:343–347, 1985.

[260] A. Chander, K. R. Dhariwal, R. Viswanathan, and T. A. Venkitasubramanian. Pyridine nucleotides in lung and liver of hypoxic rats. *Life Sci.*, 26:1935–1945, 1980.

[261] S. Yu, W. Q. Cao, P. Kashireddy, K. Meyer, Y. Jia, Dd. Hughes, Y. Tan, J. Yeng, A. V. Yeldandi, M. S. Rao, R. H. Costa, F. J. Gonzalez, and J. K. Reddy. Human peroxisome proliferator-activated receptor alpha (PPAR-alpha) supports the induction of peroxisome proliferation in PPAR-α deficient mouse liver. *J. Biol. Chem.*, 276:42485–91, 2001.

[262] U. Hoch and P. R. Ortiz de Montellano. Covalently linked heme in cytochrome P4504A fatty acid hydroxylase. *J. Biol. Chem.*, 276:11339–11346, 2001.

[263] A. M. Lesk, M. Levitt, and C. Chothia. Alignment of the amino acid sequences of distantly related proteins using variable gap penalties. *Protein Eng.*, 1:77–78, 1986.

[264] H. M. Berman, J. Westbrook, Z. Feng, G. Gilliland, T. N. Bhat, H. Weissig, I. N. Shindyalov, and P. E. Bourne. The Protein Data Bank. *Nucl. Acids Res.*, 28:235–242, 2000.

[265] Http. http://www.rcbs.org/pdb/.

[266] D. F. Lewis, E. Watson, and B. G. Lake. Evolution of the cytochrome p450 superfamily: sequence aligments and pharmacogenetics. *Mutat. Res.*, 410:245–270, 1995.

[267] C. N. Palmer, T. H. Richardson, K. J. Griffin, M. H. Hsu, A. S. Muerhoff, J. E. Clark, and E. F. Johnson. Characterisation of a cDNA encoding a human kidney, cytochrome P450 4A fatty acid ω-hydroxylase and the cognate enzyme expressed in Escherichia coli. *Biochimica et Biophysica Acta*, 1172:161–166, 1993.

[268] P. A. Loughran, L. J. Roman, R. T. Miller, and B. S. Masters. The kinetic and spectral characterization of the E. coli-expressed mammalian CYP4A7: cytochrome b5 effects vary with substrate. *Arch. Biochem. Biophys.*, 385:311–321, 2001.

[269] L. J. Roman, C. N. Palmer, J. E. Clark, A. S. Muerhoff, K. J. Griffin, E. F. Johnson, and B. S. Masters. Expression of rabbit cytochrome P4504A which catalyse the omega-hydroxylation of arachidonic acid, fatty acids and prostaglandins. *Arch. Biochem. Biophys.*, 307:57–65, 1993.

[270] J. R. Okita, S. B. Johson, P. J. Castle, S. C. Dezellem, and R. T. Okita. Improved separation and immunodetection of rat cytochrome P450 4A forms in liver and kidney. *Drug Metabolism and Disposition*, 25:1008–1012, 1997.

[271] Y. Suzuki, M. Iai, A. Kamei, Y. Tanabe, S. Chiba, S. Yamaguchi, S. Zbang, Y. Takemoto, N. Shimozawa, and N. Kondo. Peroxisomal acyl CoA oxidase deficiency. *The Journal of Pediatrics*, 140:128–130, 2002.

[272] L. T. Braiterman, P. A. Watkins, A. B. Moser, and K. D. Smith. Peroxisomal very long chain fatty acid β-oxidation activity is determined by the level of adrenodeukodystrophy protein (ALDP) expression. *Mol. Genet. Metab.*, 66:91–99, 1999.

[273] B Fournier, J. Saudubray, B. Benichou, S. Lyonnet, A. Munnich, H. Clevers, and B. T. Poll The. Large delection of the peroxisomal acyl-CoA oxidase gene in Pseudoneonetal Adrenoleukodystrophy. *J. Clin. Invest.*, 94:526–531, 1994.

[274] T. Aoyama, Y. Souri, T. Kamijo, S. Ushikubo, and T. Hashimoto. Peroxisomal acyl-coenzyme A oxidase is a rate-limiting enzyme in a very-long-chain fatty acid β-oxidation system. *Biochem. Biophys. Res. Com.*, 201:1541–1547, 1994.

[275] C. Nohammer, Y. El-Shabrawi, S. Schauer, M. Hiden, M. Berger, S. Forss-Petter, E. Winter, R. Eferl, R. Zechner, and G. Hoefler. cDNA cloning and analysis of tissue-specific expression of mouse peroxisomal straight-chain acyl-CoA oxidase. *Eur. J. Biochem.*, 267:1254–60, 2000.

[276] T. Aoyama, K. Tsushima, M. Souri, T. Kamijo, Y. Suzuki, N. Shimozawa, T. Orii, and T. Hashimoto. Molecular cloning and functional expression of a human peroxisomal acyl-coenzyme A oxidase. *Biochem. Biophys. Res. Com.*, 198:1113–1118, 1994.

[277] C. Setoyama, H. Tamaoki, Y. Nishina, K. Shiga, and R. Miura. Functional expression of two forms of rat acyl-CoA oxidase and their substrate specificities. *Biochem. Biophys. Res. Com.*, 217:482–487, 1995.

[278] P. P. Van Veldhoven, P. V. Rompuy, M. Fransen, B. D. Bethune, and G. P. Mannaerts. Large-scale purification and further characterisation of rat pristanoyl-coa oxidase. *J. Biochem.*, 222:795–801, 1994.

[279] U. Varanasi, R. Chu, Q. Huang, R. Castellon, and A. V. Yeldandi. Isolation of the human peroxisomal acyl-CoA oxidase gene: Organisation, promoter analysis, and chromosomal localisation. *Proc. Natl. Acad. Sci. USA.*, 91:3107–3111, 1994.

[280] K. Okazaki, T. Takechi, N. Kambara, S. Fufui, I. Kubota, and T. Kamiryo. Two acyl-coenzyme A oxidase in peroxisomes of the yeast candida tropicalis : primary structures deduced from genomic DNA sequence. *Proc. Natl. Acad. Sci.*, 83:1232–1236, 1986.

[281] M. A. Hooks, F. Kellas, and I. A. Graham. Long-chain acyl-CoA oxidases of Arabidopsis. *The Plant journal*, 20:1–13, 1999.

[282] M. Casteels, L. Schepers, P. P. V. Veldhoven, H. J. Eyssen, and G. P. Mannaerts. Separate peroxisomal oxidases for fatty acyl-CoAs and trihydroxycoprostanoyl-CoA in human liver. *J. Lipid. Res.*, 31:1865–1872, 1990.

[283] M. Souri, T. Aoyama, and T. Hashimoto. A sensitive assay of acyl-Coenzyme A oxidase by coupling with beta-oxidation multienzyme complex. *Anal. Biochem.*, 221:362–367, 1994.

[284] C. Qi, Y. Zhu Y., J. Pan, N. Usuda, N. Maeda, A. V. Rao, J. K. Reddy, and T. Hashimoto. Peroxisomal β-oxidation and peroxisome proliferator-activated receptor alpha: an adaptive metabolic system. *Annu Rev Nutr.*., 21:193–230, 2001.

[285] T. C. Aldridge, J. D. Tugwood, and S. Green. Identification and characterisation of DNA elements implicated in the regulation of CYP4A1 transcription. *Biochem. J.*, 306:473–479, 1995.

[286] E. F. Johnson, C. N. Palmer, and M. H. Hsu. The peroxisome proliferator-activated receptor: transcriptional activation of the CYP4A6 gene. *Ann N Y Acad Sci.*, 804:373–386, 1996b.

[287] B. G. Lake. Peroxisome proliferation: current mechanisms relating to nongenotoxic carcinogenesis. *Toxicol. Lett.*, 82-83:673–81, 1995.

[288] C. De-Duve and P. Baudhuin. Peroxisomes (microbodies and related particles). *Physiol. Rew.*, 46:323, 1966.

[289] D. E. Moody and J. K. Reddy. Morphometric analysis of the ultrastructural changes in rat liver induced by the peroxisome proliferator SaH 42-348. *J. Cell Biol.*,. 71:768–780, 1976.

[290] J. Rhodin. *Corelation and ultrastructural organisation and functions in normal and experimentally changed peroxisomal convoluted tubube cells of the mouse kidney.* Institutet Stockholm, Sweden, 1954.

[291] C. Rouiller and W. Bernhard. " Microbodies" and the problem of mitochondrial regeneration in liver cells. *J. Biophys. Biochem. Cytol. Suppl.*, 2:355, 1956.

[292] J. M. Allen and M. Beard. α-hydroxy acid oxidase: localisation in the renal microbodies. *Science.*, 149:1507, 1965.

[293] Z. Hruban and M. Jr. Rechcigl. Microbodies and related particles. Morphology, biochemistry and physiology. *Int. Rev. Cytol. Suppl.*, 1:20, 1969.

[294] T. K. Shnitka. Comparative ultrastructure of hepatic microbodies in some mammals and birds in relation to species difference in uricase activitypyridine nucleotide levels in the liver of rats fed clofibrate- or pyrazinamide-containing diets. *J. Ultrastruct. Res.*, 16:598, 1966.

[295] C. De-Duve. Functions of microbodies (peroxisomes). *J. Cell Biol.*, 27:25A, 1965.

[296] C. De-Duve. Exploring cells with a centrifuge. *Science.*, 189:186, 1975.

[297] F. Leighton, B. Poole, H. Beautay, P. Baudhuin, J. W. Coffey, S. Fowler, and C. de-Duve. Cytochrome P450x. Structure, Function and Mechanism. The large scale separation of peroxisomes, mitochondria, and lysosomes from the livers of rats injected with Triton WR-1339. *J. Cell Biol.*, 37:482, 1968.

[298] A. B. Novikoff and S. Goldfischer. Visualisation of peroxisomes (microbodies) and peroxisomes and mitochondria with diaminobenzidine. *J. Histochem. Cytochem.*, 17:675, 1969.

[299] H. Beevers. Microbodies in higher plants. *Ann. Rev. Plant Physiol.*, 30:159, 1979.

[300] J. K. Reddy and T. P. Krishnakantha. Hepatic peroxisome proliferation: induction by two novel compounds structurally unrelated to clofibrate. *Science*, 190:787–230, 1975.

[301] P. B. Lazarow. Rat liver peroxisomes catalyse the β-oxidation of fatty acids: enhancement by clofibrate, a hypolipidermic drug. *J. Biolo.Chem.*, 253:1522, 1978.

[302] T. Osumui and T. Hashimoto. Peroxisomal β-oxidation of rat liver. Copurification of enoyl-CoA hydratase and 3-hydroxyacyl CoA dehydrogenase. *Biochem. Biophys. Res. Commun.*, 89:580, 1979.

[303] B. Chance, H. Sies, and A. Boveris. Hydroperoxide metabolism in mammalian organs. *Physiol. Rev.*, 59:527, 1979.

[304] Jr. R. C. Graham and M. J. Karnovsky. The histochemical demonstration of uricase activity. *J. Histochem. Cytochem.*, 13:448, 1965.

[305] F. Roels, B. D. Prest, and G. D. Prest. Liver and chorion cytochemistry. *J. Inher. Metab. Dis.*, 18, Suppl. 1:155–171, 1995.

[306] M. A. Hayat. *Principles and Techniques of Electron Microscopy*, pages 1–137. The MacMillan Press Ltd. London, 1989.

Available online at www.sciencedirect.com
SCIENCE DIRECT®
Gene 309 (2003) 91–99
GENE
AN INTERNATIONAL JOURNAL ON GENES AND GENOMES
www.elsevier.com/locate/gene

Identification and cloning of two forms of liver peroxisomal fatty *Acyl CoA Oxidase* from the koala (*Phascolarctos cinereus*)

Suong Ngoc Thi Ngo, Ross Allan McKinnon*, Ieva Stupans

Centre for Pharmaceutical Research, College of Pharmacy, University of South Australia, City East Campus, North Terrace, Adelaide, SA 5000, Australia

Received 15 October 2002; received in revised form 10 February 2003; accepted 18 February 2003
Received by T. Gojobori

Abstract

In the present study, the cloning, expression and characterization of the rate-limiting enzyme of the peroxisomal β-oxidation spiral, acyl CoA oxidase (AOX), from koala (*Phascolarctos cinereus*) liver is described. It has been previously reported that peroxisomal cyanide-insensitive palmitoyl-CoA oxidation activity was absent in koala liver [Comp. Biochem. Physiol. (C) 127 (2000) 327]. This activity is a measure of the overall peroxisomal β-oxidation minus the final step catalysed by thiolase. Two 2039 bp koala liver *AOX* cDNAs, designated *AOX1* and *AOX2*, were cloned by reverse transcription–polymerase chain reaction and rapid amplification of cDNA ends. The koala *AOX* cDNAs encode proteins of 662 amino acids. Transfection of the koala *AOX* cDNAs into Cos-7 cells resulted in the expression of proteins with palmitoyl-CoA oxidase activity. The apparent K_m values for *AOX1* and *AOX2* cDNA-expressed enzymes were 28 and 38 μM, respectively, which are within the range of order of magnitude reported for rat and human purified AOX enzymes (approximately 10 μM). Northern analysis, utilizing the koala *AOX1* cDNA as probe, detected a more intense AOX mRNA band in the koala liver as compared to rats and humans. Southern blot analysis of liver genomic DNA samples revealed a single *AOX* gene fragment of less than 14 kb in koalas, rat and humans, suggesting a single *AOX* gene. Collectively, the results of this study suggest that the absence of peroxisomal cyanide-insensitive palmitoyl-CoA oxidation activity in the koala liver is possibly due to deficiencies of one or more enzymes downstream of acyl-CoA oxidase and/or deficiencies of mitochondrial β-oxidation enzymes.
© 2003 Elsevier Science B.V. All rights reserved.

Keywords: Palmitoyl-coenzyme A; Peroxisomal β-oxidation; Reverse transcription–polymerase chain reaction; Rapid amplification of cDNA ends

1. Introduction

Peroxisomes are single membrane bound cytoplasmic organelles that participate in a variety of metabolic processes. These organelles are present in virtually all eukaryotic cells and are most abundant in mammalian liver and kidney. The most extensively characterized process performed by peroxisomes is fatty acid β-oxidation. Via β-oxidation, peroxisomes play an essential role in the metabolism of lipids and also in bile acid synthesis (Aoyama et al., 1998).

Peroxisomal β-oxidation is responsible for the chain-shortening oxidation of a variety of acyl-coenzyme A (CoA) substrates. These include long-chain and very long-chain fatty acyl-CoAs, long-chain dicarboxylyl-CoAs, the CoA esters of eicosanoids, 2-methyl-branched fatty acyl-CoAs, and the CoA esters of the bile acid intermediate di- and tri-hydroxycoprostanoic acids (Reddy and Hashimoto, 2001). In this process, hydrogen peroxide is generated. Very long chain fatty acids are oxidized predominantly, if not exclusively, in peroxisomes; long chain fatty acids are

Abbreviations: A, adenosine; aa, amino acid(s); AOX, acyl coenzyme A oxidase; bp, base pair(s); BSA, bovine serum albumin; C, cytidine; cDNA, DNA complementary to RNA; CMV, cytomegalovirus; CYP, cytochrome P450; DMEM, Dulbecco's modified Eagle's medium; dNTP, deoxyribonucleoside triphosphate; EDTA, ethylenediaminetetraacetic acid; FAD, flavine adenine dinucleotide; G, guanosine; HVA, homovanillic acid; MOPS, 3-(*N*-Morpholino) propane-sulfonic acid; NEM, ethylmaleimide; RACE, rapid amplification of cDNA ends; RT–PCR, reverse transcription–polymerase chain reaction; SDS, sodium dodecyl sulphate; T, thymidine; U, uridine; UPM, universal primer mix; UTR, untranslated region(s).

* Corresponding author. Tel.: +61-8-8302-2372; fax: +61-8-8302 2389.
E-mail address: ross.mckinnon@unisa.edu.au (R.A. McKinnon).

0378-1119/03/$ - see front matter © 2003 Elsevier Science B.V. All rights reserved.
doi:10.1016/S0378-1119(03)00491-8

Table 1
Details of oligonucleotide primers

Name	Sequences (5′–3′)	Direction	Origin[a]	Accession no.
UPM*	CTAATACGACYCACTATAGGGCAA GCAGTGGTAACAACGCAGAGT (0.4 μM)	Sense	–	–
	CTAATACGACTCACTATAGGGC (2 μM)	Sense	–	–
kAOXf2	GAATTCACGGAACTCATCTTCGAGG	Sense	(+)479–(+)498	UO7866[b]
kAOXr2	GAATTCGTGCCTCACTTGCTCGAACA	Antisense	(+)1621–(+)1640	UO7866[b]
kAOX3′f	CGAGCAGCCCGATTAGTAGA	Sense	(+)1532–(+)1551	AF463453[c]
kAOX3′r	CTTCAGAGCTTCGACTGCAG	Antisense	(+)2021–(+)2040	UO7866[b]
kAOX5′r	GGTTTTCCCAAGTCCACCAG	Antisense	(+)588–(+)607	AF463453[c]
kAOXf	CCGCTCGAGTTCTGATCGTCGTCACCTTCTGC	Sense	(−)41–(−)18	AF463453[c]
kAOXr	AAAAAGGAAAAGCGGCCGCCTTCACAGCT TAGACTGCAG	Antisense	(+)1969–(+)1988	AF463453[c]
rAOXf	CCGCTCGAGCATGAACCCCGACCTGCGCAA	Sense	(+)1–(+)20	J02752[d]
rAOXr	AAAAGGAâ = AAAGCGGCCGCCCAGGGA AACTTCAAAGCT	Sense	(−)1978–(+)1997	J02752[d]
M13	GTAAAACGACGGCCAGT	Sense	–	–
M13r	CACACAGGAAACAGCTATGACCATG	Antisense	–	–
T_3	AATTAACCCTCACTAAAGGG	Sense	–	–
T_{7PCI}	TTAATACGACTCACTATAGGC	Antisense	–	–

[a] Corresponding to the position of the nucleotides relative to the start codon (designated +1).
[b] GenBank accession number of human fatty AOX mRNA (Aoyama et al., 1994), degenerate primers were derived from the alignment of *AOX* cDNAs from rat, human and mouse with the origine relative to human *AOX* cDNA.
[c] GenBank accession number of koala AOX mRNA (Ngo et al., 2000, direct submission).
[d] GenBank accession number of rat AOX mRNA (Miyazawa et al., 1987).

oxidized predominantly in mitochondria (Mannaerts et al., 2000).

The peroxisomal β-oxidation spiral is divided into two interconnected pathways, based on the substrate specificity of the participating enzymes (Baes et al., 2000; Qi et al., 2001). The L-hydroxy specific classical β-oxidation pathway acts on straight chain saturated fatty acyl-CoAs, whereas the D-hydroxy-specific β-oxidation pathway utilizes branched chain acyl-CoAs as substrates (Baes et al., 2000; Qi et al., 2001). Of these two β-oxidation systems, the enzymes of the L-hydroxy specific classical pathway, including the H_2O_2-generating fatty acyl-CoA oxidase (AOX), the L-enoyl-CoA hydratase/3-hydroxyacyl-CoA dehydrogenase bifunctional enzyme and 3-ketoacyl-CoA thiolase, are markedly induced in the liver of rats and mice by a diverse group of chemicals collectively termed peroxisome proliferators (Qi et al., 2001).

Among the inducible enzymes of the peroxisomal β-oxidation pathway, fatty acyl CoA oxidase is the first and rate-limiting enzyme. This enzyme is critical for completion of straight chain fatty acid β-oxidation. It has been previously reported that in the liver of the Australian marsupial koala (*Phascolarctos cinereus*), peroxisomal cyanide-insensitive palmitoyl-CoA oxidation is absent (Ngo et al., 2000). This is a measure of the overall peroxisomal β-oxidation activity minus the final step catalysed by thiolase. In the present study, we have focused on the molecular characterization of the koala liver fatty acyl-CoA oxidase. We have investigated the hypothesis that koala liver expresses active AOX proteins and that the absence of peroxisomal cyanide-insensitive palmitoyl-CoA oxidation is due to deficiency of one or more of the non-rate limiting enzymes down stream of acyl-CoA oxidase.

2. Materials and methods

2.1. Materials

Oligonucleotide primers for polymerase chain reaction (PCR) were custom-made by Sigma Genosys (Castle Hill, Australia). The SMART RACE cDNA Amplification kit was purchased from Clontech Laboratories (Palo Alto, CA, USA). mRNA purification kit and ultra-pure dNTPs were purchased from Amersham Pharmacia Biotech (USA). pCI-neo mammalian expression vector, restriction enzymes and DNA markers were obtained from Promega (Madison, WI, USA). QIAfilter midiprep spin kit was obtained from Qiagen (Melbourne, Australia). The Gigaprime DNA labelling kit was purchased from Geneworks (Adelaide, Australia). Palmitoyl-CoA, homovanillic acid (HVA), flavine adenine dinucleotide (FAD), ethylmaleimide (NEM), peroxidase, defatted bovine serum albumin (BSA), uric acid, and uricase were obtained from Sigma (St. Louis, MO, USA). Solvents and other chemicals were at least of analytical reagent grade.

2.2. Human and animal hepatic tissues

Livers were scavenged from six male road injured koalas (*Phacoslarctos cinereus*) and tammar wallabies (*Macropus eugenii*), a possum (*Trichosurus vulpecular*) and a bandicoot

(*Isoodon obesulus*), ultimately euthanized using pentobarbital. Male Hooded Wistar rats were used as the source of rat liver. All animals were sexually mature and the Ethic Committees of the appropriate institutions have approved the use of these tissues. Human liver tissue was obtained from a male renal transplant donor from the Flinders Medical Centre (Adelaide, Australia). Details of human liver tissue (H21) have been previously published (McKinnon et al., 1991). Livers from all species were quickly removed at the time of death, frozen in liquid nitrogen and stored at −80 °C.

2.3. Cloning and sequencing of full length koala liver acyl CoA oxidase (AOX) cDNAs

Total RNA was isolated from koala and rat livers by a modification of the method of Chomcynski and Sacchi (1998). Purification of mRNA from total RNA samples was performed using a mRNA purification kit (Amersham Pharmacia, USA) as per the manufacturer's protocol. Koala first-strand cDNA was synthesized using the First-strand cDNA kit (Amersham Pharmacia, USA) according to the manufacturer's instructions. Degenerate primers were derived from *AOX* cDNA sequences from other species in the GenBank database (Table 1). The following overlapping koala hepatic *AOX* cDNA fragments were amplified by reverse transcription polymerase chain reaction (RT–PCR): a 1161 bp cDNA fragment (position 479–1640 within the coding region of the human *AOX* cDNA) using kAOXf2 and kAOXr2 degenerate primers; a 3′-end 550 bp cDNA fragment (position 1532–2040 within the coding region of the human *AOX* cDNA) including the stop codon TGA using degenerate reverse primer kAOX3′r and gene specific forward primer kAOX3′f, derived from the 1161 bp *AOX* cDNA sequence. The conditions for PCR amplifications of the 1161 bp cDNA fragment were: denaturing at 94 °C for 5 min; 30 cycles of 94 °C for 45 s, 55 °C for 45 s, and 72 °C for 1 min; final extension at 72 °C for 10 min. The cycling conditions for amplification of the 3′-end were similar to that of the 1.2 kb *AOX* cDNA fragment except that Q solution (Qiagen) was included and the gene specific forward primer kAOX3′f was added to the PCR reactions after reaction mixtures were cycled for five cycles of 94 °C for 45 s, 55 °C for 45 s, and 72 °C for 1 min, in order to enhance yield and specificity. To obtain the 5′-end of koala AOX mRNA, a RACE protocol was applied using SMART RACE cDNA Amplification kit (Clontech) according to the manufacturer's protocol. Koala 5′-end *AOX* cDNA fragments were amplified utilizing Universal Primer Mix (UPM) and gene specific reverse primer kAOX5′r (Table 1), based on the koala 1.2 kb *AOX* cDNA sequence. Touchdown PCR conditions for RACE reactions were as follows: 5 cycles of 94 °C for 5 s and 72 °C for 2 min; 5 cycles of 94 °C for 5 s, 70 °C for 10 s and 72 °C for 2 min, and 32 cycles of 94 °C for 5 s, 68 °C for 10 s and 72 °C for 2 min. Two 5′ cDNA fragments of sizes 850 and 650 bp were amplified. Amplified DNA fragments were subcloned into pGEM-T vector (Promega, Madison, WI) in accordance with the manufacturer's instructions and subsequently sequenced using M13 universal (M13) and M13 reverse (M13r) sequencing primers (Table 1).

Full-length koala *AOX* cDNAs were then amplified by RT–PCR, using forward primer kAOXfF and reverse primer kAOXfR (Table 1), derived from the 5′- and 3′-sequences obtained. Restriction sites, *Xho*I and *Not*I, were included at the 5′- and 3′-ends of the forward and reverse primers, respectively, to facilitate subsequent directional cloning into the pCI-neo expression vector. KAOXfF and kAOXfR primers amplified a 2039 bp fragment corresponding to the entire coding region of the koala AOX, including the start and stop codons and 51 bp upstream of the start codon. PCR reactions were cycled at 94 °C for 30 s, 65 °C for 30 s and 72 °C for 2 min, for 35 cycles, followed by a final 10-min extension at 72 °C. PCR reaction products were separated on 0.7% w v^{-1} low melt agarose gels, excised and purified using a QIAEX II Gel Extraction kit as per the manufacturer's instructions (Qiagen). After digestion with *Xho*I and *Not*I, the purified koala *AOX* 2039 bp cDNA fragment was ligated into the pCI-neo expression vector and transformed into *Escherichia coli* strain DH5α competent cells. Plasmid DNA was isolated from approximately 100 colonies using a modified alkaline lysis miniprep procedure and screened for the presence of the 2039 bp inserts by restriction digest with *Xho*I and *Not*I. Plasmid DNA with the correct size inserts were then purified using the Qiaspin Spin kit (Qiagen), according to the manufacturer's instructions, and subsequently sequenced in both forward and reverse directions using T_3 and T_{7PCI} primers (Table 1) and internal primers, designed based on sequencing data obtained from the T_3 and T_{7PCI} primers.

For the purpose of control experiments, two full-length rat *AOX* cDNAs, designated r*AOX1* and r*AOX2*, were isolated by RT–PCR using RAOXfF and RAOXfR primers, derived from published rat *AOX* cDNA sequences (Table 1). These two cDNAs are identical to those previously cloned and characterized and designated rat ACO-I and ACO-II (Setoyama et al., 1995). The amplification, subcloning into pCI-neo vector, screening and sequencing of rat *AOX1* and *AOX2* cDNAs was performed essentially as described for koala *AOX* cDNAs.

2.4. Expression of koala liver acyl-CoA oxidase in Cos-7 cells

COS-7 cells were grown as a monolayer in Dulbecco's modified Eagle's Medium (DMEM) supplemented with 10% fetal bovine serum (FBS), 50 U ml^{-1} penicillin/streptomycin and 4 mM Glutamax I supplement (Invitrogen, Melbourne, Victoria) at 37 °C and 5% CO_2. COS-7 cells were seeded at 6×10^5 cells per 90-mm tissue culture plates. The cells were then allowed to grow in DMEM containing 10% FBS until 90% confluent. Immediately prior to

```
1    GGGGGGGGAC TTCTGATCGT CGTCACCTTC TGCCCCATCG CCGCCTTTAC CATGAACCCA
1                                                                M  N  P
61   GACTTGCGCA GGGAGCGGGA CGCTGCCAGC TTCGATGCGG AAAAACTCAC TTACATCCTG
4     D  L  R  R  E  R  D  A  A  S  F  D  A  E  K  L  T  Y  I  L
121  GATGGGGGCT CCGAGAGGAC CCGGCGCCGC CGGGAGATCG AGAACCTGAT TCTGAATGAT
24    D  G  G  S  E  R  T  R  R  R  R  E  I  E  N  L  I  L  N  D
181  CCGGACTTTA AGCATGAAGA CTTGAATTTC CTTACCCGGA GCGAGCGCTA TGAGATAGCT
44    P  D  F  K  H  E  D  L  N  F  L  T  R  S  E  R  Y  E  I  A
241  GTCAGAAAGA GTGCCACAAT GGTGAAGAAG ATGCGAGATT TTGGCATTGC TGATCCTGAA
64    V  R  K  S  A  T  M  V  K  K  M  R  D  F  G  I  A  D  P  E
301  GAGATCATGT GGTTTAAAAA CTTTGTGCAT CGTGGGCGTC CTGAGCCTTT GGACCTTCAC
84    E  I  M  W  F  K  N  F  V  H  R  G  R  P  E  P  L  D  L  H
361  TTGGGTATGT TTCTGCCCAC ATTACTTCAC CAGGCAACCC AGGAGCAGCA GGAACGCTTC
104   L  G  M  F  L  P  T  L  L  H  Q  A  T  Q  E  Q  Q  E  R  F
421  TTCATACCAG CCTGGAACCT GGAGATTATT GGCACTTATG CCCAGACAGA AATGGGCCAT
124   F  I  P  A  W  N  L  E  I  I  G  T  Y  A  Q  T  E  M  G  H
481  GGAACTCACC TTCGAGGCCT AGAAACCACA GCAACTTATG ACCCTAAAAC ACAGGAGTTT
144   G  T  H  L  R  G  L  E  T  T  A  T  Y  D  P  K  T  Q  E  F
541  ATTCTTAACA GCCCTACTGT TACTTCCATT AAGTGGTGGC CTGGTGGACT TGGGAAAACC
164   I  L  N  S  P  T  V  T  S  I  K  W  W  P  G  G  L  G  K  T
601  TCAAATCATG CCATAGTTCT GGCTCAGCTC TACACTAAGG GAGAGTGCTA TGGATTGCAT
184   S  N  H  A  I  V  L  A  Q  L  Y  T  K  G  E  C  Y  G  L  H
661  GCCTTCATTG TACCTATTCG AGAAATGGGA ACCCACAAAC CTTTTCCAGG CATTATCGTG
204   A  F  I  V  P  I  R  E  M  G  T  H  K  P  F  P  G  I  I  V
721  GGAGACATCG GGCCCAAGTT TGGCTATGAT GAAATGGATA ATGGTTATCT AAAGATGGAC
224   G  D  I  G  P  K  F  G  Y  D  E  M  D  N  G  Y  L  K  M  D
781  AACTATCGAA TTCCTCGGGA AAATATGCTG ATGAAGTACG CCCAGGTCAA ACCTGATGGC
244   N  Y  R  I  P  R  E  N  M  L  M  K  Y  A  Q  V  K  P  D  G
841  ACATATGTGA AGCCTTTAAG TAACAAACTG ACTTATGGAA CCATGGTGTT TGTCAGATCC
264   T  Y  V  K  P  L  S  N  K  L  T  Y  G  T  M  V  F  V  R  S
901  TTTCTTGTGG GAGAGGCAGC TCGATCATTG TCTAAAGCTT GCACTATTGC TATCCGCTAC
284   F  L  V  G  E  A  A  R  S  L  S  K  A  C  T  I  A  I  R  Y
961  AGTTTAATAA GGCACCAGTC TGAAATCCAG CCAGGTGATC CTGAACCCCA GATCTTGGAT
304   S  L  I  R  H  Q  S  E  I  R  P  G  D  P  E  P  Q  I  L  D
1021 TTTCAGACCC AGCAATATAA ACTTTTTCCT CTCTTGGCCA CTGCCTATGC CTTTCAATTT
324   F  Q  T  Q  Q  Y  K  L  F  P  L  L  A  T  A  Y  A  F  Q  F
1081 GTGGGAGCCT ACATGAAGGA AACCTATCAT CGCATTAATG TGGACATCAG CCAAGGGAAC
344   V  G  A  Y  M  K  E  T  Y  H  R  I  N  V  D  I  S  Q  G  N
1141 CTGAATGAAC TACCTGAGCT TCATGCACTG ACAGCTGGGC TTAAGGCTTT CACCTCTTGG
364   L  N  E  L  P  E  L  H  A  L  T  A  G  L  K  A  F  T  S  W
1201 ACAACTAATT CTGGCATTGA AGCCTGCCGG ATGGCTTGTG GTGGGCATGG ATACTCCCAC
384   T  T  N  S  G  I  E  A  C  R  M  A  C  G  G  H  G  Y  S  H
1261 TGCAGTGGCC TCCCAAACAT TTATGTCACT TTTACCCCCA CCTGCACCTT TGAAGGCGAA
404   C  S  G  L  P  N  I  Y  V  T  F  T  P  T  C  T  F  E  G  E
1321 AACACTGTGA TGATGCTCCA GACAGCTCGG TTTTTGATGA AAAGCTATGA TCAGGTTCAC
424   N  T  V  M  M  L  Q  T  A  R  F  L  M  K  S  Y  D  Q  V  H
1381 TCAGGAAAGT TGGTGGGTGG CATGGTGTCC TACTTGAATG ACCTGCCTAG TCAGCGCATC
444   S  G  K  L  V  G  G  M  V  S  Y  L  N  D  L  P  S  Q  R  I
1441 CAGCCACAGC AGGTGGCAGC TTGGCCAGCG ATGGTGGATA TCAACAACCC AGACAGCCTC
464   Q  P  Q  Q  V  A  A  W  P  A  M  V  D  I  N  N  P  D  S  L
1501 ACAGAAGCCT ATAAACATCG AGCAGCCCGA TTAGTAGAAG CTGCAGCAAG GAACCTTCAA
484   T  E  A  Y  K  H  R  A  A  R  L  V  E  A  A  A  R  N  L  Q
1561 GCCGAAATGA AGCACAGAAA AAGCAAAGAG ATAGCATGGA ACTTCACCTC GGTGGACCTT
504   A  E  M  K  H  R  K  S  K  E  I  A  W  N  F  T  S  V  D  L
1621 GTTCGAGCAA GTGAGGCTCA TTGTCACTAT GTGGTAGTAA AGCTCTTTTC TGGAAATCTC
524   V  R  A  S  E  A  H  C  H  Y  V  V  V  K  L  F  S  G  N  L
1681 TCTAAAATTG ATGACAAACCCATTCAGGCA GTCCTGACGA ATTTGTGTCT CTTATATGCC
544   G  I  S  S  K  I  D  D  K  P  I  Q  A  V  L  T  N  L  C  L
1741 CTGTATGGAA TCAGTCAGAA TTCTGGGGAC TTTCTACAGG GGGGCATCTT GACAGAGTCC
564   L  Y  A  L  Y  Q  N  S  G  D  F  L  Q  G  G  I  L  T  E  S
1801 CAACTTACCC AAGTGAACCA GCGGGTGAAG GAGCTCCTGA CACTGATCCG CCCCGAATCT
584   Q  L  T  Q  V  N  Q  R  V  K  E  L  L  T  L  I  R  P  E  S
1861 GCTGCTTTAG TGGATGCATT TGATTTTCAA GATGTTTCAC TTGGCTCTGT GCTTGGCCGC
604   A  A  L  V  D  A  F  D  F  Q  D  V  S  L  G  S  V  L  G  R
1921  TATGATGGCA ATATTTATGA AAATATGTTT GAATGGGCCA AGAAATCTCC ACTGAATAAA
624   Y  D  G  N  I  Y  E  N  M  F  E  W  A  K  K  S  P  L  N  K
1981 TCAGAGGTCC ATGAATCTTA TCACAAACAC CTGAAGCCAC TGCAGTCTAA GCTGTGAAG
644   S  E  V  H  E  S  Y  H  K  H  L  K  P  L  Q  S  K  L  X
```

Fig. 1. Nucleotide and deduced amino acid sequences of fatty acyl-CoA oxidase (AOX) type 1 full-length cDNA isolated from koala liver. Nucleotides and the corresponding amino acids, shown by single-letter codes, are numbered as indicated at the left-hand side of the figure. The ATG start codon is boxed at position 51. The sequence consists of an open reading frame encoding 662 amino acids. Underlined amino acid sequences correspond to the conserved unique fatty acyl CoA oxidase motif KWWPGG found at residues 174–180, the FAD binding motif CGGHGY located at residues 396–400 and the C-terminus containing an SKL motif, which was proposed to be an import signal present in several peroxisomal matrix proteins. The koala AOX1 sequence has been submitted to GenBank and its accession number is AF463453. Amino acids are shown by the single-letter code nomenclature as follows: A, alanine; C, cysteine; D, aspartic acid; E, glutamic acid; F, phenylalanine; G, glycine; H, histidine; I, isoleucine; K, lysine.; L, leucine; M, methionine; N, asparagine; P, proline; Q, glutamine; R, arginine; S, serine; T, threonine; V, valine; W, tryptophan; Y, tyrosine.

transfection, cells were washed with DMEM with no serum and media removed. Full-length koala *AOX* cDNAs cloned in pCI-neo vector were transfected into COS-7 cells using Lipofectamine 2000 reagent (Invitrogen, MD, USA). The Lipofectamine–DNA complexes were allowed to form for 30 min at room temperature before overlaying the cells. Cells were harvested 3 days following transfection. The cells were rinsed briefly in 0.1 M phosphate buffer (pH 7.4), homogenized, and the crude cell lysates were used directly for protein determination and palmitoyl-CoA oxidase activity assay.

2.5. Preparation of liver homogenates

Liver homogenates 10% (w/v) were prepared at 4 °C, 15 min prior to starting the activity incubations. Livers were homogenized in cold homogenization medium (0.25 M sucrose, 5 mM 3-(*N*-morpholino)-propane-sulfonic acid (MOPS, pH 7.5) and 1 mM ethylenediaminetetraacetic acid (EDTA), pH 7.5) using a Teflon probe. The liver homogenates were filtered through cotton gauze and stored on ice until needed. The protein concentration of each homogenates was determined by the method of Lowry et al. (1951).

2.6. Determination of palmitoyl-CoA oxidase activity

Palmitoyl-CoA oxidase activity determination was performed using a modification of the method described by Van Veldhoven (1995) using palmitoyl-CoA as the substrate. Activity was determined following the formation of H_2O_2 coupled to the dimerization of homovanillic acid (HVA) into a fluorescent product, catalysed by peroxidase in the presence of the generated H_2O_2. Test and blank incubations were performed for each individual liver sample with no substrate palmitoyl-CoA in the blank incubations. For determination of total palmitoyl-CoA oxidase activity, test and blank reaction mixtures contained 160 μl of diluted homogenate (1 in 10 dilution of the above prepared homogenate) and 40 μl of pre-incubation mixture containing 25 mM NaN_3 and 25 μM FAD. The assay mixtures were pre-incubated for 10 min on ice in order to inhibit catalase activity and to saturate the oxidase with its cofactor FAD. The reaction was initiated by adding 800 μl of appropriate warm test reaction mixture to the test incubations and 800 μl of blank reaction mixture to the blank incubations and the mixed preparations were placed in a shaking water bath at 37 °C. The test and blank reaction mixtures contained 50 mM K-phosphate buffer (pH 8.0), 0.1 mg ml^{-1} peroxidase, 0.15% (wv^{-1}) defatted BSA, 125 μM palmitoyl-CoA and 0.75 mM HVA, except that palmitoyl-CoA was not included in the blank incubation mixture. The reaction was terminated at the following time points by removing 200 μl of the incubated samples from the test and blank incubations after 8, 16, 24 and 32 min and adding 80 μl of stop buffer containing 8% ($w\ v^{-1}$) $HClO_4$. The resultant mixtures were centrifuged, followed by alkalinization of the supernatant with 2.8 ml of 0.5 M sodium carbonate and 10 mM EDTA buffer (pH 10.7) and fluorescence was then read after 10 min. Fluorescence was standardized by mean of uric acid and urate oxidase, essentially as described by Van Veldhoven (1995).

The determination of acyl-CoA oxidase-dependent palmitoyl-CoA oxidase activity was performed essentially as described for that of total palmitoyl-CoA oxidase, except that 5 mM NEM was included in the pre-incubation mixture to inhibit other CoA oxidases (Van Veldhoven, 1995). For determination of palmitoyl-CoA oxidase activity of koala and rat *AOX1* and *AOX2* cDNA-expressed proteins, crude cell homogenates were used.

2.7. Analysis of acyl CoA oxidase (AOX) mRNA by Northern blotting

Northern blot analysis was performed using a koala liver *AOX* 320 bp cDNA probe. Blotting was performed essentially as described previously (Kong et al., 2002). The integrity of mRNA was assessed by visualization with ethidium bromide (results not shown). To assess equal loading of mRNA, the filter was stripped and reprobed with [^{32}P]dCTP-labelled *β-actin* cDNA probe (Ambion, Austin, Texas, USA).

2.8. Southern blot analysis of koala genomic DNA with AOX cDNA

Genomic DNA was digested with *Eco* RI overnight at 37 °C. DNA fragments were separated by gel electrophoresis and transferred to a nylon membrane. Prehybridization and hybridization with [^{32}P]dCTP-labelled koala *AOX* 320 bp cDNA probe were performed at 42 °C in a hybridization solution containing 50% formamide. Transblotting was then performed and the blot exposed to X-ray film (Curix Blue HC-S plus, Agfa-Gevasrt, Mortsel, Belgium) with intensifying screens at −80 °C for several days.

3. Results and discussion

3.1. Cloning of koala liver acyl-CoA oxidase cDNAs

Previous studies in our laboratory have demonstrated that peroxisomal cyanide-insensitive palmitoyl-CoA oxidation is absent in the koala liver (Ngo et al., 2000). In the present study, we have focused on the molecular characterization of the first and rate-limiting enzyme in this pathway, fatty acyl-CoA oxidase (AOX).

Two 2039 bp koala *AOX* cDNAs were isolated from koala liver utilizing PCR-based approaches and were designated k*AOX1* and k*AOX2*. The nucleotide and deduced amino acid sequences of k*AOX1* and k*AOX2* are shown in Figs. 1 and 2. These sequences differ in a small area of the

```
AOXI
317 AACTTTGTGCAT CGTGGGCGTC CTGAGCCTTT GGACCTTCAC TTGGGTATGT TTCTGCCCAC
 89   N  F  V  H  R  G  R  P  E  P  L  D  L  H  L  G  M  F  L  P  T
379 ATTACTTCAC CAGGCAACCC AGGAGCAGCA GGAACGCTTC TTCATACCAG CCTGGAACCT
110    L  L  H  Q  A  T  Q  E  Q  Q  E  R  F  F  I  P  A  W  N  L
439 GGAGATTATT GGCACTTATG CCCAGACAGA AATGGGCCAT
130    E  I  I  G  T  Y  A  Q  T  E  M  G  H

AOXII
317 AAACCACAGTTG ATCAATTTTG TGGAACCGGT TGGCCTCACT TACTCCATGT TTATCCCTAC
 89   K  P  Q  L  I  N  F  V  E  P  V  G  L  T  Y  S  M  F  I  P  T
379 CTTGCTGGAT CAGGGCACCA CTGCTCAGCA ACAGAAATGG CTGCCTCCAA CCCAAGGACT
110    L  L  D  Q  G  T  T  A  Q  Q  Q  K  W  L  P  P  T  Q  G  L
439 CCAGATAATT GGCACCTACG CCCAGACCGA GATGGGGCAC
130    Q  I  I  G  T  Y  A  Q  T  E  M  G  H
```

Fig. 2. AOX1 and AOX2 cDNA and corresponding deduced amino acid sequences in the coding region located between nucleotides 269-429, where sequence differences were found. The accession number of koala AOX2 is AF463454.

coding region, between nucleotides 269–429. This finding is consistent with results reported in both the rat and humans (Miyazawa et al., 1987; Varanasi et al., 1994). In each species, a single *AOX* gene was identified which gives rise to alternative mRNA species via differential splicing (Miyazawa et al., 1987; Varanasi et al., 1994). Two *AOX* cDNAs have also been described in the yeast, *Candida tropicalis* (Okazaki et al., 1986).

Each koala *AOX* cDNA has an open reading frame of 1988 bp, which encodes a protein of 662 aa, and both contain a 51 bp 5′-UTR. Both k*AOX1* and k*AOX2* cDNAs exhibit high nucleotide sequence identity to the reported human and rat *AOX* cDNA sequences (Table 2). The k*AOX1* and k*AOX2* cDNA sequences were submitted to GenBank (Bethesda, MD, USA) and have been assigned the accession numbers AF463453 and AF463454, respectively.

As shown in Fig. 1, the k*AOX1* and k*AOX2* cDNAs share several common features with other published *AOX* sequences: the conserved unique fatty acyl CoA oxidase sequence KWWPGG found at residues 174–180 (Hooks et al., 1999), the FAD binding motif CGGHGY located at residues 396–400 (Hooks et al., 1999), and the C-terminus containing an SKL motif which has been proposed to be an import signal present in several peroxisomal matrix proteins (Fig. 1) (Nöhammer et al., 2000).

3.2. Determination of palmitoyl-CoA oxidase activity in koala liver homogenates

To determine the acyl-CoA oxidase activity present in koala liver, total palmitoyl-CoA oxidase and acyl-CoA oxidase-dependent palmitoyl-CoA oxidase activities were determined in koala liver homogenates. Activities were also determined for rat and human liver homogenates and results are shown in Table 3. As shown in Table 3, total palmitoyl-CoA and acyl-CoA oxidase-dependent palmitoyl-CoA activities detected in liver homogenates revealed that total palmitoyl-CoA activity of koala livers was about 12- and 5-fold less than that in rat and human liver homogenates, respectively. This finding suggests that the level of functional acyl-CoA oxidase protein in koala liver is significantly lower than in rat and human livers. The acyl-CoA oxidase activity of rat liver homogenate determined in our study is consistent with that reported by Van Veldhoven et al. (1994).

3.3. Expression of koala AOX1 and AOX2 in COS-7 cells and determination of palmitoyl-CoA oxidase (AOX) activity

To confirm that the cloned koala *AOX* cDNAs encode functional enzymes, the k*AOX1* and k*AOX2* cDNAs were each cloned into the pCI-neo vector and the resultant

Table 2
Nucleotide and amino acid sequence identity (shown in bold) between the koala AOX and AOX subfamilies from other species

	AOX1[a]	AOX2[b]	hAOX1[c]	hAOX2[d]	rAOX[e]	mAOX[f]
kAOX1	100	96	83	81	78	77
	100	**95**	**88**	**84**	**81**	**80**
kAOX2		100	80	83	80	79
		100	**84**	**86**	**83**	**82**
hAOX1			100	96	82	81
			100	**96**	**85**	**83**
hAOX2				100	85	83
				100	**88**	**86**
rAOX1					100	93
					100	**95**
mAOX						100
						100

[a] Koala liver fatty *AOX* cDNA type 1 nucleotide and deduced amino acid sequences, GenBank accession number AF463453 (Ngo et al., 2000, direct submission).

[b] Koala liver fatty *AOX* cDNA type 2 nucleotide and deduced amino acid sequences, GenBank accession number AF463454 (Ngo et al., 2000, direct submission).

[c] Human fatty *AOX* cDNA type 1 nucleotide and deduced amino acid sequences, GenBank accession number UO7866 (Aoyama et al., 1994).

[d] Human fatty *AOX* cDNA type 2 nucleotide and deduced amino acid sequences, GenBank accession number UO7866 (Aoyama et al., 1994).

[e] Rat fatty *AOX* cDNA nucleotide and deduced amino acid sequences, GenBank accession number J02752 (Miyazawa et al., 1987).

[f] Mouse fatty *AOX* cDNA nucleotide and deduced amino acid sequences, GenBank accession number AF006688 (Nöhammer et al., 2000).

Table 3
Total palmitoyl-CoA and acyl-CoA oxidase-dependent palmitoyl-CoA oxidase activities determined in koala and rat liver homogenates

Sample	Total palmitoyl-CoA oxidase activity	AOX-dependent palmitoyl-CoA oxidase activity
Koala ($n = 6$)	389.4 ± 192.7	292.5 ± 100.7
Rat ($n = 3$)	4323.9 ± 191.63	3515.0 ± 508.5
Human ($n = 1$)	1881.7	

Values are expressed as mean ± SD. Activity is expressed as nM min^{-1} (g protein)$^{-1}$.

plasmids transfected into COS-7 cells. The palmitoyl-CoA oxidase activity of the cDNA-expressed koala AOX1 and AOX2 proteins was determined and compared with cDNA-expressed rat AOX1 and AOX2. Liver homogenates from koala, human and rat were included as positive controls. Palmitoyl-CoA activities for expressed koala and rat AOX1 and AOX2 enzymes are shown in Table 4. Based on sequence alignments, koala AOX1 displays higher sequence identity with rat AOX2 (ACO-II). The activity of cDNA-expressed koala AOX1 protein was significantly higher than that observed with cDNA-expressed rat AOX2 (1472.70 versus 471.65 nM min^{-1} (g protein)$^{-1}$, respectively). The activity of cDNA-expressed koala AOX2 protein was significantly lower (543.3) while no activity was observed for cDNA-expressed rat AOX1. Each reported activity for cDNA-expressed proteins represents the average of two experiments.

Kinetic analysis was performed for both cDNA-expressed koala AOX1 and AOX2 using palmitoyl-CoA substrate concentrations ranging from 25 to 175 μM, as previously described by Van Veldhoven and colleagues (Van Veldhoven et al., 1992, 1994; Van Veldhoven, 1995). Results of these analyses are shown in Table 4. Table 4 shows apparent K_m values of 28 and 38 μM for cDNA-expressed koala AOX1 and AOX2 enzymes, respectively. Previous studies have reported apparent K_m values for purified rat and human AOX1 enzymes of approximately 10 μM (Chu et al., 1995; Casteels et al., 1990). Our reported K_m values for cDNA-expressed koala AOX1 and AOX2 are within the range of order of magnitude. The apparent K_m for human liver homogenate observed in our study was 70 μM, which is comparable to that reported (62 μM) by Casteels and colleagues (Casteels et al., 1990). Decreases in palmitoyl-CoA oxidase activity of cDNA-expressed koala and rat AOX1 and AOX2 enzymes as well as liver homogenates were also observed with substrate concentrations just above the V_{max} values (not shown). The situation was similar to that reported for activity measurements of rat purified AOX1 by Souri and other colleagues (Setoyama et al., 1995; Souri et al., 1994; Van Veldhoven et al., 1992).

Table 4
Palmitoyl-CoA activity[a] catalysed by cDNA-expressed koala and rat AOX enzymes

Sample	Palmitoyl-CoA oxidase activity	K_m[b]	V_{max}
Expressed koala AOX1	1472.70	28	1499.10
Expressed koala AOX2	543.30	38	677.00
Expressed rat AOX1	n.d.		
Expressed rat AOX2	471.65	–[c]	–
Rat liver homogenate	4643.95	–	–
Koala liver homogenate	375.90	78	610.40
Human liver homogenate	1883.65	70	2600.85

[a] Acyl-CoA oxidase-dependent palmitoyl-CoA activity and V_{max}, expressed as nM min^{-1} (g protein)$^{-1}$, were determined following the formation of H_2O_2 coupled to the dimerization of homovanillic acid into a fluorescent product catalysed by peroxidase, using a modification of the method described by Van Veldhoven (1995). Data are derived from multiple time points and duplicate determinations. Activity determined in untransfected Cos-7 cell lysates was not detectable. n.d., no activity detected.

[b] K_m values are expressed as μM.

[c] –, Enzyme kinetic parameters not determined.

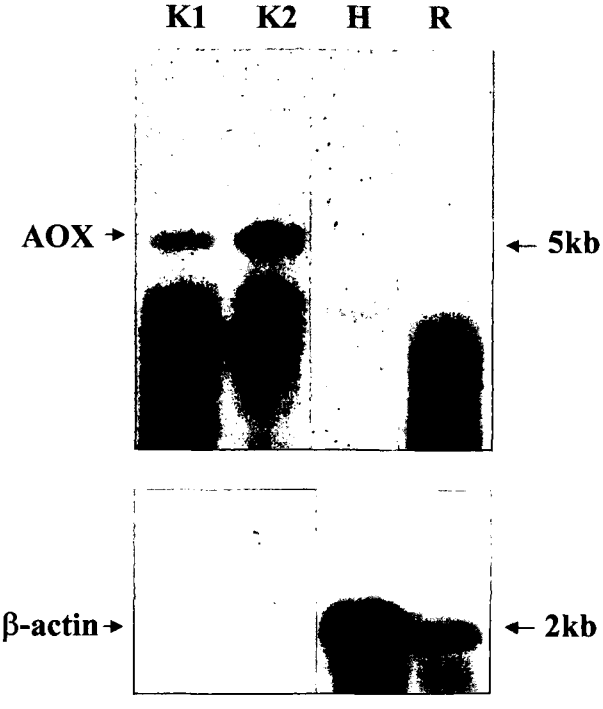

Fig. 3. Representative Northern blot analysis of hepatic AOX mRNA. mRNAs were purified from human, rat and two koala liver samples, electrophoresed on 1% denaturing (formaldehyde) agarose gel and transferred to nylon filter. Koala AOX cDNA probe was ^{32}P-labelled, hybridized and autoradiographed for several days. H, human mRNA (10 μg); R, rat mRNA (10 μg); K_1, koala mRNA sample 1 (4 μg); K_2, koala mRNA sample 2 (10 μg). The blot demonstrated higher expression of AOX mRNA in koala liver as compared to human and rat. (a) Hybridization with koala AOX cDNA probe. (b) Hybridization with mouse β-actin.

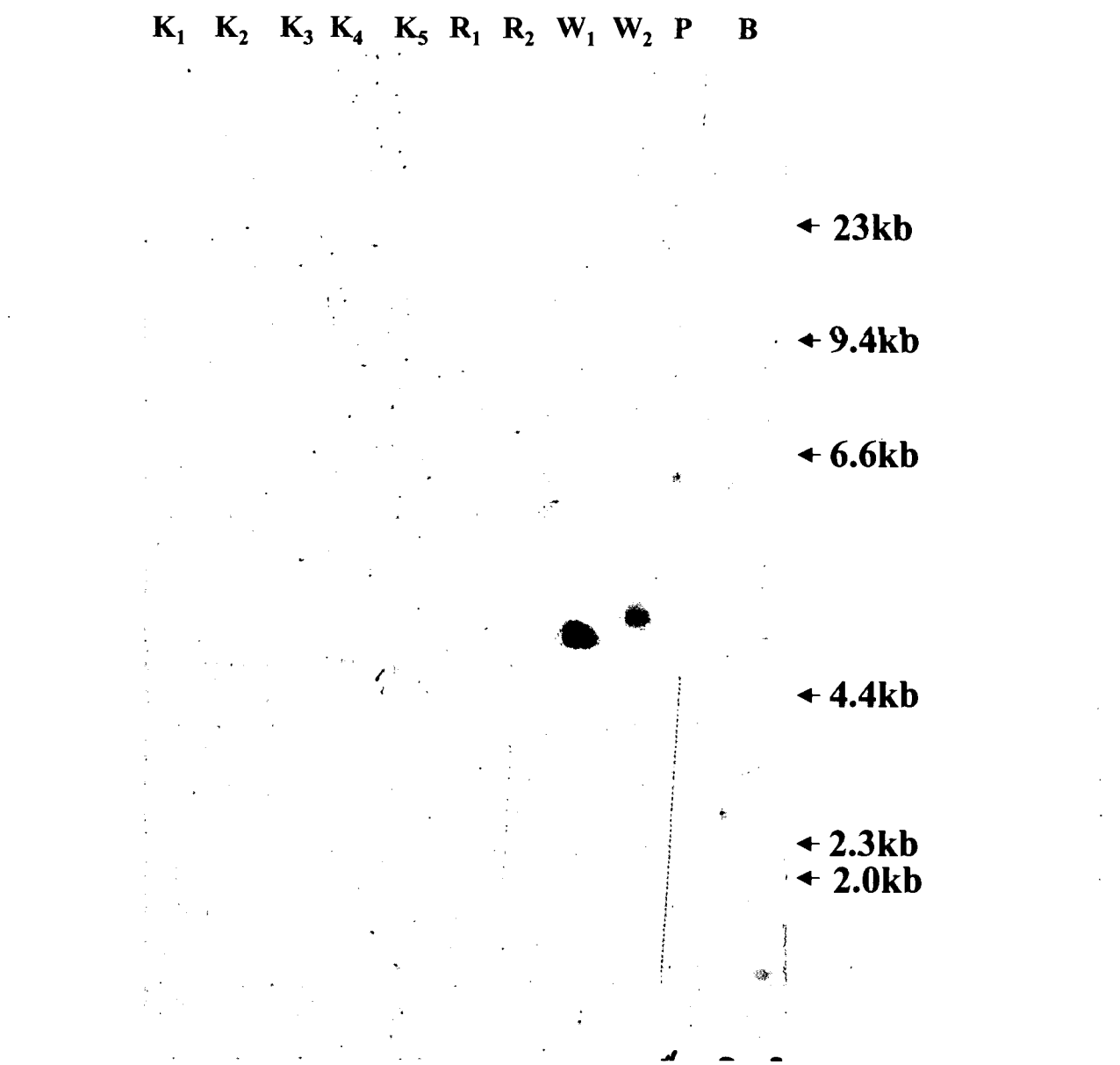

Fig. 4. Representative Southern blot analysis of AOX gene. Genomic DNA was extracted from five koala (K_1-K_5), two rat (R_1-R_2), two wallabies (W_1-W_2), one possum (P), and one bandicoot (B) liver samples, electrophoresed on 1% agarose gel and transferred to nylon filter. Koala AOX cDNA was ^{32}P-labelled, hybridized and autoradiographed for several days. A single AOX gene fragment of size less than 14 kb was observed for the koala and other examined species.

3.4. Northern analysis of acyl CoA oxidase (AOX) mRNA

The expression of AOX mRNA was examined in koala, rat and human livers. A representative Northern blot is shown in Fig. 3.The koala *AOX* cDNA probe recognized mRNA in all mRNA samples studied. In koala, a single band corresponding to a mRNA species of approximately 5 kb was observed in all livers studied. A single band of lower intensity was detected in rat and human liver mRNA samples, of approximately 4 and 3 kb, respectively. The intensity of signal indicates higher expression of koala hepatic AOX mRNA as compared to rat and human. The sizes of human and rat AOX mRNAs detected in the present study are comparable with previously reported values of 3.2 and 3.8 kb, respectively (Aoyama et al., 1994). Our studies also show higher expression of rat AOX mRNA as compared to human, which is consistent with previous studies (Aoyama et al., 1994).

3.5. Southern analysis of the AOX gene

Southern blot analysis of *Eco* RI-digested genomic DNA from male koala, rat, wallaby, possum, and bandicoot livers is shown in Fig. 4. From this blot, it is apparent that *Eco* RI-digestion of genomic DNA produced only one *AOX* gene fragment of size less than 14 kb for koala, wallaby and rat samples, suggesting a single *AOX* gene.

3.6. Conclusion

1. Two koala *AOX* cDNAs have been isolated and differ only in a small area of the coding region, between nucleotides 269 and 429. This finding is consistent with results reported in both rat and humans.
2. Expression of koala AOX1 and AOX2 in Cos-7 cells and kinetic analysis confirm that the cloned koala *AOX* cDNAs encode functional enzymes with palmitoyl-CoA oxidase activity.
3. The results of this study suggest that the absence of peroxisomal cyanide-insensitive palmitoyl-CoA oxidation, a measure of the overall peroxisomal β-oxidation spiral activity minus the final step catalysed by thiolase, in the koala liver, is possibly due to deficiencies of one or more enzymes downstream of acyl-CoA oxidase such as enoyl-CoA hydratase/3-hydroxyacyl-CoA dehydrogenase bifunctional enzyme and 3-ketoacyl-CoA thiolase and/or deficiencies of mitochondrial β-oxidation enzymes.

Acknowledgements

The authors acknowledge the assistance of Mr Chris Lee and Dr Brett Jones in procuring tissues for this study.

References

Aoyama, T., Tsushima, K., Souri, M., Kamijo, T., Suzuki, Y., Shimozawa, N., Orii, T., Hashimoto, T., 1994. Molecular cloning and functional expression of a human peroxisomal acyl-coenzyme A oxidase. Biochem. Biophys. Res. Commun. 198, 1113–1118.

Aoyama, T., Peters, J.M., Iritani, M., NakaJima, T., Furihata, K., Hashimoto, T., Gonzalez, F.J., 1998. Altered constitutive expression of fatty acid-metabolizing enzymes in mice lacking the peroxisome proliferator-activated receptor alpha (PPAR-α). J. Biol. Chem. 273, 5678–5684.

Baes, M., Huyghe, S., Carmeliet, P., Declercq, P.E., Collen, D., Mannaerts, G.P., Van Van Veldhoven, P.P., 2000. Inactivation of the peroxisomal multifunctional protein-2 in mice impedes the degradation of not only 2-methyl-branched fatty acids and bile acid intermediates but also very long-chain fatty acids. J. Biol. Chem. 275, 16329–16336.

Casteels, M., Schepers, L., Van Veldhoven, P.P., Eyssen, H.J., Mannaerts, G.P., 1990. Separate peroxisomal oxidases for fatty acyl-CoAs and trihydroxycoprostanoyl-CoA in human liver. J. Lipid. Res. 31, 1865–1872.

Chomcynski, P., Sacchi, N., 1998. Single step method for RNA isolation by acid guanidinium thiocyanate-phenol-chloroform extraction. Anal. Biochem. 162, 156–159.

Chu, R., Usuda, N., Reddy, M.K., Liu, C., Hashimoto, T., Alvares, K., Rao, M.S., Reddy, J.K., 1995. Functional expression of rat peroxisomal acyl-CoA oxidase in *Spodoptera frugiperda* cells. Biochem. Biophys. Res. Commun. 200, 178–186.

Hooks, M.A., Kellas, F., Graham, I.A., 1999. Long-chain acyl-CoA oxidases of Arabidopsis. Plant J. 20, 1–13.

Kong, S., McKinnon, R.A., Mojarrabi, B., Stupans, I., 2002. Absence of type 1 11beta-hydroxysteroid dehydrogenase enzyme in koala liver. Comp. Biochem. Physiol. (C) 131, 39–50.

Lowry, O.H., Rosebrough, N.J., Farr, A.L., Randall, R.J., 1951. Protein measurement with the Folin phenol reagent. J. Biol. Chem. 193, 265–275.

Mannaerts, G.P., Van Veldhoven, P.P., Casteels, M., 2000. Peroxisomal lipid degradation via β- and α-oxidation in mammals. Cell Biochem. Biophys. 32, 73–87.

McKinnon, R.A., Hall, P.D.L.M., Quattrochi, L.C., Tukey, R.H., McManus, M.E., 1991. Localisation of CYP1A1 and CYP1A2 messenger RNA in normal human liver and in hepatocellular carcinoma by in situ hybridization. Hepatology 14, 848–856.

Miyazawa, S., Hayashi, H., Hijikata, M., Ishii, N., Furuta, S., Kagamiyama, H., Osumi, T., Hashimoto, T., 1987. Complete nucleotide sequence of cDNA and predicted amino acid sequence of rat acyl-CoA oxidase. J. Biol. Chem. 262, 8131–8137.

Ngo, S., Kong, S., Kirlich, A., McKinnon, R.A., Stupans, I., 2000. Cytochrome P450 4A, peroxisomal enzymes and nicotinamide cofactors in koala liver. Comp. Biochem. Physiol. (C) 127, 327–334.

Nöhammer, C., El-Shabrawi, Y., Schauer, S., Hiden, M., Berger, M., Forss-Petter, S., Winter, E., Eferl, R., Zechner, R., Hoefler, G., 2000. cDNA cloning and analysis of tissue-specific expression of mouse peroxisomal straight-chain acyl-CoA oxidase. Eur. J. Biochem. 267, 1254–1260.

Okazaki, K., Takechi, T., Kambara, N., Fufui, S., Kubota, I., Kamiryo, T., 1986. Two acyl-coenzyme A oxidase in peroxisomes of the yeast *Candida tropicalis*: primary structures deduced from genomic DNA sequence. Proc. Natl. Acad. Sci. USA 83, 1232–1236.

Qi, C., Zhu, Y., Pan, J., Usuda, N., Maeda, N., Yeldandi, A.V., Rao, M.S., Reddy, J.K., Hashimoto, T., 2001. Peroxisomal β-oxidation and peroxisome proliferator-activated receptor alpha: an adaptive metabolic system. Annu. Rev. Nutr. 21, 193–230.

Setoyama, C., Tamaoki, H., Nishina, Y., Shiga, K., Miura, R., 1995. Functional expression of two forms of rat acyl-CoA oxidase and their substrate specificities. Biochem. Biophys. Res. Commun. 217, 482–487.

Souri, M., Aoyama, T., Hashimoto, T., 1994. A sensitive assay of acyl-Coenzyme A oxidase by coupling with beta-oxidation multienzyme complex. Anal. Biochem. 221, 362–367.

Van Veldhoven, P.P., 1995. Activity measurements of acyl-CoA oxidases in human liver. J. Inher. Metab. Dis. 18 (Suppl. 1), 125–134.

Van Veldhoven, P.P., Vanhove, G., Assselberghs, S., Eyssen, H.J., Mannaerts, G.P., 1992. Substrate specificities of rat liver peroxisomal acyl-CoA oxidase (inducible acyl-CoA oxidase), pristanoyl-CoA trihydroxycoprostanoyl-CoA oxidase. J. Biol. Chem. 267, 20065–20074.

Van Veldhoven, P.P., Rompuy, P.V., Fransen, M., Bethune, B.D., Mannaerts, G.P., 1994. Large-scale purification and further characterisation of rat pristanoyl-CoA oxidase. J. Biochem. 222, 795–801.

Varanasi, U., Chu, R., Huang, Q., Castellon, R., Yeldandi, A.V., 1994. Isolation of the human peroxisomal acyl-CoA oxidase gene: Organisation, promoter analysis, and chromosomal localisation. Proc. Natl. Acad. Sci. USA 91, 3107–3111.

ELSEVIER

Comparative Biochemistry and Physiology Part C 136 (2003) 165–173

CBP

www.elsevier.com/locate/cbpc

The effects of *Eucalyptus* terpenes on hepatic cytochrome P450 CYP4A, peroxisomal Acyl CoA oxidase (AOX) and peroxisome proliferator activated receptor alpha (PPARα

Suong Ngoc Thi Ngo, Ross Allan McKinnon*, Ieva Stupans

Centre for Pharmaceutical Research, School of Pharmaceutical, Molecular and Biomedical Sciences, University of South Australia, SA 5000, Adelaide, Australia

Received 21 June 2002; received in revised form 6 June 2003; accepted 18 August 2003

Abstract

Eucalyptus leaves contain a high proportion of essential oils comprising of a complex mixture of monoterpenes such as 1,8-cineole, α-pinene, *d*-limonene and *p*-cymene. In this study, hepatic levels of microsomal lauric acid hydroxylase and peroxisomal cyanide-intensive palmitoyl coenzyme A oxidative activities were examined in livers of possums given an artificial diet consisting of the above monoterpenes for 10 days. These values were compared with those of possums fed a control diet containing only fruits and cereals. Peroxisomal cyanide-intensive palmitoyl coenzyme A oxidative activity was significantly higher in livers of treated possums relative to that of control possums (2.96 ± 0.93 vs. 0.98 ± 0.88 nmol/mg protein per min, $P < 0.01$) (mean $\pm$ S.D., $n = 4$). A small increase in microsomal lauric acid hydroxylase activity was observed in the treated possum in comparison with the control group (4.40 ± 0.85 vs. 3.60 ± 0.48 nmol/mg protein per min) (mean $\pm$ S.D., $n = 4$). A higher NAD/ NADP ratio was observed in treated possums as compared with control possums (4.73 ± 0.65 vs. 3.51 ± 0.64 nmol/mg protein per min, $P < 0.05$) (mean $\pm$ S.D., $n = 4$). No other statistically significant differences in pyridine nucleotide contents were found between control and treated possums. Northern blot analysis of mRNA from rat, human, terpene treated and control possum livers, using the corresponding koala cDNA probes, detected a more intense acyl CoA oxidase (AOX) mRNA band in livers of terpene fed possums. Negligible differences in the intensity of CYP4A and PPARα mRNA bands were observed between the two groups. These data suggest that *Eucalyptus* terpenes elevate hepatic AOX expression in possums.
© 2003 Elsevier Inc. All rights reserved.

Keywords: Lauric acid hydroxylase (LAH); Cyanide-intensive palmitoyl coenzyme A oxidation; Peroxisome proliferator activated receptor alpha (PPARα); CYP4A; AOX; Nicotinamide-adenine dinucleotide (NAD); Nicotinamide-adenine dinucleotide phosphate (NADP); Brush tail possum (*Trichosurus vulpecula*); *Eucalyptus*; Terpenes

1. Introduction

Australian native *Eucalyptus* species are widely distributed throughout Australia and grow in a wide range of climatic environments (Ghisalberti, 1996). Although *Eucalyptus* leaves are low in protein, high in fibre and contain a high proportion of phenolics and essential oils, Australian Eucalypt forests are an essential food source for several folivorous marsupials (Cork and Foley, 1997). Koalas (*Phascolarctos cinereus*) ingest the leaves of certain *Eucalyptus* species as their only food source, while brush tail possums (*Trichosurus vulpecula*) living in non-residential environments rely on these leaves as their major food supply

*Corresponding author. Tel.: +61-8-8302-2372; fax: +61-8-8302-2389.

E-mail address: ross.mckinnon@unisa.edu.au (R.A. McKinnon).

1532-0456/03/$ - see front matter © 2003 Elsevier Inc. All rights reserved.
doi:10.1016/S1532-0456(03)00197-2

(Stupans et al., 2001). As a result, these *Eucalyptus* herbivores ingest and absorb large amounts of dietary monoterpenes such as 1,8-cineole, α-pinene, *d*-limonene and *p*-cymene, which are major constituents of essential oils in *Eucalyptus* species (Corrigan, 1992). Such large quantities of *Eucalyptus* oil would be toxic, even potentially fatal, to humans and many other mammalian species (Patel and Wiggins, 1980; Spoerke et al., 1989). It has been hypothesised that specialist *Eucalyptus* herbivores, for example koalas and brush tail possums, utilise highly efficient enzyme systems to metabolise the plant secondary metabolites, such as terpenes and phenolics, to non-toxic substances, which can then be readily excreted in the urine (Freeland and Janzen, 1974; McLean and Foley, 1997). Enzymes that carry out the biotransformation of the unique *Eucalyptus* diet of these folivorous animals have been partially identified to be the cytochromes P450 (Pass et al., 2001).

It has been reported that essential oils, extracted from wood and leaves, induced the levels and activities of some cytochrome P450 enzymes in rat liver (Hiroi et al., 1995). Similarly, oral administration of the terpene, β-myrcene, caused induction of CYP isozymes in the rat liver (De-Oliveira et al., 1997). Citral, a component of *Eucalyptus* leaves, has also been reported to cause induction of peroxisomal β-oxidation enzymes and microsomal enzyme such as CYP4A in the rat liver (Roffey et al., 1990). Known CYP4A inducers such as clofibrate, di(2-ethylhexyphthalate), and tridiphane, which constitute a class of chemicals collectively termed peroxisome proliferators, have been reported to cause peroxisome proliferation and induction of peroxisomal β-oxidation enzymes and CYP4A (reviewed in Simpson, 1997). Structurally diverse peroxisome proliferators have also been reported to significantly induce hepatic pyridine nucleotides, in particular the highest abundance nicotinamide cofactors, NAD and NADPH, in the rat liver (Shin et al., 1998, 1999a,b; Labrie, et al., 1997).

A novel member of the steroid/nuclear superfamily known as the peroxisome proliferator activated receptor alpha (PPARα), has been reported to mediate induction of genes encoding peroxisomal fatty acyl-CoA oxidase (AOX) and microsomal CYP4A6 by peroxisome proliferators in the liver of mouse and human, through transcriptional activation of these target genes (Yu et al., 2001). Induction of PPARα in the rat liver after exposure to peroxisome proliferators has also been reported to signify one important measurement of the effects of peroxisome proliferator (Gebel et al., 1992; Sterchele et al., 1996).

In the present study, the enzymatic activities of CYP4A and AOX were examined in livers of possums treated with an artificial diet containing 1,8-cineole, α-pinene, *d*-limonene and *p*-cymene and compared to livers of possums treated with the artificial diet only. Enzyme and mRNA levels were investigated by Western and Northern blot analyses. The hepatic pyrimidine dinucleotide contents and the expression of peroxisome proliferator activated receptor-alpha (PPAR-α) protein and mRNA were also examined.

2. Materials and methods

2.1. Materials

Bovine serum albumin, unlabelled lauric acid, coenzyme A, palmitoyl coenzyme A, flavin adenine dinucleotide, NADPH, alcohol dehydrogenase, glucose-6-phosphate and glucose-6-phosphate dehydrogenase were obtained from Sigma (St. Louis, MO, USA). [1-^{14}C]Lauric acid (spec. act. 37 mCi/mmol) and mRNA purification kit were purchased from Amersham Pharmacia Biotech (Sydney, Australia). The Gigaprime DNA labelling kit was purchased from Geneworks (Adelaide, Australia). Reagents for immunoblotting were obtained from Biorad (Sydney, Australia) unless otherwise stated. All solvents and other chemicals were of analytical grade.

2.2. Hepatic tissue and sample preparation

Eight possum livers (four treated and four control possums) were kindly donated by Dr Georgia Pass (University of Tasmania). The possum tissues have been used in other studies (Pass et al., 1999, 2001; Liapis et al., 2000). Briefly, control possums were fed an artificial diet containing apple, silver beet, carrot, lucerne, brown sugar and water (39.6%, 26.6%, 8.2%, 4.5%, 3% and 14.9% wet matter, respectively) for 10 days. Treated possums were fed the same artificial diet into which 1,8-cineole, α-pinene, *d*-limonene and *p*-cymene were included. The amount of 1,8-cineole, α-pinene, *d*-limonene and *p*-cymene added into the wet mash were 566, 16, 69 and 214 mg/kg, respectively, for the first 5 days, then 1212, 32, 138, and 428 mg/

kg respectively, for the next 5 days. Livers were scavenged from male road injured koalas (*Phacoslarctos cinereus*), ultimately euthenased using pentobarbital. Male Hooded Wistar rats (*Rattus norvegicus*) were used as the source of rat liver. Human liver tissue was obtained from a renal transplant donor from the Flinders Medical Centre (SA, Australia). The details of the human liver tissue H21 have been published previously (McKinnon et al., 1991). All animals were sexually mature and the Ethic Committees of the appropriate institutions had approved the use of these tissues. Livers from all species were quickly removed and chilled immediately at the time of death and frozen in liquid nitrogen before storage at −80 °C.

Preparation of hepatic microsomes, cytosolic and post-nuclear supernatants were carried out as previously described (Kong et al., 2002; Ngo et al., 2000). Nuclear extracts were prepared using a modification of the method described by Gebel et al., 1992. Liver tissue was homogenised in three volumes of homogenisation buffer containing 20 mM Tris–HCl (pH 7.4), 1 mM EDTA, 25 mM KCl, 1 mM PMFS (phenylmethanesulfonyl fluoride), 1 mM DTT and 10% glycerol using 10 strokes of a drilling Teflon probe. The homogenate was centrifuged at $1000\times g$ for 5 min and the resultant pellet was resuspended in three volumes of the above homogenisation buffer. The resultant suspension was centrifuged $1000\times g$ for 5 min to remove the remainder of cytosol. After removal of the supernatant, the pellet was resuspended in two volumes of homogenisation buffer containing 0.4 M NaCl using a Potter Elvehjem homogeniser. The obtained suspension was stirred gently at 4 °C for 20 min with a magnetic stir bar and then centrifuged at $1000\times g$ for 60 min. The collected supernatant representing the nuclear extract was stored at −80 °C until use. Protein concentrations of various subcellular fractions were determined by the method of Lowry et al., (1951).

2.3. Enzyme assay

Lauric acid hydroxylase activity (a CYP4 marker) was determined using a modification of the method described by Parker and Orton (1980). Peroxisomal cyanide-intensive fatty acid β-oxidation was performed essentially as described by Lazarow (1981). Hepatic pyridine nucleotide contents were determined by the procedure of Klingenberg (1974) as previously described (Ngo et al., 2000).

To ensure linearity, all assay conditions were optimised with respect to time, protein and substrate concentrations.

2.4. Western blot analysis

Immunodetection of CYP4A in liver micromes from control and treated possum, koala, rat and human livers was performed as previously described (Pass et al., 1999), using rat polyclonal CYP4A primary antibody (1:200) raised in sheep (Chemicon International-UT, UK). Horseradish peroxidase (HRP) conjugated rabbit-anti-sheep IgG (1:2000) was use as the secondary antibody (Silenus Laboratories, Hawthorn, Australia). For immunodetection of PPARα in cytosol and nuclear extracts, a polyclonal PPARα antibody (1:200) raised in rabbit (Santa Cruz, Germany) and a mouse-anti-rabbit (1:2000) IgG (Santa Cruz, Germany) were used as the primary and secondary antibody, respectively.

2.5. Northern blot analysis

Total RNA from livers was isolated by a modification of the method of Chomczynski and Sacchi (1987). The phenol–chloroform extraction step of total RNA was repeated twice in order to obtain cleaner total RNA. Purification of mRNA from total RNA samples was performed using the mRNA purification kit (Amersham, Sydney, Australia) as per the manufacturer's protocol. Northern blot analysis of hepatic mRNAs were carried out as previously described (Kong et al., 2002), using corresponding koala cDNA probes. Spectrophotometric quantification of mRNA and ethidium bromide staining of the blot were used for mRNA loading control. After probing with the koala cDNA probe, the filter was stripped and re-probed with [^{32}P]dCTP labelled *β actin* cDNA probe (Ambion, Austin, TX, USA) used as an additional loading control.

2.6. Data analysis

Data were expressed as the mean of triplicate observations, except that the quantification of hepatic pyridine nucleotide contents was performed in duplicate. Population variability was indicated by the S.D. Statistical analysis was per-

Table 1
LAH activities in liver microsomes prepared from control and terpene treated possums

	LAH activity (nmol LA metabolite/mg protein per min)
Control possums ($n=4$)	3.60 ± 0.48
Treated possums ($n=4$)	4.40 ± 0.85*

LAH, lauric acid hydroxylase. Results are expressed as means $\pm$ S.D. of four animals for each group. *The mean was different from that of control possums, analysis of data using a two-sample t-test for a one-tail hypothesis showed that the difference was not statistically significant ($P<0.1$).

formed using a two-sample t-test for a one-tail hypothesis.

3. Results

3.1. Lauric acid hydroxylase activity

Lauric acid hydroxylase activity was determined as a measure of CYP4A activity. Data for hepatic microsomal lauric acid hydroxylase activity are summarised in Table 1. Lauric acid hydroxylase activity was 22% higher in livers of treated possums, as compared with the control group (4.40 ± 0.85 vs. 3.60 ± 0.48 nm/mg protein per min). Statistical analysis using t-test showed that the difference reaches significance at $P<0.1$ (Table 1).

3.2. Peroxisomal cyanide-intensive palmitoyl coenzyme A oxidation activity

Data for peroxisomal cyanide-intensive palmitoyl coenzyme A oxidation activity are shown in Table 2. A statistically significant (202%) higher rate of peroxisomal cyanide-intensive palmitoyl-CoA oxidation was observed in livers of terpene fed possums relative to that of the control possums (2.96 ± 0.93 vs. 0.98 ± 0.88 nmol/mg protein per min, $P<0.01$).

3.3. Changes in hepatic pyridine nucleotides in treated possums

Data for hepatic pyridine nucleotide contents are summarised in Table 3. In livers of treated possums, a higher NAD/NADP ratio was observed as compared to control possums (4.73 ± 0.65 vs. 3.51 ± 0.64 nmol/mg protein per min, $P<0.05$). No other statistically significant differences in hepatic pyridine nucleotide contents were observed between the two groups.

3.4. Western blot analysis

3.4.1. Detection of CYP4A immunoreactive proteins in control and treated possum hepatic tissues

CYP4A immunoreactive bands of mass approximately 51 kDa and 54 kDa were detected in livers of both control and treated possums, with no clear difference in the density of the immunoreactive bands detected between terpene-treated and control possum groups (Fig. 1).

3.4.2. Detection of PPARα

The anti-human PPARα polyclonal antibody recognised immunoreactive bands of mass approximately 52 kDa and 54 kDa, of greater intensity, in both cytosol and nuclear extracts of treated possums as compared to the control group (Fig. 2a,b).

Table 2
Peroxisomal cyanide-intensive palmitoyl coenzyme A oxidation activities in post-nuclear supernatant prepared from control and terpene treated possums

	Peroxisomal cyanide-intensive palmitoyl coenzyme A oxidation activity (nmol/mg protein per min)
Control possums ($n=4$)	0.98 ± 0.88
Terpene possums ($n=4$)	2.96 ± 0.93*

Results are expressed as means $\pm$ S.D. of four animals for each group.*Significantly different from control group at $P<0.01$. Statistical analysis was performed using a two-sample t-test for a one-tail hypothesis.

Table 3
Nicotinamide cofactor concentrations in homogenates prepared from control and treated possum liver tissues

	Cofactor (nmol/g tissue)			
	NAD	NADH	NADP	NADPH
Control group ($n=4$)	487.5±147.8	136.3±59.3	139.0±37.6	146.3±77.8
Terpene group ($n=4$)	435.0±87.5	152.0±22.7	92.5±17.1	299.0±171.0**
	Ratio			
	NAD/NADP	NAD/NADH	NADP/NADPH	
Control group ($n=4$)	3.51±0.64	4.00±1.40	1.40±1.16	
Terpene group ($n=4$)	4.73±0.65***	2.98±1.02*	0.35±0.10**	

Results are expressed as means±S.D. of four animals for each group. The nicotinamide ratios were calculated for each individual animal and results are expressed as means of ratios±S.D.* and **: The means were different from that of control possums, however, analysis of data (using a two-sample t-test for a one-tail hypothesis) showed that the differences were far from and not statistically significant ($P<0.25$ and $P<0.1$, respectively). ***Significant different from control group at $P<0.05$.

3.5. Northern blot analysis of CYP4A, AOX and PPARα

Hybridisation of mRNAs with a koala *CYP4A* 417 bp cDNA probe detected a slightly more intense CYP4A mRNA band of size 2.6 kb in the livers of treated group relative to control group (Fig. 3). mRNA hybridisation with a koala *AOX* 320 bp cDNA probe detected a much more intense AOX mRNA band of size 5 kb observed in the treated group (Fig. 4). Using a koala *PPARα* 1.2 kb cDNA probe, PPARα mRNA species detected in livers of treated possums were of size approximately 2 kb and 4.5 kb and mRNA of size approximately 8 kb was detected in koala liver (Fig. 5). No signal was observed for control possum and rat and human livers.

4. Discussion

We have previously reported a reproducibly high CYP content and the possible *Eucalyptus* dietary induction of hepatic lauric acid hydroxylation activity and NAD cofactor content in koala liver (Stupans et al., 1999; Ngo et al., 2000). In the present study, a significantly higher peroxisomal cyanide-intensive palmitoyl coenzyme A oxidation activity was observed in livers of terpene-treated possums. This higher activity was not accompanied by an increase in CYP4A enzyme activity. In comparison to the maximal induction of up to 15-fold reported for rats exposed to peroxisome proliferators, the induction of palmitoyl coenzyme A oxidation activity by *Eucalyptus* terpenes in this study is smaller (Bell et al., 1991; Bell and Elcombe, 1991; Bars et al., 1993). The induction protocol used in this study had previously been shown to result in a significant increase in both CYP2C and CYP2E (Pass et al., 1999).

It has been reported that there is a temporally separated, but usually closely associated induction of microsomal CYP4A and peroxisomal β-oxidation enzymes by structurally diverse peroxisome proliferators (Sharma et al., 1988; Bell et al., 1991; Bell and Elcombe, 1991; Bars et al., 1993: reviewed in Simpson, 1997). Our results were similar to the results of Roffey and co-workers,

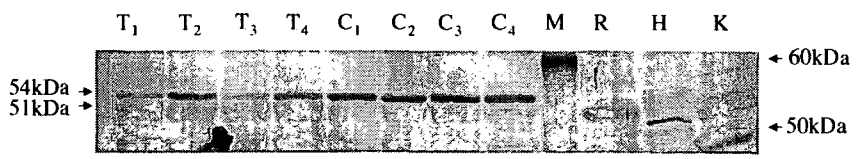

Fig. 1. Immunoblot analysis of CYP4A (50 μg microsomal protein/lane) in hepatic microsomes from brush tail possums, using sheep anti-rat CYP4A polyclonal antibody. C1–C4, possums given control diet of fruits and vegetables only; T1–T4, possums given mixture of four terpenes in control diet over 10 days; M, prestained protein ladder; R, rat; H, human; K, koala.

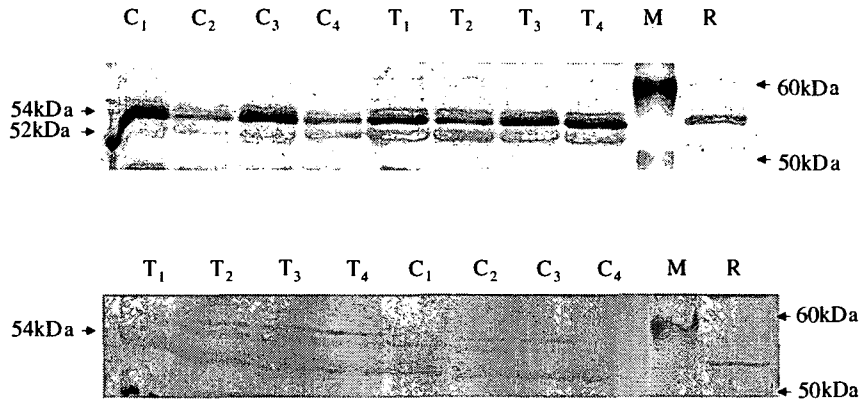

Fig. 2. Immunoblot analysis of PPRAα (50 μg nuclear extract or cytosol protein/lane) in nuclear extracts and cytosol from brush tail possums, using rabbit anti-human PPRAα polyclonal antibody. C1–C4, possums given control diet of fruits and vegetables only; T1–T4, possums given mixture of four terpenes in control diet over 10 days; M, prestained protein ladder; R, rat. (a) Nuclear extracts; (b) cytosol.

who found that oral administration of linalool, a monoterpene, caused two-fold induction of palmitoyl coenzyme A oxidation activity but not of CYP4A activity (Roffey et al., 1990).

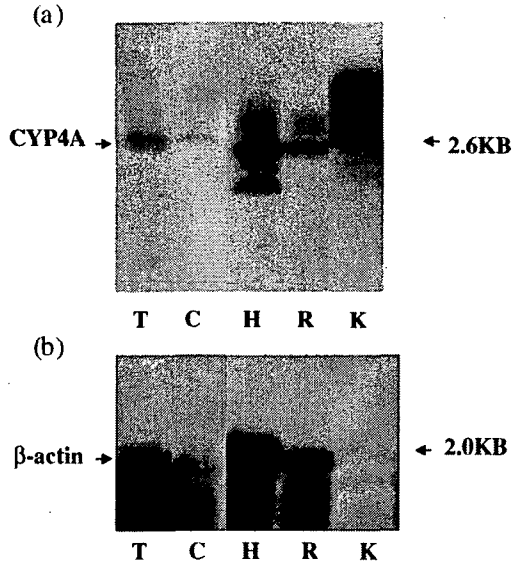

Fig. 3. Northern blot analysis of hepatic mRNA from terpene fed possum (T), control possum (C), human (H), rat (R) and koala (K), hybridised with koala *CYP4A15* 417bp cDNA probe. mRNA (10 μg per lane) was electrophoresed, blotted and hybridised with ^{32}P-labelled *CYP4A* cDNA probe as described, the filter was stripped and re-probed with a [^{32}P]dCTP labelled β *actin* cDNA probe (Ambion, Austin, TX, USA) for loading control. (a) Hybridised with koala *CYP4A15* 417bp cDNA probe. (b) Hybridised with β *actin* cDNA probe.

Peroxisome proliferators have been previously reported to cause significant induction of hepatic pyridine nucleotides NAD, NADP and NADPH, with a significant decrease in the NAD/NADH ratio, reflecting stimulation of fatty acid oxidation in peroxisomes (Shin et al., 1998). In this study, the ratio of NAD/NADP of treated possums was

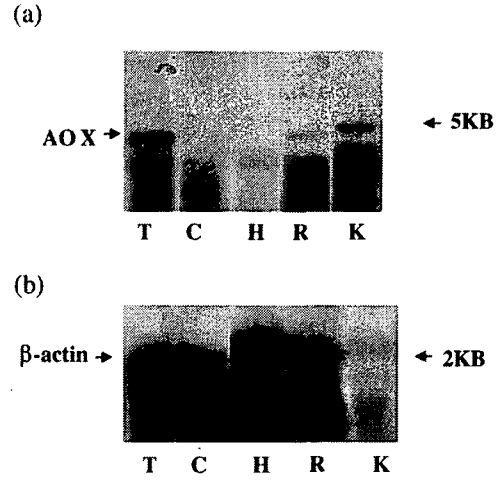

Fig. 4. Northern blot analysis of hepatic mRNA from terpene fed possum (T), control possum (C), human (H), rat (R) and koala (K), hybridised with koala *AOX* 320bp cDNA probe. mRNA (10 μg per lane) was electrophoresed, blotted and hybridised with P^{32} labelled *AOX* 1.2 kb cDNA probe as described, the filter was stripped and re-probed with [^{32}P]dCTP labelled β *actin* cDNA probe (Ambion, Austin, TX, USA) for loading control. (a): Hybridised with koala *AOX* 1.2 kb cDNA probe. (b) Hybridised with β *actin* cDNA probe.

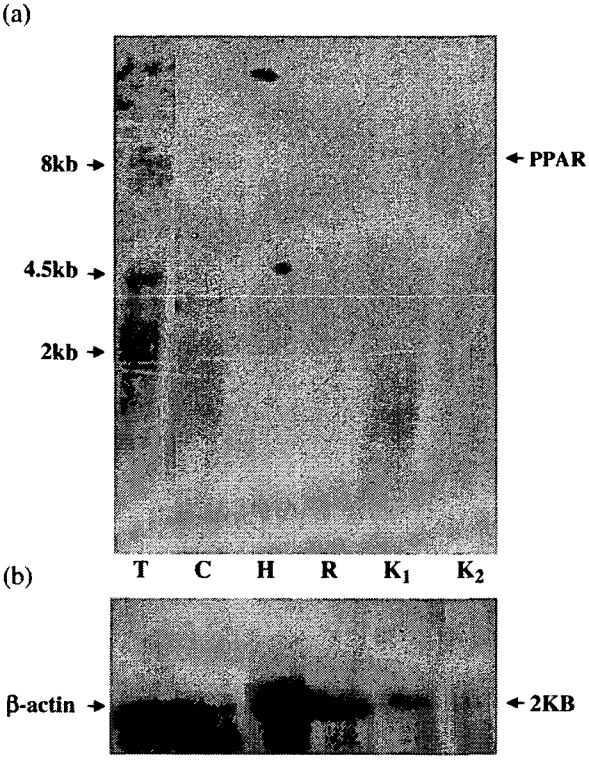

Fig. 5. Northern blot analysis of hepatic mRNA from terpene fed possum (T), control possum (C), human (H), rat (R) and koala sample 1 (K_1), Koala sample 2 (K_2), hybridised with koala *PPARα* cDNA 1.2 kb probe. mRNA (10 μg per lane, K_1 was 4 μg) was electrophoresed, blotted and hybridised with ^{32}P-labelled *PPARα* cDNA probe as described, the filter was stripped and re-probed with [^{32}P]dCTP labelled *β actin* cDNA probe (Ambion, Austin, TX, USA) for loading control. (a) Hybridised with koala *PPARα* cDNA 1.2 kb probe. (b) Hybridised with *β actin* cDNA probe.

higher than in control possums (Table 3). Mean NADPH content observed in terpene treated possums appeared to be much higher as compared with that of the control group, data analysis showed that this difference was not statistically significant (Table 3). Similarly, the lower means NAD/NADH and NADP/NADPH ratios observed in treated possums relative to control possums were found not to be statistically significant (Table 3). Our results suggested that *Eucalyptus* terpenes elevated hepatic NAD/NADP ratio with no significant changes in other hepatic pyridine nucleotide parameters.

No significant difference in the intensity of CYP4A immunoreactive bands were observed in immunoblots of the terpene-treated and control possum groups (Fig. 1). This result was consistent with the activity studies in which CYP4A activity was only 22% higher in livers of terpene-fed possums as compared with that of control possums.

A novel member of the steroid/nuclear superfamily, peroxisome proliferator activated receptor alpha (PPARα), has been reported to mediate induction of genes encoding peroxisomal AOX and microsomal CYP4A6 by peroxisome proliferators in the liver of mouse and human, through transcriptional activation of these target genes (Yu et al., 2001). In addition, disruption of PPARα gene has been reported to result in abolition of the pleiotropic effects of peroxisome proliferators (Lee et al., 1995). Induction of PPARα protein after exposure to peroxisome proliferators has been observed in rat liver (Gebel et al., 1992; Sterchele et al., 1996), which was thought to represent one important measurement of the effects of peroxisome proliferators.

From the immunoblot analysis of cytosolic and nuclear extracts (Fig. 2a,b), stronger signals for PPARα immunoreactive proteins detected in both cytosol and nuclear extracts of treated possums appeared to be due to higher PPARα protein expression, as compared with that of control possums.

The signal intensity for reactive CYP4A mRNA species in livers of test possums as compared to that of control group suggests that there is no significant difference in the expression of CYP4A mRNA between the two groups. In contrast, much stronger AOX mRNA signal detected for liver samples of treated possums relative to control possums appeared to be due to significantly higher AOX mRNA expression. This finding was consistent with the results obtained above for the activity studies that hepatic AOX enzyme activity was 202% higher ($P<0.01$), while lauric acid hydroxylase activity was only 22% higher ($P<0.1$). The expression of PPARα mRNA appeared to be higher in liver of treated possum since PPARα mRNA reactive species were not detected in liver of the control possum (Fig. 5). Although clearly visible on autoradiography film, the bands observed in livers of the test possum (2 kb, 4.5 kb) and koala (8 kb) in Fig. 5, resolution has been lost in photographic reproduction and imaging. The results in our study indicate that induction of peroxisomal β-oxidation enzymes are not always associated with induction of microsomal enzymes such as CYP4A.

Variation in the sizes of PPARα mRNA detected by northern blot analysis has been reported. Issemann and Green reported that two major mRNA species of approximately 1.8 and 2 kb were detected in mouse liver (Issemann and Green, 1990) while the size of mouse PPARα mRNA detected by others was approximately 8.5–9.5 kb (Lee et al., 1995; Tugwood et al., 1998). In addition, the size of the rat PPARα mRNA detected by Gebel et al. (1992) was approximately 6 kb, whereas that reported by others was approximately 9.5 kb (Tugwood et al., 1998). The size of human PPARα mRNA was reported to be approximately 9.5 kb (Tugwood et al., 1998). In our study, no bands of either size (6 kb or 9.5 kb) were observed for either human and rat livers. The absence of PPARα mRNA in rat tissue observed in our study was similar to the results of Sterchele and co-workers, who found that the expression level of PPARα mRNA in untreated rat liver was quite low limiting detection by Northern analysis (Sterchele et al., 1996). Gebel et al. (1992) also found no hybridisation signal when probing untreated rat RNA with a PPARα cDNA probe.

Species differences in response to peroxisome proliferators have been reported. Humans and guinea pigs were reported to be either non-responsive or obviously less responsive, whereas mice and rats were shown to be extremely responsive (Lake et al., 1989; Bell et al., 1993, 1998).

Induction of CYP expression by structurally diverse compounds has been reported to be mediated via the action of the constitutive androstane receptor (Waxman, 1999; Kliewer et al., 1999). Further work needs to be carried out in order to identify the mechanisms by which *Eucalyptus* terpenes exert their effects on peroxisomal AOX and microsomal CYP4A expression.

In conclusion, this study has demonstrated that dietary terpenes cause a significant increase in hepatic AOX expression at both the protein and mRNA level, with little increase in PPARα and cytochrome P450 CYP4A expression. Whether the effects of *Eucalyptus* monoterpenes are mediated via the nuclear receptor PPARα or the constitutive androstane receptor remains to be determined.

Acknowledgments

The authors would like to thank Assoc. Prof. Stuart McLean and Dr Georgia J Pass (University of Tasmania, Australia) for supplying the hepatic brush tail possum tissues used in this study.

References

Bars, R.G., Bell, D.R., Elcombe, C.R., 1993. Induction of cytochrome P450 and peroxisomal enzymes by clofibric acid in vivo and in vitro. Biochem. Pharmacol. 45, 2045–2053.

Bell, D.R., Elcombe, C.R., 1991. Induction of acyl-CoA oxidase and cytochrome-P4504A1 RNA in rat primary hepatocyte culture by peroxisome proliferators. Biochem. J. 280, 249–253.

Bell, D.R., Bars, R.G., Gibson, G.G., Elcombe, C.R., 1991. Localisation and differential induction of cytochrome-P450iva and acyl-CoA oxidase in rat liver. Biochem. J. 275, 247–252.

Bell, D.R., Plant, N.J., Na, L., Rider, C.G., Brown, S., Ateitalla, I., et al., 1993. Species-specific induction of cytochrome P-450 4A RNAs: PCR cloning of partial guinea pig, human and mouse CYP4A cDNA. Biochem. J. 294, 173–180.

Bell, D.R., Savory, R., Horley, N.J., Choudhury, A.I., Dickins, M., Gray, T.J.B., et al., 1998. Molecular basis of non-responsiveness to peroxisome proliferators: the guinea pig PPAR-α is functional and mediates peroxisome proliferator-induced hypolipidemia. Biochem. J. 332, 689–693.

Chomczynski, P., Sacchi, N., 1987. Single step method for RNA isolation by acid guanidinium thiocyanate–phenol–chloroform extraction. Anal. Biochem. 162, 156–159.

Cork, S.J., Foley, W.J., 1997. Digestive and metabolic adaptations of arboreal marsupials for dealing with plant antinutrients and toxins. In: Saunders, N.K., Hinds, L.A. (Eds.), Marsupial Biology, Recent Research, New Perspectives. UNSW Press, Sydney, pp. 204–226.

Corrigan, D., 1992. In: De Smet, P.A.G.M., Keller, R., Hansel, R., Chandler, R.F. (Eds.), Adverse Effect of Herbal Drugs. Springer, Berlin, pp. 125–133.

De-Oliveira, A.C.A.X., Ribeiro-Pinto, L.F., Otto, S.S., Goncalves, A., Paumgartten, F.J.R., 1997. Induction of liver monoxygenases by β-myrcene. Toxicology 124, 135–140.

Freeland, W.J., Janzen, H., 1974. Strategies in herbivory by mammals: the role of plant secondary compounds. Am. Nat. 108, 269–287.

Gebel, T., Arand, M., Oesch, F., 1992. Induction of peroxisome proliferator activated receptor by fenofibrate in rat liver. FEBS Lett. 309, 37–40.

Ghisalberti, E.L., 1996. Bioactive acylphloroglucinol derivatives from *Eucalyptus* species. Phytochemistry. 41, 7–22.

Hiroi, T., Miyazaki, Y., Kobayashi, Y., Imaoka, S., Funae, Y., 1995. Induction of hepatic P450s in rat by essential wood and leaf oils. Xenobiotica 25, 457–467.

Issemann, I., Green, S., 1990. Activation of a member of the steroid hormone receptor superfamily by peroxisome proliferators. Nature 347, 645–650.

Kliewer, S.A., Lehmann, J.M., Willson, T.M., 1999. Orphan nuclear receptors: shifting endocrinology into reverse. Science 284, 757–760.

Klingenberg, M., 1974. Nicotinamide-adenine dinucleotides (NAD, NADP, NADH. NADPH): spectrophotometric and fluorometric methods. In: Bergmeyer, H.U. (Ed.), Methods

of Enzymatic Analysis, Vol. 4. Verlag Chemie, New York, pp. 2045–2059 and 2298–2299.

Kong, S., McKinnon, R.A., Mojarrabi, B, Stupans, I., 2002. Absence of type 1 11beta-hydroxysteroid dehydrogenase enzyme in koala liver. Comp. Biochem. Physiol. C 131, 39–50.

Labrie, F., Luu-The, V., Lin, S.X., Labrie, C., Simard, J., Breton, R., Belanger, A., 1997. The key role of 17 beta-hydroxysteroid dehydrogenases in sex steroid biology. Steroids 62, 148–158.

Lake, B.G., Evans, J.G., Gray, T.J.B., Korosi, S.A., North, C.J., 1989. Comparative studies on nafenopin induced hepatic peroxisome proliferation in the rat, Syrian hamster, guinea pig and marmoset. Toxicol. Appl. Pharmacol. 99, 148–160.

Lazarow, P.B., 1981. Assay of peroxisomal (-oxidation of fatty acids. In: Lowenstein, J.J. (Ed.), Lipids. Methods in Enzymology, Vol. 72. Academic Press, New York, pp. 315–319.

Lee, S.S.T., Pineau, T., Drago, J., Lee, E.J., Owens, J.W., Kroetz, D.L., et al., 1995. Targeted disruption of the alpha isoform of the peroxisome proliferator-activated receptor gene in mice results in abolishment of the pleiotropic effects of peroxisome proliferators. Mol. Cell Biol. 15, 3012–3022.

Liapis, P., Pass, J.G., McKinnon, R.A., Stupans, I., 2000. Characterisation of tolbutamide hydroxylase activity in the common brush tail possum, (*Trichosurus vulpecula*) and koala (*Phascolarctos cinereus*): inhibition by the *Eucalyptus* terpene 1,8-cineole. Comp. Biochem. Physiol. C 127, 351–357.

Lowry, O.K., Rosebrough, N.J., Farr, A.I., Randall, R.J., 1951. Protein measurement with the Folin phenol reagent. J. Biol. Chem. 193, 265–275.

McKinnon, R.A., Hall, P.D.L.M., Quattrochi, L.C., Tukey, R.H., McManus, M.E., 1991. Localisation of CYP1A1 and CYP1A2 messenger RNA in normal human liver and in hepatocellular carcinoma by in situ hybridisation. Hepatology 14, 848–856.

McLean, S., Foley, W.J., 1997. Metabolism of *Eucalyptus* terpenes by herbivorous marsupials. Drug Metab. Rev. 29, 213–218.

Ngo, S.N.T., Kong, S., Kirlich, A., Mckinnon, R.A., Stupans, I., 2000. Cytochrome P450 4A, peroxisomal enzymes and nicotinamide cofactors in koala liver. Comp. Biochem. Physiol. C 127, 327–334.

Parker, G.L., Orton, T.C., 1980. Induction by oxyisobutyrates of hepatic and kidney microsomal cytochrome P-450 4A with specificity towards hydroxylation of fatty acids. In: Gustafsson, J.A., Carlstedt-Duke, J., Mode, A., Rafter, J. (Eds.), Biochemistry, Biophysics and Regulation of Cytochrome P-450. Elsevier, Amsterdam, pp. 373–377.

Pass, J.G., McLean, S., Stupans, I., 1999. Induction of xenobiotic metabolising enzymes in the common brush tail possum, *Trichosurus vulpecula*, by *Eucalyptus* terpenes. Comp. Biochem. Physiol. C 124, 239–246.

Pass, J.G., Mclean, S., Stupans, I., Davies, N., 2001. Microsomal metabolism of the terpene 1,8-cineole in the common brush tail possum (*Trichosurus vulpecular*), koala (*Phascolarctos cinereus*), rat and human. Xenobiotica 31, 205–221.

Patel, S., Wiggins, J., 1980. *Eucalyptus* oil poisoning. Arch. Dis. Child. 55, 405–406.

Roffey, S.J., Walker, R., Gibson, G.G., 1990. Hepatic peroxisomal and microsomal enzyme induction by citral and linalool in rats. Food Chem. Toxicol. 28, 403–408.

Sharma, R.A.J., Lake, B.G., Foster, J., Gibson, G.G., 1988. Co-induction of microsomal cytochrome P-452 and the peroxisomal fatty acid beta-oxidation pathway in the rat by clofibrate and di-(2-ehtylhexyl)phthalate. Biochem. Pharmacol. 37, 1203–1206.

Shin, M., Ohnishi, M., Iguchi, S, Umezawa, C., 1999. Peroxisome-proliferator regulates key enzymes of the tryptophan-NAD+ pathway. Toxicol. Appl. Pharmacol. 158, 71–80.

Shin, M., Sano, K, Umezawa, C., 1999. Effect of peroxisome proliferators on the TRP-NAD pathway. In: Huether, A. (Ed.), Tryptophan, Seretonin, and Melatonin: Basic Aspects and Applications. Kluwer Academic, Plenum Publishers, New York, pp. 333–340.

Shin, M., Iwamoto, N., Yamashita, M., Sano, K., Umezawa, C., 1998. Pyridine nucleotide levels in the liver of rats fed clofibrate- or pyrazinamide-containing diets. Biochem. Pharmacol. 55, 367–371.

Simpson, A.E., 1997. The cytochrome P450 4 (CYP4) family. Gen. Pharmacol. 28, 351–359.

Spoerke, D.G., Vandenberg, S.A., Smolinske, S.C., Kulig, K., Rumack, B.H., 1989. *Eucalyptus* oil: 14 cases of exposure. Vet. Hum. Toxicol. 31, 166–168.

Sterchele, P.F., Sun, H., Peterson, R.E., Heuvel, J.P.V., 1996. Regulation of peroxisome proliferator-activated receptor alpha mRNA in rat liver. Arch. Biochem. Biophys. 326, 281–289.

Stupans, I., Kong, S., Kirlich, A., Murray, M., Bailey, E.L., Jones, B.R., et al., 1999. Hepatic microsomal enzyme activity in the koala and tammar wallaby: high 17beta-hydroxysteroid oxidoreductase activity in koala liver microsomes. Comp. Biochem. Physiol. C 123, 67–73.

Stupans, I., Jones, B., McKinnon, R.A., 2001. Xenobiotic metabolism in Australian marsupials. Comp. Biochem. Physiol. C 128, 367–376.

Tugwood, J.D., Holden, P.R., James, N.H., Prince, R.A., Roberts, R.A., 1998. A peroxisome proliferator-activated receptor-alpha (PPAR() cDNA cloned from guinea-pig liver encodes a protein with similar properties to the mouse PPARα: implications for species differences in responses to peroxisome proliferators. Arch. Toxicol. 72, 169–177.

Waxman, D.J., 1999. P450 gene induction by structurally diverse xenochemicals: central role of nuclear receptors CAR, PXR, and PPAR. Arch. Biochem. Biophys. 369, 11–23.

Yu, S., Cao, W.Q., Kashireddy, P., Meyer, K., Jia, Y., Hughes, D.E., et al., 2001. Human peroxisome proliferator-activated receptor alpha (PPARalpha) supports the induction of peroxisome proliferation in PPARalpha-deficient mouse liver. J. Biol. Chem. 276, 42485–42491.